DOTTORATO DI RICERCA IN BIOCHIMICA
CICLO XXVI (A.A. 2010-2013)

Nitric Oxide and Melatonin in Cell Bioenergetics and Neurodegeneration

Dottoranda
Maria Chiara Magnifico

Docente guida   **Coordinatore**
Prof. P. Sarti   **Prof. F. Malatesta**

Correlatore
Dr. M. Arese

Dicembre 2013

ACKNOLEDGMENT

III

IV

V

VI

1. INTRODUCTION

1.1 Cell respiration

Cell respiration is the principal metabolic pathway by which eukaryotic and prokaryotic cells, in the presence of oxygen produce energy for their needs. It consists of a series of redox (reduction-oxidation) reactions, called oxidative phosphorilation (OXPHOS), during which substrates, such as glucose, are converted into H_2O and CO_2. The energy is stored in the form of ATP, a molecule discovered in 1899 by Karl Lohmann and whose central role in bioenergetics was defined by Fritz Lipmann in 1941. ATP carries chemical energy to be used by all the energy-consuming cell functions, including protein biosynthesis, locomotion or transportation of molecules across cell membrane and compartments. Not only OXPHOS, but also glycolysis is set to produce ATP in the cells, particularly under low O_2 tension. Interestingly, most cancer cell types, despite their apparently intact mitochondria and a virtually efficient OXPHOS, commonly switch from OXPHOS to the energetically less favorable glycolysis in a metabolic transition termed the Warburg effect and the condition facilitaties a shift to anabolic pathways [1]. In eukaryotes, glycolysis occurs in the cell cytoplasm whereas both OXPHOS and the Krebs cycle occur in the mitochondrion, in the inner mitochondrial membrane and in the mitochondrial matrix, respectively. Mitochondria are the central organelles in a variety of essential cell functions and have been, therefore, the focus of numerous studies for many years. Mitochondria are membrane-enclosed organelles distributed in the cytosol of most eukaryotic

cells. Mitochondria are typically 0.7 - 1 μm in length. The number of mitochondria in a cell varies widely within organisms and tissue types. Mitochondria are compartmentalized by two membranes, made of phospholipids and containing highly specialized proteins. The outer membrane bilayer encloses the entire organelle and is freely permeable to ions and most small metabolites. The inner mitochondrial membrane is assembled in many folds called *"cristae"*, which expand the surface area of the membrane. The inner membrane is highly impermeable to all molecules and most ions, which require specific membrane transporters to enter or exit the matrix. The protein-mediated and -regulated permeability of the inner membrane is of vital importance for the morphological and functional integrity of the mitochondrion. As mentioned before, the oxidative phosphorylation occurs at the level of the inner mitochondrial membrane while the citric acid cycle and the oxidation of fatty acids, i.e. the main sources of NADH and $FADH_2$, occur in the matrix. NADH or $FADH_2$ convey electrons to the electron transport respiratory system. The system contains membrane-bound electron carriers that are organized in the so called respiratory chain. The NADH:ubiquinone oxidoreductase (also called NADH dehydrogenase) is the mitochondrial Complex I and catalyzes the first step of oxidative phosphorylation, through the transfer of two electrons from NADH to a lipid-soluble carrier, ubiquinone (Q). The succinate dehydrogenase is Complex II and may directly catalyze the reduction of quinone. The ubiquinol-cytochrome c oxidoreductase is complex III and oxidizes ubiquinol while reducing cytochrome c (cyt c). The cytochrome c oxidase (CcOX), complex IV, carries electrons from cyt c to molecular oxygen that is reduced to water using up protons in the matrix (scalar protons). The ATP synthase (Complex V) catalyzes the synthesis of ATP. Ubiquinone and cyt c are freely-diffusible molecules that shuttles electrons from

2

one complex to the next one, according to their redox potential. At the level of complex I, III and IV, the free energy released is used to traslocate protons (H^+) from the mitochondrial matrix into the intermembrane space (vectorial proton pumping). Both vectorial and scalar reactions generate a proton electrochemical potential gradient across the inner mitochondrial membrane ($\Delta\mu H^+$), the so called proton–motive force. $\Delta\mu H^+$ is used to drive endoergonic reactions; among them, the synthesis of ATP by ATP synthase is, indeed, the main responsible reaction for the back flux of protons into the matrix and the gradient dissipation. The proton motive force has two components: *i)* the trasmembrane electrical potential ($\Delta\psi$), which arises from the net accumulation of positive charges (H^+) in the intermembrane space, while under standard matrix bears a net negative charge and *ii)* the trasmembrane pH gradient (ΔpH). The relationship between these two components is expressed by the Mitchell equation:

$$\Delta\mu H^+ = \Delta\Psi - 60\ \Delta pH$$

Cytochome c oxidase contributes to the energyzation of the inner mitochondrial membrane, by reduction of O_2 to H_2O and by the proton-pumping out of the mitochondrial matrix.

1.1.1 *Cytochrome c oxidase*

Cytochrome c oxidase (CcOX) (EC 1.9.3.1) is a complex metalloprotein located in the inner mitochondrial membrane. The enzyme catalyzes the oxidation of cytochrome c and reduction of oxygen to water. CcOX is a member of the superfamily of heam-copper oxidases. The 3D crystallographic structure of several heme-copper oxidases has been solved since 1995 (see Fig. 1) [2-4]. The mammalian purified CcOx is a dimer where each monomer is 204.5 kDa. The

enzyme is formed by 3-4 subunits in prokaryotes, in eukaryotes by 13 subunits; of these, subunit I, II and III are forming the core of the enzyme and are coded by mitochondrial genes; these subunits are very similar to the corresponding subunits in *Paracoccus Denitrificans*.
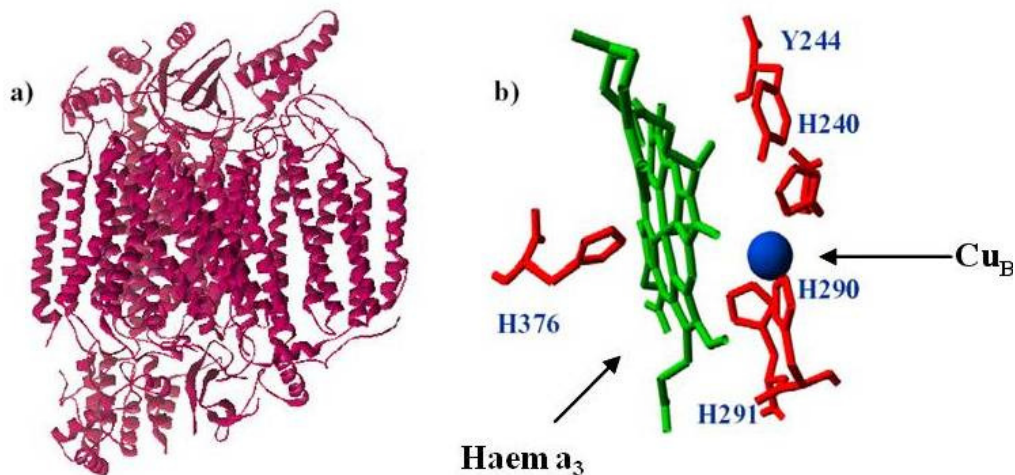
Fig. 1: a) Structure of the CcOX from beef heart. b) Oxidized active site of the beef heart enzyme *(modified from Tsukihara et al, 1995; Tsukihara et al, 1996)*.

The subunit I, tightly in contact with subunit II and III, is made by 12 transmembrane helices and contains 3 of the 4 redox centres of the enzyme, namely haem a, a_3 and Cu_B. The subunit II is constituted by 2 hydrophilic transmembrane helices and one hydrophilic domain protruding in the cytosolic side of the mitochondrial membrane, and containing the bimetallic site Cu_A. The subunit III is constituted by 7 transmembrane helices involved in the control of the proton pumping activity [5]. It presents a large cavity in which two molecules of lipids (phosphatidylethanolamine and phosphatidylglycerol) have been

detected. The enzyme contains 4 redox-active metal sites: Cu_A (two coppers organised in a single site), haem a, haem a_3 and Cu_B. The enzyme contains also redox inactive metals such as Mg^{2+} and Zn^{2+} playing most probably a structural role. The bimetallic site Cu_A, presents a tetrahedric structure in which two Cu (copper-copper dimer) are bound by the sulfhur of Cys^{196} and Cys^{200}, like a centre (2Fe-2S). Haem a is a low-spin haem with two histidine (His^{61}, His^{378}) residues as axial Fe-ligands. It transfers electrons from Cu_A to the binuclear centre. The binuclear centre is formed by the high spin haem a_3 and the copper ion (Cu_B). It is the catalytic centre for O_2 reduction. The haem a_3 appears to be penta-coordinated and its ligand is the His^{376}. Cu_B is coordinated by His^{290}, His^{291} and His^{240}, the latter is covalently linked to the highly conserved tyrosine Tyr^{244}; this tyrosine has a radical character in one of the catalytic intermediates, possibly playing a crucial role in catalysis. The bimetallic active site (haem a_3-Cu_B) of CcOX, O_2 is reduced to H_2O and all CcOX ligands, such as NO, CO and CN^-, bind.

In the O_2 reduction to water, 4 electrons are transferred to CcOX from cytochrome c following this pathway:

$$\text{cyt } c \rightarrow Cu_A \rightarrow \text{cyt } a \rightarrow \text{cyt } a_3\text{-}Cu_B \rightarrow O_2$$
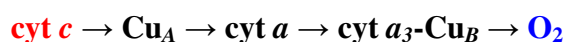
The binuclear haem a_3-Cu_B centre is reduced by the electrons donated by cytochrome c and arriving intramolecularly *via* Cu_A and haem a; after complete reduction the binuclear site is oxidized by oxygen completing the reaction cycle. Also for the sake of identifying the intermediates relevant in the nitric oxide

binding chemistry, the catalytic cycle can be divided into a reductive and an oxidative part as shown in the scheme:
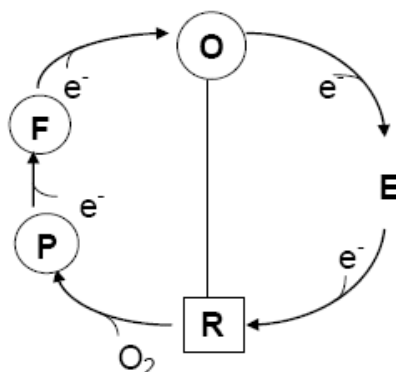
In the reductive part the oxidized active site **O** (haem a_3-Cu_B), accepts two electrons sequentially from Cu_A via cytochrome a. This is an intra-molecular electron transfer that yields the fully two-electrons reduced site **R**, via a single-electron reduced intermediate **E** in which the electron can reside either on haem a_3 (species **E**1) or on Cu_B (species **E**2) [6]. The rate-limiting step of the catalytic cycle is the intramolecular reduction of the binuclear site. In the much faster oxidative part (μs vs ms), upon reaction with O_2, **R** restores the fully oxidized enzyme **O**, by populating the O_2 intermediates **P** and **F** [7]. Interestingly and at substantial variance with O_2, NO proved able to react with all intermediate CcOX species [8].

6

1.1.2   Mitochondrial nitro-oxidative stress

Mitochondrial respiration is the most important energy product process, but it is also recognized as the most relevant source of reactive oxygen and nitrogen species (RONS) in the majority of eukaryotic cell types [9]. RONS are small molecules which are highly reactive due to their unpaired valence shell electrons; average life-time values are 10^{-6}, 10^{-5}, 10^{-9} seconds for singlet oxygen, superoxide radical and hydroxyl radical, respectively (Fig. 2). In response to a variety of stressors, RONS production increases. When this occurs in conjunction with a limited antioxidant defense availability, a nitro-oxidative stress occurs, such a condition may ultimately lead to oxidative damage of cellular components, DNA, proteins and lipids. Despite their dark side, RONS are involved in the regulation of vital processes such as cellular signaling, the activation of cellular antioxidant defence system, the immune response, apoptosis and gene transcription, all functions serving several key roles in human physiology. Due to the high RONS reactivity, under optimal conditions, cells possess various molecular mechanism responsible for their control: these consist of both non-enzymatic and enzymatic systems. Non-enzymatic systems include hydrophylic and lipophylic radical scavengers, such as glutathione, cytochrome c (cyt-c), ascorbic acid, reduced coenzyme Q10, vitamin E, vitamin C and melatonin. Enzymatic components include manganese superoxide dismutase (Mn-SOD), catalase (CAT), glutathione peroxidase (GPx), glutaredoxin reductases (Grd) and peroxiredoxin. The regeneration of glutathione by glutathione reductase and reduced thioredoxin by thioredoxin reductase depends on NADPH. Gene-mutations involving these enzymes, mutations in their corresponding genes have been associated with idiopathic   cardiomyopathy,   neurological   sufferance,   impairment   glucose

metabolism, and cancer, all pathological states invariably displaying increased RONS level. In structurally and functionally intact cells and mitochondria, antioxidant defense capacity balances RONS generation, limiting RONS bioavailability.
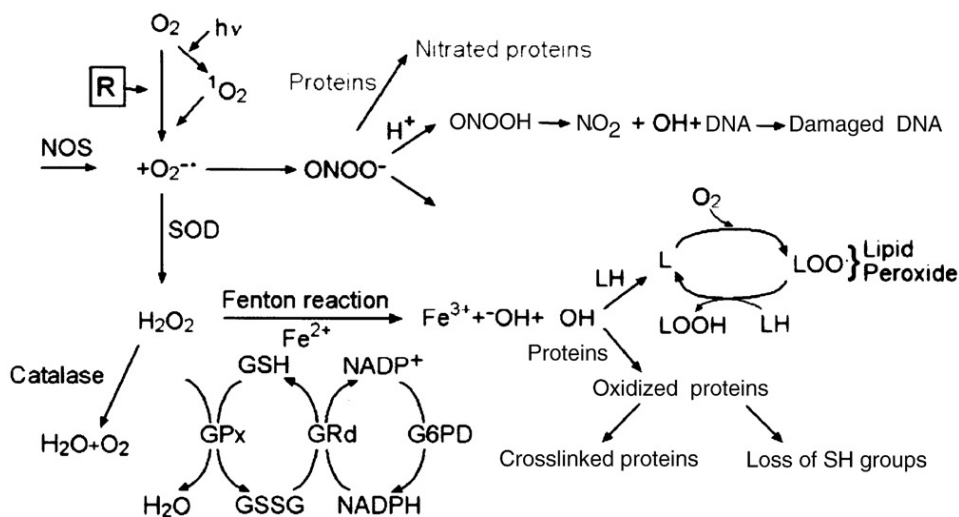
Fig. 2: RONS *(modified from Barzilai et al., 2002).*

Decreased antioxidant defense capacity is a prerequisite for increased net RONS production and nitro-oxidative stress. The primary RONS generated by mitochondria is superoxide anions (O_2^-). Formation of O_2^- in the mitochondrion occurs at the level of complex I and complex III. O_2^- is converted in the more stable, still highly reactive, H_2O_2 in mitochondria through the activity of matrix Mn-SOD and in the intermembrane through the activity of Cu,Zn-SOD [10, 11]. H_2O_2 generated in mitochondria has a number of fates. Because H_2O_2 is relatively stable and membrane-permeable (transported by the aquaporins located in the inner mitochondrial membrane [12]), it can diffuse within the cell where it is

removed by cytosolic antioxidant systems such as catalase, glutathione peroxidase and thioredoxin peroxidase [13]. Mitochondrially generated H_2O_2 can also act as a signaling molecule in the cytosol, affecting multiple networks that control, for example, cell cycle, stress response, energy metabolism, and redox balance [14]. If not metabolized by the mitochondrial antioxidant systems, H_2O_2 is promptly decomposed via the Fenton reaction forming hydroxyl radicals. The hydroxyl radical is a potent reactive species, able to oxidize important targets, including nucleic acids, amino acids (tyrosine, phenylalanine, histidine), sugars and lipids [15]. Due to the high risk bound to the Fenton chemistry, it is feasible that mitochondria have developed both an efficient H_2O_2 and metal-chelating removal systems. Experiments carried out using iron chelators proved their efficiency to prevent mitochondrial damage and loss of integrity due to enhanced ROS generation [16, 17].

Mitochondria have also been credited as a source of reactive nitrogen species derived from nitric oxide (NO). The mitochondrial role of NO and its putative physiological signaling function will be extensively analyzed in the next chapter. Here it is important to underline that the intracellular redox state, might favor to a different extent the formation of peroxynitrite ($ONOO^-$) using superoxide anions and NO. In turn, peroxynitrite nitrates and inhibits Mn-SOD, thereby preventing the breakdown of locally produced superoxide, which further fuels the formation of peroxynitrite [18].

$ONOO^-$ exerts its harmful effects directly and indirectly (Fig. 3). $ONOO^-$ causes activation of transcriptional factors, including nuclear factor kappa B (NF-kB) and activator protein-1 (AP-1) leading to pro-inflammatory gene expression, including tumor necrosis factor a (TNF-α) and interleukin 1 (IL-1) [19]. Peroxynitrite can react with CO_2, giving rise to CO_3^- and NO_2^- radicals. $ONOO^-$ directly interacts

9

with and covalently modifies all major types of biomolecules including membrane lipids, thiols, proteins, and DNA [15, 19]. Using both cultured cells and isolated submitochondrial fractions, peroxynitrite has been shown to exert significant inhibition to most components of the electron transport chain, through mechanisms involving, to various extents, cysteine oxidation, tyrosine nitration, and damage of iron sulfur centers.
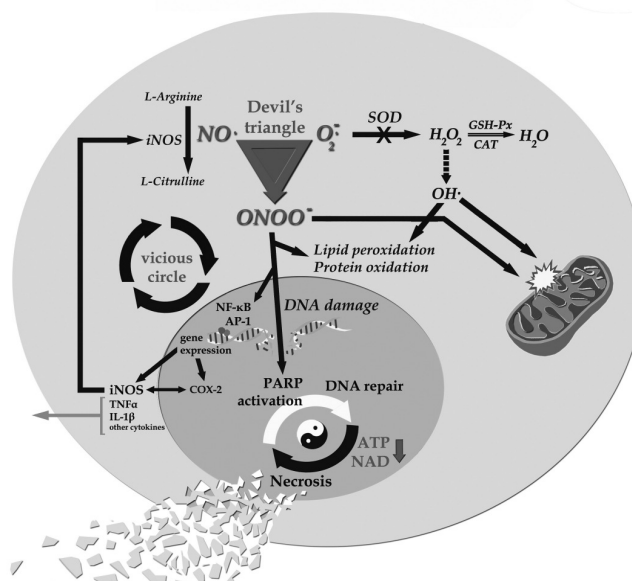
Fig. 3: Effects of ONOO⁻ (*modified from Korkmaz et al., 2009*).

A major protein target for nitrosation and nitration is respiratory Complex I [20]. ONOO⁻ activates matrix metallo proteinases (MMPs) and inactivates several enzymes that are critically involved in the repair of DNA damage. Another target of peroxynitrite is cytochrome c, the nitration of which significantly impairs its redox properties [21, 22]. Notably, cytochrome c nitration increases its

10

peroxidatic activity, leading to the generation of hydrogen peroxide and exacerbation of oxidative damage to mitochondrial proteins. $ONOO^-$ further impairs energy metabolism by inhibiting the tricarboxylic acid cycle enzyme aconitase, as well as the mitochondrial creatine kinase, which is present in the intermembrane space. Nicotinamide nucleotide transhydrogenase, which allows formation of NADPH from NADH and $NADP^+$, is another important mitochondrial protein oxidized, nitrated, and inactivated by peroxynitrite. The ensuing depletion of NADPH reduces the mitochondrial ability to regenerate GSH, contributing to the amplification of oxidative stress within the organelle. $ONOO^-$ induces cell apoptosis but also necrosis of cells. When the exposure to this agent persists, the activation of the DNA repair enzyme poly (ADP ribose) polymearase-1 (PARP-1) also occurred [23].

Mitochondrial bioenergetics and redox state are also dependent on intracellular Ca^{2+} levels. Mitochondria are endowed with Ca^{2+} uniporters capable of rapidly promoting $\Delta\Psi$-driven Ca^{2+} uptake into the matrix, most notably when Ca^{2+} is released by the endoplasmic reticulum [24]. Ca^{2+} can be accumulated in vast quantities in mitochondria, by mean of mitochondrial Ca^{2+} transporters despite their affinity for Ca^{2+} is lower than that the reticulum and plasma membrane transporters. Consistently, an elevated Ca^{2+} accumulation has been associated with mitochondrial oxidative stress [16, 25-28]. Increased cytoplasmatic Ca^{2+} levels may increase mitochondrial RONS formation by several mechanisms; these include the enhancing of citric acid cycle activity and NADH formation [26], activating ROS-generating enzymes such as glycerol phosphate and α-ketoglutarate dehydrogenase [29]; but also the enhancement of NO generation via activation of the eNOS enzyme and consequent respiratory inhibition [30, 31], and promoting the loss of cytochrome c due to the mitochondrial permeability

transition, which is promoted by excessive Ca^{2+} accumulation [32-34]. At molecular level, the nitro-oxidative stress could facilitate the opening of the mitochondrial permeability transition pore (MPTP). Activation of the MPTP might render the inner mitochondrial membrane permeable to protons, increasing the eventually need of glycolytic ATP in the attempt to maintain the mitochondrial membrane potential. In the absence of glycolysis, an oxidative damage and the associated mitochondrial dysfunction may result in energy depletion, manifested as an irreversible drop of membrane potential, accumulation of cytotoxic mediators and cell death [35].

Mitochondrial nitro-oxidative stress has been linked to the pathophysiology of a large number (>100) of human diseases (such as Alzheimer disease), as well as to the aging process [36]. Pathological conditions characterized by a lower respiratory rate, in fact, are often accompanied by enhanced RONS release: this is the case of respiratory deficiencies associated with neurodegenerative diseases and mitochondriopathies [37-39].

1.2 Patho-physiological role of Nitric Oxide

Nitric oxide (NO) is a gaseous biological messenger which regulates several physiological responses [40] including relaxation of smooth muscles [41], neurotransmission [42], platelet aggregation [43, 44] and inflammation [45]. Made of oxygen and nitrogen, it can be classified as a ROS better as a RONS. In the late 1980s, the labile endothelium-derived relaxing factor (EDRF) was unveiled to be NO [46, 47]. Many of the physiological functions of NO are mediated through the activation of soluble guanylyl cyclase (sGC). NO interacts allosterically with sGC to increase cyclic GMP (cGMP) concentration, leading to

cGMP-response. Murad first showed that the activation of sGC by nitrovasodilators could occur via the formation of NO. He was fascinated by the idea that a gas and free radical was regulating smooth muscle contraction and proposed that hormones as other endogenous factors could also act by releasing NO [48, 49]. About 25 years ago nitric oxide was discovered to act as an efficient, to a large extent reversible inhibitor of cellular respiration [50]. NO exerts a controlled inhibitory role on the mitochondrial respiratory chain through the reaction with complex I and complex IV. The interaction between NO and complex IV is rapid and reversible [51-55], leading under controlled conditions (pulses of NO) to a limited depression of OXPHOS and to activation of glycolysis, indeed in those cells able to sustain it [56, 57]. NO is a modulator of neuronal function [58, 59] and several studies have suggested that NO plays a role in the circadian and homeostatic regulation of sleep [60-67]. NO is also implicated in the pathophysiology of many diseases, such as cardiovascular dysfunctions [68-74], neurodegeneration [75-81], arthritis, asthma, diabetes and septic shock [82-85]. Evidence is growing that the toxic effect of NO resides on its concentration levels and on the production of peroxynitrite and other reactive oxygen and nitrogen species. Low concentration of NO (piconanomolar) appears to be by and large physiological, whereas high concentration of NO (micromolar) may turn to pathological. The type of biomolecule reacting with NO and, when occurring, the cell bioenergetic changes induced, strongly contribute to physiological or pathological outcomes.

1.2.1   NO generation and the Nitric Oxide Synthases

Nitric oxide is produced endogenously by the nitric oxide synthase enzymes, NOS(s).

NOS catalyzes the following reaction:

L-Arginine   N^{G}hydroxy L-Arginine   L-Citrulline
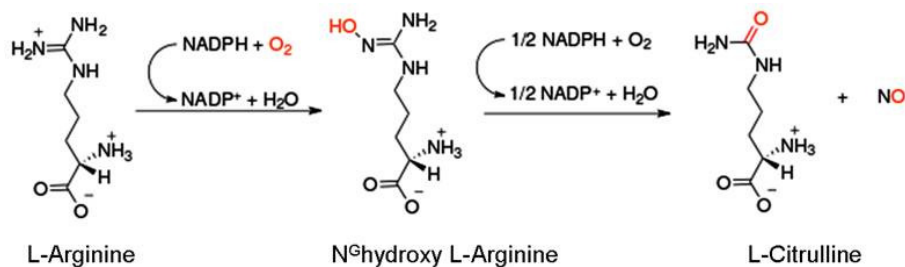
The NOS enzyme activity take advantage of the presence of differents cofactors and prosthetic groups: FAD, FMN, tetrahydrobiopterin (BH$_4$) and iron protoporphyrin (haem). NOS generates NO using one of the terminal N atoms of the L-arginine that is transformed into L-citrulline [86]. Oxidation of L-arginine to L-citrulline occurs via two successive mono-oxygenation reactions producing N^{G}hydroxy L-arginine (NOHLA) as an intermediate [87, 88].

Three NOSs isoforms have been identified, named according to the cell type or the environment where they were first detected. The constitutive NOSs (cNOSs) are the endothelial NOS (eNOS or NOS III) and the neuronal NOS (nNOS or NOS I), whereas the inducible NOS (iNOS or NOS II) is typically produced on stimulation of immunocompetent cells. In general the nNOS and eNOS isoforms are known to be constitutively expressed and their function is Ca^{2+}-dependent. These enzyme releases NO, in the nanomolar concentration range, for short time periods in response to receptor or physical stimulation. The NO released by these

enzyme isoforms acts as a transduction mechanism underlying several physiological responses. The third isoform iNOS display a completely different regulation of activity: it is induced after activation of macrophages, endothelial cells and a number of other cells by cytokines. Once expressed, thus mainly under infection circunstances, the iNOS synthesizes NO, in the (high) micromolar concentration range and for long periods of time. Furthermore, this enzyme is Ca^{2+}-independent since calmodulin (CaM) is already bound to the enzyme. The nNOS and iNOS have a cytosolic location and eNOS is associated to the cell membrane. The three distinct genes for the human NOS isoforms, exist as a single copy of each in the aploid human genome. The three isoforms share a 50–60% sequence homology and some basic features: (1) the N-terminal domain, holding one Fe–haem, (2) the L-arginine- and the tetrahydrobiopterin (BH4)-binding domains, (3) a calmodulin binding region and (4) the reductase C-terminal domain.
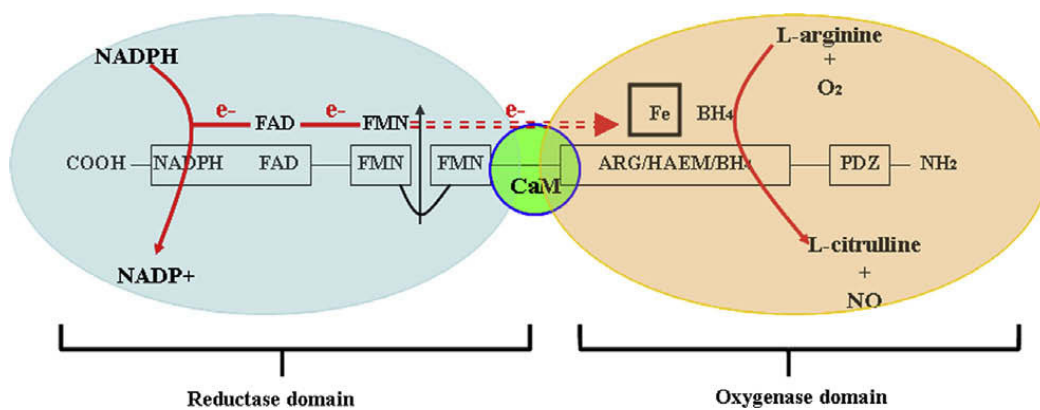
Fig. 4: Schematic representation of nNOS structure (*from Li Zhou, Dong-Ya Zhu; Review 2009*).

The NOSs are homodimers consisting of two identical monomers, which can be functionally and structurally divided into two major domains: a C-terminal reductase-carboxy domain, containing binding sites for FAD, FMN and NADPH, and an N-terminal oxygenase-amino domain, containing the binding sites for haem, BH_4 and L-arginine [88-91] (Fig. 4). In between the two domains of a NOS monomer a calmodulin binding site is located (green circle in figure 4).

The electrons are donated by NADPH to the reductase domain of the enzyme and proceed *via* FAD and FMN redox carriers to the oxygenase domain. In the oxygenase domain, they interact with the haem iron and BH_4 at the active site to catalyze the reaction of oxygen with L-arginine, generating L-citrulline and NO as products. Electron flow through the reductase domain requires the presence of bound Ca^{2+}-Calmodulin (CaCaM) [92].

1.2.1.1 Regulation of NOS activity

 Intrinsic factors

The small acidic calcium binding protein, calmodulin (CaM) was the first protein shown to interact with NOS and is necessary for the enzymatic activity of all three isoforms [93]. Calmodulin is a member of a superfamily of structurally related calcium signaling proteins. Members of this superfamily share a 29-residue helix-loophelix motif called the EF-hand that is responsible for high affinity calcium binding. Calmodulin has four EF-hand domains, arranged as two pairs separated by an eight-turn central helix. The exact mechanism of how CaM activates the NOS is not fully understood [94]. Studies have shown that CaM is placed just between the two domains of the enzyme (reductase and oxygenase domain); on this basis it has been proposed that CaM acts like a switch that causes a conformational change in the NOS thus allowing the transfer of an electron

between the reductase and oxygenase domains, by a process that is thought to be highly dynamic. Under physiological conditions, the calmodulin (CaM)-binding site of the iNOS is always occupied by CaM, whereas CaM binding to nNOS and eNOS is dependent on the increase of intracellular calcium. The nNOS and eNOS differ in their primary structure from iNOS in the former having 40 ± 50 amino acids inserts in the middle of the FMN-binding subdomain, which has been described as an autohinibitory loop [95]. Analysis of mutants of cNOS with this loop deleted has shown that the insert acts by destabilizing CaM binding at low Ca^{2+} and by inhibiting the electron transfer from flavin domain to the heam domain in the absence of CaCaM [96]. Factors stimulating an intracellular Ca^{2+} increase, stimulate also CaM binding to cNOS that became activated. In contrast, when intracellular Ca^{2+} concentrations decrease to basal levels, calmodulin dissociates from cNOS and it becomes inactive.

Extrinsic factors

Several extrinsic factors regulating NOS(s) activity have been identified and here below summarized.

- Phosphorilation

cNOS activity is regulated by phosphorilation. The eNOS is target of phosphorylation at the level of key residues, namely serine Ser^{116} and Ser^{1177} and threonine Thr^{495} (human enzyme, numbering). Phosphorylation increases the eNOS sensitivity to Ca^{2+} and modulates its catalytic function, although with mechanisms only partly understood [97]. In contrast, the phosphorylation of nNOS at Ser^{847} by CaM-dependent kinases leads to a decrease in nNOS activity [98].

Chapter 1. Introduction

- Proteins binding to PDZ domain of nNOS

The N-terminal 220 aminoacids of nNOS realise a PDZ domain (post-synaptic density protein, discs-large/ ZO-1 homology domain) [99]. The nNOS PDZ domain contains two non-overlapping binding sites, one site binds PDZ domains of other proteins (residues 100–130, comprising a β-hairpin) while the other site binds COOH-terminal peptide ligands [100]. Proteins bearing PDZ domains typically localize to specialized cell compartments and are believed to be important in linking components of signal transduction pathways in multiple complexes [101]. The result of anchoring nNOS to membrane or cytosolic protein via direct PDZ–PDZ domain or C-terminal-PDZ interactions, leads to an altered NO signaling. PSD95 (post-synaptic density protein-95), a multivalent synaptic scaffolding protein, can link nNOS to N-methyl-D-aspartate receptor (NMDAR), and accounts for the efficient activation of nNOS by NMDAR stimulation [102].

- Protein inhibitor of NOS (PIN)

The initial report suggested that the N-terminus of nNOS (amino acids 163–245) could bind to the 89-aminoacid protein PIN which destabilizes nNOS dimers and inhibits nNOS activity [103]. PIN was only co-immunoprecipitated with nNOS and not with eNOS or iNOS [103]. However, other report claim that PIN neither inhibits nNOS nor promotes monomerization. Alternatively PIN might act as a dynein light chain, participated in nNOS axonal transport rather than as a nNOS inhibitor [104]. It remains to be established whether PIN can influence nNOS activity and if so, the mechanism involved.

- Heat-shock protein 90 (Hsp90)

Heat shock protein 90 (hsp90), an abundant molecular chaperone (constituing almost 1~2 % of total cytosolic protein) is highly conserved from prokaryotes to eukaryotes, and is involved in the folding, stability and maturation of numerous

18

client proteins including NOS [105]. Hsp90 has been identified as a regulator of eNOS activity, possibly as an allosteric modulator [106]. The nNOS-hsp90 heterocomplex has been detected; but rather than a direct activation of nNOS by hsp90 wasn't observed, it has been suggested for the chaperone protein in the process of incorporation of the haem into nNOS [107]. Regarding to the iNOS isoform, this is thought to be primarily regulated at transcriptional level and the identification of a protein interacting with iNOS in the central nervous system has been reported [108].

- Myristoylation, palmitoylation

Of the three NOS isoforms, only the eNOS was found to be acylated by both myristate and palmitate [109]. eNOS undergoes a series of covalent modifications, including co-translational N-myristoylation at Gly^2, as well as post-translational thiopalmitoylation at Cys^{15} and Cys^{26} [110, 111]. Myristoylation of eNOS is required for the subsequent palmitoylation of the enzyme, and both acylations are required for the efficent localization of eNOS to the plasmalemmal caveolae [112]. Specifically, eNOS is associated with caveolin-1 and caveolin 3 isoforms in endothelial cells and cardiac myocytes, respectively [113]. Relevant to the melatonin chemistry here presented, caveolin negatively impact the eNOS activity through a direct interaction with the enzyme. When interacting with caveolin, eNOS is in an inactive form. CaM acts as a direct allosteric competitor (*vs* caveolin) to promote the Ca^{2+}-dependent activation of eNOS [114].

1.2.2 NO reactivity

NO is a highly diffusible molecule, freely permeable to membranes. Once NO is produced it may reacts with a large number of targets according to the specific kinetic and affinity constants (Fig. 5).
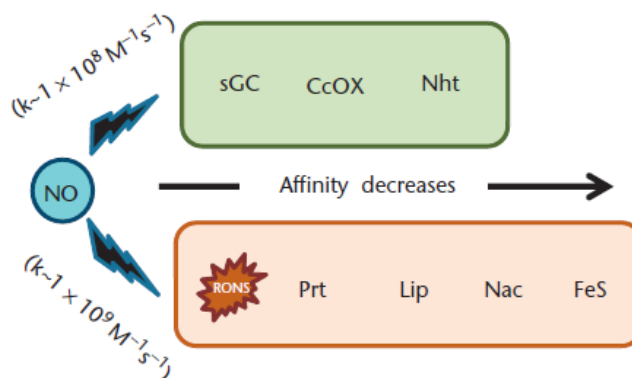
Fig. 5: Cell targets of NO and RONS. The affinity of NO for the targets decreases from left to right. sGC, soluble guanylate cyclase; CcOX, cytochrome c oxidase; Nht, nonheme targets; RONS, reactive oxygen and nitrogen species; Prt, proteins; Lip, lipids; Nac, nucleic acids and FeS centres (*from Sarti P., 2013*).

NO reacts rapidly and with high affinity to ferrous iron (Fe^{2+}) of haemproteins such as guanylate cyclase, haemoglobin, myoglobin and cytochrome c oxidase. The reaction is:

$$NO + Fe^{2+} \leftrightarrow Fe^{2+}\text{-}NO$$
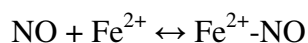
The binding of NO to the ferrous iron (Fe^{2+}) occurs with a mechanism similar only overall to that of CO and O_2; interestingly, the kinetic binding constant is very similar to that O_2 binding (k' ~ 10^7- 10^8 M^{-1} s^{-1}), and faster than CO binding

20

to the ferrous iron ($k' \sim 10^4 \, M^{-1} \, s^{-1}$). In order to carry out its physiological action, NO has to bind efficiently to the target enzyme but also to leave it rapidly. *In vivo* the dissociation of NO from the ferrous haem iron of both guanylate cyclase and cytochrome oxidase is very rapid, with rate constant values $k' = 0,05 \, s^{-1}$ [115] and $k' = 1,2 \times 10^{-2} \, s^{-1}$ [116], respectively.

Many of the physiological functions of NO in the cardiovascular, neuronal, gastrointestinal and other systems are mediated by the binding to the ferrous haem iron of soluble guanylyl cyclase (sGC) [41]. Among targets, indeed sGC presents the highest affinity for NO, with a Kd in the sub-μM range [117]; following binding to NO, a 200 fold increases activity of sGC occurs [118] while the reaction of NO with other haemproteins, such as cytochrome oxidase [51] and aconitase [119] induces their inhibition.

NO can also bind to the porfirinic Fe(III) of meta-haemoglobin; in this reaction an electron is transferred from NO to the ferric iron forming Fe (II) NO^+. The reaction is:

$$NO + Fe^{3+} \leftrightarrow Fe^{3+}\text{-}NO \leftrightarrow Fe^{2+}\text{-}NO^+$$
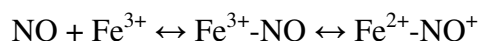
Differently from the bent Fe^{2+}-NO geometry, a linear geometry of the Fe^{3+}-NO bond is favoured [120]. NO binds less tightly to ferric, compared to ferrous iron and the NO dissociation from the Fe^{3+}-NO complex is much faster than for the respective Fe^{2+}-NO complex. It is worth noticing that some Fe^{3+}-NO complexes are quite stable (e.g. catalase, horse radish peroxidase, cytochrome c peroxidase), whereas others (e.g. metmyoglobin, methaemoglobin, cytochrome c) react further [119].

1.2.2.1 NO, haemoglobin and myoglobin

The reaction of NO with oxygenated myoglobin is rapid (k= 5×10^7 M^{-1} s^{-1}) and results in the formation of nitrate and Met-Mb. The reaction is:

$$Mb (Fe^{2+})O_2 + NO \rightarrow Mb (Fe^{3+}) + NO_3$$
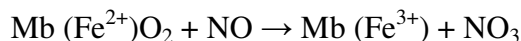
A physiological role for this reaction was first proposed by Brunori, who hypothesized that the oxygenated myoglobin has high capacities of NO scavenging and may, therefore, protect tissues from NO-mediated inhibition of mitochondrial respiration, if necessary [121].

In addition deoxygenated myoglobin possess a nitrite reductase activity. The reaction is:

$$NO_2^- + deoxyMb (Fe^{2+}) + H^+ \rightarrow NO + metMb (Fe^{3+}) + OH^-$$
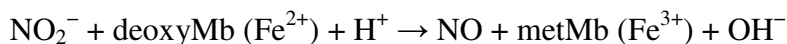
This is a slow reaction (k = 12 $M^{-1}s^{-1}$ at pH = 7.4, T = 37°C) generating metMb and NO, thus participating in nitrite recycling.

1.2.2.2 The S-nitroso compounds (R-SNO)

NO may reacts with thiols producing S-nitrosothiols (R-SNO).
The reaction is:

$$R-SH + NO \leftrightarrow R-SNO$$

S-nitrosothiols are nitro-thio-esters with the general structure R-S-N=O; naturally occurring examples include S-nitrosocysteine, S-nitrosoglutathione and S-nitrosoalbumin, in which R is an amino acid, a polypeptide and a protein, respectively. The R-SNO concentration in blood is 5-7 μM but probably this value is overestimated [122]. R-SNO play an important role in plasma and in

circulating erythrocytes, where they are believed to act as a buffer and transport systems for NO, involved in the regulation of vascular tone and blood flow [123].

1.2.2.3 The nitrotyrosine

Protein bound L-tyrosines are prone to be attacked by reactive nitrogen intermediates to form 3-nitrotyrosine (3-NT), leading to a post-translational modification. Tyrosine is modified in the 3-position of the phenolic ring through the addition of a nitro group (NO_2) [124]. $ONOO^-$ is the most widely RONS involved in protein nitration [125]; the formation of nitrotyrosine has been detected in various pathological conditions including atherosclerosis, myocardial infarction, myocarditis, heart failure, shock, diabetic complication and neurodegenerative and inflammatory disorders [126-128].

1.2.3   NO and mitochondrial respiration

About 25 years ago, it was discovered that nitric oxide inhibits mitochondrial respiration by reacting with respiratory chain complexes, particularly with Complex I and IV [50, 51, 129-131]. The reaction of NO with Complex III has been also described, but it is sluggish [132]. The reaction of NO with Complex I and Complex IV has been studied in detail and, presently, appears to be the most promising to elucidate the bioenergetic relevance of the mitochondrial nitrosative stress to cell pathophysiology. Depending on a variety of parameters, it is now evident that the reaction of NO with mitochondrial respiratory complexes causes *positive* or *negative* effects. The first ones elucidated were the inhibitory *negative* effects, though later on also signaling-like *positive* effects were found. The predominance of *positive* or *negative* effects is, indeed, different and testifies the

existence of different reaction mechanisms, whose predominance directly depends on the actual concentration and persistence in the mitochondrial environment of NO. The cellular concentration of NO depends, first of all, on NOS activity, controlled by different stimuli and effectors; relevant to its bioavailability, however, NO is also produced by recycling cell's and body's nitrite.

The functional implication of the reactivity of NO at the level of the respiratory chain is different owing not only to the protein complex targeted (Complex I and/or complex IV), but also and particularly dealing with complex IV to the reaction mechanism undergoing. Both Complex I and IV are inhibited by NO, though in a well different way: inhibition of complex IV is rapid (milliseconds) and reversible, occurring at nanomolar NO concentrations, whereas inhibition of complex I occurs after a prolonged exposure to higher NO concentrations and is persistent. The inhibition of Complex I involves the reversible S-nitrosation of a key cysteine residue on the ND3 subunit. The reaction of NO with cytochrome c oxidase (CcOX) directly involves the active site of the enzyme: two mechanisms have been described leading to formation of either a relatively stable nitrosyl-derivative (CcOX-NO) or a more labile nitrite-derivative (CcOX-NO$_2^-$) [8, 116]. Following NO inhibition of respiration, the O$_2$ consumption and thereby the OXPHOS dependent synthesis of ATP may decrease while glycolysis takes place [133].

1.2.3.1 NO and Complex I

At (high) μM concentrations, as typically in the presence of activated iNOS, NO inhibits complex I via the S-nitrosation of critical thiol residues [131]. Inhibition of complex I can be reverted by destabilizing the S-nitrosothiols. This is achieved with thiol-reducing agents such as dithiothreitol *in vitro*, or ascorbate and GSH in

24

cells and *in vitro* as well as *in vivo* [134]. The S-nitrosation of Complex I crucially depends on the structural conformation of the complex, which in turn depends on the availability of O_2 and mitochondrial NADH [135]. Complex I can assume an active (A) form and a so-called *dormant* (D) or de-activated form [136]. The cysteine residues exposed at the surface of the enzyme are different in the A and D conformation [137]. The A-form exposes several (up to 10 - 15) cysteine residues, whose S-nitrosation or derivatization with thiol-blocking agents, such as N-ethyl maleimide (NEM), is almost ineffective [138]. Once in the D-state, the enzyme exposes on the surface of the mitochondrially-encoded ND3 subunit the residue cys 39 whose blockage fully inhibits the enzyme [137]. Thus the A to D conformational change of Complex I, provides a feasible mechanistic interpretation of its inactivation by NO observed in turnover and under conditions favoring nitrosative stress. Complex I upon reacting with NO may trigger cell physiological or pathological events [131, 139, 140]. Complex I inhibition has been observed particularly during sepsi [141]; it has been also reported to play a role in the progression of neurodegenerative diseases (such as Alzheimer disease (AD), Parkinson disease (PD) and amyotrophic lateral sclerosis (ALS)) (see [140] for review).

1.2.3.2 NO and Complex IV

Nitric oxide, at low (nM) concentrations, reacts very rapidly with complex IV (CcOX), producing important physiological and pathological effects at mitochondrial level [130]. This reaction has been studied at all integration levels ranging from the isolated enzyme, to mitochondria, cells and tissues [31, 51, 82, 129, 130, 142-149]. The reaction of NO with CcOX involves the catalytic metals in the active site of the enzyme, i.e. the Fe and Cu ions of the haem a_3-Cu_B site

[53, 150]. It can occur through two alternative reaction pathways (PWs), named PW1 and PW2 [8, 151]. PW1 leads to a CcOX-mediated NO oxidation to nitrite, whereas PW2 is responsible for formation of the more persistently inhibited, Fe^{2+}–NO, nitrosyl CcOX [116]. One pathway can prevails over the other depending on NO, cyt c^{2+} and O_2 concentrations (Fig. 6). Interestingly, PW2 proved to occur only in the presence of higher concentrations of reduced cytochrome c ([151] and ref. therein cited) and/or during hypoxia [152], whereas under standard condition the formation of the nitrite derivative has been demonstrated to take place.
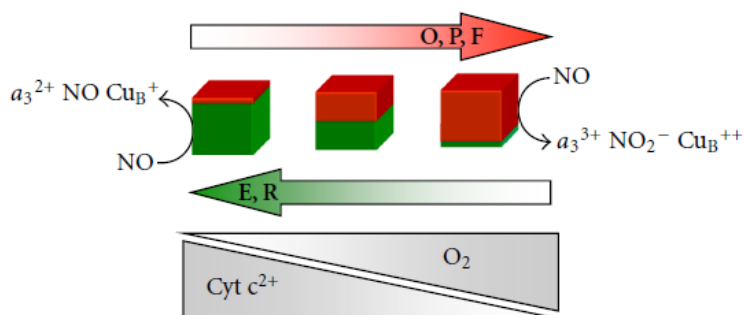
Fig. 6: Two alternative reaction pathways for the interaction of NO with CcOX (*from Sarti P., 2013*).

Despite small or even no changes in the mitochondrial respiratory efficiency caused by PW1, the persistence of NO in the environment may induce a transient (physiological) shift to glycolysis (PW1) or a more severe (cell dangerous) inhibition of the respiratory chain (PW2) [8]

- The 'nitrite' pathway (PW1)

NO reacts with the fully oxidized **O** binuclear site of CcOX [153] [154] or with the same site in the oxi-catalytic intermediates (**P** and **F**) generated during reaction of the enzyme with O_2 [155, 156], to form nitrite (NO_2^-). During the reaction with the oxidized Cu_B ($k = 2 \: x \: 10^5 \: M^{-1} \: s^{-1}$ at 20 °C), NO is transiently oxidized to nitrosonium ion (NO^+), that in turn is subsequently hydroxylated (or hydrated) to nitrite (or nitrous acid). Thus, after the reaction, the enzyme displays nitrite bound to ferric heme a_3 and is inhibited. The affinity of nitrite for the reduced heme a_3, however, is much lower than the affinity for the oxidized active site. The intramolecular electron transfer to heme a_3-Cu_B, therefore, causes the prompt dissociation of nitrite and the subsequent full restoration of activity [156, 157]. Relevant to possible patho-physiological effects of CcOX inhibition by NO, it is worth to notice that the nitrite dissociation upon reduction of heme a_3 (~ $6 \: x \: 10^{-2} \: s^{-1}$ at pH = 7.3, T = 20°C) is faster than the NO dissociation from the nitrosylated site [156, 158, 159]. A recent evidence was provided in favor of a nitrite reductase activity of CcOX [160-162]. Torres et al. [155] and Giuffrè et al. [156] established that a fairly rapid reaction of NO also occurs with intermediates **P** and **F** of CcOX. With these intermediates the NO reaction is slower than with the **O** species ($k \sim 10^4 \: M^{-1} \: s^{-1}$ *vs* $k = 2 \: x \: 10^5 \: M^{-1} \: s^{-1}$ at 20°C), still leading to nitrite-inhibited CcOX.

- The 'nitrosyl' pathway (PW2)

NO binds to the fully reduced (**R**) binuclear site of CcOX very rapidly at a rate similar to that of O_2 ($k = 0.4 - 1 \: x \: 10^8 \: M^{-1} \: s^{-1}$) [163, 164]; the high affinity Fe^{2+} nitrosyl adduct ($a_3^{2+}NOCu_B^+$) is formed [165, 166]. The dissociation reaction is relatively slow ($k_{off} = 3.9 \: x \: 10^{-3} \: s^{-1}$ at 20 °C) and photosensitive [116]. The fully

reduced (**R**) binuclear site commonly reacts with O_2, thus the inhibition of CcOX *via* formation of a nitrosyl R-adduct is expected to occur in competition with O_2. Under these conditions, the inhibition reverts upon exposing the inhibited enzyme to O_2; indeed, the rate of activity recovery matches that one of NO dissociation from reduced heme a_3. The reversal of inhibition has been proposed to involve formation of superoxide (O_2^-) produced by reaction of O_2 with reduced Cu_B reacting, in turn, with the NO molecule bound to heme a_3, to yield peroxynitrite ($ONOO^-$) [159]. According to this hypothesis, the peroxynitrite formed at the active site would be rapidly reduced to nitrite, and eventually released as such in the bulk. Although intriguing, a more recent study disproved this mechanism, showing that recovery of CcOX activity more simply results from O_2-mediated displacement of NO bound to reduced heme a_3 [167]. NO has been suggested to combine also with the single-electron reduced (**E**) site, in which the electron resides either on heme a_3 or on Cu_B [166, 168].

1.2.3.3 Mitochondrial respiration, NO and bioenergetic implications

Different studies using isolated mitochondria [142, 169] and intact cells [56] have shown that inhibition of respiration by NO induces the immediate collapse of mitochondrial membrane potential, inhibition of mitochondrial ATP synthesis and depletion of ATP. Experiments carried out with exogenous NO donors showed that the reversible inhibition of respiration induced by NO was confined to CcOX [170]. As already mentioned, however, after prolonged exposure to NO, the respiratory chain inhibition becames persistent and is mainly localized at Complex I. Inhibition of CcOX by NO enhances the formation of superoxide anions and subsequent generation of hydrogen peroxide that can induce the stabilization of HIF-1α [171]. This could explain, at least in part, the increased stability of HIF-1α

that is observed during treatment with NO. The increase in superoxide-anion generation by the electron-transport chain in the presence of NO might also explain the local formation of peroxynitrite observed under some circumstances and hence its pathophysiological relevance [125, 172, 173]. Almeida and co-authors compared the responses of rat cortical astrocytes and neurons to nitric oxide mitochondrial inhibition [56]. Neurons and astrocytes are two cell types that differ greatly in their ability to invoke anaerobic glycolysis under stress. In both cell types, inhibition of respiration by NO decreased the ATP concentrations by ~ 25 %, and within 10 minutes. This resulted in the stimulation of anaerobic glycolysis in astrocytes, but not in neurons. Astrocytes responded to inhibition of respiration by increasing their glycolytic metabolism, and by using glycolytically-generated ATP to maintain their mitochondrial membrane potential. Lymphoid T cells, which, like astrocytes, are highly glycolytic, were previously reported to exhibit a similar response to NO [174]. These cells were protected against apoptosis that is induced by the protein-kinase inhibitor staurosporin. By contrast, in neurons, ATP concentrations and the membrane potential continued to decrease and the cells showed signs of early apoptotic cell death. Further studies into this differential response led to the observation that, following inhibition of respiration, astrocytes undergo a rapid, cGMP-independent increase in the activity of 6-phosphofructo-1-kinase (PFK1), a master regulator of glycolysis [175]. The rate of activity of this enzyme in astrocytes was found to be twice of the neuronal one, under basal conditions. The concentration of fructose-2,6-bisphosphate (F2,6P2), the powerful allosteric activator of PFK1, was also significantly greater in astrocytes than in neurons and, following inhibition of respiration, the concentration increased further in astrocytes but did not change in neurons. The increased glycolytic rate in astrocytes served to preserve cells from ATP depletion

29

and cell death, possibly because glycolytic ATP served to drive the reverse activity of ATP synthase in order to maintain the mitochondrial membrane potential [56]. All together, these set of correlations suggest that the inhibition of mitochondrial respiration by NO would up-regulate the glycolytic flux in astrocytes to prevent the depletion of ATP. In contrast, cortical neurons showed that the glutamate-receptor activation, leading to NO release, causes a loss of mitochondrial membrane potential [176]. In addition to that, the enhancement of mitochondrial Ca^{2+} that follows glutamate receptor activation [177, 178] reinforces mitochondrial membrane potential loss, causing MPTP opening. MPTP opening promotes the exchange of solutes and small proteins between the mitochondrial matrix and the cytosol [179]. These events all coexist and lead to mitochondrial swelling, rupture of the outer mitochondrial membrane, and release of pro-apoptotic factors such as cytochrome c [179]. It is worth recalling also that the prolonged exposure of cells to NO and/or to peroxynitrite might induce the depletion of the intracellular reduced glutathione, thus rendering mitochondria more vulnerable to the deleterious effects of RONS. Furthermore, it has been shown that the generation of intracellular NO during exposure of neurons to glutamate results in a progressive depletion of NADPH, contributing to the decrease of the reduced/oxidized glutathione ratio. In addition, the activity of cytoplasmic enzymes, such as glutathione reductase and glyceraldehyde-3-phosphate dehydrogenase is, like complex I, inhibited by NO in a manner that indicates the occurrence of S-nitrosylation [174]. The action of endogenous NO on mitochondrial respiration provides the clue to understand both the physiological bioenergetic regulation and the activation of cellular response to energy failure; indeed, under some extreme circumstances, such as ischemia,

hypoxia or altered composition of the respiratory chain, the reaction of Complex IV with NO may become pathological.

1.3 Melatonin

Melatonin (Fig. 7), the N-acetyl-5-methoxytryptamine, is an hormone, secreted mainly by the pineal gland, but also produced in many other sites such as retina, skin, gut, and bone marrow cells, although the physiological implication of the extrapineal synthesis is only beginning to be revealed [180, 181].
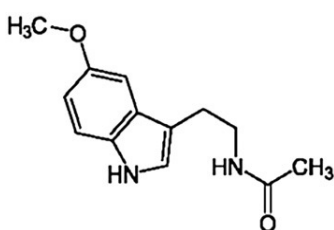
Fig. 7: Chemical structure of melatonin (*from Ambriz-Tututi et. Al, 2009*).

Melatonin was discovered in 1956 by the American dermatologist Aaron Lerner and his co-authors as an amphibian skin-lighting factor present in extracts of bovine pineal glands [182]. Subsequently, melatonin was reported to be present in a wide spectrum of organisms, including bacteria, fungi, plants, protozoa, invertebrates and vertebrates, including man [183-185]. The fact that melatonin is evolutionarily highly conserved molecule suggest for this molecule an important physiological role(s). In humans, melatonin secretion by the pineal gland is synchronized to the light ∕ dark cycle, with a nocturnal maximum (in young

subjects, $\approx$ 200 pg x mL^{-1} plasma corresponding to ~ 1 nM) and low diurnal baseline levels ($\approx$ 10 pg x mL^{-1} plasma corresponding to ~ 50 pM) [186, 187].

1.3.1 Biosynthesis and catabolism

The enzymatic machinery for the biosynthesis of melatonin in the pineal gland pinealocytes was first identified by Axelrod (Fig. 8) [188]. Melatonin is synthesized from a dietary amino acid precursor, L-tryptophan, through the action of four enzyme: tryptophan hydroxylase (TPH), aromatic aminoacid decarboxylase (AADC), arylalkylamine N-acetyltransferase (AA-NAT) and hydroxyindole-O-methyltransferase (HIOMT). The rate of melatonin formation depends on the activity of the two enzymes AA-NAT [189, 190] and, to a lesser extent TPH, which controls the availability of serotonin [191, 192]. In mammals, the regulation of pineal melatonin biosynthesis is mediated by the retinohypothalamic tract, whose signal activates the suprachiasmatic nucleus (SCN) [193]. Postganglionic sympathetic fibers reach the pineal gland and regulate melatonin biosynthesis through the presynaptic release of norepinephrine (NE) [194]. NE, by binding to β-adrenergic receptors on the pinealocytes, activates adenylate cyclase via the α-subunit of G(s) protein. The increase in cAMP promotes the synthesis of proteins, among them the melatonin-synthesizing enzymes, and in particular the rate-limiting AA-NAT [195]. The nocturnal exposure to bright light suppresses melatonin production immediately by degradation of pineal AA-NAT (Fig. 8b) [196]. Pineal melatonin production occurs during the dark phase and is acutely suppressed by light and in addition melatonin is quickly cleared from the circulation following the cessation of its production, therefore, for both reasons, plasma melatonin exhibits a circadian

rhythm: highest levels occurs at night, and lowest levels during the day, attaining peak plasma concentrations between 02:00 and 04:00 h [197] (Fig. 8c).
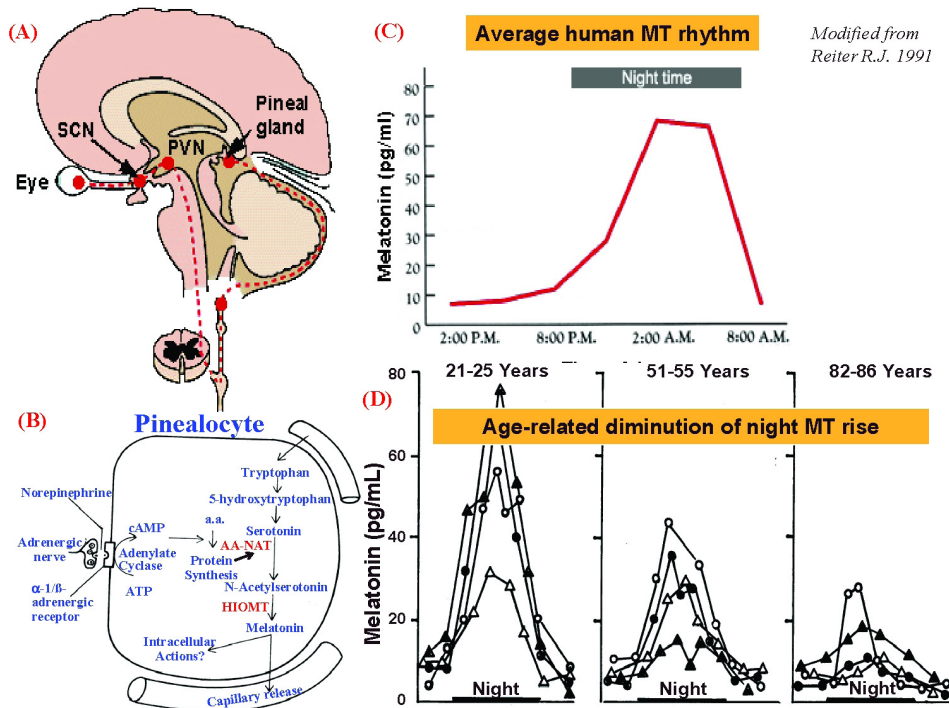
Fig. 8: a) Pineal gland. b) Melatonin biosynthesis by pinealocyte. c) Averege human melatonin rhythm. D) Age-related diminution of night melatonin rise (*modified from Reiter, 1991*).

The onset of secretion is usually at ~ 21.00 to 22.00 h and the offset at 07.00 to 09.00 h in adults, leaving in temperate zones [197, 198]. Due to its lipophylic nature, melatonin readily crosses the blood–brain barrier. Once synthesized, the majority of melatonin diffuses directly towards the cerebrospinal fluid of the brain's third ventricle, while another fraction is released into the blood stream,

whereby it is distributed to all tissues [180, 199]. Melatonin released to the cerebrospinal fluid is ~ 20–30 times higher than that released into the blood. More than 90% of circulating melatonin is degraded by the liver; in the hepatocyte is first hydroxylated in the C6 position by cytochrome P_{450} mono-oxygenases (isoenzymes CYP1A2, CYP1A1 and, to a lesser extent, CYP1B1) being, thereafter, conjugated with sulfate, to a lesser extent with glucuronic acid, to be excreted as 6-sulfatoxymelatonin (aMT6S) in urine [180].
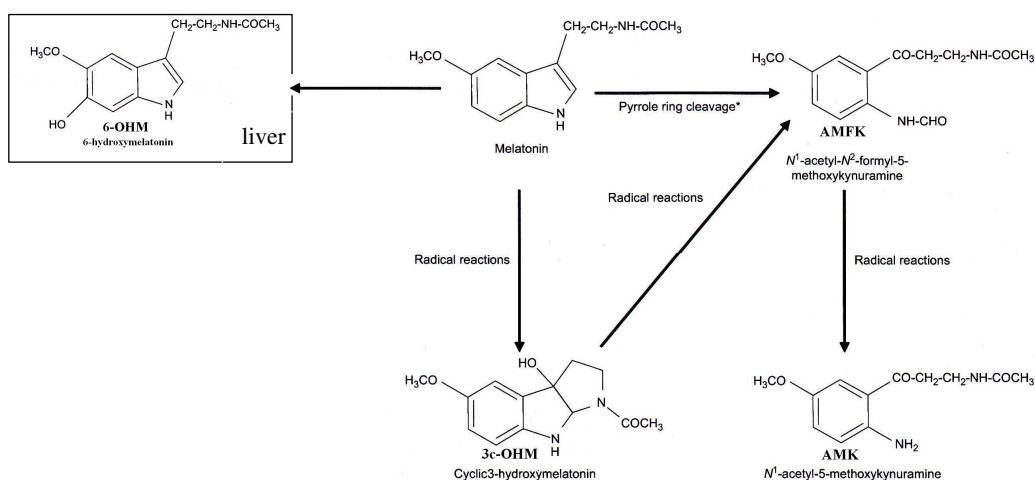
Fig. 9: The metabolism and the antioxidant cascade of melatonin. Circulating melatonin is metabolized to 6-sulfatoxymelatonin (6-OHM) in the liver. In the brain, melatonin is metabolized to N1-acetyl-N2-formyl-5-methoxykynuramine (AFMK) through the pyrrol-ring cleavage. When melatonin interacts with RONS it generates cyclic 3-hydroxymelatonin (c3-OHM). The c3-OHM acts likewise a scavenger, leading to the formation of AFMK. AFMK interacts with RONS to form N1-acetyl-5-methoxykynuramine (AMK); this latter molecule is a radical scavenger as well. This cascade of reactions greatly enhances the effective functional concentration of melatonin and its scavenging efficacy (*modified from Reiter et al., 2009*).

The metabolism of melatonin is rapid, and its half-life in humans following exogenous administration is short, ranging between 10 and 60 min [200] (Fig. 9). In the brain, a substantial fraction of melatonin is degraded via oxidative pyrrole-ring cleavage and is metabolized to N1-acetyl-N2-formyl-5-methoxykynuramine (AFMK) [201]. Melatonin can be also metabolized non-enzymatically in the cells, but also extracellularly, by mean of a free radical chemistry and a few other oxidants. Melatonin is converted into cyclic 3-hydroxymelatonin (c3-OHM) by directly scavenging two hydroxyl radicals. The c3-OHM itself is an effective radical scavenger and generates AFMK. AFMK is not the terminal molecule in melatonin's antioxidative cascade. Rosen and co-authors have documented that it interacts with RONS to form N1-acetyl-5-methoxykynuramine (AMK) [202]. This latter molecule is a radical scavenger as well. This is of interest as the antioxidant and anti-inflammatory properties of melatonin are shared by these metabolites, AFMK and, with considerably higher efficacy AMK [203, 204].

1.3.2 *Physiological role*

Melatonin is involved in various physiological functions [187, 201, 205, 206], such as sleep propensity [207], control of sleep ∕ wake rhythm [208], blood pressure regulation [209], energy metabolism [210], immune function [199, 211], circadian rhythm regulation [212], retinal functions [189], detoxification of free radicals [203, 204, 213], control of tumor growth [214], bone protection [215] and the regulation of bicarbonate secretion in the gastrointestinal tract [216]. Melatonin was initially studied for its role in endocrine physiology regulating circadian and, sometimes, seasonal rhythms [217]. It acts as a photoperiod messenger molecule, transducing photoperiod changes to reproductive organs, and

plays a vital role in the seasonal control of reproduction in certain animals. Melatonin participates in reproductive function by acting at hypothalamic, pituitary and gonadal levels [218, 219]. Melatonin may have a significant role in the onset of human puberty [220]. Melatonin can be used as a chronobiotic that is capable of normalizing the disturbed bodily rhythms, including sleep–wake rhythms [201, 221, 222]. In fact, melatonin is used for preventing jetlag or as adjuvant in elderly people with sleep-problems [205]. The direct effects in region containing high density of melatonin receptors, such as the circadian pacemaker, the suprachiasmatic nucleus (SNC), or the pars tuberalis (PT) strongly supported the original hypothesis of its physiological role. In the perception by many investigators, the control of circadian and seasonal rhythmicities represents melatonin's main physiological function. Although this view is not generally disputed, during more recent decades, melatonin has been shown to possess a number of additional functions and to act in tissues or cells that express melatonin receptors at much lower level [187, 201, 206, 223]. Several evidence has been accumulated showing that melatonin influences the function of a variety of tissues not related to the endocrine system [217] and display an exceptional multiplicity of actions. The presence of melatonin in the gastrointestinal tract suggests that it has a protective role in this organ system [224]. Melatonin has significant bone-protecting properties [225] and plays a role in energy expenditure and body mass regulation [226]. Melatonin has been demonstrated as an efficient antioxidant under both *in vivo* and *in vitro* conditions. Not only melatonin, but also the kynuric pathway of melatonin, provides a series of radical scavengers [204]. Melatonin up-regulates antioxidative enzymes. The complex pattern of protective actions of melatonin may turn out to be of major clinical significance, for example in retarding the progression of neurodegenerative diseases such as Alzheimer's or

Parkinson's disease [227-229]. Deficiencies in melatonin production or melatonin receptor expression, and decreases in melatonin levels (such as those which occur during aging) can be associated with a multitude of pathophysiological changes, which, again, reflect the pleiotropy of this molecule. Changes in the amplitude and phasing of the melatonin rhythm have been described in patients with major depressive, bipolar affective, mood and seasonal affective disorders. Melatonin reduces the systolic, diastolic and mean blood pressure of hypertensive patients [230, 231]. The antitumor effects of melatonin seem to be exerted at multiple levels, from modulation of the glutathione system to interference with lipid mediators and receptors of other hormones [232-235]. The immune-enhancing actions of melatonin, in conjunction with its antioxidant properties, suggest a therapeutic value in a variety of diseases, including bacterial and viral infections [199, 201]. In comparison with other signaling molecules, the numerous actions that have been attributed to melatonin are exceptional. This should be taken as an expression of its overall importance as a modulator at various levels of hierarchy. The practical applicability of melatonin, however, remains unconfirmed in fact most of the effects described have not been demonstrated at clinically relevant concentrations. Moreover, a pleiotropic agent may have side-effects, which, to date, have still not been investigated in detail.

1.3.3 On the cell stage

Melatonin interacts with cells in a receptor-dependent or -independent manner (Fig. 10). The receptor-mediated melatonin signaling involves different types of cell surface and nuclear receptors, expressed to a different extent by cell-lines and tissues. Several major actions of melatonin are mediated by the membrane

receptors MT1 (Mel 1a) and MT2 (Mel 1b) [205, 223]. They belong to the superfamily of G-protein coupled receptors containing the typical seven transmembrane domains. The human MT2 receptor has a lower affinity (K_d = 160 pmol/l) for ^{125}I-melatonin as compared to the human MT1 receptor (K_d = 20–40 pmol/l); both are, therefore, of a fairly high affinity and the agonist binding is guanosine triphosphate (GTP)-sensitive [223]. Activating G protein signaling, specifically Gi/Go, the receptors mediate a wide variety of effects; among others, inhibition of the adenylate cyclase (AC), with a consequent cyclic AMP (cAMP) decrease, regulation of gene transcription, activation of protein kinase C subtypes and changes of intracellular Ca^{2+} levels [205]. MT1 and MT2 receptors are expressed both singly and together in various tissues of the body [223]; also their mRNA levels vary on a circadian basis, with expression levels affected by light and melatonin concentration in plasma. Besides membrane receptor signaling, melatonin has been extensively proposed to freely cross the cell membrane [236], to reach and interact with subcellular components, such as nucleus [237] and mitochondria [210]. This suggests the potential for melatonin to widely interact with low affinity intracellular enzymes, transporters, cytoskeletal proteins, and nuclear receptors, which can generate further signals independently or by secondary interaction with components of receptor-dependent pathways. The enzyme quinone reductase 2 is a classic example of these protein targets that was originally identified as a third melatonin receptor (MT3) with possible regulatory functions on cellular redox status [238]. However, the biochemical characteristics and physiological role of this low-affinity binding protein remain poorly understood [239]. Melatonin binds nuclear (orphan) receptors of the family of RORs and RZRs (RZR/RORa) regulating the expression of several enzymes. Members of these families have been suggested to play a role in the

immunostimulatory effect of melatonin in B and T lymphocytes, by sustaining its potential to inhibit Fas ligand-mediated apoptosis and cytokine production [240]. RORα inactivation by melatonin has been proposed to follow its interaction with calmodulin, an upstream component of melatonin signaling, and it is ultimately responsible for the control of transcription factor NF-kB-dependent genes including, among others, inflammatory mediators and antioxidant enzymes [241].
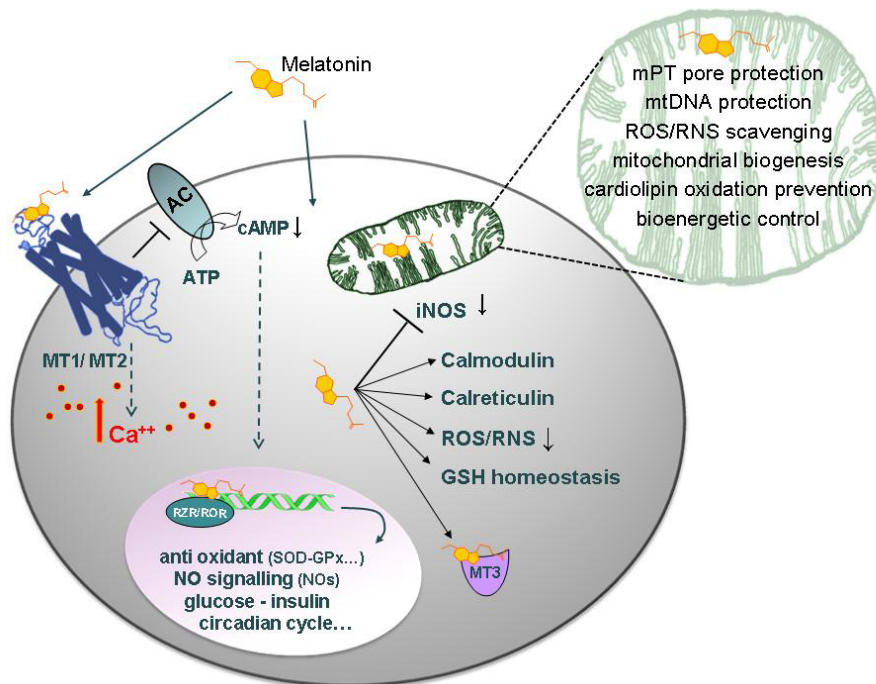
Fig. 10: Melatonin on the cell stage (*from Sarti P., 2013*).

Binding nuclear receptor melatonin also down-regulate pro-oxidant enzymes, such as the NOSs, particularly the iNOS [242]. Although antioxidative protection by melatonin is partially based on receptor mechanisms, Tan and co-workers

reported in 1993 [243, 244] that melatonin functioned as a direct free radical scavenger, an action that is receptor-independent. Melatonin has the capability of donating electrons *in vitro* to reduce the reactivity of molecules with an unimpaired electron in their valance orbital, i.e. free radicals.

The antioxidant properties of melatonin have been world-widely recognized, likely accounting for a number of protective effects exerted in different cellular compartments [204]. Melatonin is more effective than the majority of its naturally occurring molecular analogs [244, 245], suggesting that the substituents of the central indole structure controls the reactivity of the adducts. Rate constants determined for the reaction of melatonin with hydroxyl radicals are very high, almost diffusion limited, approaching $k \approx 10^{10}$ M^{-1} s^{-1} [246, 247]. Receptor-independent activities of intracellular melatonin can be also sustained by low-affinity interactions with specific targets of cell signaling. These include calcium binding proteins, cytoskeletal and scaffold proteins, other signaling proteins in the cytosol and in some organelles, and, in particular, components of mitochondrial signaling. Among the intracellular targets of melatonin, the Ca^{2+}-calmodulin (CaCaM) complex plays a major role in both receptor-dependent and -independent functions [248, 249]. The mitochondrion is proposed to play a key role in cell signaling and in the transcriptional and post-translational events induced by melatonin, which integrate with the signaling activity of the cell during normal or stress-related conditions.

1.3.4   The mitochondrial connection

The discovery that mitochondria are a target for melatonin opened a new prospective to understand the mechanism of action of this indoleamine. It is

generally agreed that melatonin has a role in the mitochondrial metabolic homeostasis [250-253]. Melatonin may be a critical molecule that preserves mitochondrial integrity and physiology [252]. Melatonin is accumulated in the mitochondrion in a concentration dependent manner [254, 255] where it interferes with mitochondrial bioenergetics. The highest intracellular melatonin concentration are found in mitochondria (~ 100–200 times more than in the cytosol) [256]. It has been proposed that melatonin can: (i) protect cells against mitochondrial oxidative stress and apoptosis through its antioxidant and RONS scavenging properties; (ii) accelerate the electron flow through the mitochondrial respiratory chain, thus increasing the efficiency of ATP production [257, 258]; (iii) stabilize and optimize the membrane potential across the inner mitochondrial membrane by regulating the mitochondrial permeability transition pore (MPTP) [259-261]. The molecular mechanism(s) underlying the functional effects of melatonin, particularly those related to cell bioenergetics, and therefore of putative patho-physiological relevance, remain as yet only partly understood.

1.3.4.1 Melatonin and mitochondrial oxidative stress

Melatonin has been repeatedly shown to reduce the mitochondrial formation of RONS thus protecting eTC proteins and mitochondrial membranes against oxidative, nitrosative or nitrative damage [252-254, 262, 263]. Melatonin reacts at a high rate with radicals like $OH^{\cdot}$ and relatively, more slowly with the O_2^{-}. Melatonin is not only a potent scavenger of hydroxyl radicals, but also of NO, $ONOO^{-}$ and carbonate radicals [203, 264]. Many studies demonstrate the protective effect of melatonin and its derivatives on lipid peroxidation induced by oxidative stress in mitochondrial membranes [265]. It is presumed that melatonin achieves this high degree of lipid protection by interfering with the radicals that

41

initiate this process, especially the OH˙ and ONOO⁻, and by positioning itself among the membrane lipids in such a way as to impede the oxidation of the polyunsaturated fatty acids [266]. Melatonin was reported to protect the mitochondria from oxidative damage in part by preventing cardiolipin oxidation [210, 261]. Alterations in cardiolipin structure, content and acyl chain composition have been associated with mitochondrial dysfunction in various tissues under a variety of pathophysiological conditions [210, 262]. The antioxidant effect of melatonin could be also ascribed to its ability of down-regulating the free radical production *via* two different mechanisms [267]. The first one consists in the acceleration of the electron flow through the eTC, thus avoiding leakage from the chain responsible for formation of partially reduced oxygen species. The optimization of eTC is achieved by promoting the activity of complex I and complex IV, the main electron leakage sites of the chain [257, 268]. The second one involves the control of the mitochondrial membrane potential. An elevated mitochondrial membrane potential slows down the eTC and may result in an accumulation of reducing equivalents with electron leakage generating free radicals. A moderate down-regulation of the mitochondrial membrane potential significantly reduces free radical formation [269]. Melatonin improves the GSH redox cycling and increases GSH content by stimulating its synthesis in the cytoplasm. Under normal conditions, in fact, melatonin is able to stimulate the expression and activity of the two enzyme involved in the GSH-GSSG balance, i.e., glutathione peroxidase (GPx) and glutathione reductase (GRd) [256, 262, 270]. Up-regulation of antioxidant enzymes and down-regulation of pro-oxidant enzymes are other mechanisms that contribute to the protective effects of melatonin on mitochondria. Melatonin, for instance, enhances the activity of superoxide dismutase [271-273], catalase [274], glutathione

peroxidase and heme oxygenase1 [275]. Conversely, melatonin inhibits activities of some pro-oxidant enzymes including iNOS [242, 276, 277], the cyclo-oxidase 2 (COX2) and the myeloperoxidase [278, 279]. The effects of melatonin on these enzymes likely contribute to its protective effects against mitochondrial oxidative stress.

1.3.4.2 Melatonin and respiratory complex

The high redox potential of melatonin 0.94 V suggests that this indoleamine may be redox active interacting with the complexes of the eTC, thereby increasing electron flow. Martin and co-workers observed that pharmacological concentration of melatonin increases the activity of brain and liver mitochondrial respiratory complexes I and IV in a time-dependent manner, whereas no significant changes were detected at the level of Complex II and III [257]. The same authors extended this observation to sub-mitochondrial particles isolated from rats liver and brain: the organelles incubated with increasing quantities of melatonin, from $\sim 10^{-9}$ M up to $\sim 10^{-4}$ M showed, once again, an enhancement of Complex I and Complex IV activity [258]. Despite the clear experimental evidence, the molecular mechanism by which melatonin administered in the diet, injected i.p., or added to a suspension of isolated mitochondria would sustain the mitochondrial complexes activity is still obscure. Interestingly, and somewhat in contrast with these findings also a decrease of the O_2 consumption rate by rat liver mitochondria has been reported [280]. Other studies have described one possible mechanism by which melatonin increases the activity of complex IV; this protection action may be due, at least in part, to an effect on the expression of mtDNA encoded polypeptide subunits I, II and III of complex IV in mitochondria from rat liver in a time-dependent manner which correlates with the increase in

complex IV activity. These effects were also produced by AMK and this compound was more potent than melatonin itself [281].

1.3.4.3 Melatonin and mitochondrial membrane potential

Electrophysiological experiments demonstrate the antagonism of melatonin on the ionotropic glutamate receptor N-methyl-d-aspartate (NMDA receptor) [282, 283]. This effect is dose-dependent and, as a consequence of the treatment, the NMDA receptor channel pore remains closed, thereby preventing the opening of L-type calcium channels and calcium influx [284]. Further experiments demonstrate that melatonin is able to diminish the rises in cytosolic calcium induced by NMDA in cultured mouse striatal neurons [285]. Experiments carried out using rat brain astrocytes [286] and cultured PC12 cells [287] show that melatonin limits cytosolic calcium rises and, as a consequence, the concomitant production of free radicals. In these two reports, melatonin indirectly inhibited the opening of the MPTP and blocked MPTP dependent cytochrome c release, the downstream activation of caspase 3 and the cell death by apoptosis [286]. Melatonin strongly inhibits MPTP currents in a dose dependent manner with an IC50 of 0.8 μM [285]. Melatonin was repeatedly shown to prevent, at pharmacological concentrations, a fatal decline in mitochondrial membrane potential, in various cell types and with high efficacy against different noxes [285, 286, 288]. Recently it was hypothesized a dual effects of melatonin on the MPTP [263]. Under normal conditions, melatonin activates MPTP and mildly reduces the mitochondrial membrane potential [254]. Under oxidative stress conditions that damage MPTP function, melatonin significantly inhibits the MPTP and thus preserves the membrane potential to avoid mitochondrial collapse [259, 260, 289-291]. The dual functions of melatonin on MPTP establish the indoleamine as an excellent

molecule, which balances mitochondrial membrane potential and maintains the optimal function of mitochondria to generate ATP under both favorable and unfavorable conditions.

1.3.5   Melatonin and NOS

At least 20 years ago it has been proposed that melatonin down-regulates the NO synthase [276, 277, 292, 293]. Several experiments have documented the inhibiton of expression and activity of iNOS by melatonin [206, 276, 277, 294-298]. Whether the effects of melatonin on iNOS are direct or depend on its metabolites (AMK and AMFK) remain to be tested. In any case, the decrease of iNOS expression by melatonin leads to a significant reduction of NO levels and of its toxic effects, such as the $ONOO^-$ generation [299]. Much more work has been published on the downregulation of iNOS in models of inflammation and sepsis treated with pharmacological doses of melatonin [300]. In liver and lung of LPS-treated rats, melatonin antagonized iNOS as well as NO-dependent decrease in the activity of complex I and IV [299]. It was observed that melatonin administration had no effect on NOS activity and NO levels in mice lacking the iNOS gene, a finding suggesting that melatonin acts specifically on iNOS [295]. The effects of melatonin on eNOS expression and activity are unclear. It has been observed that melatonin prevents decrease of eNOS levels observed during cerebral ischemia, inducing, through its activation, vasodilation and vascular protection [301, 302]. Several experiments have shown that melatonin inhibits the activation of nNOS through inhibition of calcium–calmodulin complex (CaCaM), as well as through its binding and consequent closing of NMDA [249, 281, 296, 303]. Melatonin inhibits CaCaM in a receptor-dependent and independent manner. Melatonin can

directly bind CaCaM, avoiding the activation of the CaCaM dependent enzymes, including nNOS [248, 249]. The binding of melatonin with MT1/MT2 can regulate CaCaM activity through its phosphorilation or regulating the intracellular Ca^{2+} concentration. One of the melatonin metabolites, AMK also binds CaCaM and reduces nNOS activity in a dose dependent manner [249]. Interestingly, AMK induces an inhibition of nNOS higher than melatonin [281]. While several studies sustain that melatonin is an inhibitor on nNOS, recently Ortiz and co-worker observed that melatonin consistently inhibits the expression and activity of iNOS, which was related to its efficacy in preventing mitochondrial failure during sepsis but interestingly preserve the expression and activity of nNOS [298]. Overall, melatonin seems to maintain the levels of NO in a concentration range necessary to perform its physiological role while inhibiting the occurrence of high levels of NO (also to pathological concentration range). It is interesting that the C-terminal extremity of the MT1 receptor has been identified as containing a class III recognition motif for PDZ domains [304]. nNOS is another PDZ domain-containing protein that was previously described as a potential interacting candidate for the MT1 receptor [305]. In this work a novel role of melatonin exerted on the nNOS expression and activity has been unveiled and will be described in details.

1.3.6   *Melatonin: physiological versus pharmacological concentration*

It could be argued by the people in favor of the antioxidant melatonin function that the physiological concentration of melatonin, even at night, *in vivo* is too low to be a relevant antioxidant. As a matter of fact, the circulating melatonin concentrations at night peak are in the low nanomolar range. It is also often

assumed that melatonin levels in blood are reflective of its concentrations within tissues and cells, i.e. that the circulating melatonin concentrations is the result of an equilibrium within all body compartments. This assumption is true only in part, since it should be considered that other body fluids, e.g. ovarian follicular fluid [306], cerebrosprinal fluid [307], bile [308] contain much higher concentrations of melatonin than blood. Moreover, as knowledge in this field grows, it became apparent that a large number of tissues/cells have the capability of producing melatonin. High levels of melatonin have been identified in mitochondria, that require valid protection from free radicals and the associated stress. Recently, evidence has emerged to show that mitochondria may have the capacity to synthesize and metabolize melatonin [263]. With a few exceptions [254], the majority of the data have been collected under μM to mM melatonin concentration regimes, i.e. pharmacological-like concentrations, though using a wide variety of experimental systems, from cell organelles, to cultured cells up to in *vivo*. Under these conditions, melatonin has been reported to induce optimisation of cell bioenergetics homeostasis [257], due to its mitochondrial accumulation [254], with a direct action on the respiratory chain complexes, and prevention of oxidative mitochondrial DNA damage [251]. It remains to be determined whether the direct free radical scavenging activity is the exclusive mechanism, by which melatonin abates radical-mediated molecular destruction. It has been proposed, alternatively, that melatonin might act indirectly as stimulator of antioxidant enzymes [271-275] and inhibitor of pro-oxidant enzymes, such as NOS [206, 276, 277, 294-298]. Whatever the mechanism is, it is argued that melatonin markedly reduces excessive oxidative damage, under many experimental and clinical conditions where the molecular distruction occurs as a consequence of a high free radical-related disease or to aging [309-311]. Whether

this protection occurs at physiological melatonin concentration, or can only be achieved with pharmacological doses continues to be debated [203].

The experimental evidence suggests that the mitochondrial antioxidant melatonin activity is more evident at high concentration ($\geq$ µM), while its hormonal-like function can be detected at the lower ($\leq$ nM) concentrations.

1.4 Nitro-oxidative stress and neurodegeneration

1.4.1 Alzheimer's disease

Alzheimer's disease (AD) is among the principal debilitating conditions of the current century, affecting around 15 million people worldwide [312]. Most of the cases are sporadic whereas 5-10% are familiar and associated with mutations in gene of proteins involved in amyloid-β (Aβ) metabolism. This disorder is an age-related neurodegenerative disorder characterized by progressive cognitive decline, memory loss and neuropathological alterations. Accumulation of extracellular amyloid plaques mainly composed of Aβ peptides and deposition of intracellular neurofibrillary tangles (NFTs) built up of hyperphosphorilated tau are the main features of AD. Because of this, AD has been identified as a protein-misfolding disease (proteopathy) caused by abnormally folded Aβ and tau protein in the brain. Gross brain atrophy prominent in AD is caused by massive loss of neurons mostly in brain regions involved in learning and memory. Although the hallmark lesions of the disease were described by Alois Alzheimer already in 1906, the molecular mechanisms underlying the disorder are still unknow and an efficient therapy is still missing. Many lines of evidence suggest that oxidative stress is one of the earliest changes and plays an important role in the pathological process in

AD, and more recently, energy deficiency and mitochondrial dysfunction have been recognized as a prominent, early event in AD [312-317].

1.4.2 *Amyloid β*

Substantial genetic, animal modeling and biochemical data have emerged to suggest that Aβ plays a central role in AD [318, 319]. Aβ is a 4-KDa peptide derived from the β-amyloid precursor protein (APP) by the action of two aspartyl proteases referred to as β- and γ-secretases [320, 321]. APP is a trasmembrane polypeptide containing a single membrane-spanning domain, a large ectoplasmatic N-terminal region and a shorter cytoplasmatic C-terminal region. During and after the trafficking through the secretory pathway APP can undergo a variety of proteolytic cleavages to release secreted derivatives into vescicle lumens and extracellular space [322]. The α-secretase cleavage of APP releases the N-terminal ectodomain soluble APPα from the cell surface leaving an 83-amino-acid-long C-terminal membrane-bound fragment (C83). This fragment can be further processed by γ-secretase giving rise to the small peptide p3 and a C-terminal fragment called amyloid intracellular domain (AICD). In contrast, APP may be cut by β-secretase to produce a soluble version of APP (β-APP) and a 99-residues COOH-terminal fragment (C99) that remains membrane-bound. C99 is a substrates for γ-secretase activity, which cleaves in the middle of trasmembrane domain to produce the 4 KDa Aβ and AICD. Depending on the exact point of cleavage by γ-secretase, three principal forms of Aβ, comprising 38, 40 or 42 amino acid residues, respectively are produced. Aβ is a natural product and is present in the brains and cerebrospinal fluid (CSF) of normal humans throughout

life [321, 323]. The levels of Aβ in the CSF are known to fluctuate as part of daily sleep-wake cycles [324], strongly suggesting that a dynamic balance between Aβ production and clearance is a normal physiological event in the brain. Thus, the mere presence of Aβ does not cause neurodegeneration; rather neuronal injury appears to ensue as an abnormally accumulation of Aβ and a result of its self-association [325-327]. Aβ peptides are amphipathic molecules, containing a hydrophilic N-terminal stretch (residues 1-28) and a hydrophobic C-terminal domain (residues 29-40/42) [311]. In solution, Aβ display a substantially unfolded conformation. The misfolded Aβ usually contains stacks of β sheets organized in an arrangement known as a 'cross-β' structure. Because β-sheets can be stabilized by intermolecular interactions, Aβ have a high tendency to form oligomers, AβOs and spontaneously assemble into amyloid protofibrils and fibrils [328]. Emerging studies have shown a robust correlation between soluble, low molecular weight AβOs levels and the severity of cognitive impairment [329]. Aβ42 is far more prone to oligomerize and form amyloid fibrils than is the more abundantly produced Aβ40 peptide [330] and because of this the over-production of all Aβ, or an increased proportion of the 42 amino acid form, appears sufficient to cause early onset AD [331-334]. However, mechanism underlying Aβ-induced neurotoxicity remain to be fully elucidated. Growing evidence suggests that Aβ has deleterious effects on mitochondrial function and contributes to energy failure, neuronal apoptosis and production of RONS in AD brain [314].

1.4.3   Amyloid β and mitochondria

Extracellular soluble AβOs are believed to cause synaptic and cognitive dysfunction in AD [335, 336]; however, several evidences have indicated that intraneuronal accumulation of Aβ is an early event in AD [337, 338] and contributes to synaptic pathology [339-341]. In brains affected by AD, intraneuronal Aβ, predominantly in the form of Aβ42, has been found to accumulate within several organelles, including the endosomes/lysosomes [342], autophagosomes [343], and mitochondria [344-346]. Endoplasmic reticulum (ER) as well is likely a target of intracellular Aβ [347]. Intraorganelle accumulation of Aβ appears to damage these organelles and affects cell viability. Morphologic studies provide further evidence of the presence of Aβ in mitochondria [314, 345]. Confocal microscopy demonstrated that Aβ co-localized with HSP60, a marker of mitochondrial matrix. The origin of intramitochondrial Aβ is far from certain. It is assumed that mitochondrial Aβ is transported from other intracellular compartments [348-350]. This is due to cross-talk between cellular organelles [351], in particular between ER and mitochondria. The potential origin of mitochondrial Aβ, in fact, is possibly the ER and/or the endosomes/lysosomes [352]. It is logical to presume that Aβ might gain access into the mitochondrial matrix by an intracellular trafficking mechanism with involvement of a specific transport mechanism on the mitochondrial membrane [352]. Aβ can be imported into mitochondria via the TOM and TIM import machinery [312, 348, 353, 354]. However, Aβ has the ability by itself to permeabilize membranes. Recently, Rosales-Corral and co-worker found important evidence on Aβ-induced alterations in the lipid content of mitochondrial membranes, in part related possibly to a direct Aβ molecular interaction and in part related to Aβ-induced

oxidative stress [354]. The observation that both APP and γ-secretase components, including presenilin, nicastrin, Aph-1, and Pen-2, localize into mitochondria and that APP has a mitochondrial targeting signal sequence has gained attention [355, 356]. These observations indicate the possibilities that at least a portion of mitochondrial Aβ is generated in mitochondria and that Aβ may play a physiological, beneficial role for mitochondrial function. However, there is no evidence to confirm the physiological role of mitochondrial Aβ; instead, Aβ has been demonstrated to impair mitochondrial function [345, 346, 357-360]. A direct effect of Aβ on mitochondrial processes is further suggested by *in vitro* experiments in which cultured cells or isolated mitochondria were exposed to Aβ. In the micromolar concentration range, Aβ induced dose-dependent generation of ROS and ATP depletion associated with depolarization of the mitochondrial membrane, decreased oxygen consumption and inhibition of respiratory chain enzymes in PC12 cells [361]. A study by Tillement and co-worker showed that as low as 0.1 pM of Aβ42 decreased the mitochondrial respiratory coefficient in mitochondria isolated from rat forebrain, suggesting that Aβ impairs oxidative phosphorylation[362]. Moreira and co-worker demonstrated that 2 μM Aβ40 can exacerbate calcium-dependent formation of the MPTP, resulting in decreased mitochondrial membrane potential, decreased capacity to accumulate calcium, and uncoupling of respiration [363, 364]. Further study by Takuma and co-worker showed that neuronal culture from Tg mAPP/ABAD mice displays spontaneous generation of ROS, decreased ATP production, decreased CcOX activity, release of cytochrome c from mitochondria with subsequent induction of caspase-3-like activity followed by DNA fragmentation and loss of cell viability [365]. For APPOSK-transfected cells, Umeda and co-worker demonstrated that mitochondrial accumulation of AβOs caused altered mitochondrial membrane

potential and cytochrome c release from mitochondria [352]. According to Casley and co-worker, addition of Aβ to isolated rat brain mitochondria inhibited respiration and CcOX activity [366]. This is consistent with studies in neuroblastoma SHSY-5Y cells [367] and Tg2576 mice [346], both overexpressing APP. It was observed that also patients with AD showed impaired cytochrome c oxidase activity in the central nervous system. In 1990, Parker et al. reported about 50% reduction of CcOX activity in platelet mitochondria isolated from patients with AD [368]. Depressed CcOX activity has also been shown in homogenates of various brain regions, including frontal (−26%), temporal (−17%) and parietal (−16%) cortices as reported by Kish et al. [369]. Recently Bobba and co-worker observed that Aβ42 inhibits mitochondrial respiration and that this inhibition is accomplished by efficiently blocking the activity of respiratory Complexes I and IV [370]. This is maybe due to a direct interaction of Aβ with complexes IV and complex I, documented *in vitro* or to an increase in RONS production [370]. Several studies have demonstrated decreased pyruvate dehydrogenase (PDH) [371, 372] and α-ketoglutarate dehydrogenase (KGDH) activity [373] in the temporal and parietal cortex of AD brains. *In vitro* binding studies demonstrated that Aβ interact with the mitochondrial matrix protein, amyloid-beta-binding alcohol dehydrogenase (ABAD), leading to mitochondrial dysfunction [313]. Aβ interactions with cyclophilin D, a suggested subunit of the permeability transition pore, may also contribute to similar mitochondrial dysfunctions and exacerbate cell death [374]. Aβ influences the fission/fusion dynamic by altering the fission/fusion-related protein levels, increasing the expression of mitochondria fission genes and decreasing that of fusion genes. The increased fission gene expression prompted by Aβ alters mitochondrial morphology through fragmentation, resulting in a significantly increased number

of mitochondria [375, 376]. Intramitochondrial Aβ is able to perturb mitochondrial function in several ways by directly influencing extracellular transport chain complex activities, impairing mitochondrial dynamics, or disturbing calcium storage, thus increasing apoptotic pathways.

Despite all these observations, the presence of Aβ into the mitochondria is still debated and the mechanisms by which Aβ induces mitochondrial impairment are still unknown. An hypothesis is that Aβ may be caused mitochondrial dysfunction by the formation of pore-like structures in the mitochondrial membranes. Alternatively, Aβ may generate free radicals during aggregation and therefore cause oxidative damage to mitochondrial membranes and proteins. In this frame, it is worth considering that mitochondria are the leading sites for RONS production, and that nitric oxide, as part of them, has been proposed to play a major role in neurodegenerative disease, AD included.

1.4.4 Alzheimer's disease and NO

Numerous reports demonstrate that AD is characterized by a pathological rise of RONS concentrations [377]. Markers of lipid peroxidation, nucleic acid damage or protein modification were found to be upregulated in brains of AD patients (3-nitrotyrosine (3-NT) or protein carbonyls). Importantly, increased oxidative and nitrosative damage seems to be an early event in the process of neurodegeneration associated with AD [378-380]. One simple explanation of increased nitro-oxidative stress in AD is directly linked to Aβ toxicity. It is well known that the accumulation of Aβ in plaques as well as AβOs may produce sequential inflammatory/oxidative events and excitotoxicity, causing neurodegeneration and

cognitive impairment [311, 381, 382]. On one side, the potential of Aβ to generate free radicals has been observed by *in vitro* experiments, on the other side, however, other experimental models showed that the nitro-oxidative stress seems to precede the Aβ plaques formation [383]. There are also data showing that the oxidative stress can actually alter the metabolism of both the Aβ precursor protein and tau, thus promoting formation of plaques and tangles [384-386]. An apparent hallmark of AD is the decreased brain energy metabolism, attributed to mitochondrial dysfunction and the increased RONS production. Last but not least, inflammatory processes seem to be part of AD pathology. *In vitro* experiments have shown that Aβ can activate microglia [387]. Glia cells are present in the Aβ plaques and in their surroundings [354, 388]. Activation of microglia is associated with production of RONS and potentially leads to damage of the neighbouring neurons, further supporting the idea that NO may play a critical role in the pathogenesis of AD [354, 389]. Consistently, several studies have shown that the NOS expression is altered in AD and it has been suggested that the iNOS plays a role in the plaques and neurofibrillary tangles formation [390]. In this line, it has been shown that the NO overproduction, in fact, occurs much earlier than amyloid deposition. Luth and co-worker analyzed the expression of all NOS isoforms in AD and control brains; they also compared the NOS(s) localization with the distribution of nitrotyrosine [391]. In their study, nitrotyrosine was detected in AD neurons, astrocytes, and blood vessel. Aberrant expression of nNOS in cortical pyramidal cells was highly co-localized with nitrotyrosine. Furthermore, iNOS and eNOS were highly expressed in AD astrocytes where a double immunolabeling revealed that iNOS and eNOS were co-localized with nitrotyrosine. The increased expression of NOS in astrocytes and neurons contribute to the formation of peroxynitrite and to the generation of nitrotyrosine

[391]. The iNOS expression is associated with immune activation and thus is observed mainly in the reactive astrocytes and microglia surrounding the Aβ deposits. The presence of L-arginine in astrocytes *in vivo* suggests that glia may store L-arginine for NO production in the brain [42, 392, 393]. The eNOS immunoreactivity has been localised around the blood vessels of AD patients. The data of Colton and co-author support a role for nNOS neurons in AD [394]. Cetin et al. [395] found a decrease of nNOS expression in the hippocampus of Aβ42 injected aged rats, while Aβ42 injected young adult rats showed a significant increase of the nNOS expression. The authors hypothesize that the damaging effects of low physiological concentrations of Aβ might initially, in young adults, be overcome at least by an adaptive response. However, when age related secondary stress occurs, mitochondrial impairment might lead to the induction of cell death. Under this condition a decrease in nNOS expression was observed [395]. The impairment of the nNOS, induces loss of the NO-dependent neuronal functions, such as memory [78]. It has also been observed that aggregated Aβ inhibits the NO signaling pathway and suppresses the protective effects of endogenous NO in the brain [396]. In this respect the NO produced by the neuronal NOS (nNOS) and the endothelial NOS (eNOS) plays a protective role against Aβ-induced neuronal cell death, cerebrovascular dysfunction, and cerebral amyloid angiopathy [397].

2. AIM

This work has been developed following two different experimental approaches, sharing the common purpose of investigating the putative role of nitric oxide (NO) in the bioenergetic context of different cell lines.

In one set of experiments, carried out using human keratinocytes (HaCaT cells), a new role of melatonin related to the NO signaling has been envisaged and studied. In a second set of experiments, the mitochondrial functional state of a validated cell model of Alzheimer's disease (AD) has been investigated and related to the NO chemistry.

NO is implicated in the control of both the mitochondrial oxidative phosphorylation and the sleep/wake cycle; the latter is compatible with the night accumulation of NO and its oxidation products, nitrite and nitrate.

In this work it has been suggested that NO could be part of the complex signaling pathway triggered by melatonin, the main regulator of the circadian rhythm, that, through modulation of the NO synthase activity, could increase the cell NO bioavailability, with relevant effects on mitochondria.

Beside these physiological effects, NO has been recently reported to be implicated in neurodegenerations, such as AD, thus a link between NO and mitochondrial failure has been envisaged.

The bioenergetics of melatonin-treated and AD cells has been investigated with a particular attention devoted to measure the NOSs expression, as determined by Real-Time PCR and Western Blot analysis; the nitrite and nitrate accumulation in the cell culture medium was also assessed. The mitochondrial membrane potential was investigated by measuring the accumulation of the fluorescent probe JC-1 in

the mitochondrial matrix and the mitochondrial respiration was evaluated using intact and permeabilized cells. Cell bioenergetic changes were further explored by measuring the production of ATP and lactate.

3.   MATERIALS AND METHODS

3.1 Cell cultures

Human keratinocyte (HaCaT) cell line, were grown at 37 °C, 5% CO_2, 95% air in DMEM (Dulbecco's modified Eagle's) medium containing 4.5 g/L glucose, 10% FBS, supplemented with 2 mM L-glutamine and 50 μg/ml gentamicin in 75-cm^2 flasks, 25-cm^2 flasks or multiwall plates. The day before the experiments, cells were grown in DMEM containing 1 g/L glucose and 2 mM L-glutamine (w/o FBS, phenol red and gentamicin).

Chinese hamster ovary (CHO) cells, were grown in Ham's F12 media supplemented with 2 mM L-glutamine, 10% FBS and 1% penicillin/streptomycin. The 7WD4 and 7PA2 (kindly provided by Dr. Denis Selkoe, Harvard Medical School, Boston, thanks to Prof. Antonino Cattaneo, European Brain Research Institute (EBRI), Rome) are CHO cell lines stably expressing human wtAPP751 (7WD4 cells) and APP751 harboring mutation V717F (7PA2 cells). The 7WD4 and 7PA2 cells were cultured in Ham's F12 containing 10% FBS, 2 mM L-glutamine, 1% penicillin/streptomycin and G418 for maintaining selection of hAPP stable transfect. Before the experiments, 7WD4 and 7PA2 cells were plated without G418 antibiotic in order to be in the same culture conditions as control CHO cells.

3.2 Citrate Synthase

Cells (1x10^6), harvested by trypsinization and centrifugation (1.000 x g for 5 min at 20 °C), were lysed by CelLytic^{TM}MT Cell Lysis Reagent in the presence of the

Protease Inhibitor Cocktail and centrifuged at 20.000 x g for 10 min. Cell lysates were assayed for the determination of citrate synthase activity [398]. Citrate synthase is localized in the mitochondrial matrix and is commonly used as a quantitative marker enzyme for the content of intact mitochondria. Citrate synthase catalyzes the reaction between acetyl coenzyme A (acetyl CoA) and oxaloacetic acid (OAA) to form citric acid. The hydrolysis of the thioester of acetyl CoA results in the formation of CoA with a thiol group (CoA-SH). The thiol reacts with the DTNB in the reaction mixture to form 5-thio-2-nitrobenzoic acid (TNB). This yellow product (TNB) is observed spectrophotometrically by measuring absorbance at 412 nm.

3.3 Melatonin Determination

The presence of melatonin in living cells was evaluated by immunoassay using the ''Direct saliva Melatonin ELISA kit'' (BÜHLMANN), as adapted to cell lysates. HaCaT cells ($3x10^6$) were incubated with melatonin (1 nM) for 1 h and 5 h. After incubation, both melatonin-treated and control cells were harvested, resuspended (at 10^6/mL density), and lysed by CelLytic^{TM}MT Cell Lysis Reagent in the presence of the Protease Inhibitor Cocktail. The cell lysates were incubated for 15 minutes on a shaker and centrifuged at 20.000 x g for 10 minutes. Aliquots of lysates were loaded on a plate containing anti-melatonin polyclonal antibody for enzyme-linked immunosorbent assay (ELISA). After overnight incubation (16-20 hours), the melatonin contained in the lysates and in the calibrators competed for the binding sites of a highly specific antibody with biotinylated melatonin added during following 3 hours incubation. After suitable washing, the enzyme label, streptavidin conjugated to horseradish peroxidase (HRP) was

added, which binds during further 60 minutes incubation to the melatonin-biotin-antibody complexes captured on the coated wells. Unbound enzyme label was then removed by washing and TMB substrate (tetramethylbenzidine) was added to the wells. In a fourth 30 minutes incubation step, a chromophore was formed in inverse proportion to the amount of melatonin present in the sample. The colour turned from blue to yellow after the addition of an acidic stop solution and was observed spectrophotometrically by measuring absorbance at 450 nm.

3.4 Real Time PCR

Quantitative Real Time Polymerase Chain Reaction (QRT-PCR) was carried out in HaCaT cells, incubated 6 h with increasing amount of melatonin or at different time with melatonin 1 nM, using specific oligonucleotide primers in order to identify and quantify the different Nitric Oxide Synthase (NOS) isoforms. After incubation, cells were harvested by trypsinization and centrifugation (1000 x g for 5 min at 20°C), washed twice with Hank's buffer and counted. Cells ($1x10^{6}$) were lysed by Trizol reagent and total RNA was isolated by phenol-chloroform extraction [399]. RNA purity was measured using a spectrophotometer by determining the ratio of absorbance at 260 nm to the absorbance at 280 nm (A_{260}/A_{280}). Pure RNA shows an A_{260}/A_{280} ratio of 1.9 - 2.1 in 10 mM Tris at pH 7.5. Contamination by phenol or urea will show absorbance at 230 nm or 270 nm, respectively. Protein contaminants have a high absorbance at 280 nm and therefore produce a low A_{260}/A_{280} ratio. Absorbancies at 235 nm indicates the presence of contaminants. RNA quality was assayed by gel electrophoresis, which allows to visualize discrete intact ribosomal bands and determine the degree of

Chapter 3. Materials and Methods

RNA degradation. High-quality total RNA was indicated by sharp bands corresponding to 28S and 18S rRNA, at a ratio of approximately 2:1 (Fig. 11).
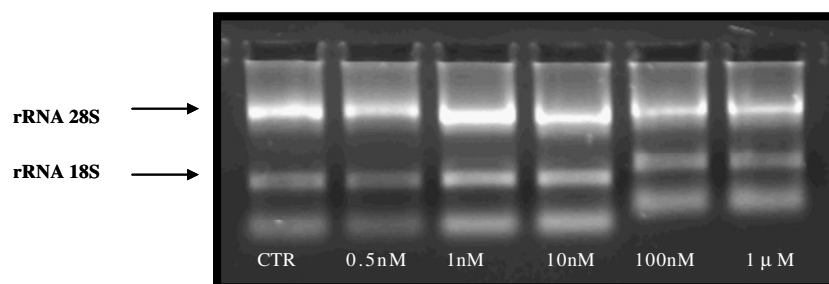
Fig. 11: Electrophoretic analysis of total RNA extracted from HaCaT cells. HaCaT cells were incubated for 6 h at increasing melatonin concentrations.

1 μg of total RNA was used as a template for the cDNA synthesis. The reverse transcription reaction was performed using Side-Step™ II QRT-PCR cDNA Synthesis Kit (Stratagene). QRT-PCR was performed using primers designed by BioRad Laboratories (Software Beacon Designer) and purchased by PRIMM. β-actin gene (PRIMM) was used for normalization.

nNOS (NOS1)
Forward : 5' **GCGGTTCTCTATAGCTTCCAGA** 3'
Reverse : 5' **CCATGTGCTTAATGAAGGACTCG** 3'
eNOS (NOS3)
Forward : 5' **GCCGTGCTGCACAGTTACC** 3'
Reverse : 5' **GCTCATTCTCCAGGTGCTTCAT** 3'
β-actina
Forward : 5' **GCGAGAAGATGACCCAGATC** 3'
Reverse : 5' **GGATAGCACAGCCTGGATAG** 3'

SYBR Green has been used as intercalating-dye which is able to bind double-stranded DNA and upon excitation to emit light (excitation = 470 nm; emission = 510 nm). Thus, as a PCR product accumulates, fluorescence increases. This method require a special thermocycler equipped with a sensitive camera (Stratagene Mx3005p System, Agilent Technologies) that monitors the fluorescence in each well of the 96-well plate at frequent intervals during the PCR reaction. The cDNAs were amplified using 45 cycles consisting of denaturation step (95 °C for 5 min) and amplification step (95 °C for 10 sec, 55 °C for 30 sec). A normal amplification curve from a dilution series of a sample is shown in Fig. 12a. Amplification plots are created when the fluorescent signal from each sample is plotted against cycle number; therefore, amplification plots represent the accumulation of product over the duration of the real-time PCR experiment. The initial PCR cycles produce low fluorescent signals that cannot be detected by the CCD camera. The linear portion of each curve is in the exponential phase of PCR, where the amount of product, and therefore the signal, doubles after each cycle. The top portion of the curves shows minimal signal increase, as PCR slows due to the depletion of reaction components, such as primers and dNTPs. Melting curve analysis was performed at the end of every run to ensure a single amplified product for each reaction. During a Melting Curve Analysis, all products generated during the PCR amplification reaction were melted at 95 °C, then annealed at 55 °C and subjected to gradual increases in temperature. The results is a plot of raw fluorescence data units, R, versus temperature. Fig. 12b shows the melt data as the negative first derivative of raw fluorescence, R'(T), plotted against an increase in temperature. In this view, every peak in the curve indicates

a specific product melting. Most QPCR products will melt somewhere in the range of 70 - 90 °C.
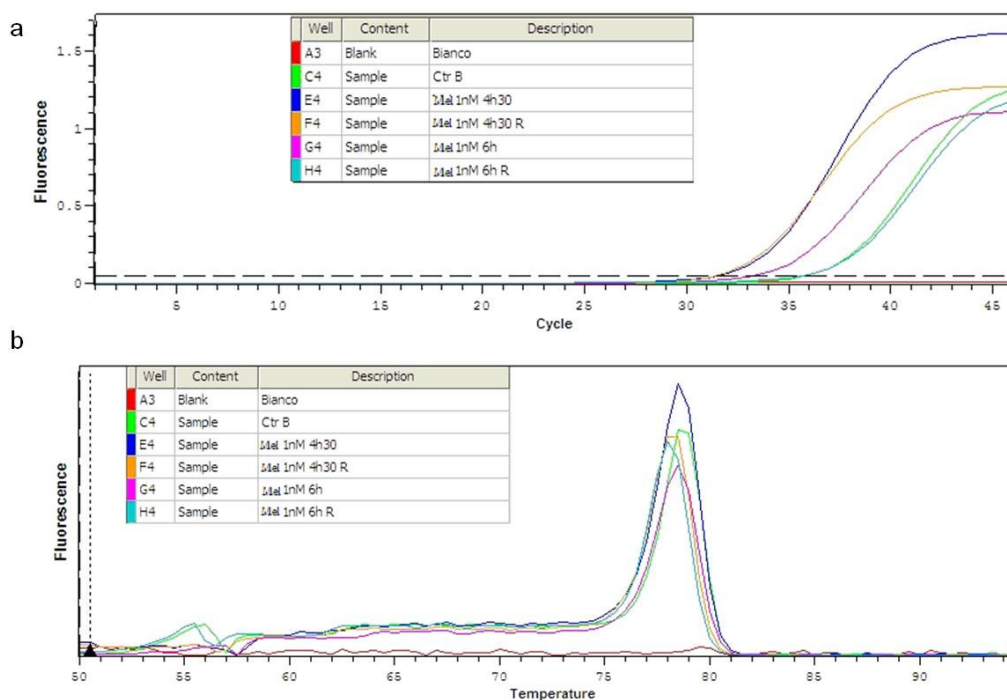
Fig. 12: a) Relative fluorescence versus Cycle number. Amplification plots are created when the fluorescent signal from each sample is plotted against cycle number; therefore, amplification plots represent the accumulation of product over the duration of the real-time PCR experiment. Real-time PCR amplification plot. Fluorescent signal is plotted against cycle number. b) The $-\Delta F/\Delta T$ (change in fluorescence/change in temperature) is plotted against temperature to obtain a clear view of the melting dynamics.

Ideally, a single peak within this temperature range is observed and the melting temperature should be the same in all the reactions where the same sample is amplified. If any secondary peaks are seen on the peak of interest, this indicates

that something other than the gene of interest is present among the reaction products. The strategies employed to quantify the results obtained by QRT-PCR is termed comparative threshold (Ct = cycle threshold) method. This involves comparing the Ct values of the samples of interest with a control or calibrator such as a non-treated sample. The Ct value is the cycle number at which the fluorescence generated within a reaction crosses the fluorescence threshold, a fluorescent signal significantly above the background fluorescence. At the threshold cycle, a detectable amount of amplicon product has been generated during the early exponential phase of the reaction. The threshold cycle is inversely proportional to the original relative expression level of the gene of interest. The Ct values of both the calibrator and the samples of interest are normalized to the endogenous housekeeping, β-actin. The comparative Ct method is also known as the $2^{-(\Delta)(\Delta)Ct}$ method, where

$$(\Delta)(\Delta)Ct = (\Delta)Ct_{sample} - (\Delta)Ct_{reference}$$

Here, $(\Delta)Ct_{sample}$ is the Ct value for any sample normalized to the endogenous housekeeping gene and $(\Delta)Ct_{reference}$ is the Ct value for the control also normalized to the endogenous housekeeping gene.

3.5 Western Blot

HaCaT cells, grown overnight in DMEM containing 1 g/L glucose, 2 mM L-glutamine without FBS, were incubated with melatonin (1 nM) at different time. After melatonin incubation, HaCaT cells were harvested by trypsinization and centrifugation (1000 x g for 5 min at 25°C), washed twice with Hank's buffer and lysed with CelLytic™MT Cell Lysis Reagent in the presence of protease inhibitors. The cell lysates were incubated for 15 minutes on a shaker and

centrifuged at 20.000 x g for 10 min. The protein concentration was determined by Bradford assay [400]. Samples were run on gel electrophoresis, 10 % SDS-PAGE gels in order to obtain protein separation. 20 µg of total protein from cell lysate was loaded into wells in the gel. One lane was reserved for the marker (Invitrogen, SeeBlue® Plus2 prestained standard), a commercially available mixture of proteins having defined molecular weights. SDS-PAGE (SDS polyacrylamide gel electrophoresis) maintains polypeptides in a denatured state once they have been treated with strong reducing agents, in these case dithiothreitol (DTT) to remove secondary and tertiary structure and thus allows separation of proteins by their molecular weight. The gel was run at 90 V through the stacking part of the gel and the volts were turned up to 150 V after the proteins have gone through the stack and are migrating through the resolving gel. Following electrophoresis, the protein was transferred on nitrocellulose membranes (Whatman, GE Halthcare UK) for 1 h at 100 mA. Blocking of non-specific binding was achieved by placing the membrane in PBS with 0.1 % tween and 3 % BSA for 2 h at room temperature. After blocking, the membrane was incubated overnight at 4°C with primary rabbit polyclonal anti-nNOS antibodies (from BD Transduction Laboratories); α-tubulin was used as the reference. A secondary ECL TM anti-rabbit antibody HRP (Jackson) was thereafter incubated 1 h at 25°C. Washing steps (consisting to washes of PBS, 0.1 % Tween, 5 minutes each) were necessary to remove unbound reagents and reduce background. The imagine was determined for chemiluminescence (Amersham, GE Halthcare UK). Densitometric analysis was carried out by the KODAK 1D Image Analysis Software (Eastman Kodak Company).

Chapter 3. Materials and Methods

3.6 Nitrate / Nitrite (NO$_X$) determination

The total concentration of nitrite and nitrate (NO$_X$) is used as a quantitative measure of NO production. Accumulation of the NO$_X$ in the culture medium of HaCaT cells (~ 2.5×10^5 cells/mL), grown over night in DMEM 1 g/L glucose (without FBS and phenol red), was measured after 6 h and 8 h exposure to melatonin at the given concentrations or at different times of incubation with 1 nM melatonin. In the case of CHO and 7PA2 cells, the NO$_X$ content in the supernatants was evaluated after 4 h of accumulation. Incubations of cells for NO$_X$ measurements were performed in serum-free DMEM without phenol red, because both FBS and phenol red can cause a significant reduction in the intensity of the fluorescence. After incubation, the cell supernatants were centrifuged at 4°C, 1000 x g for 10 min and the NO$_X$ content was determined fluorometrically (Nitrate/Nitrite Fluorometric Assay Kit, Cayman Chemical Co.). Nitrate/Nitrite Fluorometric Assay Kit provides an accurate and convenient measurement of total nitrate/nitrite concentration in a simple two-step process. In the first step nitrate is converted to nitrite by nitrate reductase:

$$NO_3^- + e^- + 2H^+ \rightarrow NO_2^- + H_2O$$
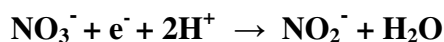
In the second step, nitrite reacts with the fluorescent probe DAN (2, 3-diaminonaphthalene). NaOH enhances the detection of the fluorescent product, 1(H)-naphthotriazole (NAT) (Fig. 13).
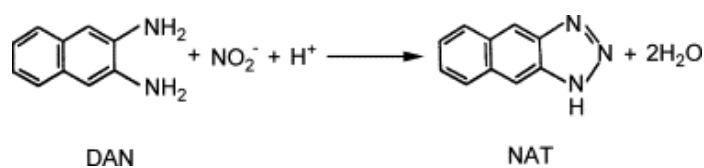
Fig. 13: Reaction of 2,3-Diaminonaphthalene (DAN) with NO$_2^-$.

Chapter 3. Materials and Methods

The fluorescent intensity is proportional to the total nitric oxide production and was measured at the Fluorescence Plate Reader VICTOR^{TM} Multilabel Counter (Perkin Elmer) using an excitation wavelength of 375 nm and an emission wavelength of 420 nm.

The NO$_X$ concentrations were determined using the following equation:

$$[\text{Nitrate} + \text{Nitrite}] \ (\mu M) = \left(\frac{\text{fluorescence - y-intercept}}{\text{slope}} \right) \left(\frac{1}{\text{volume of sample used } (\mu l)} \right) \times \text{dilution}$$

3.7 Mitochondrial membrane potential measurement

The mitochondrial membrane potential was measured exploiting the accumulation of the cationic fluorescent probe JC-1 (Fig. 14) into the mitochondrial negatively charged matrix [401]. The fluorescence emission of JC-1 depends both on its concentration and on the excitation wavelength.
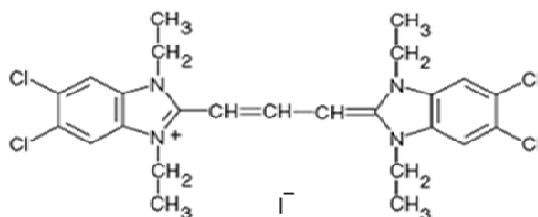
Fig. 14: Structure of JC-1 (5,5',6,6'-tetrachloro-1,1',3,3' tetraethylbenzimidazolylcarbocyanine iodide).

Upon exciting at 490 nm, JC-1 monomers display a cytoplasmic fluorescence emission centered at 537 nm (green band). Above a critical concentration, better

reached at high mitochondrial membrane potential value ($\Delta\Psi \geq 200$ mV), JC-1 aggregates are formed in the mitochondria, characterised by an intense emission band centred at 590 nm (red band) (Fig. 15).
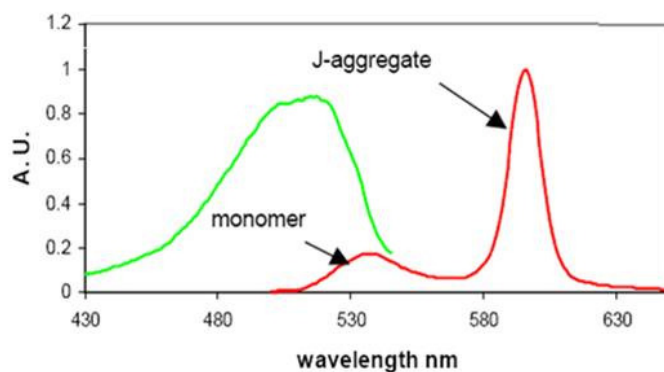
Fig. 15: Excitation and Emission Spectra of JC-1. JC-1 is a cationic dye that exhibit a potential-dependent accumulation in mitochondria, indicated by a fluorescence emission shift from green (~525 nm) to red (~590 nm). The potential-sensitive colour shift is due to concentration-dependent formation of red fluorescent J-aggregates.

Before the fluorescence measurement, HaCaT cells, grown at the semi-confluence in flask of 25 cm^2 and incubated 6 h in the presence or absence of melatonin (0.5 - 100 nM), are washed twice with PBS (containing 8 g/L NaCl, 0.2 g/L KCl, 1.11 g/L Na$_2$HPO$_4$, 0.2 g/L KH$_2$PO$_4$) and pre-incubated for 1 h at 37 °C in a physiological low-K$^+$ buffer (containing 137 mM NaCl, 3.6 mM KCl, 1.8 mM CaCl$_2$, 0.5 mM MgCl$_2$, 4 mM Hepes and 1 x mixed aminoacids from GIBCO plus 0.5 mM L-arginine at pH 7.2) in the presence of melatonin and in the absence of glucose to stimulate the oxidative phosphorilation (OXPHOS). For the experiment, cells were trypsinized, gently centrifuged at 1100 x g, for 5 min at 20 °C, and resuspended in high-K$^+$ buffer (containing 137 mM KCl, 3.6 mM NaCl,

1.8 mM CaCl$_2$, 0.5 mM MgCl$_2$, 4 mM Hepes at pH 7.2), to obtain a cell suspension of 1×10^6 cells/ml. In the case of CHO and 7PA2 cells, a similar condition was used to measure $\Delta\Psi$, with the only difference consisting in the use of DMEM (w/o glucose) as pre-incubation buffer, due to a high sensitivity of these cells to K$^+$ buffer. For the same reason, the experiment were carried out in DMEM (containing glucose, 1 g/L) without phenol red, to obtain a cell suspension of 3×10^6 cells/ml. The kinetics of JC-1 accumulation was followed in the presence of ouabain 2 μM in order to dissipate the plasma membrane potential, possibly abolishing any aspecific cytoplasmatic fluorescence. Accumulation of the JC-1 aggregates into mitochondria was started by adding 0.6 μM nigericin to the cells, pre-mixed with the 0.3 μM JC-1. Nigericin is an electroneutral K$^+$/H$^+$ antiporter ionophore which converts the ΔpH component of $\Delta\mu$H$^+$ into the electrical membrane potential gradient $\Delta\Psi$, allowing full expression of mitochondrial $\Delta\mu$H$^+$ as $\Delta\Psi$ [402] (Fig. 16a).
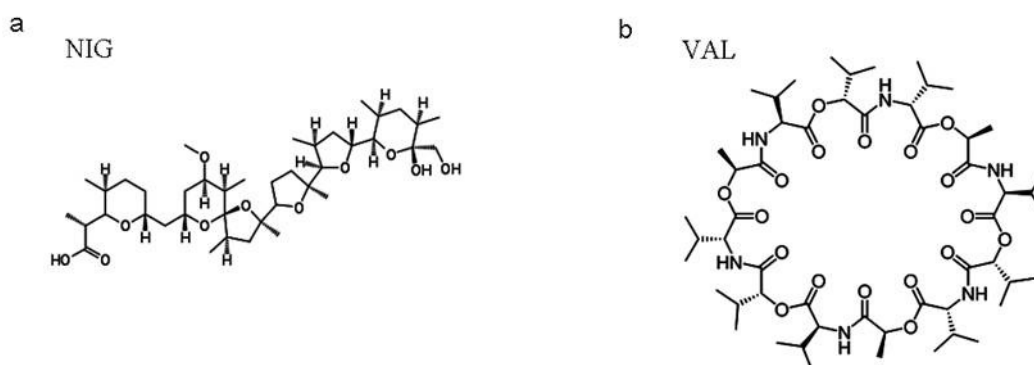
Fig. 16: Structure of nigericin (a) and valinomycin (b).

70

After addition of nigericin, the fluorescence level reached a maximum within approximately 60 min; thereafter, the fluorescence signal was rapidly dissipated by 0.2 μM valinomycin, a mobile carrier ionophore which catalyses the electrical uniport of K^+ (Fig. 16b). The kinetics of JC-1 accumulation was measured in 24-well black plates using the Fluorescence Plate Reader VICTOR^{TM} Multilabel Counter (Perkin Elmer); the excitation filter was selected at 490 nm and the emission filters at 595 nm, to detect the red aggregates of the probe JC-1.

3.8 Polarographic measurements

Oxygen consumption was measured with the OROBOROS Oxygraph 2k (Fig. 17) (Oroboros Instruments). The software DatLab (Oroboros, Innsbruck, Austria) was used for data acquisition (1 s time intervals) and analysis, including calculation of the time derivative of oxygen concentration normalized per mg of protein (O_2 flux per mass: pmol sec^{-1} mg^{-1}), signal deconvolution dependent on the response time (τ) of the oxygen sensor and correction for instrumental background oxygen flux [403, 404]. In all applications the chamber volume is 1.5 ml. The large inner diameter of the chamber (16 mm) provides space for additional electrodes, light guide and mechanical transducer. Each chamber is equipped with a polarographic oxygen sensor (POS) with a large cathode (2-mm diameter) that increases the sensitivity and signal-to-noise ratio and decreases the signal drift at zero oxygen. Gas-aqueous phase boundaries must be avoided to exclude uncontrolled oxygen gradients within the measuring system. Measurements of oxygen back-diffusion and mathematical correction for background were carried out to perform high accuracy of flux.

3.8.1 *Polarographic oxygen sensor (POS)*

In the O_2 Clark-type electrode, the probe is a platinum wire coated with Ag/AgCl, serving as reference electrode. The selectivity towards the specific gas is achieved by i) a gas-permeable hydrophobic membrane isolating the probe from the other redox-active non-gaseus species which might be present in the solution and ii) the polarization voltage applied. This is $- 0.67$ V for O_2 ($1/2\ O_2 + 2\ e^- + 2\ H^+ \rightarrow H_2O$).
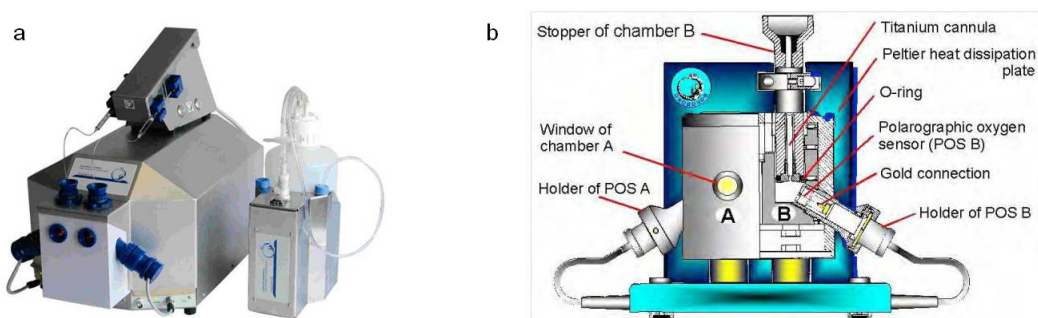
Fig. 17: a) The OROBOROS Oxygraph 2k with the Titration-Injection microPump (Tip-2k) on top and the Integrated Suction System (ISS) on the right. b) Inside view of the OROBOROS Oxygraph 2k instruments. A, left: external of chamber; B, right: internal of chamber.

The oxygen electrode was calibrated by recording the signal in air-equilibrated buffer (corresponding to $[O_2]$ in the range 200-300 μM, calculated from the solubility of the gas in the experimental conditions used) and subtracting the signal measured upon addition of excess sodium dithionite ($[O_2] = 0$).

Chapter 3. Materials and Methods

3.8.2 Air and oxygen calibration

The oxygen sensors were calibrated by a two-point calibration, routinely achieved at air saturation and zero oxygen concentration. Accordingly, static calibration involves the determination of the constant signal of the polarographic oxygen sensor at 0 % and 100 % air saturation (R_0 and R_1, respectively) under the particular experimental conditions (temperature, signal amplification by electronic gain, polarization voltage, stirring speed, medium). Air saturation was achieved by stirring the medium without sample in the chambers in contact with air, until the oxygen signal (the slope expressed as pmol sec^{-1} ml^{-1}) becomes constant (in about 20 min). After stabilization of the oxygen signal, R1 must be < 10 Volts. Zero oxygen calibration was achieved by allowing complete oxygen depletion or alternatively by use a freshly prepared a 2-5 % solution of Na-dithionite (sodium hydrosulfite: $Na_2S_2O_4$) in water. The instrumental background test is necessary for a calibration of the O_2k chamber performance. The chamber was closed without sample and after stabilization for 10 min, oxygen consumption was obtained by the polarographic oxygen sensor at air saturation and it was indicated as J°1 (the uncorrected oxygen slope expressed as pmol sec^{-1} ml^{-1}). In the next steps the oxygen concentration was reduced by nitrogen gas. At progressively lower steps of oxygen concentration, the oxygen consumption by the sensor decreased linearly and the effect of oxygen backdifussion was finally apparent as a positive slope or negative flux. The linear dependence of background oxygen flux from oxygen concentration is described by the equation with slope $b°$ and intercept $a°$:

$$J_{O2}° = b° \, cO_2 + a° \quad (Y = b°x + a°)$$

The linear regression was automatically displayed in the DatLab4-Excel file "O_2k-Background.xls", plotting background oxygen flux as a function of oxygen flux as a function of oxygen concentration with intercept $a°$ and slope $b°$ (Fig. 18).
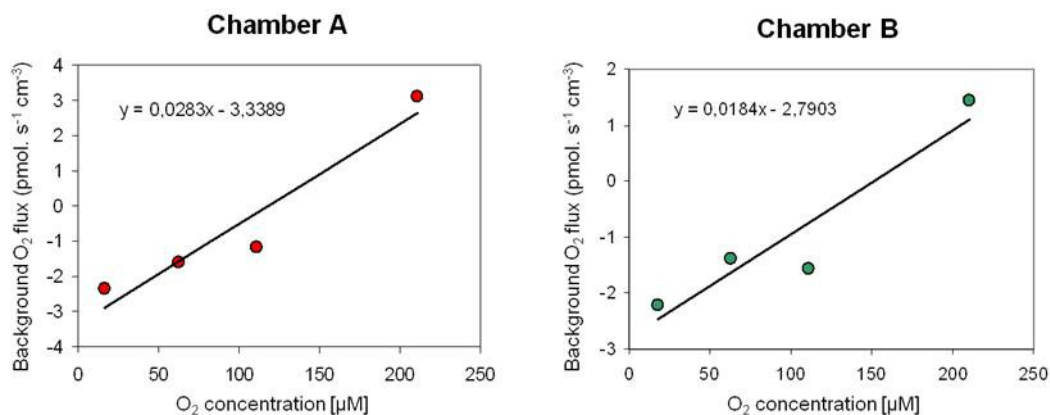
Fig. 18: O_2k-Background. Oxygen calibration in Hank's buffer containing 5.5 mM glucose. The graphs show oxygen flux as a function of oxygen concentration, with the linear regression parameters.

These values were used for on-line instrumental background correction of flux during respirometric experiments in the corresponding O_2k-chambers.

3.8.3   Measurements of oxygen consumption in intact cells

HaCaT cells, grown overnight in an antibiotic/FBS-free DMEM medium, were incubated 8 h with increasing melatonin concentrations (0.5, 1, 10, 100 nM); when required, the nNOS inhibitor, 7-nitroindazole (7N), was added (500 nM) 30 min before the measurement. For the assay, cells were harvested with trypsin–EDTA, washed twice by centrifugation at 1000 x g for 5 min at 20°C through

Hank's medium, containing 5.5 mM glucose and resuspended in Hank's medium, containing 5.5 mM glucose at a density of $3,3 \times 10^6$ cells / ml.

CHO and 7PA2 cells ($3,3 \times 10^6$ cells/ml) were resuspended in DMEM, containing glucose 1 g/L Cellular oxygen consumption was evaluated using high resolution respirometry. Value were normalized by protein determination [400].

3.8.4   *Measurements of oxygen consumption in permeabilized cells*

HaCaT cells, grown over night in 1 g/L glucose DMEM (w/o FBS and phenol red), were incubated 8 h in the presence and absence of 1 nM melatonin. CHO and 7PA2 cells were cultured in 75-cm^2 flasks in Ham's F12 containing 10 % FBS, 2 mM L-glutamine, 1 % penicillin/streptomycin without G418. Before the experiments, cells were washed twice with PBS, harvested with 0.5 % trypsin-EDTA, gently centrifuged at 1100 x g for 5 min at 20 °C, washed with respiration medium, centrifuged at 1100 x g for 5 min at 20 °C and resuspended in respiration medium. Cell density was determined by cell count and cell viability was evaluated by trypan blue exclusion test. Total protein was measured by Bradford assay. The respiration medium was added to the oxygraph chambers about ten minute before the measurements and was equilibrated with atmospheric oxygen and the required experimental temperature (37 °C). Cell suspension was added to the oxygraph chambers containing respiration medium to a final cell density of 3.3×10^6 cells / ml and the system was equilibrated again for 5 min.   The respiration medium consists of: 3 mM MgCl$_2$ x 6 H$_2$O (0.61 g/L), 20 mM taurine (2.502 g/L), 10 mM KH$_2$PO$_4$ (1.361 g/L), 20 mM HEPES (4.77 g/L), 1 g/L BSA, 110mM mannitol (20.04 g/L), 0.3mM dithiothreitol (0.046 g/L), pH 7.1, adjusted with 5 N KOH. The respiration medium was supplemented with 0.5 mM EGTA

(0.19 g/L) in respiration measurements of CHO and 7PA2 cells. EGTA was used to create the appropriate free concentration of Ca^{2+} in the physiological range. In addition, EGTA chelates contaminating heavy metals toxic for mitochondria. EGTA wasn't used in the experiments involving melatonin. EGTA may mask the action of melatonin because of its higher affinity for calcium ions. Respiration was assayed and evaluated in cells permeabilized with digitonine. Digitonin is a Cholesterol-complex forming agent that interact with cholesterol molecules of the plasma membrane (the polar heads of the cholesterol are associated with the polar heads of the phospholipids). The interaction induces a loss of membrane integrity (permeabilization), so that the barrier between the intracellular space and surrounding medium disappears. The cholesterol content of intracellular organelles like mitochondria is considerably lower and so the optimal digitonin concentration that doesn't disrupt these organelles but its action is confined to outer cell membrane needs to be experimentally determinated. The optimal digitonine concentration and the incubation time was determined according to [405]. Briefly, the digitonine titration curve for 3.3×10^{6} cells/ml was performed in mitochondrial medium, in the presence of 10 mM succinate, 0.5 μM rotenone and 1 mM ADP (Fig. 19). Time intervals between titrations were 12-14 min up to 3 μg cm^{-3} and 4-5 min at higher digitonin concentrations. Putative membrane damage produced by digitonin was also evaluated, by independently assaying the onset of sensitivity of cell respiration to externally added cytochrome c^{2+}. The optimal digitonin concentration obtained as described was added to cell suspension using a 25-μl Hamilton microsyringe and was incubated for about 10 min (at 37 °C). Typically, after addition of digitonin, the cell respiration rate markedly declines for 5–7 min. The lower rate of endogenous cellular respiration in the absence of mitochondrial substrates (e.g., pyruvate + malate) is indicative

of the plasma membrane permeabilization, followed by the leakage and dilution of intracellular metabolites when complete cell permeabilization has been achieved. Digitonin used for permeabilization does not influence mitochondrial respiration and can be present in the medium during the entire respirometric run.
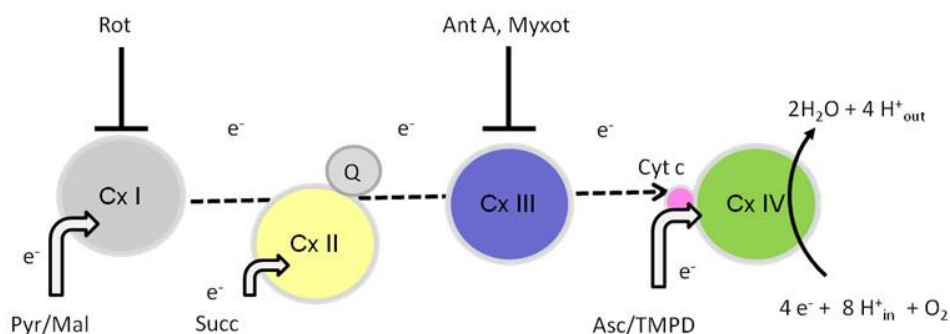
Fig. 19: Sequential representation of the mitochondrial respiratory chain. Experimental design of oxygraphic titration, using specific substrate and inhibitors. Cx I-IV: mitochondrial complex I-IV. Rot: rotenone (0.5 μM, inhibitor of Cx I), Ant A: antimycin A (5 μM, inhibitor of Cx III). Pyr/Mal: Pyruvate + Malate (8.8 mM and 4.4 mM respectively); Succ: succinate (10 mM); Asc/TMPD: ascorbate + TMPD (2 mM and 0.5 mM respectively, reductants of CxIV); Q: ubiquinol, Cyt c: cytochrome c (*modified from Krako et al. 2013*).

The contribution of the respiratory complexes to cell respiration was also evaluated according to Kuznetsov et al. with minor modifications (fig. 19) [406]:
- 8.8 mM pyruvate and 4.4 mM malate were added, using a 25-μl Hamilton microsyringe, to record resting complex I-supported respiration, without ADP.
- ADP was added, using a 25-μl Hamilton microsyringe, to obtain a final (saturating) concentration of 2 mM for maximal mitochondrial respiration (state 3). The rate of state 3 respiration at saturating ADP concentrations should be stable for at least 10–15 min.

- 0.5 µM rotenone, a specific inhibitor of complex I, was added to inhibit complex I. Respiration should be almost completely inhibited.

- 10 mM succinate was added to induce complex II-supported respiration.

- 5 µM antimycin A, a specific inhibitor of complex III was added to inhibit Complex III. Inhibition of respiration should be similar to that seen after the addition of rotenone.

- Complex IV respiration was activated by adding 0.5 mM TMPD and 2 mM ascorbate, artificial substrates specific for this complex.

- 10 mM cytochrome c was added to show the intactness of the outer mitochondrial membrane.

3.9 ATP measurements

The cell adenosine-5'-triphosphate (ATP) concentration was quantified by chemiluminescence, under stationary conditions or kinetically by following the rate of ATP production.

Depending on the experiment, the stationary ATP measurement were performed using HaCaT cells, before and after treatment with melatonin 1 nM for 6 h and seeded at a density of ~ 5 x 10^5 cells / ml in 96-well plates. A similar protocol was used with CHO and 7PA2 cells. Cells were suspended for 4 h in PBS containing 2 mM L-glutamine, in the presence or absence of 11 mM glucose; when necessary, 2.5 µg/ml oligomycin was added over the last 1.5 h incubation. The starvation of glucose is necessary to avoid the glycolytic-driven metabolism and the ATP-synthase inhibitor oligomycin to inhibit OXPHOS.

The rate of ATP production was evaluated after cell membrane permeabilization [407]. After incubation with 1 nM melatonin for 6 h, HaCaT cells were harvested

by trypsinization and centrifugation (1000 x g for 5 min at 20 °C), washed with PBS and resuspended with PBS at 3×10^6/ml cells density. In order to permeabilize cells and minimize ATP synthesis by biochemical pathways other than oxidative phosphorylation, HaCaT cells (3×10^6 cells/ml) were incubated for 20 min at room temperature with 60 μg/ml digitonin, 2 mM iodoacetamide, and the adenylate kinase inhibitor, P1,P5-di(adenosine-5') pentaphosphate pentasodium salt (25 μM), in 10 mM Tris/HCl (pH 7.4), 100 mM KCl, 5 mM KH_2PO_4, 1 mM EGTA, 3 mM EDTA and 2 mM $MgCl_2$. Complex II driven ATP synthesis was induced by adding to the permeabilized cells, succinate (20 mM) and ADP (0.5 mM), in the presence of rotenone (4 μM). The reaction was carried out at 30 °C and stopped after 5 min by the addition of 80 % DMSO. A reference sample was assayed in the absence of succinate and in the presence of antimycine A (18 μM) and oligomycin (2 μM).

Synthesized ATP was measured using the ATPlite1step kit (Perkin Elmer). The assay is based on the detection of light generated by the reaction of ATP with luciferase and D-luciferin. The reaction is catalyzed by the enzyme luciferase obtained from the firefly (Photinus pyralis). The $MgATP^{2-}$ converts the luciferin into a form which is capable of being catalytically oxidized by the luciferase in a high quantum yield chemiluminescent reaction, according to the following equation:

$$\text{D-luciferin} + \text{ATP} + O_2 \xrightarrow[\text{Mg}^{2+}]{\text{Luciferase}} \text{Oxyluciferin} + \text{PPi} + \text{AMP} + CO_2 + \text{light}$$
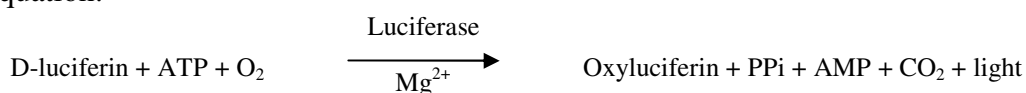
The amount of the emitted light corresponds directly to the ATP concentration. 100 μL substrate solution (containing lysis solution and luciferin/luciferase) were added to each well containing the cells in 100 μL PBS. The microplate was incubated for 10 min in the dark. The luminescence was measured by means of a

Chapter 3. Materials and Methods

VICTOR^{TM} Multilabel Counter (Perkin Elmer, Waltham, USA) equipped with 96-well (white) plates. The unknown ATP concentrations can be calculated on the basis of the ATP-standard curve.

3.10 Lactate measurements

HaCaT cells have been incubated 6 h with melatonin 1 nM in PBS (containing 8 g/L NaCl, 0.2 g/L KCl, 1.11 g/L Na_2HPO_4, 0.2 g/L KH_2PO_4), after the first 2 h, incubation cells. CHO and 7PA2 cells were grown in 6-well plates to 80–90% confluence. In order to energetically synchronize the cells, cells were starved 1 h from glucose in PBS containing Ca^{2+} 0.9 mM and Mg^{2+} 0.5 mM. Thereafter, glucose, 1 mM, was re-added to the cells for a further 3 h, in the presence or absence of myxothiazol and antimycin A (10 μM each in HaCaT cells; 5 μM each in CHO and 7PA2 cells), two inhibitors of the mitochondrial respiratory chain [408]. After incubation the cells still adherent on the flask were acidified with 80 mM $HClO_4$ and the cell supernatants were centrifuged at 4 °C, 1000 x g for 10 min; the lactate-containing supernatant was assayed (after preservation at 80 °C) spectrophotometrically (UV-visible Jasco-V550) by the method of Everse [409] following at 363 nm the production of 3-acetylpyridine-NADH catalyzed by bovine heart lactate dehydrogenase:

Lactate + 3-acetylpyridine-NAD$^+$ $\rightarrow$ Pyruvate + 3-acetylpyridine-NADH + H$^+$

The spectrophotometer was set at 363 nm on a kinetic program. 800 μl of Na-borate buffer ($Na_2B_4O_7 \cdot 10\ H_2O$; 0.01 M; pH 9.2), 100 μl of 3-acetylpyridine-NAD$^+$ (20 mg/ml solution) and 100 μl of the sample or standard or blank (PBS plus 1 mM glucose) were added into the cuvette ($V_{cuvette}$ = 1 ml). The absorbance

of the reaction mixture was followed for 2 minutes to stabilize the measure. After the addition of 10 µl of lactic dehydrogenase (LDH) enzyme (5 mg/ml), the absorbance of the reaction mixture was followed for 20 minutes to measure the lactate concentration.

3.11 Reactive Oxygen Species, measurements

Cell ROS generation was assessed by using the fluorescent probe 2´,7´-dichlorodihydrofluorescein diacetate (DCFDA). Before the experiment, HaCaT cells, incubated 6 h in the presence and absence of 100 µM and 1 nM melatonin were trypsinized, pelleted at 1000 × g for 5 min at 20 °C, and resuspended in Hank's buffer at the density 1×10^6 cells/ml. The CHO and 7PA2 cells were treated under the same conditions. Cell suspensions (1×10^6 cells/ml) were plated in 24-well (black) plates. When necessary 500 µM H_2O_2 was added. The relative fluorescence emission, after cell loading of DCFDA 100 µM, was followed of 520 nm (VICTOR^{TM} Multilabel Counter, Perkin Elmer).

3.12 Statistics

The number of independent measurements is indicated in figure legends. Significance was determined using the Student t-test, run by Excel (Microsoft Windows platform). The error bars correspond to the standard error of the mean (SEM); all P values correspond to two-sided sample t-test assuming unequal variances. A P value ≤ 0.05 was considered significant.

Chapter 3. Materials and Methods

4. RESULTS

4.1 Melatonin determination in HaCaT cells.

The effect of melatonin in HaCaT cells was explored after incubation of melatonin to the cell culture media for a variable time and at different concentration. Although melatonin is known to interact with cell surface specific receptors, the direct entry of melatonin into the cell can also occur; for these reasons first of all the presence and stability of melatonin was investigated in HaCaT cells by immunoassay using the ''Direct saliva Melatonin ELISA kit''. HaCaT cells were incubated with 1 nM melatonin for 1 h and 5 h, and the amount of melatonin up-taken by the cells was measured after cell lysis.

Cell melatonin concentration	
	pmoles / 1 x 10^{6} cells (± SEM)
Control	$1,50 \times 10^{3} \pm 0,0003$
Melatonin (1 h incubation)	$65,46 \times 10^{3} \pm 0,011*$
Melatonin (5 h incubation)	$52,86 \times 10^{3} \pm 0,0063*$

* P $\leq$ 0.05

Table 1: Cell melatonin concentration. HaCaT cells were incubated with 1 nM melatonin for 1 h and 5 h. After incubation, the cells (1 x 10^{6} / mL) were lysed for ELISA immunoassay and melatonin concentration was evaluated.

83

Chapter 4. Results

The results are reported in Table 1 and show that under the conditions chosen a significant amount of melatonin enters into the cells, without significant changes whether the incubation time is 1 h or more. The concentration of intracellular melatonin measured is, in fact, comparable after 1 h or 5 h incubation, on the other hand this value is ~ 60 times higher than that of control cells.

4.2 Effect of melatonin on NOS(s) mRNA expression in HaCaT cells.

To investigate about the possibility that melatonin could influence cellular pathways involving NO metabolism, the production of mRNA for the different NOS isoforms was tested after incubation of melatonin in HaCaT cells. At first HaCaT cells were incubated for 6 h with increasing amounts of melatonin, from 0.5 nM to 1 µM.
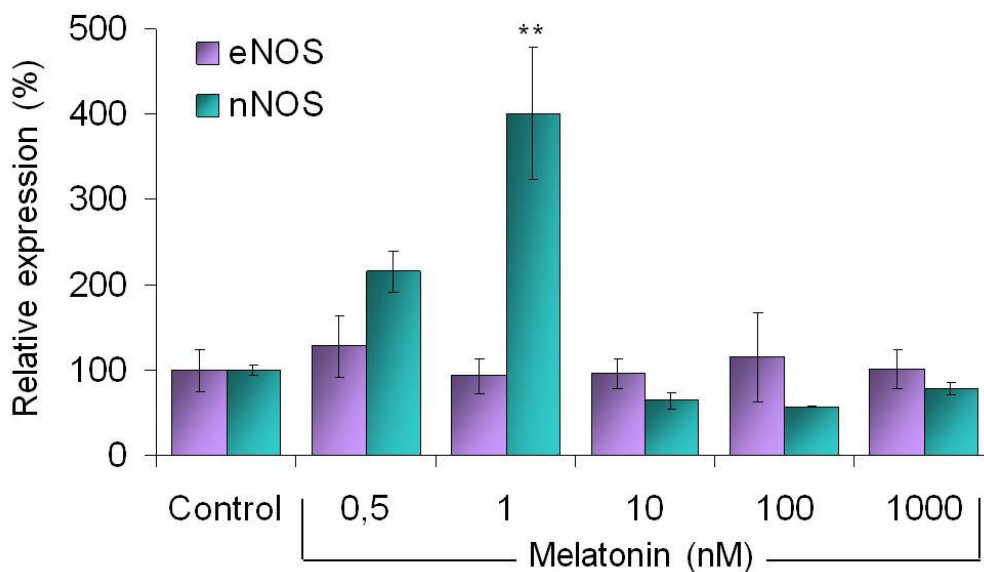
Fig. 20: Dependence of NOS expression with melatonin concentration. HaCaT cells were incubated 6 h with increasing amounts of melatonin, as indicated. QRT-PCR analysis were carried out in the presence of primers for eNOS (violet) and nNOS (cyan). Relative expression was calculated *versus* Control, after β-actin normalization. iNOS was assayed but not detected (not shown). Data ± SEM; n = 9. **$P \leq 0.01$ *versus* Control (*modified from Arese et al., 2012*).

As shown in Fig. 20, compared with controls, 0.5 and 1 nM melatonin produced a 2.15- and 4-fold increase, respectively, of the nNOS mRNA level, whereas at melatonin concentration higher than 1 nM, the nNOS mRNA expression back decreased to the level of control cells. The eNOS mRNA expression level was insensitive to melatonin under all conditions and regardless to time of incubation. The iNOS mRNA, also, remained undetectable under the same conditions (not shown).

The time dependent profile of the nNOS expression observed upon 7.5 h, 1 nM melatonin incubation, is shown in Fig. 21.
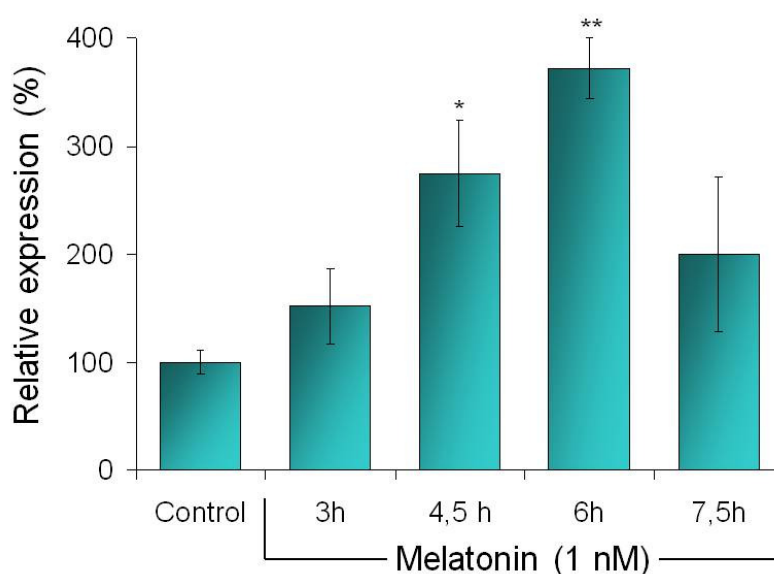
Fig. 21: Time-dependence of nNOS mRNA expression driven by 1 nM melatonin. HaCaT cells were incubated with melatonin 1 nM, as a function of time, as indicated. QRT-PCR analysis were carried out in the presence of primers for nNOS. Relative expression was calculated *versus* Control, after β-actin normalization. Data ± SEM; n = 12. ** P ≤ 0.01 *versus* Control; * P ≤ 0.05 *versus* Control (*modified from Arese et al., 2012*).

The nNOS mRNA expression level increases with the incubation time, reaching a maximum at 6 h.

4.3 nNOS protein expression in HaCaT cells driven by melatonin.

To evaluate that melatonin induces an increase not only of the mRNA but also of the protein, the protein nNOS expression level was investigated by Western Blot analysis in HaCaT cells incubated for different time with 1 nM melatonin.
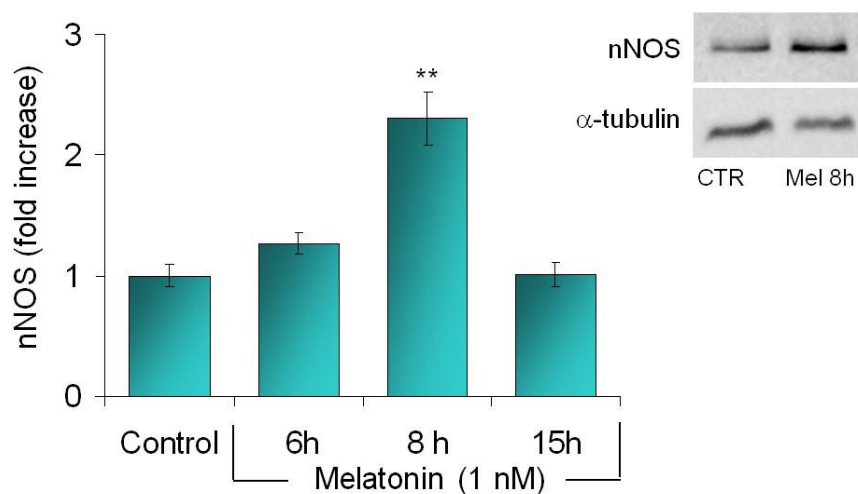
Fig. 22: Time-dependent expression of nNOS protein by melatonin. HaCaT cells were incubated with 1 nM melatonin, as a function of time, as indicated and then assayed for Western Blot with anti-nNOS antibodies. Data represent the densitometric value of each condition shown as fold increase *versus* the nNOS protein expressed by Control cells. Data ± SEM, n ≥ 3. ** $P \leq 0.01$ *versus* Control. *Inset:* Image of a typical Western Blot experiment carried out with antibody against nNOS after 8 h incubation in the presence and absence of 1 nM melatonin; α-tubulin as reference (*modified from Sarti et al., 2013*).

The nNOS protein expression changes as a function of time (Fig. 22). Compared to control, melatonin 1 nM induces a ~ 2 fold increase in nNOS expression after 8 h of incubation. The nNOS synthesis reach a maximum after ~ 8 h incubation with 1 nM melatonin, *i.e.*, ~ 2 h after cell rising of the nNOS mRNA; timing of these processes is consistent with protein synthesis and maturation (Fig. 23).
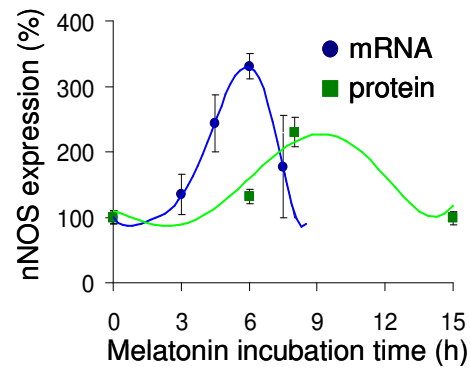
Fig. 23: Time-dependent profile of the mRNA (blue) and protein (red) nNOS expression (*modified from Sarti et al., 2013*).

4.4 Nitrate/Nitrite (NO_X) accumulation in HaCaT cells induced by melatonin.

The production of NO was assessed by measuring nitrite and nitrate levels in the medium of HaCaT cells after 6 and 8 h incubation with increasing amounts of melatonin. The result of these experiments shows that the production of NO_X by HaCaT cells is increased by melatonin compared to control (Fig. 24).

The maximal effect on NO_X accumulation is observed at about 1 nM melatonin tending to the basal level with increasing melatonin concentration by one or even two orders of magnitude.
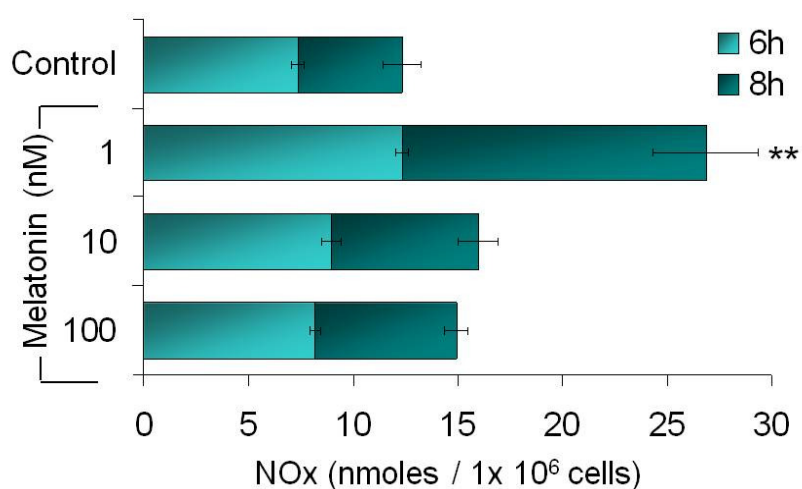
Fig. 24: Concentration dependence of NO_X production by melatonin (nanomolar). HaCaT cells were treated with increasing melatonin concentrations (1, 10, 100 nM). NO_X accumulation in the cell supernatant was quantified after 6 h (light bars) and 8 h (heavy bars) incubation with melatonin. Data ± SEM; n ≥ 5. ** P ≤ 0.01 *versus* Control (*modified from Sarti et al., 2013*).

The time dependence effect of melatonin 1 nM on NO_X accumulation are shown in Fig. 25. The production of nitrite and nitrate in the supernatant of the cells

treated with 1 nM melatonin increases with the time of incubation respect to control untreated cells and reach a peak at 8 h. Under these condition the NO_X accumulation is 2 times higher than the NO_X accumulated for a corresponding time (8 h) in controls.
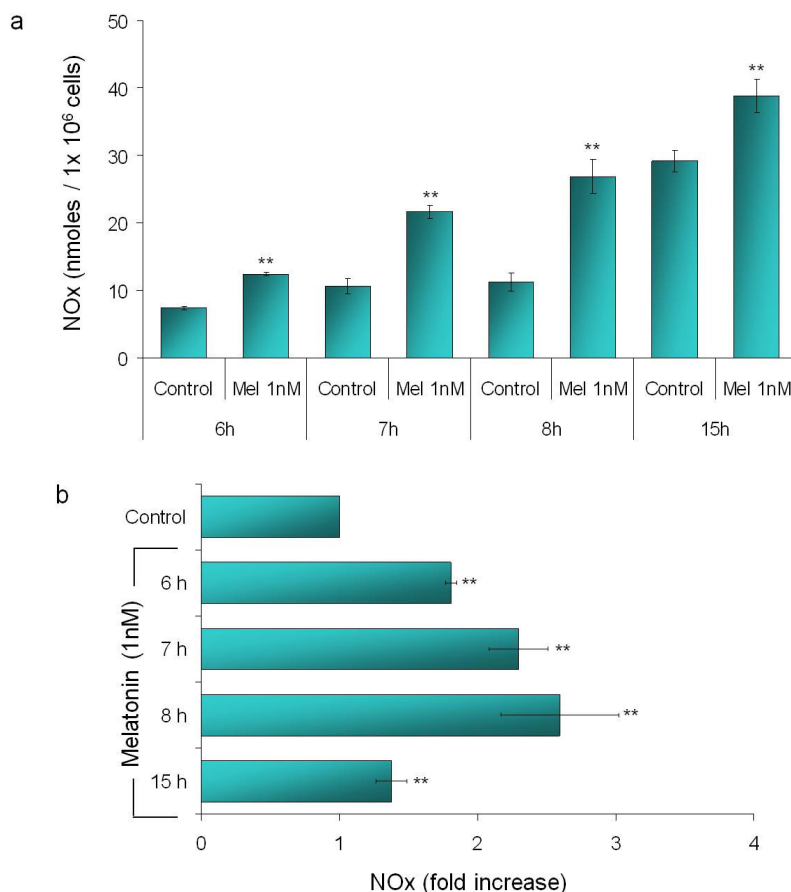
Fig. 25: Time-dependence NO_X production of nM melatonin. NO_X accumulation was measured in the cell supernatant of HaCaT cells incubated with 1 nM melatonin as a function of time. a) Data shown as nmoles NO_X / $1x10^6$ cells b) Data shown as fold increase *versus* Control (corresponding to untreated cells incubated for the same time as treated cells). Data ± SEM, n ≥ 5. ** P ≤ 0.01 *versus* Control (*modified from Sarti et al., 2013*).

4.5 Melatonin on mitochondrial membrane potential in HaCaT cells.

The mitochondrial membrane potential of HaCaT cells was measured following the import of the fluorescent probe JC-1 into mitochondria and the consequent formation of the red J-aggregates occurring when the $\Delta\Psi$ is ≥ 200 mV.

In a typical experiment, cells were pre-mixed with 300 nM JC-1 in the presence of 2 μM ouabain that prevents the hyperpolarization of the plasma membrane The reaction was started by the addition of nigericin (600 nM), a ionophore which converts $\Delta\mu H^+$ into $\Delta\Psi$.

The kinetics of JC-1 import and the formation of the aggregates where than followed, observed as the increasing level of red fluorescence and analysed. A plateau level is reached in about 60 min. Afterwards 200 nM valinomycin was added to the mixture, causing dissipation of the mitochondrial $\Delta\Psi$ and bringing back the fluorescence red signal to a basal level. The differences between the maximum fluorescence level at plateau and the minimum obtained upon addition of valinomycin, the ΔF, is proportional to $\Delta\mu H^+$. As shown in Fig. 26, after 6 h incubation with 1 nM melatonin the mitochondrial membrane potential ($\Delta\mu H^+$) is lowered, by ~ 20 %, compared to control, whereas increasing concentration of melatonin didn't affect the mitochondrial membrane potential.

Moreover, the level of fluorescence is maximal when the NOS substrate arginine is removed from the cell culture medium, pointing to a correlation between the level of $\Delta\Psi$ and the activity of NOS. Interestingly, the mitochondrial $\Delta\Psi$-depression induced by melatonin was reverted by washing cells and allowing further 3 h incubation in a melatonin-free medium.
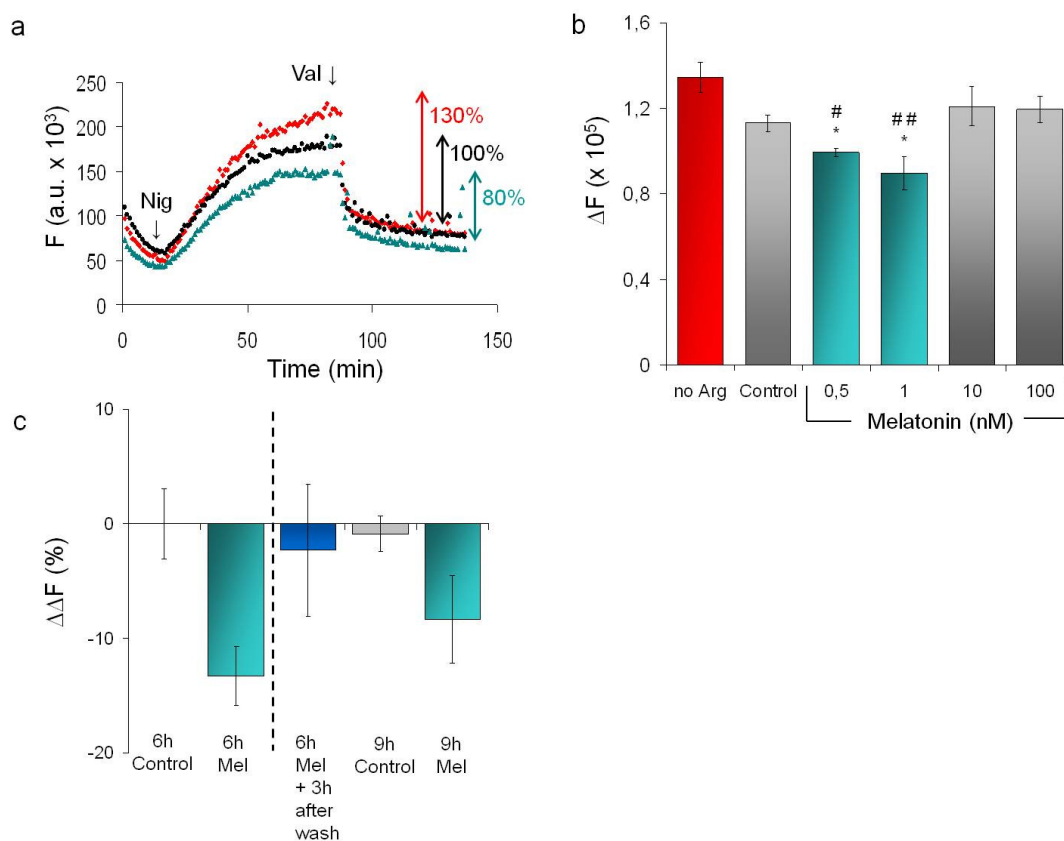
Fig. 26: Melatonin on mitochondrial membrane potential. a) Time-dependent accumulation of JC-1 in mitochondria, started by the addition to the cells of nigericin 0.6 µM (Nig). Valinomycin (Val) is added (at plateau) to collapse the membrane potential. Excitation wavelength = 490 nm, emission wavelength = 590 nm. Cells maintained in the absence of the NOS substrate arginine (red); Control cells (black). Cells after 8 h incubation with 1 nM melatonin (cyan). b) ΔFmax, calculated from plateau to the fluorescence level reached on addition of valinomycin. Data ± SEM; n = 4. * P ≤ 0.05 *versus* Control; [#] P ≤ 0.05 *versus* no Arg; [##] P ≤ 0.001 *versus* no Arg. c) ΔF decrement (ΔΔF %) of melatonin treated cells (cyan) versus Control at 6 or 9 h (gray). After melatonin incubation, cells were washed and incubated further 3 h (i) without melatonin (blue) and (ii) with melatonin renovated in the medium (cyan). Data ± SEM; n = 4 (*modified from Arese et. al., 2012*).

4.6 Evaluation of respiration efficiency of HaCaT cells treated with melatonin.

The effect of melatonin on the modulation of bioenergetic of HaCaT cells was evaluated following the spontaneous rate of oxygen consumption carried out by intact cell mitochondria.
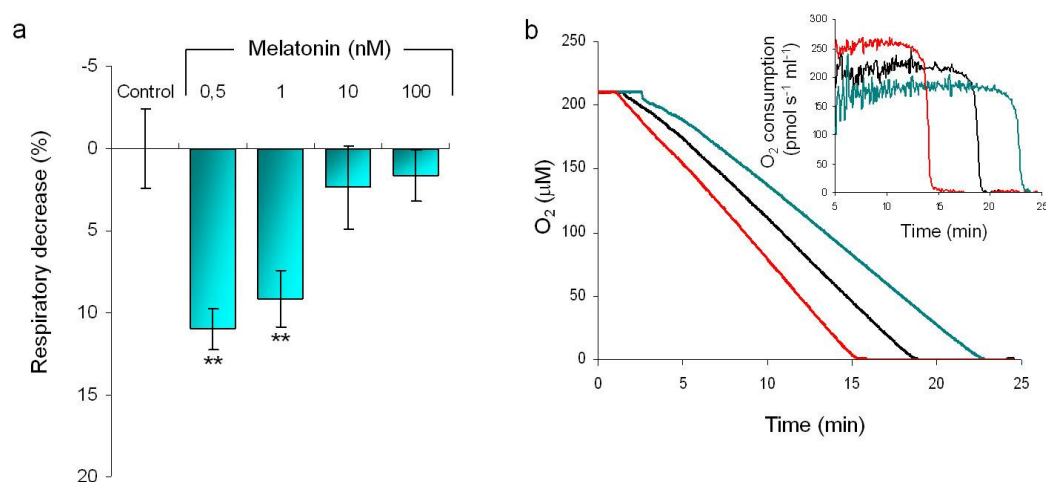
Fig. 27: Oxygen consumption rate in HaCaT cells: effect of melatonin on cell respiration. a) Comparative respiration rate of HaCaT cells incubated in the absence or in the presence of nM melatonin. Respiration was measured and reported as percent of the O_2 consumption of Control. Data ± SEM, n ≥ 3. ** P ≤ 0.01 *versus* Control. b) Typical O_2 consumption profiles of melatonin-treated HaCaT cells, in the presence (red) and absence (cyan) of the nNOS inhibitor 7-nitroindazole (7N); control untreated cells (black). *Inset:* 1st derivative plot of the traces (*modified from Sarti et al., 2013*).

After incubation for 8 h with increasing amounts of melatonin, HaCaT cells were resuspended in Hank's 1 g/L glucose at a cell density of 3.3×10^6 cells / ml and cell respiration driven by endogenous substrates was measured.

As shown in Fig. 27a, when cells are treated with 0.5-1 nM melatonin, a ~ 10 % loss of cell respiration is observed; the effect decreases at higher melatonin concentrations (up to two orders of magnitude).

Fig. 27b show typical oxygen consumption profiles of HaCaT cells treated with melatonin, in the presence (red) and the absence (cyan) of the specific nNOS inhibitor, 7-nitroindazole (7N).

The results indicate that the oxygen consumption of cells incubated 8 h with melatonin is lower than that of control cells (black line) and that the addition of 500 nM 7N 30 minutes before the measurement reverts the inhibition of respiration induced by melatonin.

To further insight the molecular mechanism responsible of this inhibition, the involvement of the mitochondrial respiratory chain complexes was evaluated after cell permeabilazation with digitonin, and making use of a mitochondrial complex specific substrate/inhibitor titration approach [406]. For this purpose, HaCaT cells, pre-treated 8 h in the presence and absence of 1 nM melatonin, were resuspended in the respiration medium (as described in Materials and Methods) at a cell density of 3.3×10^6 cells / ml. Initially the basal respiration, measured in the absence of digitonin and exogenous reducing substrates, was evaluated. Figure 28a represents a typical respiration trace of control HaCaT cells. When the signal becomes stable, digitonin is added to the cells in order to induce a loss of plasmatic membrane integrity and to allow the consequent access of substrates into the cells.
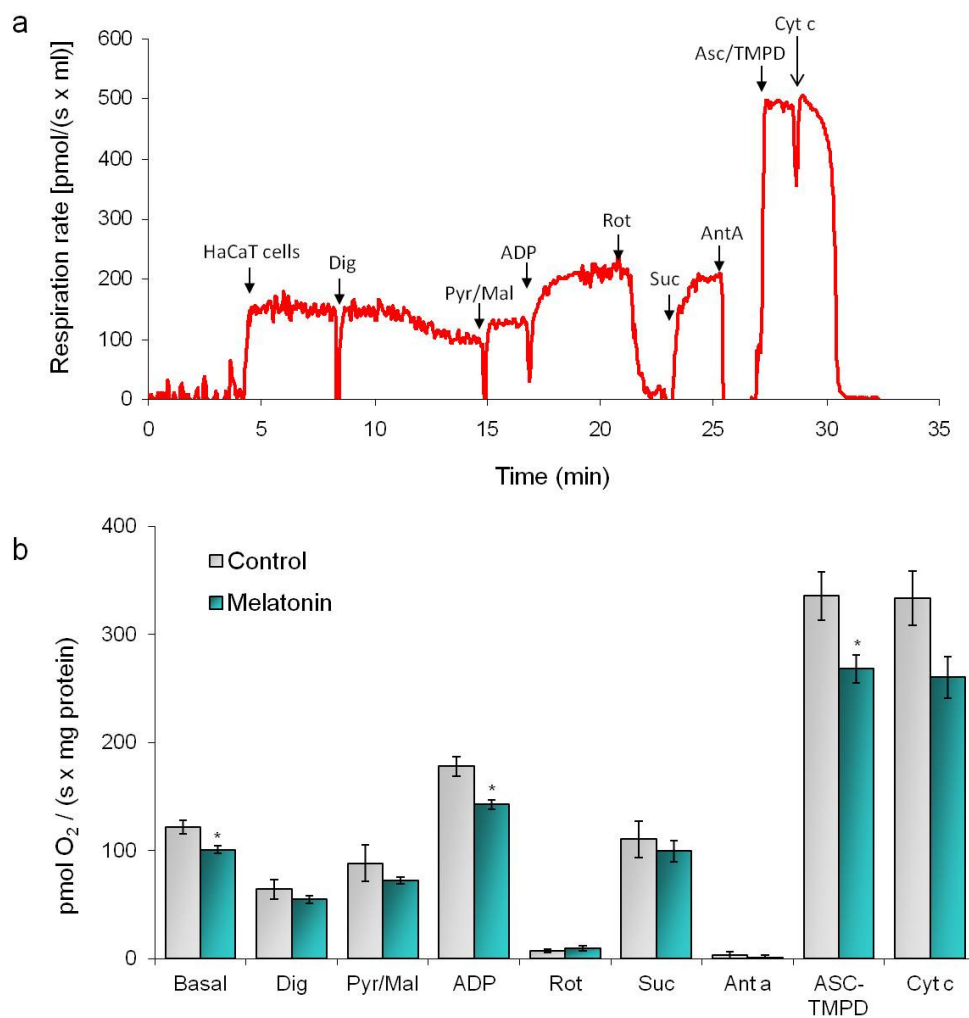
Fig. 28: Effect of melatonin on respiratory complexes activity in digitonin-permeabilized HaCaT cells. a) Oxygen consumption rate of 5×10^6 control cells. Dig: digitonine (8 μg/ml); Pyr/Mal: pyruvate (8.8 mM) and malate (4.4 mM); ADP: adenosinetriphosphate (4 mM); Rot: rotenone (0.5 μM); Suc: succinate (10 mM); Ant a: antimycin A; ASC/TMPD: ascorbate (2mM) and TMPD (0.5 mM); Cyt c: cytochrome c (10 mM). b) Respiration rate values in HaCaT cells treated 8 h in the presence and absence of 1 nM melatonin recorded after each addition step (of substrate/inhibitor) during the trace. Data values are the means ± SEM; n ≥ 4. * P ≤ 0.05 *versus* Control.

Figure 28b reports the respiration rate values of cells treated and untreated with melatonin after each addition. As shown in this figure the basal respiration is lower in HaCaT cells incubated with melatonin respect to control cells. As shown in figure 28a, within 10 minutes incubation with 8 μg/ml digitonin, cell respiration slowly decreases to approximately 50 % of the initial value, as expected due to partial membrane permeabilization and loss of reducing substrates and ADP. The addition of 2 mM ADP, 8.8 mM pyruvate and 4.4 mM malate induces an increase in cell respiration.

In the presence of digitonin, infact, pyruvate, malate and ADP can enter into the cells. Pyruvate and malate are substrates generating NADH, therefore at these stage, the respiration driven by Complex I was observed and interestingly is about 20 % lower in HaCaT cells incubated with 1 nM melatonin than in control cells (Fig. 28b). The addition of 0.5 μM rotenone (Rot), inhibitor of Complex I, abolishes almost completely respiration. After the addition of 10 mM succinate, the substrate that reacts directly with Complex II, the oxygen consumption was restored. Under these conditions the differences of respiration rate between HaCaT cells incubated in the presence and absence of melatonin are maintained, although attenuated. 5 μM Antimycin A (Ant a), by inhibiting Complex III, almost abolishes respiration, restored by adding reduced cytocrome c in the presence of ascorbate (ASC) and TMPD. Ascorbate maintains TMPD in a reduced state so that electrons can flow freely from TMPD to cytochrome c. These conditions ensure the highest electron transfer efficiency at the complex IV site. The O_2 consumption rate reached respectively 336 pmol O_2 s^{-1} mg^{-1} of proteins for control cells and 260 pmol O_2 s^{-1} mg^{-1} of proteins for cells incubated with 1 nM melatonin. The addition of exogenous cytochrome c to the respiring cells did

not affect respiration, proving the integrity of the mitochondrial outer membrane, and suggesting that, as performed, the mild digitonin treatment causes small ions and molecules permeabilization, but not loss of cytochrome c, at least on the time window explored (Fig. 28b).

4.7 Determination of variation in ATP levels in melatonin treated cells.

The effects of melatonin on the cellular metabolism were explored by measuring the ATP and lactate production. The ATP concentration levels of cells treated for 6 h with melatonin, 1 nM, was assayed either at steady state in the presence or absence of glucose or kinetically by following the rate of ATP production (Fig. 29). The stationary ATP concentration of the cells was performed in the presence or absence of 11 mM glucose for 4 h and 2.5 µg/ml oligomycin during the last 1.5 h of incubation. The starvation of glucose is necessary to minimise glycolysys and the ATP-synthase inhibitor oligomycin to inhibit OXPHOS. As shown in figure 29a in the presence of glucose the ATP concentration of cells treated or not with melatonin and/or olygomycin is similar as expected based on the contribution of both glycolysis and OXPHOS to ATP formation. After cell glucose starvation and upon minimizing the glycolitic contribution, the ATP level decreases and the addition of oligomycin induces a significant inhibition of ATP production (Fig. 29b). Under these conditions, the difference between the ATP measured in the absence and presence of olygomicyn (ΔATP) is indicative of ATP_{OXPHOS}. The ATP_{OXPHOS} value divided by the basal ATP concentration, measured in the presence of glucose, approximates the fraction of ATP_{OXPHOS}/ATP_{total}. This fraction (Fig. 29c) is lower in melatonin treated cells compared to controls.
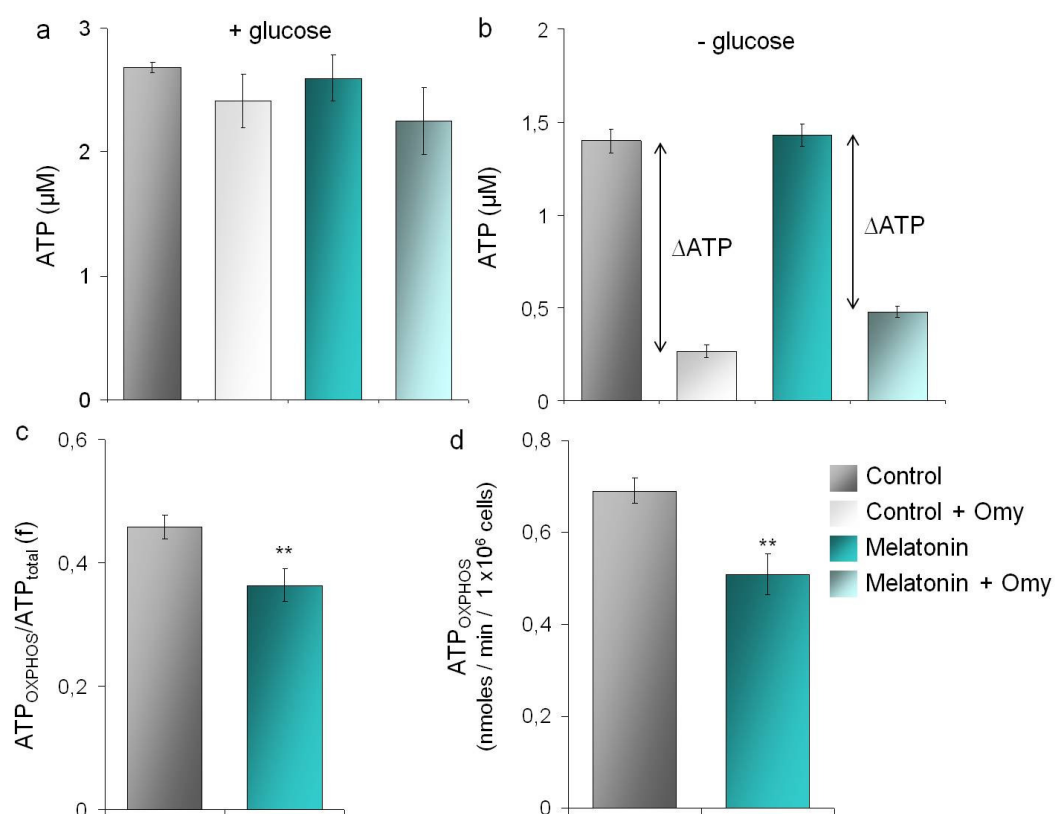
Fig. 29: Effect of melatonin on the ATP production. (a, b, c) Stationary ATP concentration levels evaluated in intact HaCaT cells (5×10^5/ml) in the presence and absence of melatonin 1 nM, oligomycin 2.5 μg/ml and glucose 11 mM, as specified in the figure. Omy: oligomycin. a) Measurements of ATP in the presence of glucose. b) Measurement of ATP in the absence of glucose. ΔATP = ATP$_{OXPHOS}$. c) Fractional ATP (f) = ATP$_{OXPHOS}$ / ATP$_{total}$; ATP$_{OXPHOS}$ = ΔATP (panel b); ATP$_{total}$ has been measured in the presence of glucose and absence of oligomycin. Data $\pm$ SEM; n = 12. ** P $\leq$ 0.01 *versus* Control. d) Rate of mitochondrial ATP synthesis. Data $\pm$ SEM, n $\geq$ 14. ** P $\leq$ 0.01 *versus* Control *(modified from Arese et al., 2013)*.

Chapter 4. Results

The effect of melatonin on the ATP_{OXPHOS} production was assessed directly by measuring the rate of succinate-driven ATP synthesis [407]. As shown in figure 29d, the rate of ATP production (nmoles ATP/minutes/$1x10^6$ cells) is lower in cells treated with melatonin than in untreated cells. After 6 h incubation with 1 nM melatonin the rate of ATP production is 0.51 ($\pm$ 0.044) nmoles/min/10^6 cells to be compared with 0.69 ($\pm$ 0.028) nmoles/min/10^6 cells of control cells. This result suggest that melatonin induces approximately 30% depression of ATP_{OXPHOS} production.

4.8 Effect of melatonin on lactate production in HaCaT cells.

The effect of 1nM melatonin on the relative contribution of OXPHOS and glycolysis to the overall ATP production was independently evaluated by comparing the concentration of lactate produced by HaCaT cells incubated for 3 h at 37 °C in a medium containing 1 mM glucose and in the absence or presence of the respiratory chain inhibitors, antymicin A and mixhotiazole both at 10 μM concentration. Cells were pre-incubated for 1 h in a glucose free medium to prevent differences in the availability of endogenous substrate. As shown in figure 30a, the basal lactate concentration in controls is on average 68 μg / 1 x 10^6 cells; this value rises to 80 μg/ 1 x 10^6 cells after melatonin treatment.

The melatonin induced increase of lactate production is consistent with the conclusion that melatonin partially inhibits OXPHOS, and glycolysis is compensating. As expected, in the presence of antimycin A and myxothiazole, the lactate increases in controls as in melatonin treated cells; in these latter, however, to a minor extent as if stimulation of glycolysis was additive. Assuming that the Warburg effect compensates exactly for the inhibition of respiration induced with

99

inhibitors, it follows that the amount of lactate, produced under basal conditions is equivalent to the glycolytic ATP, whereas the difference between the lactate produced in the presence of the inhibitors and the basal glycolitic lactate, defined as Δlactate, is proportional to ATP_{OXPHOS}.
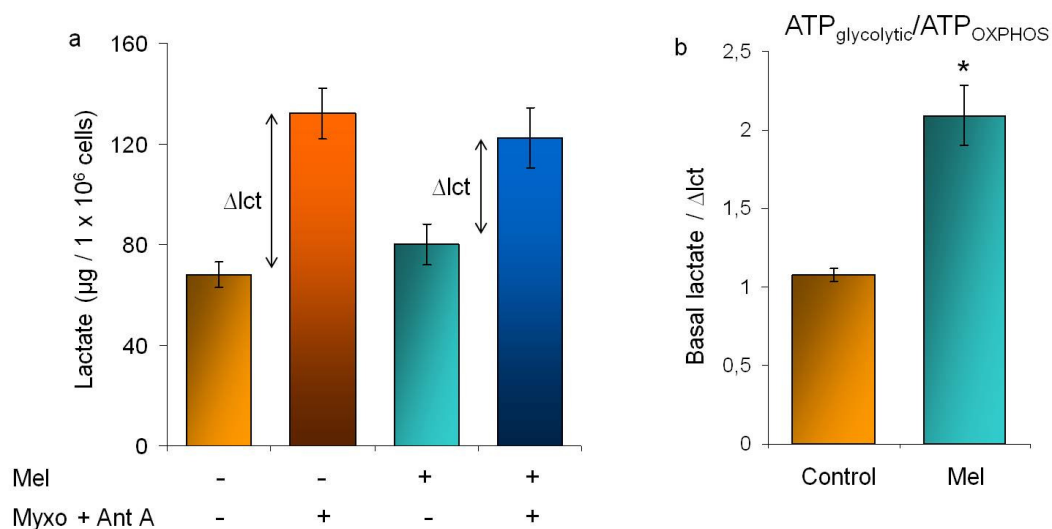
Fig. 30: Effect of melatonin on the lactate accumulation in the medium of HaCaT cells. a) Lactate production assayed in HaCaT cells incubated 6 h with 1 nM melatonin and 3 h with 1 mM glucose and in the presence and absence of myxothiazol (Myxo) and antimycin A (Ant A), 10 μM each. Basal lactate is produced by the cells in the absence of inhibitors and has been taken as ≈ $ATP_{glycolytic}$. The lactate produced in the presence of inhibitors has been taken as the maximal lactate (total). The difference between lactate produced in the presence of inhibitors and basal lactate is indicated as Δlct; Δlct ≈ ATP_{OXPHOS}. b) Ratio between basal lactate and Δlct, as indicative of the $ATP_{glycolytic}$/ATP_{OXPHOS} ratio. Values are the means ± SEM; n = 4. * p ≤ 0.05 *versus* Control *(modified from Arese et al., 2013).*

The basal lactate divided by Δlactate has been taken as indicative of the ratio between ATP glycolitic and OXPHOS. As shown in figure 30b, the

$ATP_{glycolytic}/ATP_{OXPHOS}$ ratio is lower in control (~ 1.1) than in cells treated with melatonin (~ 2.1).

4.9 Effect of melatonin on ROS production in HaCaT cells.

The evaluation of ROS production, carried out using HaCaT cells pre-loaded with the DCFDA fluorescent probe, showed that the ROS accumulation is lower in HaCaT cells incubated 6 h with melatonin 100 μM than in control cells, by ~ 20%, whereas the ROS production in HaCaT cells treated 6 h with melatonin 1 nM is comparable with Control cells (Fig. 31).
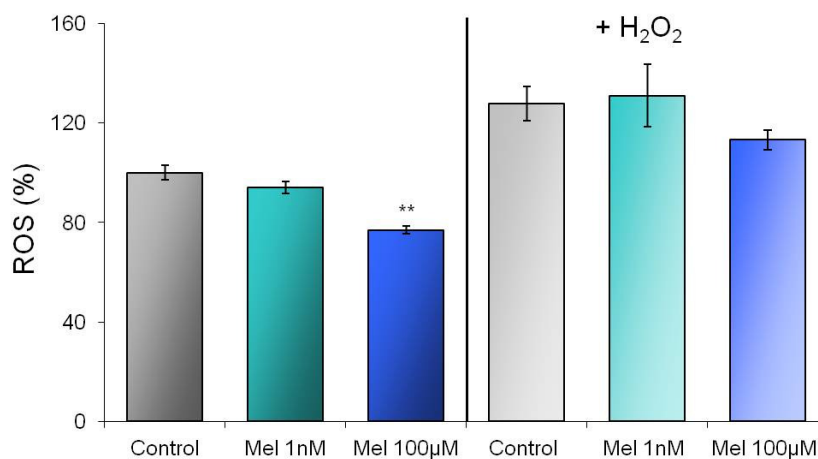
Fig. 31: Effect of melatonin on reactive oxygen species (ROS) production. ROS production was measured in cell suspension (at density 10^6/ml) containing DCFDA 0.1 mM. H_2O_2 500 μM was added, as indicated. The kinetics of DCFDA fluorescence was followed for 120 min. The percentage of ROS production is taken at 100 min. Data values are the means ± SEM; $n \geq 8$. **$P \leq$ 0.001 versus Control.

Chapter 4. Results

Consistent with literature, the addition of 500 µM H_2O_2 induced an enhancement of ROS production, less evident, however, in HaCaT cells incubated with 100 µM melatonin. Under these conditions, the effect shown in the results previously reported can not be attributed to the antioxidant activity of melatonin but rather to a specific cell signalling occurring at low nM concentration.

4.10 Citrate Synthase

The citrate synthase activity of HaCaT cell treated 8 h with melatonin was evaluated.
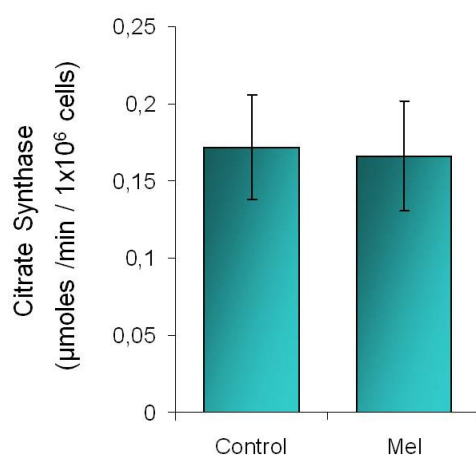
Fig. 32: Citrate Syntase in HaCaT cells. HaCaT cells, incubated in the presence and absence of 1 nM melatonin were lysed. Cell lysates were assayed for Citrate Synthase spectrophotometrically. Data values are the means ± SEM; $n \geq 3$.

As shown in Fig. 32, HaCaT cells ($1x10^6$) used as such or after incubation with melatonin display a similar citrate synthase activity.

102

4.11   Nitrate/Nitrite (NO$_X$) accumulation in CHO and 7PA2 cells

The amount of NO produced by CHO and 7PA2 cells was evaluated measuring the nitrate and nitrite (NO$_X$) content in the cell medium after 4 h of accumulation (see Methods).
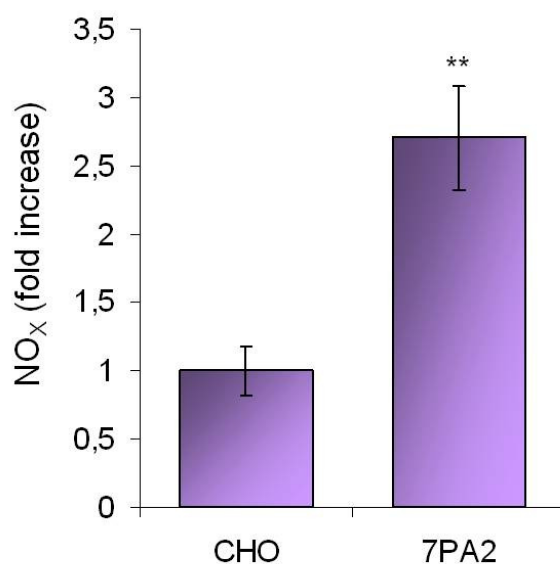
Fig. 33: NO$_X$ production in CHO e 7PA2 cells. NO$_X$ content in the supernatant of CHO and 7PA2 cells measured after 4 h of accumulation. Data shown as fold increase *versus* control (CHO). Data +/− SEM, $n \geq 7$. ** P $\leq$ 0.01 *versus* CHO.

The result is reported in figure 33 and show that the NO$_X$ produced by 7PA2 cells is significantly higher than that of control (CHO) cells. Compared to control, 7PA2 cells are characterized by a ~ 2.5 fold increase in NO$_X$ accumulation.

4.12   ROS production in CHO and 7PA2 cells

The intracellular ROS generation was measured fluorimetrically in CHO and 7PA2 cells (see Methods). The results show that the 7PA2 cells ROS level is higher compared to the CHO controls. ROS production by 7PA2 cells is ~ 25 % higher than in controls (see Fig. 34).
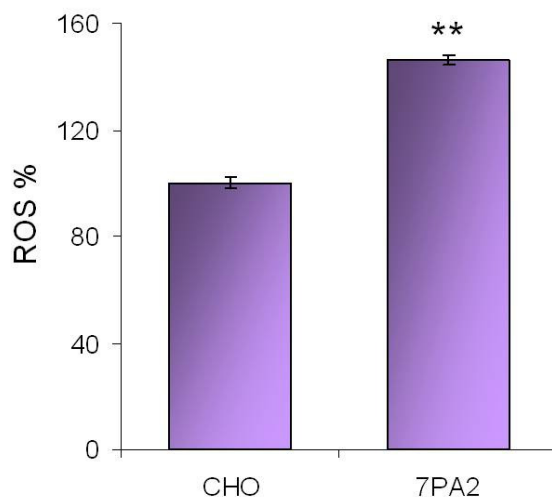
Fig. 34: ROS production in CHO e 7PA2 cells. ROS production in CHO and 7PA2 cells measured following the kinetics of DCFDA fluorescence for 120 min. The percentage of ROS production is taken at 60 min. Data values are the means ± SEM; $n = 8$. ** P ≤ 0.001 *versus* Control (CHO) *(modified from Krako et al., 2013).*

4.13   Mitochondrial membrane potential in CHO and 7PA2 cells

The mitochondrial membrane potential of CHO and 7PA2 cells was assayed following the accumulation into the mitochondrial matrix of the fluorescent cationic probe JC-1 and the accumulation of red fluorescent J-aggregates into the

mitochondrial matrix, in the presence of nigericin, converting ΔpH in $\Delta\psi$. Typical kinetics of red fluorescence accumulation in 7PA2 cells and CHO controls are shown in figure 35a. The differences between the maximum, reached about 60 minutes after addition of nigericin, and the minimum obtained upon addition of 0.2 μM valinomycin is defined as ΔF and is proportional to $\Delta\mu H^+$. Valinomycin causes mitochondrial dissipation of the $\Delta\Psi$ leading to a fast bleaching of the fluorescence signal.
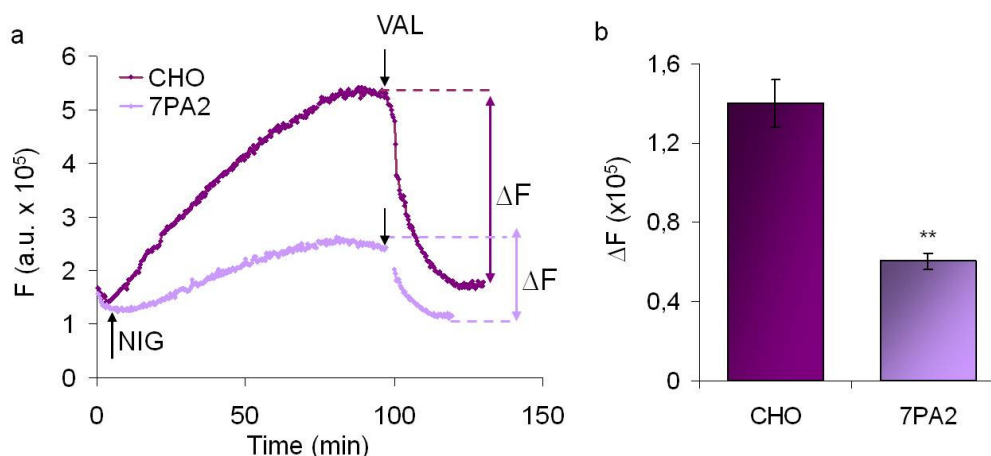
Fig. 35: Mitochondrial membrane potential in CHO and 7PA2 cells. a) Time-dependent JC-1 accumulation into mitochondria of CHO and 7PA2 cells ($3x10^6$ cells/ml). The differences between the maximal fluorescence, reached about 60 minutes after addition of 0.6 μM nigericin (NIG), and the minimum obtained upon addition of 0.2 μM valinomycin (VAL) is the ΔF proportional to $\Delta\mu H^+$. b) ΔF values, the level of mitochondrial membrane potential of CHO and 7PA2 cells normalized for $1x10^6$ cells/ml was reported as the ΔF obtained as in panel a. Data $\pm$ SEM, $n \geq 13$. ** P $\leq$ 0.001 *versus* Control (CHO) *(modified from Krako et al, 2013)*.

As shown in figure 35b, the 7PA2 cells are characterized by an approximately 60% lower mitochondrial membrane potential compared to CHO controls.

1 0 5

4.14 Mitochondrial respiration in CHO and 7PA2 cells

Cell O_2 consumption has been evaluated oxygraphically in intact CHO and 7PA2 cells respiring under basal metabolic conditions. Nigericin was added to allow maximal $\Delta\psi$ formation and once reached valynomicin was added. In the presence of both ionophores the H^+ electrochemical potential gradient is fully collapsed and the control (inhibition) exerted on the respiratory chain is abolished. The 7PA2 cells display an approximately 30% decrease of basal respiration, compared to controls (Fig. 36a). In the presence of both ionophores cell respiration increases by a factor of ~ 2.4 in control CHO cells and 1.6 in 7PA2 cells (see Fig. 36b).
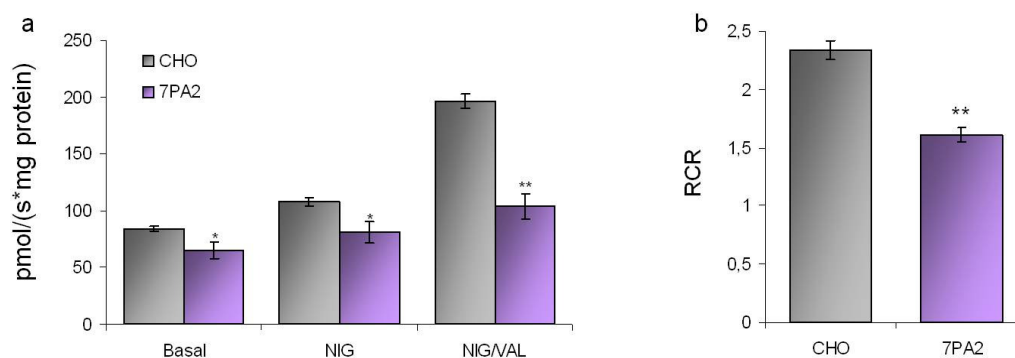
Fig. 36: Cell respiration and respiratory control ratio of CHO and 7PA2 cells. a) Oxygen consumption of intact cells ($3,3\times10^6$ cells/ml). Basal: respiration rate overall; NIG: respiration rate after addition of 0.6 μM nigericin; NIG/VAL: respiration rate measured after the subsequent addition of 0.2 μM valinomycin to cells respiring in the presence of nigericin. b) Respiratory control ratio (RCR) obtained as the ratio between the rate observed in the presence of both nigericin and valinomycin (NIG/VAL) and in their absence (Basal respiration). Data values are the means ± SEM; $n \geq 5$. ** P $\leq$ 0.001 *versus* Control (CHO) *(modified from Krako et al., 2013)*.

106

The contribution of the respiratory complexes to cellular respiration was evaluated in CHO and 7PA2 permeabilazed cells following the protocol published by Kuznetsov and collaborators, as adapted to our cell lines.
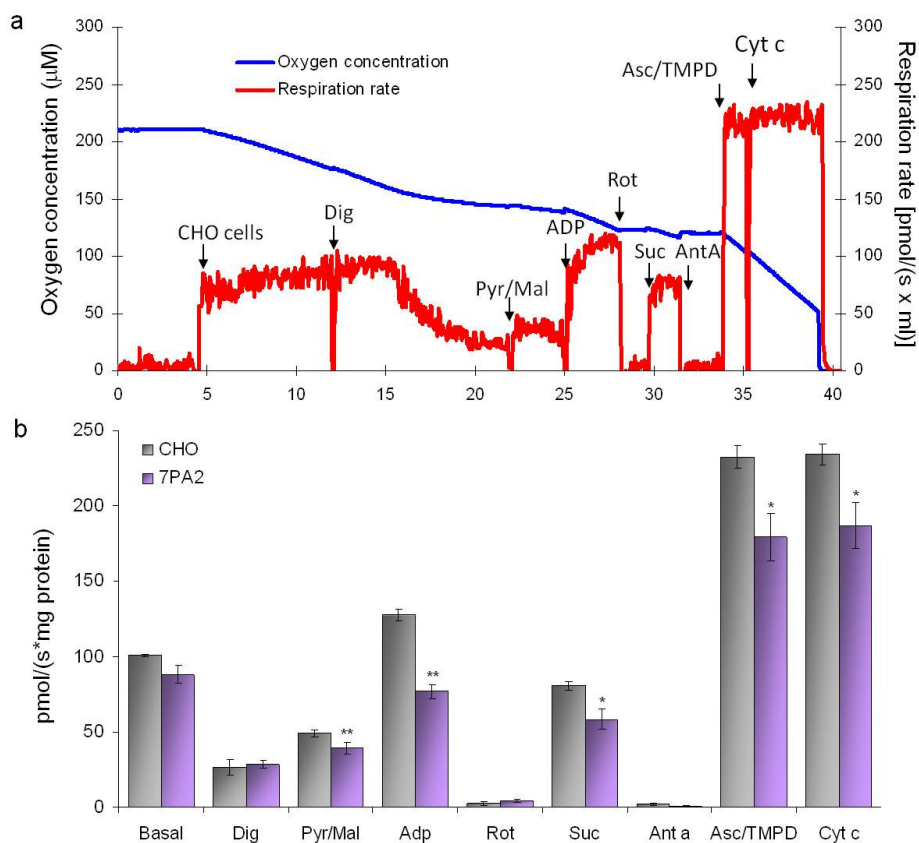
Fig. 37: Cellular respiration in digitonin-permeabilized CHO and 7PA2 cells. a) Typical oxygraph trace of 5×10^6 CHO cells. Blue line: oxygen concentration trace; red line: O_2 flux, i.e., oxygen consumption rate. b) Respiration rate values in CHO and 7PA2 cells recorded after each addition step (of substrate/inhibitor) during the trace. Data values are the means ± SEM; $n \geq 5$. * P $\leq$ 0.05 *versus* Control (CHO); ** P $\leq$ 0.001 *versus* Control (CHO) (*modified from Krako et al., 2013*) .

Briefly, as shown in figure 37a, when the oxygraphic signal becomes stable, digitonin is added to the respiring cells. The digitonin concentration used and its incubation time was optimized to the sensitivity of the cells, by mean of a concentration and time dependence titration; optimal substrate permeation was obtained using 1.8µg digitonin /$1x10^6$ cells, for 10min. After the addition of digitonin, the oxygen consumption slowly decreases and reaches a minimum value within 10 minutes of incubation. The addition of NADH generating substrates (pyruvate and malate), followed by addition of ADP fully restores respiration. As shown in figure 37b, at this step, the oxygen consumption of 7PA2 cells is significantly lower by ~ 40 % than controls. The addition of rotenone leads to the inhibition of Complex I and consequently respiration is arrested. The addition of succinate stimulates Complex II activity and allows respiration to restart bypassing Complex I. Under these conditions, the difference of respiration between 7PA2 and control cells though maintained, looks somewhat attenuated, as if impairment of Complex I in 7PA2 cells was higher than that of Complex II. To assess the Complex IV activity, the respiration was inhibited Antimycine A, a specific inhibitor of Complex III, in the presence of exogenous reductants of complex IV via cyt c, namely Ascorbate and TMPD. The respiration of 7PA2 cells at this step is more than 20 % lower respect to CHO control cells (Fig. 37b). In the last step, reduced cytochrome c is added to respiring cells; the absence of effects on the rate of respiration proves the integrity of mitochondrial outer membrane. In conclusion, the 7PA2 cells show an impairment of electron transfer, more evident at the level of complex I and complex IV.

4.15   ATP production by CHO and 7PA2 cells

The CHO and 7PA2 ATP concentration level was measured in the presence or absence of 1 mM glucose. Glucose starvation was performed to promote OXPHOS while minimizing the glycolitic contribution to the ATP production. In the absence of glucose the addition of 2.5 μg/ml oligomycin induces a dramatic decrease of ATP, due to OXPHOS inhibition. Under these condition, the difference between the ATP measured in the absence and presence of oligomycin, defined in figure 38a as ΔATP is, within a gross approximation, indicative of the ATP$_{OXPHOS}$ (fig. 38a).
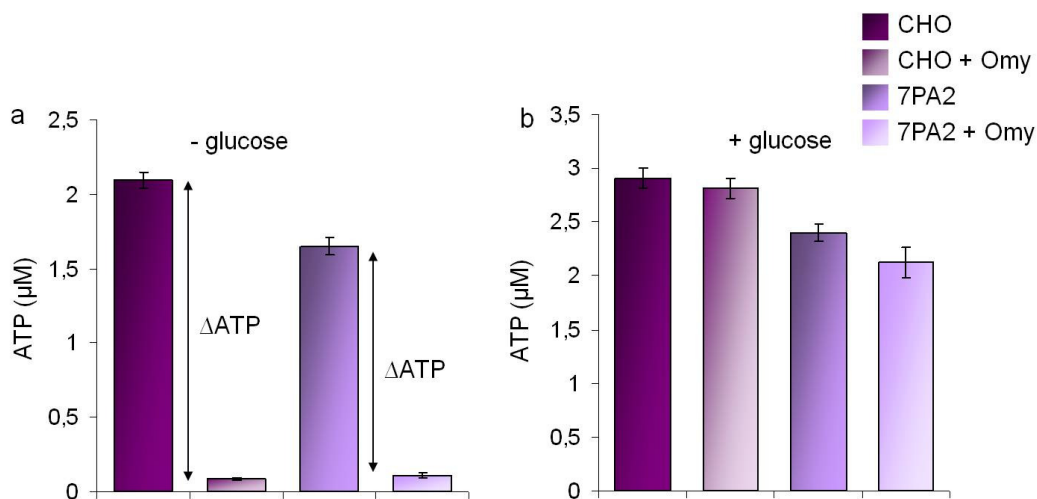
Fig. 38: ATP production in CHO and 7PA2 cells. ATP measurements evaluated in intact CHO and 7PA2 cells (5×10^5/ml) in the presence and absence of oligomycin 2.5 μg/ml and glucose 1mM. a) Measurement of ATP after 3 h cell glucose starvation. ΔATP: difference of ATP measured in the absence and in the presence of oligomycin (corresponding to ATP$_{OXPHOS}$). b) Measurements of ATP in the presence of 1mM glucose. Omy = oligomycin. Data ± SEM; $n \geq 6$ (*modified from Krako et al., 2013*).

The results suggest that the ATP_{OXPHOS} levels is more than 20 % lower in 7PA2 cells compared to CHO cells. In the presence of glucose the ATP concentration increases and the effect of oligomycin is no longer evident, this is due to glycolysis compensation to OXPHOS inhibition (Warburg effect).

As shown in figure 38b under this condition a fully efficient glycolytic induction response is operative in CHO cells where the ATP concentration is the same before and after treatment with oligomycine. This is not the case of 7PA2 cells, displaying a ~ 20 % decrease of the total ATP concentration (OXPHOS + glycolytic), that becomes even more evident when OXPHOS is inhibited by oligomycin.

4.16   Lactate production in CHO and 7PA2 cells

The lactate production by CHO and 7PA2 cells was evaluated before and after treatment of Complex III inhibitors (antymicin A and mixhotiazole). The lactate produced under basal conditions is higher in 7PA2 cells than in control CHO cells. This result is fully consistent with a different glycolytic contribution to ATP synthesis in the 7PA2 and control cell lines. As expected, in the presence of OXPHOS inhibitors, some additional lactate is produced, due to glycolytic compensation of ATP loss (Warburg effect). These results are reported in figure 39, where the histogram bar is divided in two parts, for each cell lines: the lower part (light grey) represent the basal lactate production, while the higher part (violet) represent the compensating Warburg lactate. This Warburg lactate is indicative of the OXPHOS contribution to ATP synthesis. The basal lactate production of 7PA2 cells is ~ 47 % of the total lactate, to be compared to ~ 38 %

of the CHO control cells, whereas the Warburg lactate production is ~ 53 % in 7PA2 cells and 62 % in controls.
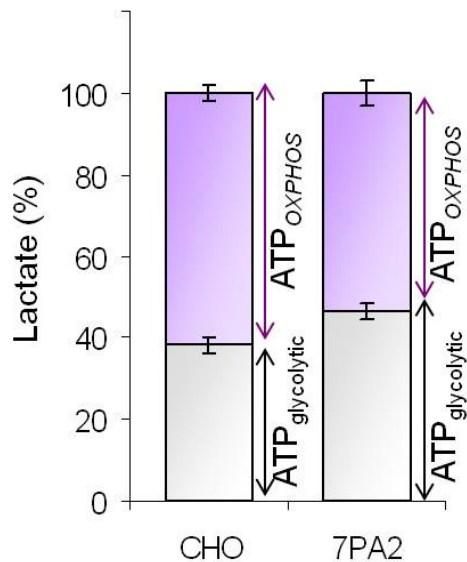
Fig. 39: Lactate production in CHO and 7PA2 cells. Lactate accumulation in the cell medium of CHO and 7PA2 cells after 2.5 h of incubation in the presence of glucose 1 mM and in the presence and absence of myxothiazol and antimycin A, 5 μM each. The lactate produced in the presence of inhibitors has been taken as the maximal lactate (total, 100 %). The difference between total and basal lactate is the Warburg lactate (violet); Warburg lactate ≈ ATP_{OXPHOS}. The lactate produced in the absence of the inhibitors is the Basal lactate (grey); Basal lactate ≈ $ATP_{glycolytic}$. Values are the means ± SEM; $n \geq 5$ *(modified from Krako et al., 2013)*.

This data strengthen the hypothesis that in 7PA2 cells OXPHOS is impaired and glycolysis compensates.

111

5. DISCUSSION AND CONCLUSION

The nitrogen monoxide (NO), nitric oxide in the literature, is a biological messenger which regulates several and important physiological responses including relaxation of smooth muscle, neurotransmission, cell migration and mitochondrial respiration [40, 41, 43-45]. NO is implicated not only in numerous physiological processes but also in several pathologies such as hypertension, cardiovascular dysfunctions, neurodegeneration, arthritis, asthma and septic shock [68-85]. Evidence is growing that the (physiological *versus* toxic) effects of NO resides on its concentration levels: NO in the low concentration range (pico-nanomolar) induces physiological responses, whereas NO in the high concentration range (micromolar) is involved in several pathologies. The NO concentration level in the cell varies depending on the relative rate of its production, degradation and scavenging. A wide variety of biological responses has been observed influencing these processes and consequently lowering or enhancing the nitric oxide availability. The enzymatic endogenous NO production depends on the activation or inhibition of the nitric oxide synthase (NOS) whose activity is controlled by different stimuli or effectors. The NO concentration level is also influenced by the specific NOS isoforms activated: the constitutive NOSs, i.e. the endothelial NOS (eNOS) and the neuronal NOS (nNOS), producing NO in the nM range, whereas the inducible NOS (iNOS) releasing up to µM NO. In the cell, the NO availability is controlled by NO scavengers, such as hemeproteins or reduced glutathione. The NO recycled from nitrite is also relevant to its bioavailability.

113

Chapter 5. Discussion and Conclusion

It is nowadays established that NO inhibits mitochondrial respiration. The inhibition is induced by the reaction of NO with some of the respiratory chain complexes, particularly with Complex I and IV, according to mechanisms studied over about 25 years. The interaction between NO and complex IV, cytochrome *c* oxidase (CcOX), is of particular interest, being rapid and reversible [51-55]. The reaction of NO with mitochondrial complexes has a potential patho-physiological relevance for the implications on cell bioenergetics and is therefore subject intensively studied. The transient and reversible inhibition of mitochondrial respiration may induce a physiological, compensatory activation of glycolysis [410]. This original observation by Warburg in our days has been re-proposed by Almeida and collaborators [56], who compared the different energetic behaviour of astrocytes and neurons inhibited by NO. In this respect, it is worth considering that different cell lines may trigger a different glycolytic compensatory activity in response to the NO inhibition of OXPHOS [56]. The evidence collected suggests that, if NO remains available in the mitochondrial environment, the mitochondrial membrane potential decreases, and glycolytic contribution became relevant to ATP synthesis. Thus, it seems crucial that cells responding to NO pulses are endowed with an efficient glycolytic machinery able to compensate for the decreased aerobic ATP production [56, 411]. In the absence of a suitable glycolytic compensation, the ATP levels could decrease dramatically, leading to cell death [57].

On this basis, we decided to explore the interplay between NO and cell bioenergetics both in a physiological context, such as HaCaT cells stimulated with physiological melatonin concentrations or in pathological frame such as cell model of Alzheimer's disease.

Chapter 5. Discussion and Conclusion

Among its multiple physiological actions, it has been suggested that NO plays a key role also in the circadian and homeostatic regulatory processes of sleep [60-63] [64-67]. NO, in fact, acts as a powerful sleep-promoting agent, as revealed following the production of nitrite and nitrate, characterized by a circadian night peak [412] and also considering that the nNOS activity is involved in the regulation of sleep-wake cycle [413, 414]. *In vivo* experiments using nNOS inhibitor or the nNOS KO mice strengthened the idea that REM sleep is regulated with nNOS-derived NO [67]. In the central nervous system (CNS), the nNOS mediates long-term regulation of synaptic transmission. In particular the nNOS seems to play an important role in long term potentiation (LTP) [415, 416]. LTP is a putative mechanism of memory formation in hippocampus [417]. Moreover, an impressive amount of evidence shows that inhibition of nNOS impairs learning and memory [90, 418-420]. Considering that sleep loss produces a decline in cognitive and motor performance [421], learning and memory deficits [422] and mood disturbances and that these effects are restored by prolongation and intensification of sleep [67], nNOS may be a joining link between the learning and memory processes and sleep.

One of the principal agent in the regulation of sleep-wake cycle is melatonin, a small, lipophylic molecule, popular for preventing jetlag or as adjuvant in elderly people with sleep-problems [423]. Originally recognized as the hormone of the pineal gland, melatonin is produced also by other extrapineal sites [180]. In humans, the melatonin-generating system is photosensitive displaying a circadian rhythm, with the highest concentration levels produced at night, in the darkness [186]. Importantly, melatonin production decline with age [186, 354]. Among the wide diversity of physiological effect reported for melatonin [187, 189, 199, 201, 203-216, 354], high relevant is the capacity to directly scavenge RONS [203, 204,

213]. The free radical-scavenging capacity of melatonin also extends to its metabolites in a free radical-scavenging cascade that prolongs its useful life [181]. Moreover, melatonin is able to induce the over-expression of antioxidant enzyme [271-275] and to inhibit pro-oxidant enzymes such as the iNOS [242, 276, 277]. Stimulated by the notion that both melatonin and NO are involved in the regulation of sleep-wake cycle and that NO controls mitochondrial respiration, we decided to investigate whether a relationship between melatonin, nitric oxide and cell bioenergetics was operative.

In contrast with what expected from the literature proposing melatonin as a simple chemical radical scavenger, using HaCaT cells in culture as targets, we have observed unexpectedly that nM melatonin induces the increase of the nNOS mRNA expression by a factor ~ 4. Consistently with a receptor mediated nuclear DNA-activated process, no effects of melatonin were observed at incubation times earlier than 3-4 h. According to our observations, the maximum peak of nNOS mRNA expression is observed after 6 hour of incubation with melatonin. At melatonin concentrations higher than nM, and/or by further extending the melatonin incubation time the nNOS expression decreases returning to a basal level; this kind of biphasic regulation suggests the existence of a time and concentration-dependent negative feed-back, finely, controlling of the nNOS mRNA expression by melatonin, at least in HaCaT cells. Moreover, within the limits of the heterogeneous distribution of melatonin among organ and tissues [263], it is intriguing that the concentrations of melatonin, in the nM range, inducing the observed changes of the nNOS mRNA are compatible with the melatonin circulating levels in the human blood at night (peak value ~ 100–200 pg/mL, corresponding to ~ 1 nM melatonin) [180, 201]. The upregulation of the nNOS mRNA expression by melatonin appears specific, as indicated by the fact

1 1 6

that over the same time period, the eNOS expression remains constant and the iNOS is not detectable. The nNOS protein synthesis lags behind the rise of the corresponding nNOS mRNA: the protein increases transiently, and within hours, returns back to its basal level. The maximum peak of nNOS protein expression is observed after 8 h of incubation with melatonin. The ~ 2 h shift between the protein and the mRNA synthesis is consistent with a nuclear DNA-dependent pathway. Almost synchronously also the production of nitrate and nitrite (NOx) increases. An increase of NO_X production in the culture medium of HaCaT cells was already observed after 6 h of incubation with melatonin and is even more increased after 8 h of incubation. This result shows that the last 2 hours of incubation are the most relevant time range where the nitrate and nitrite, and therefore NO, are produced. Interestingly, from the bioenergetic point of view, following incubation with nanomolar melatonin and on a time scale similar to that of both the nNOS changes and the NOx accumulation, the mitochondrial membrane potential decreases by ~ 20 %; the mitochondrial respiration also is slightly, but significantly depressed (~ 10 %) suggesting that under these conditions and at least in keratinocytes mitochondria, the mechanism(s) responsible for maintenance of $\Delta\Psi$ are more affected than respiration [424]. It is worth noting that when the cells were starved from the NOS substrate Arginine, the electrophoretic import of JC-1 was the highest, confirming that cultured cells express a basal NOS activity, releasing NO and depressing the mitochondrial potential to a measurable extent [31]. Furthermore the addiction of 7-nitroindazole (7N), specific nNOS inhibitor, to cells pre-incubated with melatonin reverts completely the decrease of cell respiration. These results indicate that in the presence of melatonin the inhibition of mitochondrial respiration is partial, reversible and mediated by NO. According to our measurements, the NO released

after a melatonin incubation limited in extent and time, would lead to a partial inhibition of Complex IV following predominantly the PW1 [8], leading to the formation of a labile Complex IV-NO_2^- derivative. Interestingly, and relevant to the melatonin effects herein described, the activity of Complex IV is promptly recovered upon decreasing the NO bioavailability. Under the conditions explored, that is, low NO concentration, the involvement of complex I, though possible, is less likely [131]. The analysis of the functional state of the respiratory chain complexes seems to confirm that, in the presence of melatonin, the inhibition is located at the level of complex IV.

Synchronously with the down regulation of the respiratory chain, a partial decrease of ATP_{OXPHOS} production is observed. The inhibition of ATP_{OXPHOS} production is better observed in the absence of glucose, when the contribution of glycolysis is minimized. Under these conditions, the overall ATP level is almost halved, compared with cells maintained in glucose [411]; the addition of oligomycin causes a dramatic decrease of ATP, whose amplitude is indicative of the OXPHOS contribution to the overall ATP detected. The ATP_{OXPHOS} produced by melatonin-treated cells is reproducibly smaller than in controls. The effect, though statistically significant, is small, likely due to an efficient glycolytic compensation. OXPHOS impairment and glycolytic compensation have been further substantiated measuring lactate [408]. The basal lactate, whose concentration is proportional to the $ATP_{glycolitic}$, is higher in cells treated with melatonin. These results are in accordance with the literature data showing an up-regulation of glycolytic enzymes in the rat pineal gland [425]. In the presence of OXPHOS inhibitors, the lactate production increases in both melatonin treated and untreated cells. This is due to glycolytic compensation to the overall ATP production. The difference between lactate produced in the presence and absence

of OXPHOS inhibitors is proportional to ATP_{OXPHOS}, whose value is lower in cells treated with melatonin relying on glycolysis to a significant extent.

Taken together, these findings suggest that nanomolar melatonin administered to intact HaCaT cells produces a transient but substantial rise of the constitutive nNOS, producing NO. The induced increase of NO leads to a reversible and partial inhibition of the respiratory chain with a decrease of mitochondrial $\Delta\psi$ and depression of OXPHOS. This leads, in turn, to a transient metabolic shift towards glycolysis. The mechanism through which low melatonin concentrations in the extracellular medium might induce the increase of nNOS expression is still unclear. It presumably involves a receptor-mediated melatonin signalling. Among keratinocytes, the HaCaT cell lines express the cell surface MT2-type receptor (isoform MT2b) and the nuclear receptors, that is, the retinoid orphan receptor (RORa) and the NQO2 flavoprotein, also known as the MT3 melatonin binding site [426-428]. It is tempting to speculate that a time and concentration-dependent feed-back controls the effects of melatonin on the nNOS and that the basis of this control might involve the melatonin-calmodulin interaction and signalling [429]. In this frame, when the extracellular hormone concentration is low (nanomolar or less), the nuclear mediated nNOS activation occurs, also sustained by the cell availability of calmodulin (high affinity nNOS cofactor [430]). As the incubation time increases, the intracellular concentration of melatonin (and/or its metabolites) proportionally increases; at this stage, due to the high affinity of melatonin for calmodulin [248] a competition of melatonin and nNOS both for calmodulin occurs, inducing progressive nNOS inhibition as the melatonin concentration rises [303] (Fig. 40). The existence of such equilibrium, if confirmed, would explain the results observed, also reconciling some discrepancies in the literature about the effects of melatonin, both on mitochondria and NOS. In conclusion melatonin

119

seems to act as a modulator of nNOS activity and consequently as a modulator of NO concentration in the cell.
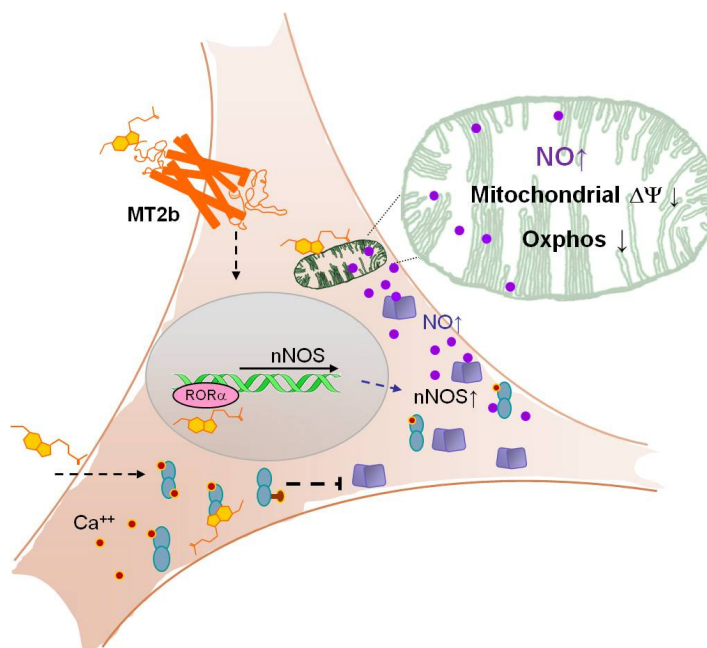
Fig. 40: Melatonin and the "keratinocyte hypothesis". At pico-nanomalar concentration, melatonin induces a significant increase of nNOS overexpression presumably trough a melatonin-receptor-mediated signaling. Under this condition, calmodulin can predominantly interact with nNOS, leading to production of NO and modulation of mitochondrial function. Upon increasing melatonin concentration (>1 nM) in the culture medium or its time of incubation, its intracellular concentration also rises: under these conditions, melatonin inactivates calmodulin (CaCaM) leading to nNOS inhibition *(from Sarti et al., 2013)*.

It has been previously reported in the literature that melatonin counteract the toxic effect of NO exerted when its level are highly increased. In this context, melatonin was proposed to act as a direct free radical scavenger of RONS, inhibits iNOS expression and seizes CaM to nNOS. In our experiments, however, we have

observed that melatonin is able to induce the nNOS expression, without leading to cell damage.

The above consideration lead to the suggestion that melatonin seems to maintain the NO concentration level in a range compatible with a physiological and positive role, such as its function in the processes of learning and memory and in the regulation of mitochondrial respiration. All together these findings could give a contribution also concerning the role played by NO in the regulation of sleep-wake cycle. This data are consistent with a physiological regulation of mitochondrial respiration and cell bioenergetics.

Nevertheless a very different scenario may arise facing a pathological condition such as the Alzheimer's disease (AD). AD is a severe neurodegenerative disorder, characterized by a progressive loss of neurons and synapses particularly in brain region involved in learning and memory. The clinical hallmarks of AD are progressive impairment of memory, learning, judgment and decision making, eventually causing dementia in older people [312, 431].

The key factor in these illness is the amyloid β-protein, also named Aβ-peptides or simply Aβ. The Aβ peptides are produced proteolytically by β- and γ-secretase acting on the β-amyloid precursor protein (APP). The Aβ-peptides are prone to aggregation in highly toxic oligomeric assemblies (Aβ-oligomers).

Recently, the hypothesis that a mitochondrial dysfunction contributes significantly to pathogenesis and evolution of AD was formulated, supporting strong evidence that correlate AD to mitochondrial damage in brain cells. The molecular mechanism underlying the mitochondrial dysfunctions observed in AD is still mostly obscure and the question of a possible role for NO in this context suggests experimental investigation.

In this work, we used 7PA2 cells as a cellular model system of AD. 7PA2 cells are Chinese Hamster Ovary cell lines (CHO) that stably express the human APP isoform, 751 aminoacids in length (APP751) that contains the human Val717Phe (V717F) mutation associated with familial Alzheimer's disease [432-434]. These cells are among the best characterized cellular models of Aβ production and oligomerisation [435].

We have addressed the issue concerning the involvement of NO in the mitochondrial dysfunction in AD by comparing the nitrate and nitrate (NOx) accumulation in the supernatant of CHO (WT) and 7PA2 (mutated) cells. Interestingly, the NOx production is ~ 3 times higher in 7PA2 cells respect to CHO cells. This result suggests a possible bioenergetic impairment in 7PA2 cells and consistently with this finding we have also observed that the oxygen consumption and the mitochondrial membrane potential of 7PA2 cells are strongly impaired. The step by step analysis of the respiratory complexes activity shows a fairly uniform gradual depression of the functional activity of the respiratory chain in AD cells, though more evident at the level of complex I and complex IV. These results are in accordance with a recent study describing an impairment of complex I and complex IV activity induced by synthetic Aβ added *in vitro* [370]. Simultaneously 7PA2 cells display a lower (~ 20 %) stationary production of ATP$_{OXPHOS}$. In addition, the 7PA2 cells seems to be less efficient than controls in compensating with glycolysis the olygomicin-induced OXPHOS impairment, as if the bioenergetic machinery of 7PA2 cells was less properly organized in both the oxidative and glycolytic metabolic compartments. Our findings suggest that the 7PA2 cells are bioenergetically less active than controls. Unfortunately, whether the mitochondrial impairment in AD is induced directly by NO or by Aβ remains uncertain. The Aβ peptides, also, in fact, have been

shown to directly interact with the respiratory complex IV [436] and respiratory complex I *in vitro* [437], and Aβ is detectable in mitochondria [345, 346]. Moreover, the interaction between the Aβ-peptides and membrane bilayers has been previously demonstrated [438]. The Aβ-peptides are able to deeply penetrate and perturb membrane structure, altering its viscosity and permeability properties, also contributing to formation of membrane pores [438]. In the case of 7PA2 cells, the modification of the membrane structure could possibly contribute to the explanations of the observed lower respiratory capacity in these cells. It is also worth to consider that the accumulation of Aβ oligomers may produce sequential inflammatory and oxidative events [439-441]. The literature data are fully consistent with the higher ROS and NOx production herein detected in the 7PA2 cells. Aβ plaques and Aβ oligomers are in the middle of a complex set of interaction among astrocytes, microglia and neurons originating a neuroinflammatory response [311] (Fig. 41). The over-activation of microglia induces the over-expression of pro-inflammatory cytokines and the consequent increase of iNOS expression (Fig. 41). The induction of iNOS in immunocompetent cells leads to NO production at μM (high) concentrations. These high levels of NO could lead to a persistent inhibition of the mitochondrial respiration, according to the PW2 inhibition mechanism [8]. Under these conditions, the mitochondrion produces an excess of O_2^- that reacts with NO to form highly reactive and toxic peroxinitrite ($ONOO^-$), which in turn evokes oxidative stress and damage of proteins, lipids, and finally, mitochondrial dysfunction [78]. These circumstances induced by $ONOO^-$ overproduction lead to a pathological impairment of the cell bioenergetics. It is worth considering that oxidative stress and particularly $ONOO^-$ overproduction is significant in AD. Therefore, the high levels of NO are able to inhibit also Complex I. A constantly

increased NO bioavailability has been shown to induce the S-nitrosation of Cys-39 on the ND3 subunit of Complex I, whose function becomes severely inhibited [131].
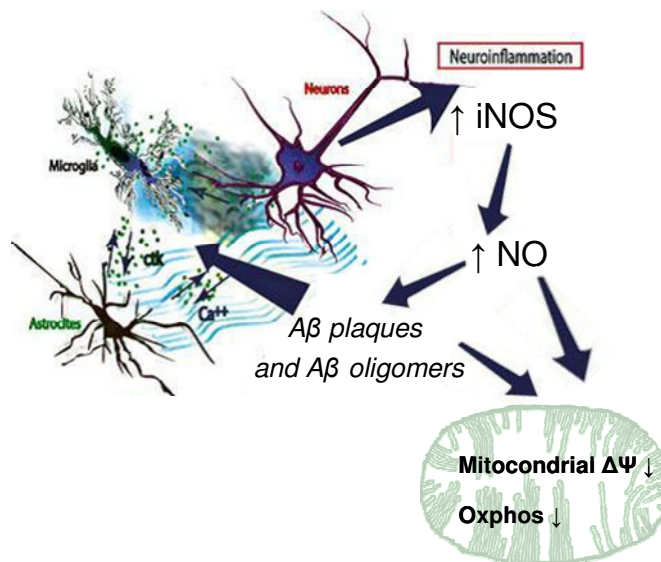
Fig. 41: Alzheimer's disease and mitochondrial dysfunction hypothesis. Aβ contributes to induce neuroinflammation and oxidative stress in early event of AD. A chronic inflammation induces the iNOS expression in immunocompetent cells. The production of high NO levels could lead to a persistent inhibition of mitochondrial respiration, which occurs at the level not only of Complex IV but also of complex I. Under these conditions a mitochondrial dysfunction take place *(modified from Rosales-Corral, 2012)*.

In this frame, it is worth to keep in mind that our AD cellular model systems are actually ovary cells, not neurons. According to our results, the 7PA2 cells display a Warburg effect. Neurons, however, do not perform glycolysis, and a more severe bioenergetic impairment would be expected in the case of neuronal cells of AD patients, due to an intrinsically lower ability to compensate an OXPHOS loss

with glycolysis [57]. The impairment of OXPHOS in neurons of AD patients could certainly lead to more serious consequences such as cell death. Moreover, it was found that neuronal death during AD is associated with increased expression of iNOS and is partially reversed by selective inhibitors of this enzyme [442]. Because iNOS enhances the cellular NO concentration to a greater extent than eNOS or nNOS, it may be an important mediator of cytotoxicity in the brain [80, 443]. Several authors showed a significant impairment of nNOS in the hippocampus of Aβ42 injected aged rats. The decrease of nNOS expression, induces loss of NO-dependent neuronal functions, such as memory and learning [78]. The same authors observed an increase of nNOS expression in the hippocampus of Aβ42 injected young rats. Under these conditions nNOS-derived NO seems to play a protective role against Aβ-induced damage, possibly by inducing an improvement in the learning and memory. In order to counterbalance insufficient tissue oxygenation in AD brain, the eNOS is activated. This can be a positive event in young patients where eNOS keeps blood vessels dilated and in this way NO favours a deeper tissue oxygenation. On the other hand in aged patients the blood vessels are less elastic and NO might fail to induce vasodilatation and brain oxygenation. If this was the case, the hypoxic condition would favor the NO-inhibition of CcOX, following PW2. All these observations indicate that a misbalance among the different isoforms of NOS occurs in AD, although still poorly understood [78]. In conclusion, based on the preliminary evidence shown in this work, we might conclude that nitric oxide plays a critical role in AD.

Is it just a coincidence that while the probability of experiencing AD grows with age, melatonin declines? It has been shown that a cerebral spinal fluid (CSF) deficiency of melatonin precedes clinical symptoms of AD [444]. Moreover sleep

disruptions, nightly restlessness, sun downing and mood disorders are frequently observed in elderly and particularly in patients with AD [311, 445, 446]. These symptoms are related with decreased levels of both melatonin and melatonin receptors in AD patients [447, 448].

A growing body of evidence supports the potential role of melatonin as an effective adjuvant in AD [449-454]. Melatonin is able to scavenge RONS including NO and ONOO$^-$, is a potent antioxidant that inhibits also iNOS expression, modulates pro-inflammatory processes, may impair calcium-dependent toxicity, prevents amyloid overproduction, mitochondrial damage and the apoptotic phenomena related with AD. Also relevant are the protective effects of melatonin on cognition in a variety of tasks of working memory, spatial reference learning and memory and basic mnemonic function, as observed in a transgenic model of AD [455]. It has been shown that MT2 receptor-deficient mice undergo impairment of synaptic plasticity and learning-dependent behaviour, suggesting that MT2 receptors participate in memory processes [456]. It is worth considering that HaCaT cells used in our experiments express the cell surface MT2 receptor and that according to our results nM melatonin induces an over-expression of nNOS in HaCaT cells.

In conclusion, we think that our work may contribute to clarify on one side the melatonin induced effect of NO on mitochondria in a physiological circadian context, while on the other side a possible role of NO in AD.

Considering that melatonin is capable of modulating NO bioavailability and cell bioenergetics, it would be interesting to investigate, therefore, in the future, whether, based on this novel function, melatonin might also have a role in the memory and learning processes altered in AD.

REFERENCES

[1]   Warburg O (1956) On respiratory impairment in cancer cells. *Science* **124**, 269-270.

[2]   Tsukihara T, Aoyama H, Yamashita E, Tomizaki T, Yamaguchi H, Shinzawa-Itoh K, Nakashima R, Yaono R, Yoshikawa S (1996) The whole structure of the 13-subunit oxidized cytochrome *c* oxidase at 2.8 Å. *Science* **272**, 1136-1144.

[3]   Tsukihara T, Aoyama H, Yamashita E, Tomizaki T, Yamaguchi H, Shinzawa-Itoh K, Nakashima T, Yaono R, Yoshikawa S (1995) Structures of Metal Sites of Oxidized Bovine Heart Cytochrome *c* Oxidase at 2.8Å. *Science* **269**, 1069-1074.

[4]   Iwata S, Ostermeier C, Ludwig B, Michel H (1995) Structure at 2.8 Å resolution of cytochrome *c* oxidase from *Paracoccus denitrificans*. *Nature* **376**, 660-669.

[5]   Sarti P, Colosimo A, Brunori M, Wilson MT, Antonini E (1983) Kinetic studies on cytochrome c oxidase inserted into liposomal vesicles. Effect of ionophores. *Biochem J* **209**, 81-89.

[6]   Zaslavsky D, Gennis RB (2000) Proton pumping by cytochrome oxidase: progress, problems and postulates. *Biochim Biophys Acta* **1458**, 164-179.

[7]   Han S, Ching YC, Rousseau DL (1990) Ferryl and hydroxy intermediates in the reaction of oxygen with reduced cytochrome c oxidase. *Nature* **348**, 89-90.

[8]   Sarti P, Forte E, Mastronicola D, Giuffre A, Arese M (2012) Cytochrome c oxidase and nitric oxide in action: molecular mechanisms and pathophysiological implications. *Biochim Biophys Acta* **1817**, 610-619.

[9]   Kowaltowski AJ, de Souza-Pinto NC, Castilho RF, Vercesi AE (2009) Mitochondria and reactive oxygen species. *Free Radic Biol Med* **47**, 333-343.

[10]   Weisiger RA, Fridovich I (1973) Mitochondrial superoxide simutase. Site of synthesis and intramitochondrial localization. *J Biol Chem* **248**, 4793-4796.

[11]   Okado-Matsumoto A, Fridovich I (2001) Subcellular distribution of superoxide dismutases (SOD) in rat liver: Cu,Zn-SOD in mitochondria. *J Biol Chem* **276**, 38388-38393.

[12]   Bienert GP, Moller AL, Kristiansen KA, Schulz A, Moller IM, Schjoerring JK, Jahn TP (2007) Specific aquaporins facilitate the diffusion of hydrogen peroxide across membranes. *J Biol Chem* **282**, 1183-1192.

[13]   Nordberg J, Arner ES (2001) Reactive oxygen species, antioxidants, and the mammalian thioredoxin system. *Free Radic Biol Med* **31**, 1287-1312.

[14]   Droge W (2002) Free radicals in the physiological control of cell function. *Physiol Rev* **82**, 47-95.

[15]   Alvarez B, Radi R (2003) Peroxynitrite reactivity with amino acids and proteins. *Amino Acids* **25**, 295-311.

[16]   Castilho RF, Kowaltowski AJ, Meinicke AR, Bechara EJ, Vercesi AE (1995) Permeabilization of the inner mitochondrial membrane by Ca2+ ions is stimulated by t-butyl hydroperoxide and mediated by reactive oxygen species generated by mitochondria. *Free Radic Biol Med* **18**, 479-486.

[17]   Paulsen CE, Carroll KS (2009) Orchestrating redox signaling networks through regulatory cysteine switches. *ACS Chem Biol* **5**, 47-62.

References

[18] Demicheli V, Quijano C, Alvarez B, Radi R (2007) Inactivation and nitration of human superoxide dismutase (SOD) by fluxes of nitric oxide and superoxide. *Free Radic Biol Med* **42**, 1359-1368.

[19] Korkmaz A, Reiter RJ, Topal T, Manchester LC, Oter S, Tan DX (2009) Melatonin: an established antioxidant worthy of use in clinical trials. *Mol Med* **15**, 43-50.

[20] Brown GC, Borutaite V (2004) Inhibition of mitochondrial respiratory complex I by nitric oxide, peroxynitrite and S-nitrosothiols. *Biochim Biophys Acta* **1658**, 44-49.

[21] Cassina AM, Hodara R, Souza JM, Thomson L, Castro L, Ischiropoulos H, Freeman BA, Radi R (2000) Cytochrome c nitration by peroxynitrite. *J Biol Chem* **275**, 21409-21415.

[22] Roberts-Kirchhoff ES, Kim CK, Kim H (2002) Nitration of cytochrome C by peroxynitrite: a putative anti-apoptotic pathway mediated by prostaglandin H2 synthase (PGHS) and nitric oxide (NO) synthase. *Adv Exp Med Biol* **507**, 427-431.

[23] Szabo C, Zingarelli B, O'Connor M, Salzman AL (1996) DNA strand breakage, activation of poly (ADP-ribose) synthetase, and cellular energy depletion are involved in the cytotoxicity of macrophages and smooth muscle cells exposed to peroxynitrite. *Proc Natl Acad Sci U S A* **93**, 1753-1758.

[24] Rizzuto R, Pinton P, Carrington W, Fay FS, Fogarty KE, Lifshitz LM, Tuft RA, Pozzan T (1998) Close contacts with the endoplasmic reticulum as determinants of mitochondrial Ca2+ responses. *Science* **280**, 1763-1766.

[25] Starkov AA, Polster BM, Fiskum G (2002) Regulation of hydrogen peroxide production by brain mitochondria by calcium and Bax. *J Neurochem* **83**, 220-228.

[26] Brookes PS, Yoon Y, Robotham JL, Anders MW, Sheu SS (2004) Calcium, ATP, and ROS: a mitochondrial love-hate triangle. *Am J Physiol Cell Physiol* **287**, C817-833.

[27] Byrne AM, Lemasters JJ, Nieminen AL (1999) Contribution of increased mitochondrial free Ca2+ to the mitochondrial permeability transition induced by tert-butylhydroperoxide in rat hepatocytes. *Hepatology* **29**, 1523-1531.

[28] Irigoin F, Inada NM, Fernandes MP, Piacenza L, Gadelha FR, Vercesi AE, Radi R (2009) Mitochondrial calcium overload triggers complement-dependent superoxide-mediated programmed cell death in Trypanosoma cruzi. *Biochem J* **418**, 595-604.

[29] Tretter L, Takacs K, Kover K, Adam-Vizi V (2007) Stimulation of H(2)O(2) generation by calcium in brain mitochondria respiring on alpha-glycerophosphate. *J Neurosci Res* **85**, 3471-3479.

[30] Ghafourifar P, Schenk U, Klein SD, Richter C (1999) Mitochondrial nitric-oxide synthase stimulation causes cytochrome c release from isolated mitochondria. Evidence for intramitochondrial peroxynitrite formation. *J Biol Chem* **274**, 31185-31188.

[31] Sarti P, Lendaro E, Ippoliti R, Bellelli A, Benedetti PA, Brunori M (1999) Modulation of mitochondrial respiration by nitric oxide: investigation by single cell fluorescence microscopy. *Faseb J* **13**, 191-197.

[32] Kowaltowski AJ, Castilho RF, Vercesi AE (2001) Mitochondrial permeability transition and oxidative stress. *FEBS Lett* **495**, 12-15.

[33] Zoratti M, Szabo I (1995) The mitochondrial permeability transition. *Biochim Biophys Acta* **1241**, 139-176.

[34] Kim JS, He L, Lemasters JJ (2003) Mitochondrial permeability transition: a common pathway to necrosis and apoptosis. *Biochem Biophys Res Commun* **304**, 463-470.

[35] Lee J, Giordano S, Zhang J (2012) Autophagy, mitochondria and oxidative stress: cross-talk and redox signalling. *Biochem J* **441**, 523-540.

References

[36] Fisher-Wellman K, Bell HK, Bloomer RJ (2009) Oxidative stress and antioxidant defense mechanisms linked to exercise during cardiopulmonary and metabolic disorders. *Oxid Med Cell Longev* **2**, 43-51.

[37] Andersen JK (2004) Oxidative stress in neurodegeneration: cause or consequence? *Nat Med* **10 Suppl**, S18-25.

[38] Fukui H, Moraes CT (2008) The mitochondrial impairment, oxidative stress and neurodegeneration connection: reality or just an attractive hypothesis? *Trends Neurosci* **31**, 251-256.

[39] Geromel V, Kadhom N, Cebalos-Picot I, Ouari O, Polidori A, Munnich A, Rotig A, Rustin P (2001) Superoxide-induced massive apoptosis in cultured skin fibroblasts harboring the neurogenic ataxia retinitis pigmentosa (NARP) mutation in the ATPase-6 gene of the mitochondrial DNA. *Hum Mol Genet* **10**, 1221-1228.

[40] Moncada S, Palmer RM, Higgs EA (1991) Nitric oxide: physiology, pathophysiology, and pharmacology. *Pharmacol Rev* **43**, 109-142.

[41] Ignarro LJ (1990) Biosynthesis and metabolism of endothelium-derived nitric oxide. *Annu Rev Pharmacol Toxicol* **30**, 535-560.

[42] Dawson VL, Brahmbhatt HP, Mong JA, Dawson TM (1994) Expression of inducible nitric oxide synthase causes delayed neurotoxicity in primary mixed neuronal-glial cortical cultures. *Neuropharmacology* **33**, 1425-1430.

[43] Radomski MW, Palmer RM, Moncada S (1987) Comparative pharmacology of endothelium-derived relaxing factor, nitric oxide and prostacyclin in platelets. *Br J Pharmacol* **92**, 181-187.

[44] Bredt DS, Snyder SH (1994) Nitric oxide: a physiologic messenger molecule. *Annu Rev Biochem* **63**, 175-195.

[45] Wei XQ, Charles IG, Smith A, Ure J, Feng GJ, Huang FP, Xu D, Muller W, Moncada S, Liew FY (1995) Altered immune responses in mice lacking inducible nitric oxide synthase. *Nature* **375**, 408-411.

[46] Ignarro LJ, Buga GM, Wood KS, Byrns RE, Chaudhuri G (1987) Endothelium-derived relaxing factor produced and released from artery and vein is nitric oxide. *Proc Natl Acad Sci U S A* **84**, 9265-9269.

[47] Palmer RM, Ferrige AG, Moncada S (1987) Nitric oxide release accounts for the biological activity of endothelium-derived relaxing factor. *Nature* **327**, 524-526.

[48] Murad F, Mittal CK, Arnold WP, Katsuki S, Kimura H (1978) Guanylate cyclase: activation by azide, nitro compounds, nitric oxide, and hydroxyl radical and inhibition by hemoglobin and myoglobin. *Adv Cyclic Nucleotide Res* **9**, 145-158.

[49] Murad F, Arnold WP, Mittal CK, Braughler JM (1979) Properties and regulation of guanylate cyclase and some proposed functions for cyclic GMP. *Adv Cyclic Nucleotide Res* **11**, 175-204.

[50] Carr GJ, Ferguson SJ (1990) Nitric oxide formed by nitrite reductase of Paracoccus denitrificans is sufficiently stable to inhibit cytochrome oxidase activity and is reduced by its reductase under aerobic conditions. *Biochim Biophys Acta* **1017**, 57-62.

[51] Cleeter MW, Cooper JM, Darley-Usmar VM, Moncada S, Schapira AH (1994) Reversible inhibition of cytochrome c oxidase, the terminal enzyme of the mitochondrial respiratory chain, by nitric oxide. Implications for neurodegenerative diseases. *FEBS Lett* **345**, 50-54.

[52] Brown GC (1995) Nitric oxide regulates mitochondrial respiration and cell functions by inhibiting cytochrome oxidase. *FEBS Lett* **369**, 136-139.

References

[53]   Sarti P, Giuffrè A, Barone MC, Forte E, Mastronicola D, Brunori M (2003) Nitric oxide and cytochrome oxidase: reaction mechanisms from the enzyme to the cell. *Free Radic. Biol. Med.* **34**, 509-520.

[54]   Cooper CE, Giulivi C (2007) Nitric oxide regulation of mitochondrial oxygen consumption II: Molecular mechanism and tissue physiology. *Am J Physiol Cell Physiol* **292**, C1993-2003.

[55]   Lundberg JO, Weitzberg E, Gladwin MT (2008) The nitrate-nitrite-nitric oxide pathway in physiology and therapeutics. *Nat Rev Drug Discov* **7**, 156-167.

[56]   Almeida A, Almeida J, Bolanos JP, Moncada S (2001) Different responses of astrocytes and neurons to nitric oxide: the role of glycolytically generated ATP in astrocyte protection. *Proc Natl Acad Sci U S A* **98**, 15294-15299.

[57]   Moncada S, Bolanos JP (2006) Nitric oxide, cell bioenergetics and neurodegeneration. *J Neurochem* **97**, 1676-1689.

[58]   Garthwaite J, Boulton CL (1995) Nitric oxide signaling in the central nervous system. *Annu Rev Physiol* **57**, 683-706.

[59]   Zhang J, Snyder SH (1995) Nitric oxide in the nervous system. *Annu Rev Pharmacol Toxicol* **35**, 213-233.

[60]   Amir S (1992) Blocking NMDA receptors or nitric oxide production disrupts light transmission to the suprachiasmatic nucleus. *Brain Res* **586**, 336-339.

[61]   Kapas L, Fang J, Krueger JM (1994) Inhibition of nitric oxide synthesis inhibits rat sleep. *Brain Res* **664**, 189-196.

[62]   Watanabe A, Hamada T, Shibata S, Watanabe S (1994) Effects of nitric oxide synthase inhibitors on N-methyl-D-aspartate-induced phase delay of circadian rhythm of neuronal activity in the rat suprachiasmatic nucleus in vitro. *Brain Res* **646**, 161-164.

[63]   Burlet S, Leger L, Cespuglio R (1999) Nitric oxide and sleep in the rat: a puzzling relationship. *Neuroscience* **92**, 627-639.

[64]   Cudeiro J, Rivadulla C, Grieve KL (2000) A possible role for nitric oxide at the sleep/wake interface. *Sleep* **23**, 829-835.

[65]   Clement P, Sarda N, Cespuglio R, Gharib A (2005) Potential role of inducible nitric oxide synthase in the sleep-wake states occurrence in old rats. *Neuroscience* **135**, 347-355.

[66]   Kalinchuk AV, Lu Y, Stenberg D, Rosenberg PA, Porkka-Heiskanen T (2006) Nitric oxide production in the basal forebrain is required for recovery sleep. *J Neurochem* **99**, 483-498.

[67]   Kalinchuk AV, Stenberg D, Rosenberg PA, Porkka-Heiskanen T (2006) Inducible and neuronal nitric oxide synthases (NOS) have complementary roles in recovery sleep induction. *Eur J Neurosci* **24**, 1443-1456.

[68]   Huang PL, Huang Z, Mashimo H, Bloch KD, Moskowitz MA, Bevan JA, Fishman MC (1995) Hypertension in mice lacking the gene for endothelial nitric oxide synthase. *Nature* **377**, 239-242.

[69]   Piech A, Dessy C, Havaux X, Feron O, Balligand JL (2003) Differential regulation of nitric oxide synthases and their allosteric regulators in heart and vessels of hypertensive rats. *Cardiovasc Res* **57**, 456-467.

[70]   Higashino H, Miya H, Mukai H, Miya Y (2007) Serum nitric oxide metabolite (NO(x)) levels in hypertensive patients at rest: a comparison of age, gender, blood pressure and complications using normotensive controls. *Clin Exp Pharmacol Physiol* **34**, 725-731.

[71]   Chatterjee A, Black SM, Catravas JD (2008) Endothelial nitric oxide (NO) and its pathophysiologic regulation. *Vascul Pharmacol* **49**, 134-140.

References

[72]   Keynes RG, Garthwaite J (2004) Nitric oxide and its role in ischaemic brain injury. *Curr Mol Med* **4**, 179-191.

[73]   Bryan NS, Calvert JW, Elrod JW, Gundewar S, Ji SY, Lefer DJ (2007) Dietary nitrite supplementation protects against myocardial ischemia-reperfusion injury. *Proc Natl Acad Sci U S A* **104**, 19144-19149.

[74]   Araujo JA, Zhang M, Yin F (2012) Heme oxygenase-1, oxidation, inflammation, and atherosclerosis. *Front Pharmacol* **3**, 119.

[75]   Gatto EM, Riobo NA, Carreras MC, Chernavsky A, Rubio A, Satz ML, Poderoso JJ (2000) Overexpression of neutrophil neuronal nitric oxide synthase in Parkinson's disease. *Nitric Oxide* **4**, 534-539.

[76]   Watanabe Y, Kato H, Araki T (2008) Protective action of neuronal nitric oxide synthase inhibitor in the MPTP mouse model of Parkinson's disease. *Metab Brain Dis* **23**, 51-69.

[77]   Malinski T (2007) Nitric oxide and nitroxidative stress in Alzheimer's disease. *J Alzheimers Dis* **11**, 207-218.

[78]   Domek-Lopacinska KU, Strosznajder JB (2010) Cyclic GMP and nitric oxide synthase in aging and Alzheimer's disease. *Mol Neurobiol* **41**, 129-137.

[79]   Ridnour LA, Dhanapal S, Hoos M, Wilson J, Lee J, Cheng RY, Brueggemann EE, Hines HB, Wilcock DM, Vitek MP, Wink DA, Colton CA (2012) Nitric oxide-mediated regulation of beta-amyloid clearance via alterations of MMP-9/TIMP-1. *J Neurochem* **123**, 736-749.

[80]   Seyidova D, Aliyev A, Rzayev N, Obrenovich M, Lamb BT, Smith MA, de la Torre JC, Perry G, Aliev G (2004) The role of nitric oxide in the pathogenesis of brain lesions during the development of Alzheimer's disease. *In Vivo* **18**, 325-333.

[81]   Aliev G, Obrenovich ME, Tabrez S, Jabir NR, Reddy VP, Li Y, Burnstock G, Cacabelos R, Kamal MA (2013) Link between cancer and Alzheimer disease via oxidative stress induced by nitric oxide-dependent mitochondrial DNA overproliferation and deletion. *Oxid Med Cell Longev* **2013**, 962984.

[82]   Zhao G, Bernstein RD, Hintze TH (1999) Nitric oxide and oxygen utilization: exercise, heart failure and diabetes. *Coron Artery Dis* **10**, 315-320.

[83]   Zhao HJ, Wang S, Cheng H, Zhang MZ, Takahashi T, Fogo AB, Breyer MD, Harris RC (2006) Endothelial nitric oxide synthase deficiency produces accelerated nephropathy in diabetic mice. *J Am Soc Nephrol* **17**, 2664-2669.

[84]   Abbasi F, Chu JW, McLaughlin T, Lamendola C, Leary ET, Reaven GM (2004) Effect of metformin treatment on multiple cardiovascular disease risk factors in patients with type 2 diabetes mellitus. *Metabolism* **53**, 159-164.

[85]   Nagareddy PR, Xia Z, McNeill JH, MacLeod KM (2005) Increased expression of iNOS is associated with endothelial dysfunction and impaired pressor responsiveness in streptozotocin-induced diabetes. *Am J Physiol Heart Circ Physiol* **289**, H2144-2152.

[86]   Stuehr DJ (1997) Structure-function aspects in the nitric oxide synthases. *Annu Rev Pharmacol Toxicol* **37**, 339-359.

[87]   Li H, Poulos TL (2005) Structure-function studies on nitric oxide synthases. *J Inorg Biochem* **99**, 293-305.

[88]   Liu Q, Gross SS (1996) Binding sites of nitric oxide synthases. *Methods Enzymol* **268**, 311-324.

[89]   Xia H, Bredt DS (1996) Cloned and expressed nitric oxide synthase proteins. *Methods Enzymol* **268**, 427-436.

References

[90]   Zhou L, Zhu DY (2009) Neuronal nitric oxide synthase: structure, subcellular localization, regulation, and clinical implications. *Nitric Oxide* **20**, 223-230.

[91]   Daff S (2010) NO synthase: structures and mechanisms. *Nitric Oxide* **23**, 1-11.

[92]   Alderton WK, Cooper CE, Knowles RG (2001) Nitric oxide synthases: structure, function and inhibition. *Biochem J* **357**, 593-615.

[93]   Bredt DS, Snyder SH (1990) Isolation of nitric oxide synthetase, a calmodulin-requiring enzyme. *Proc Natl Acad Sci U S A* **87**, 682-685.

[94]   Piazza M, Futrega K, Spratt DE, Dieckmann T, Guillemette JG (2012) Structure and dynamics of calmodulin (CaM) bound to nitric oxide synthase peptides: effects of a phosphomimetic CaM mutation. *Biochemistry* **51**, 3651-3661.

[95]   Salerno JC, Harris DE, Irizarry K, Patel B, Morales AJ, Smith SM, Martasek P, Roman LJ, Masters BS, Jones CL, Weissman BA, Lane P, Liu Q, Gross SS (1997) An autoinhibitory control element defines calcium-regulated isoforms of nitric oxide synthase. *J Biol Chem* **272**, 29769-29777.

[96]   Nishida CR, Ortiz de Montellano PR (1999) Autoinhibition of endothelial nitric-oxide synthase. Identification of an electron transfer control element. *J Biol Chem* **274**, 14692-14698.

[97]   Fleming I (2010) Molecular mechanisms underlying the activation of eNOS. *Pflugers Arch* **459**, 793-806.

[98]   Hayashi Y, Nishio M, Naito Y, Yokokura H, Nimura Y, Hidaka H, Watanabe Y (1999) Regulation of neuronal nitric-oxide synthase by calmodulin kinases. *J Biol Chem* **274**, 20597-20602.

[99]   Cui H, Hayashi A, Sun HS, Belmares MP, Cobey C, Phan T, Schweizer J, Salter MW, Wang YT, Tasker RA, Garman D, Rabinowitz J, Lu PS, Tymianski M (2007) PDZ protein interactions underlying NMDA receptor-mediated excitotoxicity and neuroprotection by PSD-95 inhibitors. *J Neurosci* **27**, 9901-9915.

[100]   Tochio H, Mok YK, Zhang Q, Kan HM, Bredt DS, Zhang M (2000) Formation of nNOS/PSD-95 PDZ dimer requires a preformed beta-finger structure from the nNOS PDZ domain. *J Mol Biol* **303**, 359-370.

[101]   Saitoh F, Tian QB, Okano A, Sakagami H, Kondo H, Suzuki T (2004) NIDD, a novel DHHC-containing protein, targets neuronal nitric-oxide synthase (nNOS) to the synaptic membrane through a PDZ-dependent interaction and regulates nNOS activity. *J Biol Chem* **279**, 29461-29468.

[102]   Sattler R, Xiong Z, Lu WY, Hafner M, MacDonald JF, Tymianski M (1999) Specific coupling of NMDA receptor activation to nitric oxide neurotoxicity by PSD-95 protein. *Science* **284**, 1845-1848.

[103]   Jaffrey SR, Snyder SH (1996) PIN: an associated protein inhibitor of neuronal nitric oxide synthase. *Science* **274**, 774-777.

[104]   Rodriguez-Crespo I, Straub W, Gavilanes F, Ortiz de Montellano PR (1998) Binding of dynein light chain (PIN) to neuronal nitric oxide synthase in the absence of inhibition. *Arch Biochem Biophys* **359**, 297-304.

[105]   Richter K, Buchner J (2001) Hsp90: chaperoning signal transduction. *J Cell Physiol* **188**, 281-290.

[106]   Garcia-Cardena G, Fan R, Shah V, Sorrentino R, Cirino G, Papapetropoulos A, Sessa WC (1998) Dynamic activation of endothelial nitric oxide synthase by Hsp90. *Nature* **392**, 821-824.

References

[107] Bender AT, Silverstein AM, Demady DR, Kanelakis KC, Noguchi S, Pratt WB, Osawa Y (1999) Neuronal nitric-oxide synthase is regulated by the Hsp90-based chaperone system in vivo. *J Biol Chem* **274**, 1472-1478.

[108] Ratovitski EA, Bao C, Quick RA, McMillan A, Kozlovsky C, Lowenstein CJ (1999) An inducible nitric-oxide synthase (NOS)-associated protein inhibits NOS dimerization and activity. *J Biol Chem* **274**, 30250-30257.

[109] Michel T (1999) Targeting and translocation of endothelial nitric oxide synthase. *Braz J Med Biol Res* **32**, 1361-1366.

[110] Liu J, Garcia-Cardena G, Sessa WC (1995) Biosynthesis and palmitoylation of endothelial nitric oxide synthase: mutagenesis of palmitoylation sites, cysteines-15 and/or -26, argues against depalmitoylation-induced translocation of the enzyme. *Biochemistry* **34**, 12333-12340.

[111] Liu J, Hughes TE, Sessa WC (1997) The first 35 amino acids and fatty acylation sites determine the molecular targeting of endothelial nitric oxide synthase into the Golgi region of cells: a green fluorescent protein study. *J Cell Biol* **137**, 1525-1535.

[112] Shaul PW, Smart EJ, Robinson LJ, German Z, Yuhanna IS, Ying Y, Anderson RG, Michel T (1996) Acylation targets emdothelial nitric-oxide synthase to plasmalemmal caveolae. *J Biol Chem* **271**, 6518-6522.

[113] Feron O, Belhassen L, Kobzik L, Smith TW, Kelly RA, Michel T (1996) Endothelial nitric oxide synthase targeting to caveolae. Specific interactions with caveolin isoforms in cardiac myocytes and endothelial cells. *J Biol Chem* **271**, 22810-22814.

[114] Michel JB, Feron O, Sase K, Prabhakar P, Michel T (1997) Caveolin versus calmodulin. Counterbalancing allosteric modulators of endothelial nitric oxide synthase. *J Biol Chem* **272**, 25907-25912.

[115] Condorelli P, George SC (2001) In vivo control of soluble guanylate cyclase activation by nitric oxide: a kinetic analysis. *Biophys J* **80**, 2110-2119.

[116] Sarti P, Giuffrè A, Forte E, Mastronicola D, Barone MC, Brunori M (2000) Nitric oxide and cytochrome *c* oxidase: mechanisms of inhibition and NO degradation. *Biochem. Biophys. Res. Commun.* **274**, 183-187.

[117] Bellamy TC, Wood J, Garthwaite J (2002) On the activation of soluble guanylyl cyclase by nitric oxide. *Proc Natl Acad Sci U S A* **99**, 507-510.

[118] Lee YC, Martin E, Murad F (2000) Human recombinant soluble guanylyl cyclase: expression, purification, and regulation. *Proc Natl Acad Sci U S A* **97**, 10763-10768.

[119] Cooper CE (1999) Nitric oxide and iron proteins. *Biochim Biophys Acta* **1411**, 290-309.

[120] Addison AW, Stephanos JJ (1986) Nitrosyliron(III) hemoglobin: autoreduction and spectroscopy. *Biochemistry* **25**, 4104-4113.

[121] Brunori M (2001) Nitric oxide, cytochrome-c oxidase and myoglobin. *Trends Biochem Sci* **26**, 21-23.

[122] Stamler JS, Jaraki O, Osborne J, Simon DI, Keaney J, Vita J, Singel D, Valeri CR, Loscalzo J (1992) Nitric oxide circulates in mammalian plasma primarily as an S-nitroso adduct of serum albumin. *Proc Natl Acad Sci U S A* **89**, 7674-7677.

[123] Hogg N (2002) The biochemistry and physiology of S-nitrosothiols. *Annu Rev Pharmacol Toxicol* **42**, 585-600.

[124] Abello N, Kerstjens HA, Postma DS, Bischoff R (2009) Protein tyrosine nitration: selectivity, physicochemical and biological consequences, denitration, and proteomics methods for the identification of tyrosine-nitrated proteins. *J Proteome Res* **8**, 3222-3238.

References

[125] Pacher P, Beckman JS, Liaudet L (2007) Nitric oxide and peroxynitrite in health and disease. *Physiol Rev* **87**, 315-424.

[126] Turko IV, Murad F (2002) Protein nitration in cardiovascular diseases. *Pharmacol Rev* **54**, 619-634.

[127] Ng JY, Chiu J, Hogg PJ, Wong JW (2013) Tyrosine nitration moderates the peptidase activity of human methionyl aminopeptidase 2. *Biochem Biophys Res Commun* **440**, 37-42.

[128] Ahsan H (2013) 3-Nitrotyrosine: A biomarker of nitrogen free radical species modified proteins in systemic autoimmunogenic conditions. *Hum Immunol* **74**, 1392-1399.

[129] Bolanos JP, Peuchen S, Heales SJ, Land JM, Clark JB (1994) Nitric oxide-mediated inhibition of the mitochondrial respiratory chain in cultured astrocytes. *J Neurochem* **63**, 910-916.

[130] Brown GC, Cooper CE (1994) Nanomolar concentrations of nitric oxide reversibly inhibit synaptosomal respiration by competing with oxygen at cytochrome oxidase. *FEBS Lett.* **356**, 295-298.

[131] Clementi E, Brown GC, Feelisch M, Moncada S (1998) Persistent inhibition of cell respiration by nitric oxide: crucial role of S-nitrosylation of mitochondrial complex I and protective action of glutathione. *Proc Natl Acad Sci U S A* **95**, 7631-7636.

[132] Poderoso JJ, Carreras MC, Lisdero C, Riobo N, Schopfer F, Boveris A (1996) Nitric oxide inhibits electron transfer and increases superoxide radical production in rat heart mitochondria and submitochondrial particles. *Arch Biochem Biophys* **328**, 85-92.

[133] Moncada S, Erusalimsky JD (2002) Does nitric oxide modulate mitochondrial energy generation and apoptosis? *Nat Rev Mol Cell Biol* **3**, 214-220.

[134] Borutaite V, Budriunaite A, Brown GC (2000) Reversal of nitric oxide-, peroxynitrite- and S-nitrosothiol-induced inhibition of mitochondrial respiration or complex I activity by light and thiols. *Biochim Biophys Acta* **1459**, 405-412.

[135] Galkin A, Moncada S (2007) S-nitrosation of mitochondrial complex I depends on its structural conformation. *J Biol Chem* **282**, 37448-37453.

[136] Vinogradov AD (1998) Catalytic properties of the mitochondrial NADH-ubiquinone oxidoreductase (complex I) and the pseudo-reversible active/inactive enzyme transition. *Biochim Biophys Acta* **1364**, 169-185.

[137] Gavrikova EV, Vinogradov AD (1999) Active/de-active state transition of the mitochondrial complex I as revealed by specific sulfhydryl group labeling. *FEBS Lett* **455**, 36-40.

[138] Galkin A AAY, Frakich N, Duchen M R, Moncada S (2009) Lack of oxigen deactivates mitochondrial complex I: implications for ischemic injury? *J Biol Chem* **in press**.

[139] Hess DT, Matsumoto A, Kim SO, Marshall HE, Stamler JS (2005) Protein S-nitrosylation: purview and parameters. *Nat Rev Mol Cell Biol* **6**, 150-166.

[140] Sarti P, Arese M, Forte E, Giuffre A, Mastronicola D (2012) Mitochondria and nitric oxide: chemistry and pathophysiology. *Adv Exp Med Biol* **942**, 75-92.

[141] Davies NA, Cooper CE, Stidwill R, Singer M (2003) Inhibition of mitochondrial respiration during early stage sepsis. *Adv Exp Med Biol* **530**, 725-736.

[142] Schweizer M, Richter C (1994) Nitric oxide potently and reversibly deenergizes mitochondria at low oxygen tension. *Biochem Biophys Res Commun* **204**, 169-175.

[143] Brown GC, Bolanos JP, Heales SJ, Clark JB (1995) Nitric oxide produced by activated astrocytes rapidly and reversibly inhibits cellular respiration. *Neurosci Lett* **193**, 201-204.

References

[144] Borutaite V, Brown GC (1996) Rapid reduction of nitric oxide by mitochondria, and reversible inhibition of mitochondrial respiration by nitric oxide. *Biochem J* **315 (Pt 1)**, 295-299.

[145] Clementi E, Brown GC, Foxwell N, Moncada S (1999) On the mechanism by which vascular endothelial cells regulate their oxygen consumption. *Proc Natl Acad Sci U S A* **96**, 1559-1562.

[146] Shen W, Hintze TH, Wolin MS (1995) Nitric oxide. An important signaling mechanism between vascular endothelium and parenchymal cells in the regulation of oxygen consumption. *Circulation* **92**, 3505-3512.

[147] Hare JM, Keaney JF, Jr., Balligand JL, Loscalzo J, Smith TW, Colucci WS (1995) Role of nitric oxide in parasympathetic modulation of beta-adrenergic myocardial contractility in normal dogs. *J Clin Invest* **95**, 360-366.

[148] Xie YW, Shen W, Zhao G, Xu X, Wolin MS, Hintze TH (1996) Role of endothelium-derived nitric oxide in the modulation of canine myocardial mitochondrial respiration in vitro. Implications for the development of heart failure. *Circ Res* **79**, 381-387.

[149] Shiva S, Brookes PS, Patel RP, Anderson PG, Darley-Usmar VM (2001) Nitric oxide partitioning into mitochondrial membranes and the control of respiration at cytochrome c oxidase. *Proc Natl Acad Sci U S A* **98**, 7212-7217.

[150] Cooper CE, Brown GC (2008) The inhibition of mitochondrial cytochrome oxidase by the gases carbon monoxide, nitric oxide, hydrogen cyanide and hydrogen sulfide: chemical mechanism and physiological significance. *J Bioenerg Biomembr* **40**, 533-539.

[151] Sarti P, Forte E, Giuffre A, Mastronicola D, Magnifico MC, Arese M (2012) The Chemical Interplay between Nitric Oxide and Mitochondrial Cytochrome c Oxidase: Reactions, Effectors and Pathophysiology. *Int J Cell Biol* **2012**, 571067.

[152] Mason MG, Nicholls P, Wilson MT, Cooper CE (2006) Nitric oxide inhibition of respiration involves both competitive (heme) and noncompetitive (copper) binding to cytochrome c oxidase. *Proc Natl Acad Sci U S A* **103**, 708-713.

[153] Cooper CE, Torres J, Sharpe MA, Wilson MT (1997) Nitric oxide ejects electrons from the binuclear centre of cytochrome c oxidase by reacting with oxidised copper: a general mechanism for the interaction of copper proteins with nitric oxide? *FEBS Lett* **414**, 281-284.

[154] Giuffre A, Stubauer G, Brunori M, Sarti P, Torres J, Wilson MT (1998) Chloride bound to oxidized cytochrome c oxidase controls the reaction with nitric oxide. *J Biol Chem* **273**, 32475-32478.

[155] Torres J, Cooper CE, Wilson MT (1998) A common mechanism for the interaction of nitric oxide with the oxidized binuclear centre and oxygen intermediates of cytochrome c oxidase. *J Biol Chem* **273**, 8756-8766.

[156] Giuffre A, Barone MC, Mastronicola D, D'Itri E, Sarti P, Brunori M (2000) Reaction of nitric oxide with the turnover intermediates of cytochrome c oxidase: reaction pathway and functional effects. *Biochemistry* **39**, 15446-15453.

[157] Torres J, Sharpe MA, Rosquist A, Cooper CE, Wilson MT (2000) Cytochrome c oxidase rapidly metabolises nitric oxide to nitrite. *FEBS Lett* **475**, 263-266.

[158] Giulivi C (2003) Characterization and function of mitochondrial nitric-oxide synthase. *Free Radic Biol Med* **34**, 397-408.

[159] Pearce LL, Kanai AJ, Birder LA, Pitt BR, Peterson J (2002) The catabolic fate of nitric oxide: the nitric oxide oxidase and peroxynitrite reductase activities of cytochrome oxidase. *J Biol Chem* **277**, 13556-13562.

References

[160]   Castello PR, David PS, McClure T, Crook Z, Poyton RO (2006) Mitochondrial cytochrome oxidase produces nitric oxide under hypoxic conditions: implications for oxygen sensing and hypoxic signaling in eukaryotes. *Cell Metab* **3**, 277-287.

[161]   Castello PR, Woo DK, Ball K, Wojcik J, Liu L, Poyton RO (2008) Oxygen-regulated isoforms of cytochrome c oxidase have differential effects on its nitric oxide production and on hypoxic signaling. *Proc Natl Acad Sci U S A* **105**, 8203-8208.

[162]   Poyton RO, Castello PR, Ball KA, Woo DK, Pan N (2009) Mitochondria and hypoxic signaling: a new view. *Ann N Y Acad Sci* **1177**, 48-56.

[163]   Gibson Q, Greenwood C (1963) Reactions of Cytochrome Oxidase with Oxygen and Carbon Monoxide. *Biochem. J.* **86**, 541-555.

[164]   Blackmore RS, Greenwood C, Gibson QH (1991) Studies of the primary oxygen intermediate in the reaction of fully reduced cytochrome oxidase. *J Biol Chem* **266**, 19245-19249.

[165]   Stubauer G, Giuffre A, Brunori M, Sarti P (1998) Cytochrome c oxidase does not catalyze the anaerobic reduction of NO. *Biochem Biophys Res Commun* **245**, 459-465.

[166]   Torres J, Darley-Usmar V, Wilson MT (1995) Inhibition of cytochrome c oxidase in turnover by nitric oxide: mechanism and implications for control of respiration. *Biochem. J.* **312**, 169-173.

[167]   Giuffre A, Forte E, Brunori M, Sarti P (2005) Nitric oxide, cytochrome c oxidase and myoglobin: competition and reaction pathways. *FEBS Lett* **579**, 2528-2532.

[168]   Giuffrè A, Sarti P, D'Itri E, Buse G, Soulimane T, Brunori M (1996) On the mechanism of inhibition of cytochrome *c* oxidase by nitric oxide. *J. Biol. Chem.* **271**, 33404-33408.

[169]   Giulivi C (1998) Functional implications of nitric oxide produced by mitochondria in mitochondrial metabolism. *Biochem J* **332 (Pt 3)**, 673-679.

[170]   Maragos CM, Morley D, Wink DA, Dunams TM, Saavedra JE, Hoffman A, Bove AA, Isaac L, Hrabie JA, Keefer LK (1991) Complexes of .NO with nucleophiles as agents for the controlled biological release of nitric oxide. Vasorelaxant effects. *J Med Chem* **34**, 3242-3247.

[171]   Boveris A, Chance B (1973) The mitochondrial generation of hydrogen peroxide. General properties and effect of hyperbaric oxygen. *Biochem J* **134**, 707-716.

[172]   Lizasoain I, Moro MA, Knowles RG, Darley-Usmar V, Moncada S (1996) Nitric oxide and peroxynitrite exert distinct effects on mitochondrial respiration which are differentially blocked by glutathione or glucose. *Biochem J* **314 (Pt 3)**, 877-880.

[173]   Packer MA, Porteous CM, Murphy MP (1996) Superoxide production by mitochondria in the presence of nitric oxide forms peroxynitrite. *Biochem Mol Biol Int* **40**, 527-534.

[174]   Beltran B, Mathur A, Duchen MR, Erusalimsky JD, Moncada S (2000) The effect of nitric oxide on cell respiration: A key to understanding its role in cell survival or death. *Proc Natl Acad Sci U S A* **97**, 14602-14607.

[175]   Almeida A, Moncada S, Bolanos JP (2004) Nitric oxide switches on glycolysis through the AMP protein kinase and 6-phosphofructo-2-kinase pathway. *Nat Cell Biol* **6**, 45-51.

[176]   Almeida A, Bolanos JP (2001) A transient inhibition of mitochondrial ATP synthesis by nitric oxide synthase activation triggered apoptosis in primary cortical neurons. *J Neurochem* **77**, 676-690.

[177]   Wang GJ, Randall RD, Thayer SA (1994) Glutamate-induced intracellular acidification of cultured hippocampal neurons demonstrates altered energy metabolism resulting from Ca2+ loads. *J Neurophysiol* **72**, 2563-2569.

References

[178]   White RJ, Reynolds IJ (1996) Mitochondrial depolarization in glutamate-stimulated neurons: an early signal specific to excitotoxin exposure. *J Neurosci* **16**, 5688-5697.

[179]   Tatton WG, Olanow CW (1999) Apoptosis in neurodegenerative diseases: the role of mitochondria. *Biochim Biophys Acta* **1410**, 195-213.

[180]   Zawilska JB, Skene DJ, Arendt J (2009) Physiology and pharmacology of melatonin in relation to biological rhythms. *Pharmacol Rep* **61**, 383-410.

[181]   Tan DX, Manchester LC, Terron MP, Flores LJ, Reiter RJ (2007) One molecule, many derivatives: a never-ending interaction of melatonin with reactive oxygen and nitrogen species? *J Pineal Res* **42**, 28-42.

[182]   Lerner AB, Case JD, Takahashi Y (1960) Isolation of melatonin and 5-methoxyindole-3-acetic acid from bovine pineal glands. *J Biol Chem* **235**, 1992-1997.

[183]   Hastings MH, Herbert J, Martensz ND, Roberts AC (1985) Annual reproductive rhythms in mammals: mechanisms of light synchronization. *Ann N Y Acad Sci* **453**, 182-204.

[184]   Hattori A, Migitaka H, Iigo M, Itoh M, Yamamoto K, Ohtani-Kaneko R, Hara M, Suzuki T, Reiter RJ (1995) Identification of melatonin in plants and its effects on plasma melatonin levels and binding to melatonin receptors in vertebrates. *Biochem Mol Biol Int* **35**, 627-634.

[185]   Hardeland R, Poeggeler B (2003) Non-vertebrate melatonin. *J Pineal Res* **34**, 233-241.

[186]   Cajochen C, Krauchi K, Wirz-Justice A (2003) Role of melatonin in the regulation of human circadian rhythms and sleep. *J Neuroendocrinol* **15**, 432-437.

[187]   Hardeland R, Cardinali DP, Srinivasan V, Spence DW, Brown GM, Pandi-Perumal SR (2011) Melatonin--a pleiotropic, orchestrating regulator molecule. *Prog Neurobiol* **93**, 350-384.

[188]   Axelrod J (1974) The pineal gland: a neurochemical transducer. *Science* **184**, 1341-1348.

[189]   Iuvone PM, Tosini G, Pozdeyev N, Haque R, Klein DC, Chaurasia SS (2005) Circadian clocks, clock networks, arylalkylamine N-acetyltransferase, and melatonin in the retina. *Prog Retin Eye Res* **24**, 433-456.

[190]   Klein DC (2007) Arylalkylamine N-acetyltransferase: "the Timezyme". *J Biol Chem* **282**, 4233-4237.

[191]   Cahill GM, Besharse JC (1990) Circadian regulation of melatonin in the retina of Xenopus laevis: limitation by serotonin availability. *J Neurochem* **54**, 716-719.

[192]   Thomas KB, Brown AD, Iuvone PM (1998) Elevation of melatonin in chicken retina by 5-hydroxytryptophan: differential light/dark responses. *Neuroreport* **9**, 4041-4044.

[193]   Moore RY (1997) Circadian rhythms: basic neurobiology and clinical applications. *Annu Rev Med* **48**, 253-266.

[194]   Buijs RM, Hermes MH, Kalsbeek A (1998) The suprachiasmatic nucleus-paraventricular nucleus interactions: a bridge to the neuroendocrine and autonomic nervous system. *Prog Brain Res* **119**, 365-382.

[195]   Klein DC (2004) The 2004 Aschoff/Pittendrigh lecture: Theory of the origin of the pineal gland--a tale of conflict and resolution. *J Biol Rhythms* **19**, 264-279.

[196]   Gastel JA, Roseboom PH, Rinaldi PA, Weller JL, Klein DC (1998) Melatonin production: proteasomal proteolysis in serotonin N-acetyltransferase regulation. *Science* **279**, 1358-1360.

[197]   Reiter RJ (1991) Melatonin synthesis: multiplicity of regulation. *Adv Exp Med Biol* **294**, 149-158.

[198]   Arendt J (1998) Melatonin and the pineal gland: influence on mammalian seasonal and circadian physiology. *Rev Reprod* **3**, 13-22.

References

[199] Ambriz-Tututi M, Rocha-Gonzalez HI, Cruz SL, Granados-Soto V (2009) Melatonin: a hormone that modulates pain. *Life Sci* **84**, 489-498.

[200] Claustrat B, Brun J, Chazot G (2005) The basic physiology and pathophysiology of melatonin. *Sleep Med Rev* **9**, 11-24.

[201] Pandi-Perumal SR, Srinivasan V, Maestroni GJ, Cardinali DP, Poeggeler B, Hardeland R (2006) Melatonin: Nature's most versatile biological signal? *FEBS J* **273**, 2813-2838.

[202] Rosen J, Than NN, Koch D, Poeggeler B, Laatsch H, Hardeland R (2006) Interactions of melatonin and its metabolites with the ABTS cation radical: extension of the radical scavenger cascade and formation of a novel class of oxidation products, C2-substituted 3-indolinones. *J Pineal Res* **41**, 374-381.

[203] Reiter RJ, Paredes SD, Manchester LC, Tan DX (2009) Reducing oxidative/nitrosative stress: a newly-discovered genre for melatonin. *Crit Rev Biochem Mol Biol* **44**, 175-200.

[204] Reiter RJ, Tan DX, Rosales-Corral S, Manchester LC (2013) The universal nature, unequal distribution and antioxidant functions of melatonin and its derivatives. *Mini Rev Med Chem* **13**, 373-384.

[205] Pandi-Perumal SR, Trakht I, Srinivasan V, Spence DW, Maestroni GJ, Zisapel N, Cardinali DP (2008) Physiological effects of melatonin: role of melatonin receptors and signal transduction pathways. *Prog Neurobiol* **85**, 335-353.

[206] Hardeland R (2008) Melatonin, hormone of darkness and more: occurrence, control mechanisms, actions and bioactive metabolites. *Cell Mol Life Sci* **65**, 2001-2018.

[207] Lavie P (1997) Melatonin: role in gating nocturnal rise in sleep propensity. *J Biol Rhythms* **12**, 657-665.

[208] Zisapel N (2001) Circadian rhythm sleep disorders: pathophysiology and potential approaches to management. *CNS Drugs* **15**, 311-328.

[209] Scheer FA, Van Montfrans GA, van Someren EJ, Mairuhu G, Buijs RM (2004) Daily nighttime melatonin reduces blood pressure in male patients with essential hypertension. *Hypertension* **43**, 192-197.

[210] Paradies G, Petrosillo G, Paradies V, Reiter RJ, Ruggiero FM (2010) Melatonin, cardiolipin and mitochondrial bioenergetics in health and disease. *J Pineal Res* **48**, 297-310.

[211] Guerrero JM, Reiter RJ (2002) Melatonin-immune system relationships. *Curr Top Med Chem* **2**, 167-179.

[212] Armstrong SM (1989) Melatonin and circadian control in mammals. *Experientia* **45**, 932-938.

[213] Reiter RJ, Tan DX, Maldonado MD (2005) Melatonin as an antioxidant: physiology versus pharmacology. *J Pineal Res* **39**, 215-216.

[214] Blask DE, Dauchy RT, Sauer LA (2005) Putting cancer to sleep at night: the neuroendocrine/circadian melatonin signal. *Endocrine* **27**, 179-188.

[215] Cardinali DP, Ladizesky MG, Boggio V, Cutrera RA, Mautalen C (2003) Melatonin effects on bone: experimental facts and clinical perspectives. *J Pineal Res* **34**, 81-87.

[216] Bubenik GA (2002) Gastrointestinal melatonin: localization, function, and clinical relevance. *Dig Dis Sci* **47**, 2336-2348.

[217] Vanecek J (1998) Cellular mechanisms of melatonin action. *Physiol Rev* **78**, 687-721.

[218] Roy D, Belsham DD (2002) Melatonin receptor activation regulates GnRH gene expression and secretion in GT1-7 GnRH neurons. Signal transduction mechanisms. *J Biol Chem* **277**, 251-258.

References

[219] Balik A, Kretschmannova K, Mazna P, Svobodova I, Zemkova H (2004) Melatonin action in neonatal gonadotrophs. *Physiol Res* **53 Suppl 1**, S153-166.

[220] Waldhauser F, Boepple PA, Schemper M, Mansfield MJ, Crowley WF, Jr. (1991) Serum melatonin in central precocious puberty is lower than in age-matched prepubertal children. *J Clin Endocrinol Metab* **73**, 793-796.

[221] Dijk DJ, Cajochen C (1997) Melatonin and the circadian regulation of sleep initiation, consolidation, structure, and the sleep EEG. *J Biol Rhythms* **12**, 627-635.

[222] Zhdanova IV, Tucci V (2003) Melatonin, Circadian Rhythms, and Sleep. *Curr Treat Options Neurol* **5**, 225-229.

[223] Dubocovich ML, Markowska M (2005) Functional MT1 and MT2 melatonin receptors in mammals. *Endocrine* **27**, 101-110.

[224] Konturek SJ, Konturek PC, Brzozowski T, Bubenik GA (2007) Role of melatonin in upper gastrointestinal tract. *J Physiol Pharmacol* **58 Suppl 6**, 23-52.

[225] Koyama H, Nakade O, Takada Y, Kaku T, Lau KH (2002) Melatonin at pharmacologic doses increases bone mass by suppressing resorption through down-regulation of the RANKL-mediated osteoclast formation and activation. *J Bone Miner Res* **17**, 1219-1229.

[226] Fideleff HL, Boquete H, Fideleff G, Albornoz L, Perez Lloret S, Suarez M, Esquifino AI, Honfi M, Cardinali DP (2006) Gender-related differences in urinary 6-sulfatoxymelatonin levels in obese pubertal individuals. *J Pineal Res* **40**, 214-218.

[227] Olakowska E, Marcol W, Kotulska K, Lewin-Kowalik J (2005) The role of melatonin in the neurodegenerative diseases. *Bratisl Lek Listy* **106**, 171-174.

[228] Srinivasan V, Pandi-Perumal SR, Maestroni GJ, Esquifino AI, Hardeland R, Cardinali DP (2005) Role of melatonin in neurodegenerative diseases. *Neurotox Res* **7**, 293-318.

[229] Pandi-Perumal SR, BaHammam AS, Brown GM, Spence DW, Bharti VK, Kaur C, Hardeland R, Cardinali DP (2013) Melatonin antioxidative defense: therapeutical implications for aging and neurodegenerative processes. *Neurotox Res* **23**, 267-300.

[230] Cagnacci A, Arangino S, Angiolucci M, Maschio E, Melis GB (1998) Influences of melatonin administration on the circulation of women. *Am J Physiol* **274**, R335-338.

[231] Arangino S, Cagnacci A, Angiolucci M, Vacca AM, Longu G, Volpe A, Melis GB (1999) Effects of melatonin on vascular reactivity, catecholamine levels, and blood pressure in healthy men. *Am J Cardiol* **83**, 1417-1419.

[232] Anisimov VN, Egormin PA, Piskunova TS, Popovich IG, Tyndyk ML, Yurova MN, Zabezhinski MA, Anikin IV, Karkach AS, Romanyukha AA (2010) Metformin extends life span of HER-2/neu transgenic mice and in combination with melatonin inhibits growth of transplantable tumors in vivo. *Cell Cycle* **9**, 188-197.

[233] Kontek R, Nowicka H (2013) The modulatory effect of melatonin on genotoxicity of irinotecan in healthy human lymphocytes and cancer cells. *Drug Chem Toxicol* **36**, 335-342.

[234] Cheng Y, Cai L, Jiang P, Wang J, Gao C, Feng H, Wang C, Pan H, Yang Y (2013) SIRT1 inhibition by melatonin exerts antitumor activity in human osteosarcoma cells. *Eur J Pharmacol* **715**, 219-229.

[235] Kim KJ, Choi JS, Kang I, Kim KW, Jeong CH, Jeong JW (2013) Melatonin suppresses tumor progression by reducing angiogenesis stimulated by HIF-1 in a mouse tumor model. *J Pineal Res* **54**, 264-270.

[236] Costa EJ, Shida CS, Biaggi MH, Ito AS, Lamy-Freund MT (1997) How melatonin interacts with lipid bilayers: a study by fluorescence and ESR spectroscopies. *FEBS Lett* **416**, 103-106.

References

[237] Menendez-Pelaez A, Reiter RJ (1993) Distribution of melatonin in mammalian tissues: the relative importance of nuclear versus cytosolic localization. *J Pineal Res* **15**, 59-69.

[238] Nosjean O, Ferro M, Coge F, Beauverger P, Henlin JM, Lefoulon F, Fauchere JL, Delagrange P, Canet E, Boutin JA (2000) Identification of the melatonin-binding site MT3 as the quinone reductase 2. *J Biol Chem* **275**, 31311-31317.

[239] Boutin JA, Marcheteau E, Hennig P, Moulharat N, Berger S, Delagrange P, Bouchet JP, Ferry G (2008) MT3/QR2 melatonin binding site does not use melatonin as a substrate or a co-substrate. *J Pineal Res* **45**, 524-531.

[240] Fildes JE, Yonan N, Keevil BG (2009) Melatonin--a pleiotropic molecule involved in pathophysiological processes following organ transplantation. *Immunology* **127**, 443-449.

[241] Tomas-Zapico C, Coto-Montes A (2005) A proposed mechanism to explain the stimulatory effect of melatonin on antioxidative enzymes. *J Pineal Res* **39**, 99-104.

[242] Alonso M, Collado PS, Gonzalez-Gallego J (2006) Melatonin inhibits the expression of the inducible isoform of nitric oxide synthase and nuclear factor kappa B activation in rat skeletal muscle. *J Pineal Res* **41**, 8-14.

[243] Tan DX, Poeggeler B, Reiter RJ, Chen LD, Chen S, Manchester LC, Barlow-Walden LR (1993) The pineal hormone melatonin inhibits DNA-adduct formation induced by the chemical carcinogen safrole in vivo. *Cancer Lett* **70**, 65-71.

[244] Poeggeler B, Reiter RJ, Tan DX, Chen LD, Manchester LC (1993) Melatonin, hydroxyl radical-mediated oxidative damage, and aging: a hypothesis. *J Pineal Res* **14**, 151-168.

[245] Poeggeler B, Thuermann S, Dose A, Schoenke M, Burkhardt S, Hardeland R (2002) Melatonin's unique radical scavenging properties - roles of its functional substituents as revealed by a comparison with its structural analogs. *J Pineal Res* **33**, 20-30.

[246] Poeggeler B, Saarela S, Reiter RJ, Tan DX, Chen LD, Manchester LC, Barlow-Walden LR (1994) Melatonin--a highly potent endogenous radical scavenger and electron donor: new aspects of the oxidation chemistry of this indole accessed in vitro. *Ann N Y Acad Sci* **738**, 419-420.

[247] Mahal HS, Sharma HS, Mukherjee T (1999) Antioxidant properties of melatonin: a pulse radiolysis study. *Free Radic Biol Med* **26**, 557-565.

[248] Romero MP, Garcia-Perganeda A, Guerrero JM, Osuna C (1998) Membrane-bound calmodulin in Xenopus laevis oocytes as a novel binding site for melatonin. *FASEB J* **12**, 1401-1408.

[249] Leon J, Macias M, Escames G, Camacho E, Khaldy H, Martin M, Espinosa A, Gallo MA, Acuna-Castroviejo D (2000) Structure-related inhibition of calmodulin-dependent neuronal nitric-oxide synthase activity by melatonin and synthetic kynurenines. *Mol Pharmacol* **58**, 967-975.

[250] Leon J, Acuna-Castroviejo D, Sainz RM, Mayo JC, Tan DX, Reiter RJ (2004) Melatonin and mitochondrial function. *Life Sci* **75**, 765-790.

[251] Leon J, Acuna-Castroviejo D, Escames G, Tan DX, Reiter RJ (2005) Melatonin mitigates mitochondrial malfunction. *J Pineal Res* **38**, 1-9.

[252] Acuna-Castroviejo D, Martin M, Macias M, Escames G, Leon J, Khaldy H, Reiter RJ (2001) Melatonin, mitochondria, and cellular bioenergetics. *J Pineal Res* **30**, 65-74.

[253] Acuna-Castroviejo D, Escames G, Rodriguez MI, Lopez LC (2007) Melatonin role in the mitochondrial function. *Front Biosci* **12**, 947-963.

[254] Lopez A, Garcia JA, Escames G, Venegas C, Ortiz F, Lopez LC, Acuna-Castroviejo D (2009) Melatonin protects the mitochondria from oxidative damage reducing oxygen

References

consumption, membrane potential, and superoxide anion production. *J Pineal Res* **46**, 188-198.

[255] Venegas C, Garcia JA, Escames G, Ortiz F, Lopez A, Doerrier C, Garcia-Corzo L, Lopez LC, Reiter RJ, Acuna-Castroviejo D (2012) Extrapineal melatonin: analysis of its subcellular distribution and daily fluctuations. *J Pineal Res* **52**, 217-227.

[256] Martin M, Macias M, Escames G, Leon J, Acuna-Castroviejo D (2000) Melatonin but not vitamins C and E maintains glutathione homeostasis in t-butyl hydroperoxide-induced mitochondrial oxidative stress. *FASEB J* **14**, 1677-1679.

[257] Martin M, Macias M, Escames G, Reiter RJ, Agapito MT, Ortiz GG, Acuna-Castroviejo D (2000) Melatonin-induced increased activity of the respiratory chain complexes I and IV can prevent mitochondrial damage induced by ruthenium red in vivo. *J Pineal Res* **28**, 242-248.

[258] Martin M, Macias M, Leon J, Escames G, Khaldy H, Acuna-Castroviejo D (2002) Melatonin increases the activity of the oxidative phosphorylation enzymes and the production of ATP in rat brain and liver mitochondria. *Int J Biochem Cell Biol* **34**, 348-357.

[259] Jou MJ (2011) Melatonin preserves the transient mitochondrial permeability transition for protection during mitochondrial Ca(2+) stress in astrocyte. *J Pineal Res* **50**, 427-435.

[260] Petrosillo G, Moro N, Paradies V, Ruggiero FM, Paradies G (2010) Increased susceptibility to Ca(2+)-induced permeability transition and to cytochrome c release in rat heart mitochondria with aging: effect of melatonin. *J Pineal Res* **48**, 340-346.

[261] Petrosillo G, Moro N, Ruggiero FM, Paradies G (2009) Melatonin inhibits cardiolipin peroxidation in mitochondria and prevents the mitochondrial permeability transition and cytochrome c release. *Free Radic Biol Med* **47**, 969-974.

[262] Cardinali DP, Pagano ES, Scacchi Bernasconi PA, Reynoso R, Scacchi P (2013) Melatonin and mitochondrial dysfunction in the central nervous system. *Horm Behav* **63**, 322-330.

[263] Tan DX, Manchester LC, Liu X, Rosales-Corral SA, Acuna-Castroviejo D, Reiter RJ (2013) Mitochondria and chloroplasts as the original sites of melatonin synthesis: a hypothesis related to melatonin's primary function and evolution in eukaryotes. *J Pineal Res* **54**, 127-138.

[264] Tan DX, Reiter RJ, Manchester LC, Yan MT, El-Sawi M, Sainz RM, Mayo JC, Kohen R, Allegra M, Hardeland R (2002) Chemical and physical properties and potential mechanisms: melatonin as a broad spectrum antioxidant and free radical scavenger. *Curr Top Med Chem* **2**, 181-197.

[265] Catala A (2007) The ability of melatonin to counteract lipid peroxidation in biological membranes. *Curr Mol Med* **7**, 638-649.

[266] Allegra M, Furtmuller PG, Regelsberger G, Turco-Liveri ML, Tesoriere L, Perretti M, Livrea MA, Obinger C (2001) Mechanism of reaction of melatonin with human myeloperoxidase. *Biochem Biophys Res Commun* **282**, 380-386.

[267] Hardeland R (2005) Antioxidative protection by melatonin: multiplicity of mechanisms from radical detoxification to radical avoidance. *Endocrine* **27**, 119-130.

[268] Solis-Munoz P, Solis-Herruzo JA, Fernandez-Moreira D, Gomez-Izquierdo E, Garcia-Consuegra I, Munoz-Yague T, Garcia Ruiz I Melatonin improves mitochondrial respiratory chain activity and liver morphology in ob/ob mice. *J Pineal Res* **51**, 113-123.

[269] Lenaz G (2012) Mitochondria and reactive oxygen species. Which role in physiology and pathology? *Adv Exp Med Biol* **942**, 93-136.

References

[270] Acuna Castroviejo D, Lopez LC, Escames G, Lopez A, Garcia JA, Reiter RJ (2011) Melatonin-mitochondria interplay in health and disease. *Curr Top Med Chem* **11**, 221-240.

[271] Garcia-Macia M, Vega-Naredo I, De Gonzalo-Calvo D, Rodriguez-Gonzalez SM, Camello PJ, Camello-Almaraz C, Martin-Cano FE, Rodriguez-Colunga MJ, Pozo MJ, Coto-Montes AM (2011) Melatonin induces neural SOD2 expression independent of the NF-kappaB pathway and improves the mitochondrial population and function in old mice. *J Pineal Res* **50**, 54-63.

[272] Mayo JC, Sainz RM, Antoli I, Herrera F, Martin V, Rodriguez C (2002) Melatonin regulation of antioxidant enzyme gene expression. *Cell Mol Life Sci* **59**, 1706-1713.

[273] Inarrea P, Casanova A, Alava MA, Iturralde M, Cadenas E (2011) Melatonin and steroid hormones activate intermembrane Cu,Zn-superoxide dismutase by means of mitochondrial cytochrome P450. *Free Radic Biol Med* **50**, 1575-1581.

[274] Zwirska-Korczala K, Jochem J, Adamczyk-Sowa M, Sowa P, Polaniak R, Birkner E, Latocha M, Pilc K, Suchanek R (2005) Influence of melatonin on cell proliferation, antioxidative enzyme activities and lipid peroxidation in 3T3-L1 preadipocytes--an in vitro study. *J Physiol Pharmacol* **56 Suppl 6**, 91-99.

[275] Wu CC, Lu KC, Lin GJ, Hsieh HY, Chu P, Lin SH, Sytwu HK (2012) Melatonin enhances endogenous heme oxygenase-1 and represses immune responses to ameliorate experimental murine membranous nephropathy. *J Pineal Res* **52**, 460-469.

[276] Crespo E, Macias M, Pozo D, Escames G, Martin M, Vives F, Guerrero JM, Acuna-Castroviejo D (1999) Melatonin inhibits expression of the inducible NO synthase II in liver and lung and prevents endotoxemia in lipopolysaccharide-induced multiple organ dysfunction syndrome in rats. *FASEB J* **13**, 1537-1546.

[277] Gilad E, Wong HR, Zingarelli B, Virag L, O'Connor M, Salzman AL, Szabo C (1998) Melatonin inhibits expression of the inducible isoform of nitric oxide synthase in murine macrophages: role of inhibition of NFkappaB activation. *FASEB J* **12**, 685-693.

[278] Wang H, Li L, Zhao M, Chen YH, Zhang ZH, Zhang C, Ji YL, Meng XH, Xu DX (2011) Melatonin alleviates lipopolysaccharide-induced placental cellular stress response in mice. *J Pineal Res* **50**, 418-426.

[279] Deng WG, Tang ST, Tseng HP, Wu KK (2006) Melatonin suppresses macrophage cyclooxygenase-2 and inducible nitric oxide synthase expression by inhibiting p52 acetylation and binding. *Blood* **108**, 518-524.

[280] Reyes-Toso CF, Ricci CR, de Mignone IR, Reyes P, Linares LM, Albornoz LE, Cardinali DP, Zaninovich A (2003) In vitro effect of melatonin on oxygen consumption in liver mitochondria of rats. *Neuro Endocrinol Lett* **24**, 341-344.

[281] Acuna-Castroviejo D, Escames G, Leon J, Carazo A, Khaldy H (2003) Mitochondrial regulation by melatonin and its metabolites. *Adv Exp Med Biol* **527**, 549-557.

[282] Castillo-Romero JL, Vives-Montero F, Reiter RJ, Acuna-Castroviejo D (1993) Pineal modulation of the rat caudate-putamen spontaneous neuronal activity: roles of melatonin and vasotocin. *J Pineal Res* **15**, 147-152.

[283] Escames G, Acuna-Castroviejo D, Leon J, Vives F (1998) Melatonin interaction with magnesium and zinc in the response of the striatum to sensorimotor cortical stimulation in the rat. *J Pineal Res* **24**, 123-129.

[284] Escames G, Macias M, Leon J, Garcia J, Khaldy H, Martin M, Vives F, Acuna-Castroviejo D (2001) Calcium-dependent effects of melatonin inhibition of glutamatergic response in rat striatum. *J Neuroendocrinol* **13**, 459-466.

142

References

[285] Andrabi SA, Sayeed I, Siemen D, Wolf G, Horn TF (2004) Direct inhibition of the mitochondrial permeability transition pore: a possible mechanism responsible for anti-apoptotic effects of melatonin. *FASEB J* **18**, 869-871.

[286] Jou MJ, Peng TI, Reiter RJ, Jou SB, Wu HY, Wen ST (2004) Visualization of the antioxidative effects of melatonin at the mitochondrial level during oxidative stress-induced apoptosis of rat brain astrocytes. *J Pineal Res* **37**, 55-70.

[287] Kilic E, Kilic U, Yulug B, Hermann DM, Reiter RJ (2004) Melatonin reduces disseminate neuronal death after mild focal ischemia in mice via inhibition of caspase-3 and is suitable as an add-on treatment to tissue-plasminogen activator. *J Pineal Res* **36**, 171-176.

[288] Xu M, Ashraf M (2002) Melatonin protection against lethal myocyte injury induced by doxorubicin as reflected by effects on mitochondrial membrane potential. *J Mol Cell Cardiol* **34**, 75-79.

[289] Petrosillo G, Colantuono G, Moro N, Ruggiero FM, Tiravanti E, Di Venosa N, Fiore T, Paradies G (2009) Melatonin protects against heart ischemia-reperfusion injury by inhibiting mitochondrial permeability transition pore opening. *Am J Physiol Heart Circ Physiol* **297**, H1487-1493.

[290] Hibaoui Y, Roulet E, Ruegg UT (2009) Melatonin prevents oxidative stress-mediated mitochondrial permeability transition and death in skeletal muscle cells. *J Pineal Res* **47**, 238-252.

[291] Fischer TW, Zmijewski MA, Wortsman J, Slominski A (2008) Melatonin maintains mitochondrial membrane potential and attenuates activation of initiator (casp-9) and effector caspases (casp-3/casp-7) and PARP in UVR-exposed HaCaT keratinocytes. *J Pineal Res* **44**, 397-407.

[292] Pozo D, Reiter RJ, Calvo JR, Guerrero JM (1994) Physiological concentrations of melatonin inhibit nitric oxide synthase in rat cerebellum. *Life Sci* **55**, PL455-460.

[293] Storr M, Koppitz P, Sibaev A, Saur D, Kurjak M, Franck H, Schusdziarra V, Allescher HD (2002) Melatonin reduces non-adrenergic, non-cholinergic relaxant neurotransmission by inhibition of nitric oxide synthase activity in the gastrointestinal tract of rodents in vitro. *J Pineal Res* **33**, 101-108.

[294] Escames G, Lopez LC, Ortiz F, Ros E, Acuna-Castroviejo D (2006) Age-dependent lipopolysaccharide-induced iNOS expression and multiorgan failure in rats: effects of melatonin treatment. *Exp Gerontol* **41**, 1165-1173.

[295] Lopez LC, Escames G, Tapias V, Utrilla P, Leon J, Acuna-Castroviejo D (2006) Identification of an inducible nitric oxide synthase in diaphragm mitochondria from septic mice: its relation with mitochondrial dysfunction and prevention by melatonin. *Int J Biochem Cell Biol* **38**, 267-278.

[296] Jimenez-Ortega V, Cano P, Cardinali DP, Esquifino AI (2009) 24-Hour variation in gene expression of redox pathway enzymes in rat hypothalamus: effect of melatonin treatment. *Redox Rep* **14**, 132-138.

[297] Tapias V, Escames G, Lopez LC, Lopez A, Camacho E, Carrion MD, Entrena A, Gallo MA, Espinosa A, Acuna-Castroviejo D (2009) Melatonin and its brain metabolite N(1)-acetyl-5-methoxykynuramine prevent mitochondrial nitric oxide synthase induction in parkinsonian mice. *J Neurosci Res* **87**, 3002-3010.

[298] Ortiz F, Garcia JA, Acuna-Castroviejo D, Doerrier C, Lopez A, Venegas C, Volt H, Luna-Sanchez M, Lopez LC, Escames G (2013) The beneficial effects of melatonin

References

against heart mitochondrial impairment during sepsis: inhibition of iNOS and preservation of nNOS. *J Pineal Res.*

[299] Escames G, Leon J, Macias M, Khaldy H, Acuna-Castroviejo D (2003) Melatonin counteracts lipopolysaccharide-induced expression and activity of mitochondrial nitric oxide synthase in rats. *FASEB J* **17**, 932-934.

[300] Srinivasan V, Pandi-Perumal SR, Spence DW, Kato H, Cardinali DP (2010) Melatonin in septic shock: some recent concepts. *J Crit Care* **25**, 656 e651-656.

[301] Wang WZ, Fang XH, Stephenson LL, Baynosa RC, Khiabani KT, Zamboni WA (2005) Microcirculatory effects of melatonin in rat skeletal muscle after prolonged ischemia. *J Pineal Res* **39**, 57-65.

[302] Koh PO (2008) Melatonin regulates nitric oxide synthase expression in ischemic brain injury. *J Vet Med Sci* **70**, 747-750.

[303] Leon J, Escames G, Rodriguez MI, Lopez LC, Tapias V, Entrena A, Camacho E, Carrion MD, Gallo MA, Espinosa A, Tan DX, Reiter RJ, Acuna-Castroviejo D (2006) Inhibition of neuronal nitric oxide synthase activity by N1-acetyl-5-methoxykynuramine, a brain metabolite of melatonin. *J Neurochem* **98**, 2023-2033.

[304] Guillaume JL, Daulat AM, Maurice P, Levoye A, Migaud M, Brydon L, Malpaux B, Borg-Capra C, Jockers R (2008) The PDZ protein mupp1 promotes Gi coupling and signaling of the Mt1 melatonin receptor. *J Biol Chem* **283**, 16762-16771.

[305] Luchetti F, Canonico B, Betti M, Arcangeletti M, Pilolli F, Piroddi M, Canesi L, Papa S, Galli F (2010) Melatonin signaling and cell protection function. *FASEB J* **2010**.

[306] Tamura H, Nakamura Y, Korkmaz A, Manchester LC, Tan DX, Sugino N, Reiter RJ (2009) Melatonin and the ovary: physiological and pathophysiological implications. *Fertil Steril* **92**, 328-343.

[307] Skinner DC, Malpaux B (1999) High melatonin concentrations in third ventricular cerebrospinal fluid are not due to Galen vein blood recirculating through the choroid plexus. *Endocrinology* **140**, 4399-4405.

[308] Tan D, Manchester LC, Reiter RJ, Qi W, Hanes MA, Farley NJ (1999) High physiological levels of melatonin in the bile of mammals. *Life Sci* **65**, 2523-2529.

[309] Poeggeler B, Cornelissen G, Huether G, Hardeland R, Jozsa R, Zeman M, Stebelova K, Olah A, Bubenik G, Pan W, Otsuka K, Schwartzkopff O, Bakken EE, Halberg F (2005) Chronomics affirm extending scope of lead in phase of duodenal vs. pineal circadian melatonin rhythms. *Biomed Pharmacother* **59 Suppl 1**, S220-224.

[310] Reiter RJ, Paredes SD, Korkmaz A, Manchester LC, Tan DX (2008) Melatonin in relation to the "strong" and "weak" versions of the free radical theory of aging. *Adv Med Sci* **53**, 119-129.

[311] Rosales-Corral SA, Acuna-Castroviejo D, Coto-Montes A, Boga JA, Manchester LC, Fuentes-Broto L, Korkmaz A, Ma S, Tan DX, Reiter RJ (2012) Alzheimer's disease: pathological mechanisms and the beneficial role of melatonin. *J Pineal Res* **52**, 167-202.

[312] Spuch C, Ortolano S, Navarro C (2012) New insights in the amyloid-Beta interaction with mitochondria. *J Aging Res* **2012**, 324968.

[313] Lustbader JW, Cirilli M, Lin C, Xu HW, Takuma K, Wang N, Caspersen C, Chen X, Pollak S, Chaney M, Trinchese F, Liu S, Gunn-Moore F, Lue LF, Walker DG, Kuppusamy P, Zewier ZL, Arancio O, Stern D, Yan SS, Wu H (2004) ABAD directly links Abeta to mitochondrial toxicity in Alzheimer's disease. *Science* **304**, 448-452.

[314] Chen JX, Yan SD (2007) Amyloid-beta-induced mitochondrial dysfunction. *J Alzheimers Dis* **12**, 177-184.

References

[315]   Moreira PI, Santos MS, Oliveira CR (2007) Alzheimer's disease: a lesson from mitochondrial dysfunction. *Antioxid Redox Signal* **9**, 1621-1630.

[316]   Eckert A, Hauptmann S, Scherping I, Rhein V, Muller-Spahn F, Gotz J, Muller WE (2008) Soluble beta-amyloid leads to mitochondrial defects in amyloid precursor protein and tau transgenic mice. *Neurodegener Dis* **5**, 157-159.

[317]   Hauptmann S, Scherping I, Drose S, Brandt U, Schulz KL, Jendrach M, Leuner K, Eckert A, Muller WE (2009) Mitochondrial dysfunction: an early event in Alzheimer pathology accumulates with age in AD transgenic mice. *Neurobiol Aging* **30**, 1574-1586.

[318]   Schellenberg GD, Montine TJ (2012) The genetics and neuropathology of Alzheimer's disease. *Acta Neuropathol* **124**, 305-323.

[319]   Masters CL, Selkoe DJ Biochemistry of amyloid beta-protein and amyloid deposits in Alzheimer disease. *Cold Spring Harb Perspect Med* **2**, a006262.

[320]   Haass C, Koo EH, Mellon A, Hung AY, Selkoe DJ (1992) Targeting of cell-surface beta-amyloid precursor protein to lysosomes: alternative processing into amyloid-bearing fragments. *Nature* **357**, 500-503.

[321]   Seubert P, Vigo-Pelfrey C, Esch F, Lee M, Dovey H, Davis D, Sinha S, Schlossmacher M, Whaley J, Swindlehurst C, et al. (1992) Isolation and quantification of soluble Alzheimer's beta-peptide from biological fluids. *Nature* **359**, 325-327.

[322]   Selkoe DJ (2001) Alzheimer's disease results from the cerebral accumulation and cytotoxicity of amyloid beta-protein. *J Alzheimers Dis* **3**, 75-80.

[323]   Vigo-Pelfrey C, Lee D, Keim P, Lieberburg I, Schenk DB (1993) Characterization of beta-amyloid peptide from human cerebrospinal fluid. *J Neurochem* **61**, 1965-1968.

[324]   Kang JE, Lim MM, Bateman RJ, Lee JJ, Smyth LP, Cirrito JR, Fujiki N, Nishino S, Holtzman DM (2009) Amyloid-beta dynamics are regulated by orexin and the sleep-wake cycle. *Science* **326**, 1005-1007.

[325]   Pike CJ, Walencewicz AJ, Glabe CG, Cotman CW (1991) In vitro aging of beta-amyloid protein causes peptide aggregation and neurotoxicity. *Brain Res* **563**, 311-314.

[326]   Busciglio J, Lorenzo A, Yankner BA (1992) Methodological variables in the assessment of beta amyloid neurotoxicity. *Neurobiol Aging* **13**, 609-612.

[327]   Geula C, Wu CK, Saroff D, Lorenzo A, Yuan M, Yankner BA (1998) Aging renders the brain vulnerable to amyloid beta-protein neurotoxicity. *Nat Med* **4**, 827-831.

[328]   Soto C, Estrada L, Castilla J (2006) Amyloids, prions and the inherent infectious nature of misfolded protein aggregates. *Trends Biochem Sci* **31**, 150-155.

[329]   Haass C, Selkoe DJ (2007) Soluble protein oligomers in neurodegeneration: lessons from the Alzheimer's amyloid beta-peptide. *Nat Rev Mol Cell Biol* **8**, 101-112.

[330]   Burdick D, Soreghan B, Kwon M, Kosmoski J, Knauer M, Henschen A, Yates J, Cotman C, Glabe C (1992) Assembly and aggregation properties of synthetic Alzheimer's A4/beta amyloid peptide analogs. *J Biol Chem* **267**, 546-554.

[331]   Citron M, Oltersdorf T, Haass C, McConlogue L, Hung AY, Seubert P, Vigo-Pelfrey C, Lieberburg I, Selkoe DJ (1992) Mutation of the beta-amyloid precursor protein in familial Alzheimer's disease increases beta-protein production. *Nature* **360**, 672-674.

[332]   Cai XD, Golde TE, Younkin SG (1993) Release of excess amyloid beta protein from a mutant amyloid beta protein precursor. *Science* **259**, 514-516.

[333]   Kumar-Singh S, Theuns J, Van Broeck B, Pirici D, Vennekens K, Corsmit E, Cruts M, Dermaut B, Wang R, Van Broeckhoven C (2006) Mean age-of-onset of familial alzheimer disease caused by presenilin mutations correlates with both increased Abeta42 and decreased Abeta40. *Hum Mutat* **27**, 686-695.

References

[334] Rovelet-Lecrux A, Hannequin D, Raux G, Le Meur N, Laquerriere A, Vital A, Dumanchin C, Feuillette S, Brice A, Vercelletto M, Dubas F, Frebourg T, Campion D (2006) APP locus duplication causes autosomal dominant early-onset Alzheimer disease with cerebral amyloid angiopathy. *Nat Genet* **38**, 24-26.

[335] Klein WL, Krafft GA, Finch CE (2001) Targeting small Abeta oligomers: the solution to an Alzheimer's disease conundrum? *Trends Neurosci* **24**, 219-224.

[336] Selkoe DJ (2002) Alzheimer's disease is a synaptic failure. *Science* **298**, 789-791.

[337] Gouras GK, Tsai J, Naslund J, Vincent B, Edgar M, Checler F, Greenfield JP, Haroutunian V, Buxbaum JD, Xu H, Greengard P, Relkin NR (2000) Intraneuronal Abeta42 accumulation in human brain. *Am J Pathol* **156**, 15-20.

[338] Fernandez-Vizarra P, Fernandez AP, Castro-Blanco S, Serrano J, Bentura ML, Martinez-Murillo R, Martinez A, Rodrigo J (2004) Intra- and extracellular Abeta and PHF in clinically evaluated cases of Alzheimer's disease. *Histol Histopathol* **19**, 823-844.

[339] Wirths O, Multhaup G, Bayer TA (2004) A modified beta-amyloid hypothesis: intraneuronal accumulation of the beta-amyloid peptide--the first step of a fatal cascade. *J Neurochem* **91**, 513-520.

[340] LaFerla FM, Green KN, Oddo S (2007) Intracellular amyloid-beta in Alzheimer's disease. *Nat Rev Neurosci* **8**, 499-509.

[341] Gouras GK, Tampellini D, Takahashi RH, Capetillo-Zarate E (2010) Intraneuronal beta-amyloid accumulation and synapse pathology in Alzheimer's disease. *Acta Neuropathol* **119**, 523-541.

[342] Takahashi RH, Nam EE, Edgar M, Gouras GK (2002) Alzheimer beta-amyloid peptides: normal and abnormal localization. *Histol Histopathol* **17**, 239-246.

[343] Yu WH, Cuervo AM, Kumar A, Peterhoff CM, Schmidt SD, Lee JH, Mohan PS, Mercken M, Farmery MR, Tjernberg LO, Jiang Y, Duff K, Uchiyama Y, Naslund J, Mathews PM, Cataldo AM, Nixon RA (2005) Macroautophagy--a novel Beta-amyloid peptide-generating pathway activated in Alzheimer's disease. *J Cell Biol* **171**, 87-98.

[344] Mucke L, Masliah E, Yu GQ, Mallory M, Rockenstein EM, Tatsuno G, Hu K, Kholodenko D, Johnson-Wood K, McConlogue L (2000) High-level neuronal expression of abeta 1-42 in wild-type human amyloid protein precursor transgenic mice: synaptotoxicity without plaque formation. *J Neurosci* **20**, 4050-4058.

[345] Caspersen C, Wang N, Yao J, Sosunov A, Chen X, Lustbader JW, Xu HW, Stern D, McKhann G, Yan SD (2005) Mitochondrial Abeta: a potential focal point for neuronal metabolic dysfunction in Alzheimer's disease. *FASEB J* **19**, 2040-2041.

[346] Manczak M, Anekonda TS, Henson E, Park BS, Quinn J, Reddy PH (2006) Mitochondria are a direct site of A beta accumulation in Alzheimer's disease neurons: implications for free radical generation and oxidative damage in disease progression. *Hum Mol Genet* **15**, 1437-1449.

[347] Hoozemans JJ, Veerhuis R, Van Haastert ES, Rozemuller JM, Baas F, Eikelenboom P, Scheper W (2005) The unfolded protein response is activated in Alzheimer's disease. *Acta Neuropathol* **110**, 165-172.

[348] Hansson Petersen CA, Alikhani N, Behbahani H, Wiehager B, Pavlov PF, Alafuzoff I, Leinonen V, Ito A, Winblad B, Glaser E, Ankarcrona M (2008) The amyloid beta-peptide is imported into mitochondria via the TOM import machinery and localized to mitochondrial cristae. *Proc Natl Acad Sci U S A* **105**, 13145-13150.

[349] Reddy PH (2009) Amyloid beta, mitochondrial structural and functional dynamics in Alzheimer's disease. *Exp Neurol* **218**, 286-292.

References

[350]   Pagani L, Eckert A (2010) Amyloid-Beta interaction with mitochondria. *Int J Alzheimers Dis* **2011**, 925050.

[351]   Ferri KF, Kroemer G (2001) Organelle-specific initiation of cell death pathways. *Nat Cell Biol* **3**, E255-263.

[352]   Umeda T, Tomiyama T, Sakama N, Tanaka S, Lambert MP, Klein WL, Mori H (2011) Intraneuronal amyloid beta oligomers cause cell death via endoplasmic reticulum stress, endosomal/lysosomal leakage, and mitochondrial dysfunction in vivo. *J Neurosci Res* **89**, 1031-1042.

[353]   Cha MY, Han SH, Son SM, Hong HS, Choi YJ, Byun J, Mook-Jung I (2012) Mitochondria-specific accumulation of amyloid beta induces mitochondrial dysfunction leading to apoptotic cell death. *PLoS One* **7**, e34929.

[354]   Rosales-Corral S, Acuna-Castroviejo D, Tan DX, Lopez-Armas G, Cruz-Ramos J, Munoz R, Melnikov VG, Manchester LC, Reiter RJ (2012) Accumulation of exogenous amyloid-beta peptide in hippocampal mitochondria causes their dysfunction: a protective role for melatonin. *Oxid Med Cell Longev* **2012**, 843649.

[355]   Hansson CA, Frykman S, Farmery MR, Tjernberg LO, Nilsberth C, Pursglove SE, Ito A, Winblad B, Cowburn RF, Thyberg J, Ankarcrona M (2004) Nicastrin, presenilin, APH-1, and PEN-2 form active gamma-secretase complexes in mitochondria. *J Biol Chem* **279**, 51654-51660.

[356]   Anandatheerthavarada HK, Biswas G, Robin MA, Avadhani NG (2003) Mitochondrial targeting and a novel transmembrane arrest of Alzheimer's amyloid precursor protein impairs mitochondrial function in neuronal cells. *J Cell Biol* **161**, 41-54.

[357]   Keil U, Bonert A, Marques CA, Scherping I, Weyermann J, Strosznajder JB, Muller-Spahn F, Haass C, Czech C, Pradier L, Muller WE, Eckert A (2004) Amyloid beta-induced changes in nitric oxide production and mitochondrial activity lead to apoptosis. *J Biol Chem* **279**, 50310-50320.

[358]   Crouch PJ, Blake R, Duce JA, Ciccotosto GD, Li QX, Barnham KJ, Curtain CC, Cherny RA, Cappai R, Dyrks T, Masters CL, Trounce IA (2005) Copper-dependent inhibition of human cytochrome c oxidase by a dimeric conformer of amyloid-beta1-42. *J Neurosci* **25**, 672-679.

[359]   Eckert A, Hauptmann S, Scherping I, Meinhardt J, Rhein V, Drose S, Brandt U, Fandrich M, Muller WE, Gotz J (2008) Oligomeric and fibrillar species of beta-amyloid (A beta 42) both impair mitochondrial function in P301L tau transgenic mice. *J Mol Med (Berl)* **86**, 1255-1267.

[360]   Yang TT, Hsu CT, Kuo YM (2009) Cell-derived soluble oligomers of human amyloid-beta peptides disturb cellular homeostasis and induce apoptosis in primary hippocampal neurons. *J Neural Transm* **116**, 1561-1569.

[361]   Shearman MS, Ragan CI, Iversen LL (1994) Inhibition of PC12 cell redox activity is a specific, early indicator of the mechanism of beta-amyloid-mediated cell death. *Proc Natl Acad Sci U S A* **91**, 1470-1474.

[362]   Tillement L, Lecanu L, Yao W, Greeson J, Papadopoulos V (2006) The spirostenol (22R, 25R)-20alpha-spirost-5-en-3beta-yl hexanoate blocks mitochondrial uptake of Abeta in neuronal cells and prevents Abeta-induced impairment of mitochondrial function. *Steroids* **71**, 725-735.

[363]   Moreira PI, Santos MS, Moreno A, Oliveira C (2001) Amyloid beta-peptide promotes permeability transition pore in brain mitochondria. *Biosci Rep* **21**, 789-800.

147

References

[364]   Moreira PI, Santos MS, Moreno A, Rego AC, Oliveira C (2002) Effect of amyloid beta-peptide on permeability transition pore: a comparative study. *J Neurosci Res* **69**, 257-267.

[365]   Takuma K, Yao J, Huang J, Xu H, Chen X, Luddy J, Trillat AC, Stern DM, Arancio O, Yan SS (2005) ABAD enhances Abeta-induced cell stress via mitochondrial dysfunction. *FASEB J* **19**, 597-598.

[366]   Casley CS, Canevari L, Land JM, Clark JB, Sharpe MA (2002) Beta-amyloid inhibits integrated mitochondrial respiration and key enzyme activities. *J Neurochem* **80**, 91-100.

[367]   Rhein V, Baysang G, Rao S, Meier F, Bonert A, Muller-Spahn F, Eckert A (2009) Amyloid-beta leads to impaired cellular respiration, energy production and mitochondrial electron chain complex activities in human neuroblastoma cells. *Cell Mol Neurobiol* **29**, 1063-1071.

[368]   Parker WD, Jr., Filley CM, Parks JK (1990) Cytochrome oxidase deficiency in Alzheimer's disease. *Neurology* **40**, 1302-1303.

[369]   Kish SJ, Mastrogiacomo F, Guttman M, Furukawa Y, Taanman JW, Dozic S, Pandolfo M, Lamarche J, DiStefano L, Chang LJ (1999) Decreased brain protein levels of cytochrome oxidase subunits in Alzheimer's disease and in hereditary spinocerebellar ataxia disorders: a nonspecific change? *J Neurochem* **72**, 700-707.

[370]   Bobba A, Amadoro G, Valenti D, Corsetti V, Lassandro R, Atlante A (2013) Mitochondrial respiratory chain Complexes I and IV are impaired by beta-amyloid via direct interaction and through Complex I-dependent ROS production, respectively. *Mitochondrion* **13**, 298-311.

[371]   Sorbi S, Bird ED, Blass JP (1983) Decreased pyruvate dehydrogenase complex activity in Huntington and Alzheimer brain. *Ann Neurol* **13**, 72-78.

[372]   Perry EK, Perry RH, Tomlinson BE, Blessed G, Gibson PH (1980) Coenzyme A-acetylating enzymes in Alzheimer's disease: possible cholinergic 'compartment' of pyruvate dehydrogenase. *Neurosci Lett* **18**, 105-110.

[373]   Gibson GE, Sheu KF, Blass JP (1998) Abnormalities of mitochondrial enzymes in Alzheimer disease. *J Neural Transm* **105**, 855-870.

[374]   Du H, Guo L, Fang F, Chen D, Sosunov AA, McKhann GM, Yan Y, Wang C, Zhang H, Molkentin JD, Gunn-Moore FJ, Vonsattel JP, Arancio O, Chen JX, Yan SD (2008) Cyclophilin D deficiency attenuates mitochondrial and neuronal perturbation and ameliorates learning and memory in Alzheimer's disease. *Nat Med* **14**, 1097-1105.

[375]   Wang X, Su B, Siedlak SL, Moreira PI, Fujioka H, Wang Y, Casadesus G, Zhu X (2008) Amyloid-beta overproduction causes abnormal mitochondrial dynamics via differential modulation of mitochondrial fission/fusion proteins. *Proc Natl Acad Sci U S A* **105**, 19318-19323.

[376]   Cho DH, Nakamura T, Fang J, Cieplak P, Godzik A, Gu Z, Lipton SA (2009) S-nitrosylation of Drp1 mediates beta-amyloid-related mitochondrial fission and neuronal injury. *Science* **324**, 102-105.

[377]   Mangialasche F, Polidori MC, Monastero R, Ercolani S, Camarda C, Cecchetti R, Mecocci P (2009) Biomarkers of oxidative and nitrosative damage in Alzheimer's disease and mild cognitive impairment. *Ageing Res Rev* **8**, 285-305.

[378]   Butterfield DA, Boyd-Kimball D (2004) Amyloid beta-peptide(1-42) contributes to the oxidative stress and neurodegeneration found in Alzheimer disease brain. *Brain Pathol* **14**, 426-432.

[379]   Emerit J, Edeas M, Bricaire F (2004) Neurodegenerative diseases and oxidative stress. *Biomed Pharmacother* **58**, 39-46.

References

[380] Moreira PI, Siedlak SL, Aliev G, Zhu X, Cash AD, Smith MA, Perry G (2005) Oxidative stress mechanisms and potential therapeutics in Alzheimer disease. *J Neural Transm* **112**, 921-932.

[381] Hardy JA, Higgins GA (1992) Alzheimer's disease: the amyloid cascade hypothesis. *Science* **256**, 184-185.

[382] Jomova K, Vondrakova D, Lawson M, Valko M (2010) Metals, oxidative stress and neurodegenerative disorders. *Mol Cell Biochem* **345**, 91-104.

[383] Ill-Raga G, Ramos-Fernandez E, Guix FX, Tajes M, Bosch-Morato M, Palomer E, Godoy J, Belmar S, Cerpa W, Simpkins JW, Inestrosa, Nc, Munoz FJ (2010) Amyloid-beta peptide fibrils induce nitro-oxidative stress in neuronal cells. *J Alzheimers Dis* **22**, 641-652.

[384] Li MH, Jang JH, Sun B, Surh YJ (2004) Protective effects of oligomers of grape seed polyphenols against beta-amyloid-induced oxidative cell death. *Ann N Y Acad Sci* **1030**, 317-329.

[385] Lovell MA, Xiong S, Xie C, Davies P, Markesbery WR (2004) Induction of hyperphosphorylated tau in primary rat cortical neuron cultures mediated by oxidative stress and glycogen synthase kinase-3. *J Alzheimers Dis* **6**, 659-671; discussion 673-681.

[386] Ohyagi Y, Yamada T, Nishioka K, Clarke NJ, Tomlinson AJ, Naylor S, Nakabeppu Y, Kira J, Younkin SG (2000) Selective increase in cellular A beta 42 is related to apoptosis but not necrosis. *Neuroreport* **11**, 167-171.

[387] Jekabsone A, Mander PK, Tickler A, Sharpe M, Brown GC (2006) Fibrillar beta-amyloid peptide Abeta1-40 activates microglial proliferation via stimulating TNF-alpha release and H2O2 derived from NADPH oxidase: a cell culture study. *J Neuroinflammation* **3**, 24.

[388] Rozemuller AJ, van Gool WA, Eikelenboom P (2005) The neuroinflammatory response in plaques and amyloid angiopathy in Alzheimer's disease: therapeutic implications. *Curr Drug Targets CNS Neurol Disord* **4**, 223-233.

[389] Block ML, Zecca L, Hong JS (2007) Microglia-mediated neurotoxicity: uncovering the molecular mechanisms. *Nat Rev Neurosci* **8**, 57-69.

[390] Thorns V, Hansen L, Masliah E (1998) nNOS expressing neurons in the entorhinal cortex and hippocampus are affected in patients with Alzheimer's disease. *Exp Neurol* **150**, 14-20.

[391] Luth HJ, Munch G, Arendt T (2002) Aberrant expression of NOS isoforms in Alzheimer's disease is structurally related to nitrotyrosine formation. *Brain Res* **953**, 135-143.

[392] Dawson DA (1994) Nitric oxide and focal cerebral ischemia: multiplicity of actions and diverse outcome. *Cerebrovasc Brain Metab Rev* **6**, 299-324.

[393] Faraci FM, Brian JE, Jr. (1994) Nitric oxide and the cerebral circulation. *Stroke* **25**, 692-703.

[394] Colton CA, Brown CM, Czapiga M, Vitek MP (2002) Apolipoprotein-E allele-specific regulation of nitric oxide production. *Ann N Y Acad Sci* **962**, 212-225.

[395] Cetin F, Yazihan N, Dincer S, Akbulut G (2012) The effect of intracerebroventricular injection of beta amyloid peptide (1-42) on caspase-3 activity, lipid peroxidation, nitric oxide and NOS expression in young adult and aged rat brain. *Turk Neurosurg* **23**, 144-150.

[396] Baltrons MA, Pedraza CE, Heneka MT, Garcia A (2002) Beta-amyloid peptides decrease soluble guanylyl cyclase expression in astroglial cells. *Neurobiol Dis* **10**, 139-149.

149

References

[397]   Puzzo D, Palmeri A, Arancio O (2006) Involvement of the nitric oxide pathway in synaptic dysfunction following amyloid elevation in Alzheimer's disease. *Rev Neurosci* **17**, 497-523.

[398]   Srere PA (1969) Citrate synthase. *methods in enzymology* **13**, 3-11.

[399]   Chomczynski P, Sacchi N (1987) Single-step method of RNA isolation by acid guanidinium thiocyanate-phenol-chloroform extraction. *Anal Biochem* **162**, 156-159.

[400]   Bradford MM (1976) A rapid and sensitive method for the quantitation of microgram quantities of protein utilizing the principle of protein-dye binding. *Anal Biochem* **72**, 248-254.

[401]   Reers M, Smith TW, Chen LB (1991) J-aggregate formation of a carbocyanine as a quantitative fluorescent indicator of membrane potential. *Biochemistry* **30**, 4480-4486.

[402]   Reed PW (1979) Ionophores. *Methods Enzymol* **55**, 435-454.

[403]   Gnaiger E, Steinlechner-Maran R, Mendez G, Eberl T, Margreiter R (1995) Control of mitochondrial and cellular respiration by oxygen. *J Bioenerg Biomembr* **27**, 583-596.

[404]   Gnaiger E (2001) Bioenergetics at low oxygen: dependence of respiration and phosphorylation on oxygen and adenosine diphosphate supply. *Respir Physiol* **128**, 277-297.

[405]   Gnaiger E, Kuznetsov AV, Lassnig B, Fuchs A, Reck M, Renner K, Stadlmann S, Rieger G, Margreiter R (1998) High resolution respirometry - optimum permeabilization of the cell membane by digitonin. . *BioThermoKinetics in the Post Genomic Era*, 89-95.

[406]   Kuznetsov AV, Veksler V, Gellerich FN, Saks V, Margreiter R, Kunz WS (2008) Analysis of mitochondrial function in situ in permeabilized muscle fibers, tissues and cells. *Nat Protoc* **3**, 965-976.

[407]   Sgarbi G, Baracca A, Lenaz G, Valentino LM, Carelli V, Solaini G (2006) Inefficient coupling between proton transport and ATP synthesis may be the pathogenic mechanism for NARP and Leigh syndrome resulting from the T8993G mutation in mtDNA. *Biochem J* **395**, 493-500.

[408]   Merlo-Pich M, Deleonardi G, Biondi A, Lenaz G (2004) Methods to detect mitochondrial function. *Exp Gerontol* **39**, 277-281.

[409]   Everse J (1975) Enzymic determination of lactic acid. *Methods Enzymol* **41**, 41-44.

[410]   Warburg O (1956) On the origin of cancer cells. *Science* **123**, 309-314.

[411]   Bolanos JP, Almeida A, Moncada S (2010) Glycolysis: a bioenergetic or a survival pathway? *Trends Biochem Sci* **35**, 145-149.

[412]   Tsikas D, Gutzki FM, Stichtenoth DO (2006) Circulating and excretory nitrite and nitrate as indicators of nitric oxide synthesis in humans: methods of analysis. *Eur J Clin Pharmacol* **62**, 51-59.

[413]   Kunieda T, Minamino T, Miura K, Katsuno T, Tateno K, Miyauchi H, Kaneko S, Bradfield CA, FitzGerald GA, Komuro I (2008) Reduced nitric oxide causes age-associated impairment of circadian rhythmicity. *Circ Res* **102**, 607-614.

[414]   Marino J, Cudeiro J (2003) Nitric oxide-mediated cortical activation: a diffuse wake-up system. *J Neurosci* **23**, 4299-4307.

[415]   Bon CL, Garthwaite J (2003) On the role of nitric oxide in hippocampal long-term potentiation. *J Neurosci* **23**, 1941-1948.

[416]   Haley JE, Wilcox GL, Chapman PF (1992) The role of nitric oxide in hippocampal long-term potentiation. *Neuron* **8**, 211-216.

[417]   Blackshaw S, Eliasson MJ, Sawa A, Watkins CC, Krug D, Gupta A, Arai T, Ferrante RJ, Snyder SH (2003) Species, strain and developmental variations in hippocampal neuronal

150

References

and endothelial nitric oxide synthase clarify discrepancies in nitric oxide-dependent synaptic plasticity. *Neuroscience* **119**, 979-990.

[418] Bohme GA, Bon C, Lemaire M, Reibaud M, Piot O, Stutzmann JM, Doble A, Blanchard JC (1993) Altered synaptic plasticity and memory formation in nitric oxide synthase inhibitor-treated rats. *Proc Natl Acad Sci U S A* **90**, 9191-9194.

[419] Rickard NS, Gibbs ME (2003) Effects of nitric oxide inhibition on avoidance learning in the chick are lateralized and localized. *Neurobiol Learn Mem* **79**, 252-256.

[420] Koylu EO, Kanit L, Taskiran D, Dagci T, Balkan B, Pogun S (2005) Effects of nitric oxide synthase inhibition on spatial discrimination learning and central DA2 and mACh receptors. *Pharmacol Biochem Behav* **81**, 32-40.

[421] Dinges DF, Pack F, Williams K, Gillen KA, Powell JW, Ott GE, Aptowicz C, Pack AI (1997) Cumulative sleepiness, mood disturbance, and psychomotor vigilance performance decrements during a week of sleep restricted to 4-5 hours per night. *Sleep* **20**, 267-277.

[422] Chee MW, Choo WC (2004) Functional imaging of working memory after 24 hr of total sleep deprivation. *J Neurosci* **24**, 4560-4567.

[423] Lynch HJ, Wurtman RJ, Moskowitz MA, Archer MC, Ho MH (1975) Daily rhythm in human urinary melatonin. *Science* **187**, 169-171.

[424] Palacios-Callender M, Quintero M, Hollis VS, Springett RJ, Moncada S (2004) Endogenous NO regulates superoxide production at low oxygen concentrations by modifying the redox state of cytochrome c oxidase. *Proc Natl Acad Sci U S A* **101**, 7630-7635.

[425] Moller M, Sparre T, Bache N, Roepstorff P, Vorum H (2007) Proteomic analysis of day-night variations in protein levels in the rat pineal gland. *Proteomics* **7**, 2009-2018.

[426] Slominski A, Fischer TW, Zmijewski MA, Wortsman J, Semak I, Zbytek B, Slominski RM, Tobin DJ (2005) On the role of melatonin in skin physiology and pathology. *Endocrine* **27**, 137-148.

[427] Slominski A, Tobin DJ, Zmijewski MA, Wortsman J, Paus R (2008) Melatonin in the skin: synthesis, metabolism and functions. *Trends Endocrinol Metab* **19**, 17-24.

[428] Slominski RM, Reiter RJ, Schlabritz-Loutsevitch N, Ostrom RS, Slominski AT (2012) Melatonin membrane receptors in peripheral tissues: distribution and functions. *Mol Cell Endocrinol* **351**, 152-166.

[429] Soto-Vega E, Meza I, Ramirez-Rodriguez G, Benitez-King G (2004) Melatonin stimulates calmodulin phosphorylation by protein kinase C. *J Pineal Res* **37**, 98-106.

[430] Zoche M, Bienert M, Beyermann M, Koch KW (1996) Distinct molecular recognition of calmodulin-binding sites in the neuronal and macrophage nitric oxide synthases: a surface plasmon resonance study. *Biochemistry* **35**, 8742-8747.

[431] Thies W, Bleiler L (2013) 2013 Alzheimer's disease facts and figures. *Alzheimers Dement* **9**, 208-245.

[432] Murrell J, Farlow M, Ghetti B, Benson MD (1991) A mutation in the amyloid precursor protein associated with hereditary Alzheimer's disease. *Science* **254**, 97-99.

[433] Chartier-Harlin MC, Crawford F, Houlden H, Warren A, Hughes D, Fidani L, Goate A, Rossor M, Roques P, Hardy J, et al. (1991) Early-onset Alzheimer's disease caused by mutations at codon 717 of the beta-amyloid precursor protein gene. *Nature* **353**, 844-846.

[434] Walsh DM, Klyubin I, Fadeeva JV, Cullen WK, Anwyl R, Wolfe MS, Rowan MJ, Selkoe DJ (2002) Naturally secreted oligomers of amyloid beta protein potently inhibit hippocampal long-term potentiation in vivo. *Nature* **416**, 535-539.

References

[435] Portelius E, Olsson M, Brinkmalm G, Ruetschi U, Mattsson N, Andreasson U, Gobom J, Brinkmalm A, Holtta M, Blennow K, Zetterberg H (2012) Mass spectrometric characterization of amyloid-beta species in the 7PA2 cell model of Alzheimer's disease. *J Alzheimers Dis* **33**, 85-93.

[436] Hernandez-Zimbron LF, Luna-Munoz J, Mena R, Vazquez-Ramirez R, Kubli-Garfias C, Cribbs DH, Manoutcharian K, Gevorkian G (2012) Amyloid-beta peptide binds to cytochrome C oxidase subunit 1. *PLoS One* **7**, e42344.

[437] Munguia ME, Govezensky T, Martinez R, Manoutcharian K, Gevorkian G (2006) Identification of amyloid-beta 1-42 binding protein fragments by screening of a human brain cDNA library. *Neurosci Lett* **397**, 79-82.

[438] Seelert H, Dani DN, Dante S, Hauss T, Krause F, Schafer E, Frenzel M, Poetsch A, Rexroth S, Schwassmann HJ, Suhai T, Vonck J, Dencher NA (2009) From protons to OXPHOS supercomplexes and Alzheimer's disease: structure-dynamics-function relationships of energy-transducing membranes. *Biochim Biophys Acta* **1787**, 657-671.

[439] Behl C, Davis JB, Lesley R, Schubert D (1994) Hydrogen peroxide mediates amyloid beta protein toxicity. *Cell* **77**, 817-827.

[440] Kadowaki H, Nishitoh H, Urano F, Sadamitsu C, Matsuzawa A, Takeda K, Masutani H, Yodoi J, Urano Y, Nagano T, Ichijo H (2005) Amyloid beta induces neuronal cell death through ROS-mediated ASK1 activation. *Cell Death Differ* **12**, 19-24.

[441] Hensley K, Carney JM, Mattson MP, Aksenova M, Harris M, Wu JF, Floyd RA, Butterfield DA (1994) A model for beta-amyloid aggregation and neurotoxicity based on free radical generation by the peptide: relevance to Alzheimer disease. *Proc Natl Acad Sci U S A* **91**, 3270-3274.

[442] Combs CK, Karlo JC, Kao SC, Landreth GE (2001) beta-Amyloid stimulation of microglia and monocytes results in TNFalpha-dependent expression of inducible nitric oxide synthase and neuronal apoptosis. *J Neurosci* **21**, 1179-1188.

[443] Dawson VL, Dawson TM, London ED, Bredt DS, Snyder SH (1991) Nitric oxide mediates glutamate neurotoxicity in primary cortical cultures. *Proc Natl Acad Sci U S A* **88**, 6368-6371.

[444] Zhou JN, Liu RY, Kamphorst W, Hofman MA, Swaab DF (2003) Early neuropathological Alzheimer's changes in aged individuals are accompanied by decreased cerebrospinal fluid melatonin levels. *J Pineal Res* **35**, 125-130.

[445] Zubenko GS, Moossy J, Martinez AJ, Rao G, Claassen D, Rosen J, Kopp U (1991) Neuropathologic and neurochemical correlates of psychosis in primary dementia. *Arch Neurol* **48**, 619-624.

[446] Ouchi Y, Yoshikawa E, Futatsubashi M, Yagi S, Ueki T, Nakamura K (2009) Altered brain serotonin transporter and associated glucose metabolism in Alzheimer disease. *J Nucl Med* **50**, 1260-1266.

[447] Garfinkel D, Laudon M, Nof D, Zisapel N (1995) Improvement of sleep quality in elderly people by controlled-release melatonin. *Lancet* **346**, 541-544.

[448] Wu YH, Zhou JN, Van Heerikhuize J, Jockers R, Swaab DF (2007) Decreased MT1 melatonin receptor expression in the suprachiasmatic nucleus in aging and Alzheimer's disease. *Neurobiol Aging* **28**, 1239-1247.

[449] Pappolla MA, Sos M, Omar RA, Bick RJ, Hickson-Bick DL, Reiter RJ, Efthimiopoulos S, Robakis NK (1997) Melatonin prevents death of neuroblastoma cells exposed to the Alzheimer amyloid peptide. *J Neurosci* **17**, 1683-1690.

References

[450]   van Rensburg SJ, Daniels WM, Potocnik FC, van Zyl JM, Taljaard JJ, Emsley RA (1997) A new model for the pathophysiology of Alzheimer's disease. Aluminium toxicity is exacerbated by hydrogen peroxide and attenuated by an amyloid protein fragment and melatonin. *S Afr Med J* **87**, 1111-1115.

[451]   Cardinali DP, Brusco LI, Liberczuk C, Furio AM (2002) The use of melatonin in Alzheimer's disease. *Neuro Endocrinol Lett* **23 Suppl 1**, 20-23.

[452]   Wang XC, Zhang J, Yu X, Han L, Zhou ZT, Zhang Y, Wang JZ (2005) Prevention of isoproterenol-induced tau hyperphosphorylation by melatonin in the rat. *Sheng Li Xue Bao* **57**, 7-12.

[453]   Yang X, Yang Y, Fu Z, Li Y, Feng J, Luo J, Zhang Q, Wang Q, Tian Q (2010) Melatonin ameliorates Alzheimer-like pathological changes and spatial memory retention impairment induced by calyculin A. *J Psychopharmacol* **25**, 1118-1125.

[454]   Spuch C, Antequera D, Isabel Fernandez-Bachiller M, Isabel Rodriguez-Franco M, Carro E (2010) A new tacrine-melatonin hybrid reduces amyloid burden and behavioral deficits in a mouse model of Alzheimer's disease. *Neurotox Res* **17**, 421-431.

[455]   Olcese JM, Cao C, Mori T, Mamcarz MB, Maxwell A, Runfeldt MJ, Wang L, Zhang C, Lin X, Zhang G, Arendash GW (2009) Protection against cognitive deficits and markers of neurodegeneration by long-term oral administration of melatonin in a transgenic model of Alzheimer disease. *J Pineal Res* **47**, 82-96.

[456]   Larson J, Jessen RE, Uz T, Arslan AD, Kurtuncu M, Imbesi M, Manev H (2006) Impaired hippocampal long-term potentiation in melatonin MT2 receptor-deficient mice. *Neurosci Lett* **393**, 23-26.

References

LIST OF PUBBLICATIONS

- Marzia Arese, Maria Chiara Magnifico, Daniela Mastronicola, Fabio Altieri, Caterina Grillo, Thomas J. J. Blanck, Paolo Sarti (2012). Nanomolar melatoin enhances nNOS expression and controls HaCaT-cells bioenergetics. *IUBMB LIFE, vol. 64; p. 251-258, ISSN: 1521-6543, doi: 10.1002/iub.603*.

- Paolo Sarti, Elena Forte, Alessandro Giuffrè, Daniela Mastronicola, Maria Chiara Magnifico, Marzia Arese (2012). The chemical interplay between nitric oxide and mitochondrial cytochrome c oxidase: reactions, effectors & pathophysiology. *In.t J. Cell. Biol., vol. 2012; doi: 10.1155/2012/571067*.

- Paolo Sarti, Maria Chiara Magnifico, Fabio Altieri, Daniela Mastronicola, Marzia Arese (2013). New Evidence for Cross Talk between Melatonin and Mitochondria Mediated by a Circadian-Compatible Interaction with Nitric Oxide. *Int. J. Mol. Sci.; vol. 14; p. 11259-11276; doi: 10.3390/ijms140611259*.

- Nina Krako[1], Maria Chiara Magnifico[1], Marzia Arese, Giovanni Meli, Elena Forte, Agnese Lecci, Annalisa Manca, Alessandro Giuffrè, Daniela Mastronicola, Paolo Sarti, Antonino Cattaneo. Characterization of mitochondrial dysfunctions in the 7PA2 cell model of Alzheimer's Disease (2013). *J. Alzheimer Disease; vol. 37(4); p. 747-58; doi: 10.3233/JAD-130728*.

---

[1] These authors have contributed equally to this work.

156

ATTACHMENTS

Research Communication

Nanomolar Melatonin Enhances nNOS Expression and Controls HaCaT-cells Bioenergetics

Marzia Arese[1], Maria Chiara Magnifico[1], Daniela Mastronicola[2], Fabio Altieri[1], Caterina Grillo[1], Thomas J. J. Blanck[3], and Paolo Sarti[1]

[1]*Department of Biochemical Sciences, Sapienza University of Rome, 00185 Rome, Italy*
[2]*CNR Institute of Molecular Biology and Pathology, 00185 Rome, Italy*
[3]*Department of Anesthesiology, The New York University, New York, NY, USA*

Summary

A novel role of melatonin was unveiled, using immortalized human keratinocyte cells (HaCaT) as a model system. Within a time window compatible with its circadian rhythm, melatonin at nanomolar concentration raised both the expression level of the neuronal nitric oxide synthase mRNA and the nitric oxide oxidation products, nitrite and nitrate. On the same time scale, a depression of the mitochondrial membrane potential was detected together with a decrease of the oxidative phosphorylation efficiency, compensated by glycolysis as testified by an increased production of lactate. The melatonin concentration, ~ nmolar, inducing the bioenergetic effects and their time dependence, both suggest that the observed nitric oxide-induced mitochondrial changes might play a role in the metabolic pathways characterizing the circadian melatonin chemistry. © 2012 IUBMB
IUBMB *Life*, 64(3): 251–258, 2012

INTRODUCTION

Melatonin (*N*-acetyl-5-methoxytryptamine) is involved in the regulation of several cellular functions. It is secreted by the pineal gland but also produced in many other sites such as retina, skin, gut, and bone marrow cells, although the physiological implication of these extrapineal sites, with the exception of retina, is mostly obscure ((*1, 2*) and ref. therein cited).

In humans, the melatonin-generating system is photosensitive displaying a circadian rhythm, with the highest concentration levels produced at night in the darkness (*3, 4*).

Popular for preventing jetlag or as adjuvant in elderly people with sleep-problems, melatonin functional versatility (*5, 6*) has been so far explained by an established antioxidant activity (*7*). Melatonin exerts its action either directly via bulk reactions or indirectly via cell receptor-mediated signaling (*8*), both favoring maintenance of the cell redox balance. Relevant to cell bioenergetics melatonin is highly liposoluble, exerting the antioxidant action also in the mitochondrion (*9, 10*). The molecular mechanisms by which melatonin acts as a hormone at this level and correlation with its circadian synthesis still remain largely obscure.

The receptor-mediated melatonin signaling involves different types of cell surface and nuclear receptors, expressed to a different extent by cell-lines and tissues. Among keratinocytes, the HaCat cell lines used in this study express the cell surface MT2-type receptor (isoform MT2b) and the nuclear receptors, that is, the retinoid orphan receptor (RORα) and the NQO2 flavoprotein, also known as the MT3 melatonin binding site (*11*). The receptor mediated chemistry triggered by melatonin appears complex and is still matter of debate (*8, 12*); it is worth considering that an uptake of melatonin by HaCaT cells has been already described, although at melatonin concentration values in the μM–mM range (*13, 14*).

Nitric oxide (NO) is produced endogenously by the nitric oxide synthase isoforms, NOSs (*15*); the constitutive NOSs, that is, the endothelial NOS (eNOS) and the neuronal NOS (nNOS), produce NO in the nM range, whereas the inducible NOS (iNOS) releases up to μM NO (*16, 17*). NO exerts a controlled inhibitory role on the mitochondrial respiratory chain through the reaction with complex I (*18*) and complex IV (*19–21*). The inhibition of complex IV is rapid and reversible (*20, 22, 23*); a pulse of NO induces a depression of oxidative phosphorylation (*OXPHOS*) and activation of glycolysis, in cells able to sustain

157

it (24, 25). Stimulated by the suggested implication of NO in the circadian cycle (26, 27) and by the finding that the major NO oxidation products, nitrite and nitrate, also follow a circadian rhythm with a night peak (28), we have investigated the interplay between melatonin, NO, and cell bioenergetics by monitoring the mitochondrial response of cultured keratinocytes. We have followed the parameters of interest over several hours incubation with nM melatonin to grossly mimic a night physiological cell exposure to melatonin. On this time scale, we have observed the rise of the nNOS mRNA, paralleled by the production of NOx and leading to a shift of the cell metabolism from *OXPHOS* to glycolysis.

MATERIALS AND METHODS

Chemicals

Dulbecco's modified Eagle's medium (DMEM) and fetal bovine serum (FBS) were from Invitrogen Life Technologies (GIBCO) (Paisley, UK) and from PAA (Linz, Au). Melatonin, JC-1, and all other reagents were purchased from Sigma (St. Louis, MO, USA), unless otherwise specified.

Cell Cultures

Stabilised human keratinocytes (HaCaT, ATCC, cell lines USA) were grown at 37 °C, 5% CO_2, 95% air in DMEM containing 4.5 g/L glucose, 10% FBS, 0.05 mg/mL gentamicin, and 2 mM L-glutamine in 25-cm^2 flasks or multiwell plates. Before melatonin treatment, cells were incubated $\sim$ 24 h in 1 g/L glucose DMEM (w/o FBS and phenol red). When necessary, HaCaT cells were harvested by trypsinization and centrifugation (1,000 $\times$ g) and carefully suspended in the working medium, at suitable density (see text). Cell lysis was performed by CelLytic[TM]M Cell Lysis reagent in the presence of the Protease Inhibitor Cocktail or by TRIzol (Invitrogen, Paisley, UK); protein content was determined according to Bradford (29).

NOS mRNA Determination

NOS mRNA was determined by Quantitative Real Time Polymerase Chain Reaction (QRT-PCR); HaCaT cells were harvested ($\sim$ 3 $\times$ 10^6 cells) and total RNA was isolated (30). The RNA (1 μg) reverse transcription was performed using Side-Step[TM] II QRT-PCR cDNA Synthesis Kit (Stratagene). QRT-PCR was performed using primers designed by BioRad Laboratories (Hercules, CA, USA) (Software Beacon Designer) and purchased by PRIMM (Milano, Italy). SYBR green-based (Brilliant_ SYBR_ Green QPCR Master Mix, Stratagene) QRT-PCR was performed using a MJ Mini Opticon Detection System (BioRad Laboratories). The following protocol was used: denaturation step (95 °C for 5 min), amplification step (95 °C for 10 sec, 55 °C for 30 sec) repeated 45 times. All reactions were performed in triplicate. Melting curve analysis was performed at the end of every run to ensure a single amplified product for each reaction. β-actin gene (PRIMM) was used for normaliza-

tion. QRT-PCR reagents, from Stratagene (Santa Clara, CA, USA). Quantification was performed using the Gene Expression analysis for iCycler iQ Real-Time PCR detection system (Version 1.10, BioRad Laboratories).

NOx (Nitrate/Nitrite) Determination

The accumulation of NOx was determined fluorimetrically (Fluorimetric Assay Kit, Cayman Chemical Co., Ann Arbor, MI, USA) in the culture medium of cells grown under standard conditions, and after 6 h incubation with melatonin (see text).

ATP Measurements

The cell adenosine-5′-triphosphate (ATP) concentration was quantified by chemiluminescence, under stationary conditions or kinetically by following the rate of ATP production. Cells were incubated overnight in an antibiotic/FBS-free DMEM medium, and the following day, melatonin (final concentration 1 nM) was added to the cells ($\sim$ 5 $\times$ 10^4 cells/well) for 6 h.

The stationary ATP measurements were performed using both melatonin treated and control cells suspended in phosphate-buffered-saline (PBS) containing L-glutamine (2 mM), in the presence or absence of glucose, 11 mM; when necessary, oligomycin (2.5 μg/mL) was added over the 1.5 h incubation. The rate of ATP production was evaluated as described in (31) and after cell membrane permeabilization with digitonin (60 μg/mL, 20 min at 25 °C). The assay was performed in the presence of iodoacetamide (2 mM) and the adenylate kinase inhibitor, P^1, P^5-di(adenosine-5′) pentaphosphate pentasodium salt (25 μM). The ATP synthesis was induced by adding to the permeabilized cells, succinate (20 mM) and ADP (0.5 mM), in the presence of rotenone (4 μM) (31). A reference sample was assayed in the absence of succinate and in the presence of antimycin A (18 μM) and oligomycin (2 μM).

ATP measurements (Perkin Elmer, ATPlite) were performed using a VICTOR[TM] Multilabel Counter (Perkin Elmer, USA) equipped with 96-well plates (ViewPlate-96, white, Perkin Elmer, Waltham, USA).

Lactate Measurements

Cells ($\sim$ 3 $\times$ 10^6), precultured $\sim$ 24 h in antibiotic/FBS-free DMEM, were incubated with melatonin, 1 nM, for 6 h and according to (32): 2 h in PBS containing glucose (1 mM), followed by 1 h in PBS without glucose. Thereafter, over the further 3 h incubation, glucose was readded to the cells, in the presence or absence of myxothiazol and antimycin A (10 μM each); the reaction was stopped using $HClO_4$ (33). Lactate was determined spectrophotometrically on the cell supernatant.

Mitochondrial Membrane Potential Measurements

The mitochondrial proton electrochemical potential gradient ($\delta\mu H^+$) of HaCaT cells after $\sim$ 6 h incubation with melatonin (1–100 nM), was measured following the accumulation into the mitochondrial matrix of the fluorescent, cationic probe JC-1
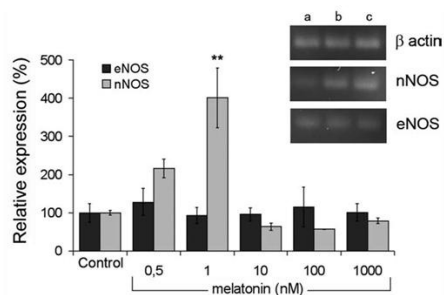
Attachments

Figure 1. Concentration dependence of the melatonin-induced expression of nNOS. Cells ($\sim 3 \times 10^6$) were incubated 6 h with melatonin at the indicated concentrations. QRT-PCR analysis in the presence of primers for eNOS (black) and nNOS (grey) was performed on 10 ng RNA extracted. Relative expression was calculated versus Control, after β-actin normalization. Notice, iNOS was assayed but not detected. Data $+/-$ SEM collected using 3 cell preparations; $n = 9$. **$P \leq 0.01$. *Inset*: gel analysis of RT-PCR amplificates obtained with nNOS, eNOS, and β-actin specific primers, after 38 amplification cycles. The number of cycles was estimated on the basis of QRT-PCR analysis to avoid any saturation effects during the amplification of DNA. a = control, b = melatonin 0.5 nM, c = melatonin 1 nM. Oligonucleotides: nNOS Forward: 5' GCGGTTCTCTATAGCTTCCAGA 3', nNOS Reverse: 5' CCATGTGCTTAATGAAGGACTCG 3'; eNOS Forward: 5' GCCGTGCTGCACAGTTACC 3', eNOS Reverse: 5'GCTCATTCTCCAGGTGCTTCAT 3'; iNOS Forward: 5' CCGAGTCAGAGTCACCATCC 3', iNOS Reverse: 5' CAGCA GCCGTTCCTCCTC 3'; β-actine Forward: 5' GCGAGAAGA TGACCCAGATC 3', β-actine Reverse: 5' GGATAGCA CAGCCTGGATAG 3'.

(Sigma Chem. Co). Briefly, JC-1 (0.4 μM) was added to cells ($\sim 1 \times 10^6$) premixed with nigericin. The kinetics of JC-1 accumulation was measured at 595 nm (VICTOR™ Multilabel Counter, Perkin Elmer) in the presence of ouabain, 0.5 μM, to avoid aspecific cell fluorescence (*34*).

Citrate Synthase

Cells (1×10^6) were lysed and centrifuged at 20,000 $\times$ g and supernatants assayed for citrate synthase (*35*) and for total protein content (*29*). HaCaT cells used as such or after incubation with melatonin display a similar protein content and citrate synthase activity (not shown).

Melatonin Determination

The presence of melatonin was evaluated by immunoassay using the "Direct saliva Melatonin ELISA kit" Bühlmann

Figure 2. Time dependence of the melatonin-induced expression of nNOS. Cells ($\sim 3 \times 10^6$) were incubated with melatonin, 1 nM, as a function of time, as indicated. QRT-PCR in the presence of primers for the nNOS. Data $+/-$ SEM collected using 4 cell preparations, $n = 12$. **$P \leq 0.01$ versus Control; *$P \leq 0.05$ versus Control.

(Schönenbuch, CH), adapted to cell lysates. Cells (3×10^6) were incubated with melatonin (1 nM) for 1 h and 5 h. After incubation, both melatonin-treated and control cells were harvested, resuspended (at 10^6/mL density), and lysed. Aliquots of lysates were loaded on enzyme-linked immunosorbent assay (ELISA) plate containing antimelatonin polyclonal antibody.

Statistics

The number of independent measurements is indicated in figure legend. Significance was determined using the Student *t*-test, run by Excel (Microsoft Windows platform). The error bars correspond to the standard error of the mean (SEM); all *P* values correspond to two-sided sample *t*-test assuming unequal variances. A *P* value ≤ 0.05 was considered significant.

RESULTS

NOSs Gene Expression

The intracellular mRNA expression levels of the eNOS, nNOS, and iNOS were measured by quantitative RT-PCR in HaCaT cells incubated for different times with increasing amounts of melatonin. As shown in Fig. 1, compared with controls, melatonin used at 0.5 and 1 nM concentrations produced a 2.15- and 4-fold increase, respectively, in nNOS mRNA level, whereas under similar conditions the eNOS mRNA did not vary significantly. The iNOS mRNA assayed in parallel remained undetectable under all conditions (not shown). The time dependent profiles of the nNOS expression stimulated up to 7.5 h by 1 nM melatonin, are shown in Fig. 2. The nNOS mRNA expression level increases with the incubation time, reaching a 1.95-

Attachments

Figure 3. Concentration dependence of NOx (nitrite and nitrate) in the cell supernatant. Cells ($\sim 2.5 \times 10^5$/well) were incubated 6 h with melatonin; NOx concentration fluorimetrically determined using the VICTOR™ Multilabel Counter (Perkin Elmer). Data +/− SEM collected using 4 cell preparations; $n = 15$ (controls and melaton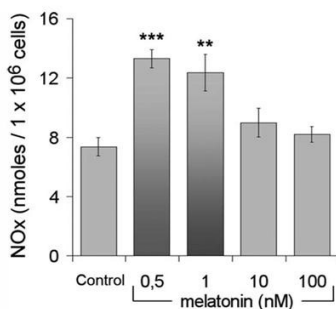in (0.5 nM); $n = 5$ (1, 10, and 100 nM melatonin). ***$P \leq 0.0001$ versus Control; **$P \leq 0.01$ versus Control (details in Materials and Methods section).

fold increase after 3 h and a maximum 3.75-fold increase after 6 h incubation.

Nitrite/Nitrate Accumulation

The accumulation of NOx in the medium after 6 h incubation with increasing amounts of melatonin is shown in Fig. 3. The production of NOx at ~ 1 nM melatonin is ~ 2 times higher than in controls. Melatonin used at 10 and 100 nM concentrations did not affect the NOx production.

Melatonin Determination in HaCaT Cells

We investigated the presence and stability of melatonin in HaCaT cells by immunoassay (ELISA). Cells were incubated with melatonin, 1 nM, for 1 h and 5 h, and the amount of melatonin up-taken by the cells was measured after cell washing and lysis. The results are reported in Table 1 and show that under the conditions chosen a significant amount of melatonin enters the cells, without significant changes over the incubation time.

Mitochondria

ATP Assays. The ATP concentration levels of cells treated for 6 h with melatonin, 1 nM, was measured either at steady state in the presence or absence of glucose or kinetically by following the rate of ATP production (Fig. 4).

When measuring the stationary levels of ATP, glucose starvation was performed to promote *OXPHOS* and minimize the glycolytic contribution to the ATP production (Warburg effect)

Table 1
Cell melatonin concentration

	pmoles/1×10^6 cells ($\pm$ SEM)
Control	$1.50 \times 10^{-3} \pm 0.0003$
Melatonin (1 h incubation)	$65.46 \times 10^{-3} \pm 0.0110$*
Melatonin (5 h incubation)	$52.86 \times 10^{-3} \pm 0.0063$*

*$P < 0.05$.
HaCaT cells (3×10^6) were incubated with melatonin (1 nM) for 1 h and 5 h. After incubation, the melatonin-treated and control cells were harvested, resuspended (at 10^6/mL density), and lysed for ELISA immunoassay (see Materials and Methods section).

(*36*). In the absence of glucose, the addition of oligomycin induces a dramatic decrease of the ATP level, due to *OXPHOS* inhibition (Fig. 4, panel a); under these conditions, the difference between the ATP measured in the absence and presence of oligomycin, defined in Fig. 4 as ΔATP is, within a gross approximation, indicative of the ATP$_{OXPHOS}$ (arrows in Fig. 4, panel a). The results suggest that the ATP$_{OXPHOS}$ is lower in melatonin treated cells with respect to control cells. In the presence of glucose, as glycolysis can take place and compensate for loss of ATP$_{OXPHOS}$ the effect of oligomycin is no longer evident, and the ATP concentration levels of melatonin treated cells and controls are similar (Fig. 4 panel b and c).

The existence of a melatonin-induced depression of the ATP$_{OXPHOS}$ production was verified directly by measuring the rate of succinate-driven ATP synthesis of the cells (*31*). After 6 h incubation with melatonin, 1 nM, the rate of ATP production is 0.51 ($\pm$ 0.044) nmoles/min $\times 10^6$ cells to be compared with 0.69 ($\pm$ 0.028) nmoles/min $\times 10^6$ cells (Fig. 4 panel d). Taken together, the results suggest that melatonin induces a significant $\sim 25\%$ depression of ATP$_{OXPHOS}$ production.

Assaying Lactate. The effect of nM melatonin on the relative contribution of *OXPHOS* and glycolysis to the overall ATP production was independently evaluated by comparing the concentration of lactate produced in the presence of glucose and in the absence or presence of the respiratory chain inhibitors, antimycin A and myxothiazole (Fig. 5). The basal lactate concentration in controls is on average 68 μg/ml $\times 10^6$ cells (Fig. 5a); this value rises to 80 μg/ml $\times 10^6$ cells after melatonin treatment. The increased lactate production induced by melatonin appears consistent with the conclusion that melatonin partially inhibits *OXPHOS*, and glycolysis is compensating: similarly, in the presence of antimycin A and myxothiazole, the lactate increases in controls as in melatonin treated cells; in these latter, to a minor extent as expected if the effect was additive. The basal lactate, that is, the lactate produced in the absence of myxothiazol and antimycin A, is proportional to glycolytic ATP, whereas the difference between the lactate detected in the presence of myxothiazol and antimycin A, and the basal lactate (defined as Δlactate) is proportional to the *OXPHOS* ATP. The basal lactate value divided by Δlactate was taken as indicative of the ratio

160

Attachments
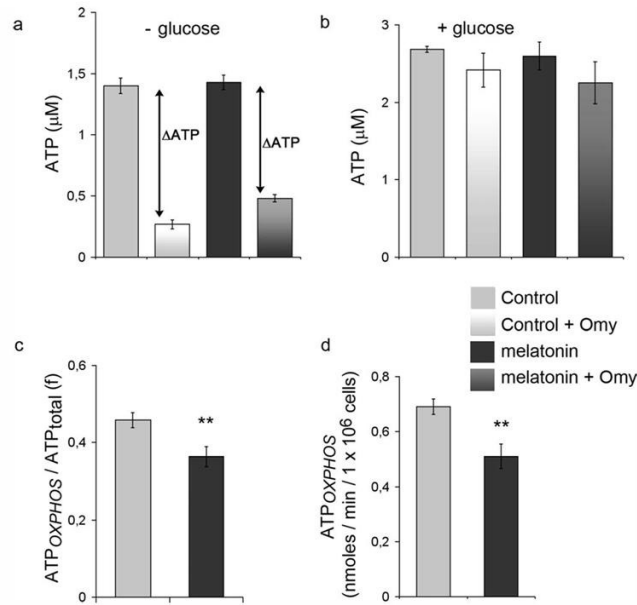
Figure 4. ATP concentration levels and production in HaCaT cells incubated with melatonin. The ATP measurements, by the luciferin/luciferase bioluminescent assay, were performed under stationary conditions (panels a,b,c) using intact HaCaT cells or kinetically after cell membrane permeabilization with digitonine (panel d). Stationary ATP concentration levels: The relative contribution of *OXPHOS* and glycolisis to the accumulation of ATP was evaluated in intact cells (5×10^4/well) in the presence and absence of melatonin 1 nM, oligomycin 2.5 μg/mL and glucose 11 mM as specified: (panel a) in the absence of glucose to avoid glycolysis (3 h cell starvation in the presence of PBS containing L-glutamine); notice that, under these conditions $\Delta ATP \propto ATP_{OXPHOS}$; (panel b) in the presence of glucose to allow glycolysis; (panel c) fractional ATP (f) = ATP_{OXPHOS}/ATP_{total}, where ATP_{OXPHOS} ΔATP (panel a); ATP_{total} was measured in the presence of glucose and absence of oligomycin (solid bars, in panel b); details in the Materials and Methods section. Data +/− SEM collected using 5 cell preparations; $n \geq 12$. **, $P \leq 0.01$ versus Control (details in Materials and Methods section). Rate of mitochondrial ATP synthesis: Complex II driven ATP synthesis was performed using cells permeabilized with digitonin, (panel d) in the presence of succinate, 20 mM, 4 μM rotenone and 0.5 mM ADP (details in Materials and Methods section).

between $ATP_{glycolytic}$ and ATP_{OXPHOS} (*37, 38*), as confirmed by (*32*). As shown in Fig. 5b, the $ATP_{glycolytic}$/ATP_{OXPHOS} ratio is ~ 1.1 in controls and ~ 2.1 in the presence of melatonin.

Mitochondrial Membrane Potential. The effect on mitochondrial $\Delta\mu H^+$ of melatonin added to the cell culture medium was evaluated by following the $\Delta\Psi$-dependent accumulation in the mitochondrial matrix of the fluorescent probe JC-1.

Typical fluorescence kinetics of JC-1 aggregates formation is shown in Fig. 6. After 6 h incubation with 1 nM melatonin, the $\Delta F \propto \Delta\Psi$ is decreased, by $\sim 20\%$. This decrement reaches

36% when cells experience starvation from arginine. The mitochondrial $\Delta\Psi$-depression induced by melatonin was reverted by washing cells and allowing further 3 h incubation in a melatonin-free medium.

DISCUSSION

The key finding of this work is that in the presence of nanomolar amounts of melatonin and after a few hours incubation, the basal level of the cellular nNOS expression rises by a factor of 4 thereafter returning to basal level. Almost synchronously

1 6 1

also the production of NOx increases while the mitochondrial membrane potential decreases. A partial decrease of ATP *OXPHOS* production is also observed, as well as a compensatory increase of glycolytic ATP, expected on the basis of the Warburg effect typically occurring in the presence of glucose

Figure 5. Melatonin-dependent accumulation of lactate in the medium of HaCaT cells. Cells (3×10^6) were incubated 6 h with melatonin (Mel) 1 nM. (a) Basal lactate $\propto$ ATP$_{glycolytic}$; Δlct $\propto$ ATP$_{OXPHOS}$. Glucose 1 mM, myxothiazol (Myxo) and antimycin A (Anti A), 10 μM each. (b) Ratio between basal lactate and Δlct, as indicative of the ATP$_{glycolytic}$/ATP$_{OXPHOS}$ ratio (*32*) (details in Materials and Methods section). Values are the means $\pm$ SEM; $n = 4$. *$P \leq 0.05$ versus Control.

sustaining glycolysis. Taken together, these findings suggest that, triggered by melatonin and over the time window explored, a fraction of mitochondrial complex IV reacts with NO and is reversibly inhibited (*20, 23, 39*).

The inhibition of ATP *OXPHOS* production is better observed in the absence of glucose, when the contribution of glycolysis is minimized. Under these conditions, the overall ATP level is almost halved, compared with cells maintained in glucose (*40*) and the addition of oligomycin causes a dramatic decrease of ATP, whose amplitude is indicative of the *OXPHOS* contribution to the overall ATP detected (ΔATP in Fig. 4). Interestingly, the ΔATP induced by oligomycin is reproducibly smaller in melatonin-treated cells, likely due to the (just mentioned) partial inhibition of complex IV because under the conditions explored, that is, low NO concentration, the involvement of complex I, though possible, is less likely (*41*). It is worth noting that when the cells were starved from the NOS substrate arginine, the electrophoretic import of JC-1 was the highest, confirming that cultured cells may express a basal NOS activity, releasing NO and depressing the mitochondrial potential to a measurable extent (*42*). The decrease of *OXPHOS* ATP induced by melatonin, though statistically significant is small, likely due to glycolytic compensation; therefore *OXPHOS* impairment was further substantiated measuring lactate (*32*). After exposure to melatonin, the ATP$_{glycolytic}$/ATP$_{OXPHOS}$ ratio, worked out through lactate measurements, is $\sim$ two-fold higher, confirming that nM melatonin drives the equilibrium between ATP$_{OXPHOS}$ and ATP$_{glycolytic}$, toward the latter (Fig. 5b).

Figure 6. Melatonin affects mitochondrial membrane potential of cells. (a) time-dependent JC-1 mitochondrial accumulation; Control without arginine (orange) and after $\sim$ 6 h incubation with melatonin 1 nM (blue). Reaction started with nigericin (0.6 μM, red arrows). Excitation wavelength = 490 nm, emission wavelength = 590 nm. ΔF_{max} values calculated from plateau to the fluorescence level reached on addition of valinomycin (black arrows). (b) ΔF_{max} at different melatonin concentrations and in controls or in the absence of arginine (the NOS substrate), color code as in panel a. Data $+/-$ SEM collected using 4 different cell preparations $n = 4$. *$P \leq 0.05$ versus Control; #$P \leq 0.05$ versus no Arg; ##$P \leq 0.001$ versus no Arg. (c) ΔF decrement ($\Delta\Delta F$ %) of melatonin treated cells (blue bar) versus Control at 6 or 9 h (gray). After melatonin, incubation cells were washed and incubated further 3 h (i) without melatonin (gray-blue) and (ii) with melatonin renovated in the medium (blue). Data $+/-$ SEM collected using 4 different cell preparations $n \geq 4$ (details in Materials and Methods section).

1 6 2

Attachments

Within the limits of the heterogeneous distribution of melatonin among organ and tissues (43), it is intriguing that the concentrations of melatonin, in the nM range, inducing the observed changes of the nNOS mRNA are compatible with the concentration of melatonin circulating in the human blood at night peak time, that is, $\sim$ 100–200 pg/mL (1, 6), corresponding to $\sim$ 1 nM melatonin. Even more interestingly, under these conditions, the upregulation of glycolytic enzymes has been observed in the rat pineal gland (44), suggesting a correlation between melatonin and mitochondrial metabolism.

The up-regulation of nNOS herein reported seems specific because, over the same time period, the eNOS expression remained constant and the iNOS was not detectable. Consistently with a receptor mediated nuclear DNA-activated process, no effects of melatonin were observed at incubation times earlier than 4–5 h. At melatonin concentrations higher than nM, and/or by further extending the melatonin incubation time the nNOS expression decreases, suggesting the existence of a time- and concentration-dependent negative feed-back control of the nNOS mRNA expression, at least in HaCaT cells. The mRNA expression level observed at 1 nM melatonin is about the double of that observed at 0.5 nM, whereas the corresponding NOx levels are similar. This finding is of complex interpretation because possibly related to post-transcriptional regulation of nNOS, as well as to different stationary stability of the nNOS mRNA and the NOx: a unique answer demands further investigation.

Indeed, it is possible that the mitochondrial effects attributed to melatonin (this article) might be also related to still active melatonin degradation products (2, 13), whose effectiveness remains to be elucidated. Regardless of their involvement, however, it is worth to consider that depending on the fraction of cytochrome-c-oxidase inhibited by NO, the O_2 consumption and thereby the *OXPHOS* ATP synthesis, may be differently affected, particularly depending on the functional state (ATP synthesis) prevailing in mitochondria (19, 45). In state IV respiration, the electron flux through the respiratory chain is controlled at the level of complex I rather than at cytochrome-c-oxidase, so that inhibition of a relatively small fraction of cytochrome-c-oxidase may not result in a significant decrease of O_2 consumption, while increasing the reduction level of the uphill respiratory chain components, hence the production of ROS (46, 47). On the contrary, when the rate-control of the respiratory chain is transferred to the cytochrome-c-oxidase, as it occurs typically with state III respiring mitochondria (21, 48), the rate of respiration together with synthesis of ATP *OXPHOS* decreases; in this case, a higher fraction of O_2 might become available for close by cells (O_2-diversion). HaCaT cells, whose relative population of state III and state IV mitochondria under the conditions explored is hard to determine and presently unknown, do not display a clear melatonin-induced depression of respiration (not shown). Still, in the presence of nM melatonin, we observe a depression of mitochondrial $\Delta\psi$ as well as a clear metabolic shift toward glycolysis.

In summary, based on the data provided by this study, nM melatonin in the environment of melatonin-sensitive cells produces a transient but substantial rise of the constitutive nNOS. The induced increase of NO production leads to transient, partial inhibition of the respiratory chain with a decrease of mitochondrial $\Delta\psi$, depression of *OXPHOS*, and rise of glycolysis. All together these findings suggest that we are facing a new role of melatonin, involving mitochondria probably in a circadian context.

REFERENCES

1. Zawilska, J. B., Skene, D. J., and Arendt, J. (2009) Physiology and pharmacology of melatonin in relation to biological rhythms. *Pharmacol. Rep.* **61**, 383–410.
2. Tan, D. X., Manchester, L. C., Terron, M. P., Flores, L. J., and Reiter, R. J. (2007) One molecule, many derivatives: a never-ending interaction of melatonin with reactive oxygen and nitrogen species? *J. Pineal Res.* **42**, 28–42.
3. Hardeland, R., Cardinali, D. P., Srinivasan, V., Spence, D. W., Brown, G. M., and Pandi-Perumal, S. R. Melatonin—a pleiotropic, orchestrating regulator molecule. *Prog. Neurobiol.* **93**, 350–384.
4. Cajochen, C., Krauchi, K., and Wirz-Justice, A. (2003) Role of melatonin in the regulation of human circadian rhythms and sleep. *J. Neuroendocrinol.* **15**, 432–437.
5. Pandi-Perumal, S. R., Trakht, I., Srinivasan, V., Spence, D. W., Maestroni, G. J., Zisapel, N., and Cardinali, D. P. (2008) Physiological effects of melatonin: role of melatonin receptors and signal transduction pathways. *Prog. Neurobiol.* **85**, 335–353.
6. Pandi-Perumal, S. R., Srinivasan, V., Maestroni, G. J., Cardinali, D. P., Poeggeler, B., and Hardeland, R. (2006) Melatonin: nature's most versatile biological signal? *FEBS J.* **273**, 2813–2838.
7. Reiter, R. J. (1998) Oxidative damage in the central nervous system: protection by melatonin. *Prog. Neurobiol.* **56**, 359–384.
8. Luchetti, F., Canonico, B., Betti, M., Arcangeletti, M., Pilolli, F., Piroddi, M., Canesi, L., Papa, S., and Galli, F. (2010) Melatonin signaling and cell protection function. *FASEB J.* **24**, 3603–3624.
9. Leon, J., Acuna-Castroviejo, D., Escames, G., Tan, D. X., and Reiter, R. J. (2005) Melatonin mitigates mitochondrial malfunction. *J. Pineal Res.* **38**, 1–9.
10. Lopez, A., Garcia, J. A., Escames, G., Venegas, C., Ortiz, F., Lopez, L. C., and Acuna-Castroviejo, D. (2009) Melatonin protects the mitochondria from oxidative damage reducing oxygen consumption, membrane potential, and superoxide anion production. *J. Pineal Res.* **46**, 188–198.
11. Slominski, A., Fischer, T. W., Zmijewski, M. A., Wortsman, J., Semak, I., Zbytek, B., Slominski, R. M., and Tobin, D. J. (2005) On the role of melatonin in skin physiology and pathology. *Endocrine* **27**, 137–148.
12. Slominski, A., Tobin, D. J., Zmijewski, M. A., Wortsman, J., and Paus, R. (2008) Melatonin in the skin: synthesis, metabolism and functions. *Trends Endocrinol. Metab.* **19**, 17–24.
13. Fischer, T. W., Sweatman, T. W., Semak, I., Sayre, R. M., Wortsman, J., and Slominski, A. (2006) Constitutive and UV-induced metabolism of melatonin in keratinocytes and cell-free systems. *FASEB J.* **20**, 1564–1566.

163

258   ARESE ET AL.

14. Nickel, A. and Wohlrab, W. (2000) Melatonin protects human keratino-cytes from UVB irradiation by light absorption. *Arch. Dermatol. Res.* **292**, 366–368.
15. Alderton, W. K., Cooper, C. E., and Knowles, R. G. (2001) Nitric oxide synthases: structure, function and inhibition. *Biochem. J.* **357**, 593–615.
16. Brown, G. C. (2001) Regulation of mitochondrial respiration by nitric oxide inhibition of cytochrome c oxidase. *Biochim. Biophys. Acta* **1504**, 46–57.
17. Cooper, C. E. and Brown, G. C. (2008) The inhibition of mitochondrial cytochrome oxidase by the gases carbon monoxide, nitric oxide, hydrogen cyanide and hydrogen sulfide: chemical mechanism and physiological significance. *J. Bioenerg. Biomembr.* **40**, 533–539.
18. Schapira, A. H. (2010) Complex I: inhibitors, inhibition and neurodegeneration. *Exp. Neurol.* **224**, 331–335.
19. Antunes, F., Boveris, A., and Cadenas, E. (2007) On the biologic role of the reaction of NO with oxidized cytochrome c oxidase. *Antioxid. Redox. Signaling* **9**, 1569–1579.
20. Brown, G. C. and Cooper, C. E. (1994) Nanomolar concentrations of nitric oxide reversibly inhibit synaptosomal respiration by competing with oxygen at cytochrome oxidase. *FEBS Lett.* **356**, 295–298.
21. Mastronicola, D., Genova, M. L., Arese, M., Barone, M. C., Giuffre, A., Bianchi, C., Brunori, M., Lenaz, G., and Sarti, P. (2003) Control of respiration by nitric oxide in Keilin-Hartree particles, mitochondria and SH-SY5Y neuroblastoma cells. *Cell Mol. Life Sci.* **60**, 1752–1759.
22. Cleeter, M. W., Cooper, J. M., Darley-Usmar, V. M., Moncada, S., and Schapira, A. H. (1994) Reversible inhibition of cytochrome c oxidase, the terminal enzyme of the mitochondrial respiratory chain, by nitric oxide. Implications for neurodegenerative diseases. *FEBS Lett.* **345**, 50–54.
23. Sarti, P., Giuffrè, A., Barone, M. C., Forte, E., Mastronicola, D., and Brunori, M. (2003) Nitric oxide and cytochrome oxidase: reaction mechanisms from the enzyme to the cell. *Free Radic. Biol. Med.* **34**, 509–520.
24. Almeida, A., Almeida, J., Bolanos, J. P., and Moncada, S. (2001) Different responses of astrocytes and neurons to nitric oxide: the role of glycolytically generated ATP in astrocyte protection. *Proc. Natl. Acad. Sci. U.S.A.* **98**, 15294–15299.
25. Bolanos, J. P., Delgado-Esteban, M., Herrero-Mendez, A., Fernandez-Fernandez, S., and Almeida, A. (2008) Regulation of glycolysis and pentose-phosphate pathway by nitric oxide: impact on neuronal survival. *Biochim. Biophys. Acta* **1777**, 789–793.
26. Kunieda, T., Minamino, T., Miura, K., Katsuno, T., Tateno, K., Miyauchi, H., Kaneko, S., Bradfield, C. A., FitzGerald, G. A., and Komuro, I. (2008) Reduced nitric oxide causes age-associated impairment of circadian rhythmicity. *Circ. Res.* **102**, 607–614.
27. Marino, J. and Cudeiro, J. (2003) Nitric oxide-mediated cortical activation: a diffuse wake-up system. *J. Neurosci.* **23**, 4299–4307.
28. Tsikas, D., Gutzki, F. M., and Stichtenoth, D. O. (2006) Circulating and excretory nitrite and nitrate as indicators of nitric oxide synthesis in humans: methods of analysis. *Eur. J. Clin. Pharmacol.* **62**, 51–59.
29. Bradford, M. M. (1976) A rapid and sensitive method for the quantitation of microgram quantities of protein utilizing the principle of protein-dye binding. *Anal. Biochem.* **72**, 248–254.
30. Chomczynski, P. and Sacchi, N. (1987) Single-step method of RNA isolation by acid guanidinium thiocyanate-phenol-chloroform extraction. *Anal. Biochem.* **162**, 156–159.

31. Sgarbi, G., Baracca, A., Lenaz, G., Valentino, L. M., Carelli, V., and Solaini, G. (2006) Inefficient coupling between proton transport and ATP synthesis may be the pathogenic mechanism for NARP and Leigh syndrome resulting from the T8993G mutation in mtDNA. *Biochem. J.* **395**, 493–500.
32. Merlo-Pich, M., Deleonardi, G., Biondi, A., and Lenaz, G. (2004) Methods to detect mitochondrial function. *Exp. Gerontol.* **39**, 277–281.
33. Everse, J. (1975) Enzymic determination of lactic acid. *Methods Enzymol.* **41**, 41–44.
34. Reers, M., Smith, T. W., and Chen, L. B. (1991) J-aggregate formation of a carbocyanine as a quantitative fluorescent indicator of membrane potential. *Biochemistry* **30**, 4480–4486.
35. Srere, P. A. (1969) Citrate synthase. *Methods Enzymol.* **13**, 3–11.
36. Warburg, O. (1956) On respiratory impairment in cancer cells. *Science* **124**, 269–270.
37. Lenaz, G., D'Aurelio, M., Merlo Pich, M., Genova, M. L., Ventura, B., Bovina, C., Formiggini, G., and Parenti Castelli, G. (2000) Mitochondrial bioenergetics in aging. *Biochim. Biophys. Acta* **1459**, 397–404.
38. Holmsen, H. and Robkin, L. (1980) Effects of antimycin A and 2-deoxyglucose on energy metabolism in washed human platelets. *Thromb. Haemost.* **42**, 1460–1472.
39. Cooper, C. E., Mason, M. G., and Nicholls, P. (2008) A dynamic model of nitric oxide inhibition of mitochondrial cytochrome c oxidase. *Biochim. Biophys. Acta* **1777**, 867–876.
40. Bolanos, J. P., Almeida, A., and Moncada, S. (2010) Glycolysis: a bioenergetic or a survival pathway? *Trends Biochem. Sci.* **35**, 145–149.
41. Clementi, E., Brown, G. C., Feelisch, M., and Moncada, S. (1998) Persistent inhibition of cell respiration by nitric oxide: crucial role of S-nitrosylation of mitochondrial complex I and protective action of glutathione. *Proc. Natl. Acad. Sci. U.S.A.* **95**, 7631–7636.
42. Sarti, P., Lendaro, E., Ippoliti, R., Bellelli, A., Benedetti, P. A., and Brunori, M. (1999) Modulation of mitochondrial respiration by nitric oxide: investigation by single cell fluorescence microscopy. *FASEB J.* **13**, 191–197.
43. Tan, D. X., Manchester, L. C., Sanchez-Barcelo, E., Mediavilla, M. D., and Reiter, R. J. (2010) Significance of high levels of endogenous melatonin in Mammalian cerebrospinal fluid and in the central nervous system. *Curr. Neuropharmacol.* **8**, 162–167.
44. Moller, M., Sparre, T., Bache, N., Roepstorff, P., and Vorum, H. (2007) Proteomic analysis of day-night variations in protein levels in the rat pineal gland. *Proteomics* **7**, 2009–2018.
45. Palacios-Callender, M., Quintero, M., Hollis, V. S., Springett, R. J., and Moncada, S. (2004) Endogenous NO regulates superoxide production at low oxygen concentrations by modifying the redox state of cytochrome c oxidase. *Proc. Natl. Acad. Sci. U.S.A.* **101**, 7630–7635.
46. Palacios-Callender, M., Hollis, V., Frakich, N., Mateo, J., and Moncada, S. (2007) Cytochrome c oxidase maintains mitochondrial respiration during partial inhibition by nitric oxide. *J. Cell Sci.* **120**, 160–165.
47. Ventura, B., Genova, M. L., Bovina, C., Formiggini, G., and Lenaz, G. (2002) Control of oxidative phosphorylation by Complex I in rat liver mitochondria: implications for aging. *Biochim. Biophys. Acta* **1553**, 249–260.
48. Shiva, S., Brookes, P. S., Patel, R. P., Anderson, P. G., and Darley-Usmar, V. M. (2001) Nitric oxide partitioning into mitochondrial membranes and the control of respiration at cytochrome c oxidase. *Proc. Natl. Acad. Sci. U.S.A.* **98**, 7212–7217.

164

Attachments

Review Article

The Chemical Interplay between Nitric Oxide and Mitochondrial Cytochrome *c* Oxidase: Reactions, Effectors and Pathophysiology

Paolo Sarti,[1,2] Elena Forte,[1] Alessandro Giuffrè,[2] Daniela Mastronicola,[2] Maria Chiara Magnifico,[1] and Marzia Arese[1]

[1] Department of Biochemical Sciences and Istituto Pasteur-Fondazione Cenci Bolognetti, Sapienza University of Rome, Piazzale Aldo Moro 5, 00185 Rome, Italy
[2] CNR Institute of Molecular Biology and Pathology, Piazzale Aldo Moro 5, 00185 Rome, Italy

Correspondence should be addressed to Paolo Sarti, paolo.sarti@uniroma1.it

Nitric oxide (NO) reacts with Complex I and cytochrome *c* oxidase (CcOX, Complex IV), inducing detrimental or cytoprotective effects. Two alternative reaction pathways (PWs) have been described whereby NO reacts with CcOX, producing either a relatively labile nitrite-bound derivative (CcOX-NO$_2^-$, PW1) or a more stable nitrosyl-derivative (CcOX-NO, PW2). The two derivatives are both inhibited, displaying different persistency and O$_2$ competitiveness. In the mitochondrion, during turnover with O$_2$, one pathway prevails over the other one depending on NO, cytochrome c^{2+} and O$_2$ concentration. High cytochrome c^{2+}, and low O$_2$ proved to be crucial in favoring CcOX nitrosylation, whereas under-*standard* cell-culture conditions formation of the nitrite derivative prevails. All together, these findings suggest that NO can modulate physiologically the mitochondrial respiratory/OXPHOS efficiency, eventually being converted to nitrite by CcOX, without cell detrimental effects. It is worthy to point out that nitrite, far from being a simple oxidation byproduct, represents a source of NO particularly important in view of the NO cell homeostasis, the NO production depends on the NO synthases whose activity is controlled by different stimuli/effectors; relevant to its bioavailability, NO is also produced by recycling cell/body nitrite. Bioenergetic parameters, such as mitochondrial $\Delta\Psi$, lactate, and ATP production, have been assayed in several cell lines, in the presence of endogenous or exogenous NO and the evidence collected suggests a crucial interplay between CcOX and NO with important energetic implications.

1. Introduction

It is nowadays established that nitrogen monoxide (NO), nitric oxide in the literature, inhibits mitochondrial respiration. The inhibition is induced by the reaction of NO with some of the complexes of the respiratory chain, according to mechanisms studied over more than 20 years. The reaction of NO with Complex III is sluggish [1], whereas the reaction of NO with Complex I and Complex IV, that is, cytochrome *c* oxidase (CcOX), is rapid and to a large extent reversible. Both reactions lead to formation of derivatives responsible of the mitochondrial nitrosative stress observed in different pathophysiological conditions, including main neurodegenerations [2–6]. The functional groups of the mitochondrial complexes reacting with NO include the metals at the catalytic active site of CcOX, namely, the Fe and Cu ions of the

heme a_3-Cu$_B$ site [7, 8]. The inhibition of Complex I results from the reversible S-nitrosation of Cys39 exposed on the surface of the ND3 subunit [9, 10]. The functional effects on cell respiration depend on the complex targeted by NO and on type of reaction. Inhibition of both Complex I and CcOX is mostly reversible, becoming irreversible, however, depending on duration of the exposure to NO and on its concentration [10, 11]. The onset of NO inhibition on Complex I is slow (minutes [10]), whereas on CcOX is very fast (milliseconds to seconds [12]). In this paper the attention is focused on the interactions between NO and CcOX. The balance between the concentrations of cytochrome c^{2+} and O$_2$ proved to be critical in inducing different CcOX inhibition patterns, spanning from a finely tuned *control* to a severe, almost irreversible enzyme inactivation [13]. The interplay between CcOX and NO is based on the inhibition
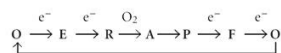
exerted by NO on the enzyme that, in turn, actively controls the NO concentration at the mitochondrial site [14].

The redox active site of CcOX contains one heme a_3 and one Cu_B tightly coupled in the so-called binuclear site, where the O_2 and NO chemistry as well as the reaction with common ligands occur. The active site receives electrons intra-molecularly from the reduced heme a and Cu_A, forming together the electron accepting pole of CcOX, maintained physiologically reduced by cytochrome c. Also relevant to the reaction of NO with CcOX, the availability in the mitochondrion of reduced cytochrome c depends on the relative rate at which it is reduced by Complex III and oxidized by O_2 via CcOX. It is also worth mentioning that the absolute cytochrome c concentration may vary in different cell lines and tissues [15]. The rate of reaction of CcOX with O_2 is close to diffusion limited ($k \approx 1 \times 10^8 \, M^{-1} \, s^{-1}$ [16, 17]), whereas the reaction with cytochrome c is slower, $k \approx 1 \times 10^6 \, M^{-1} \, s^{-1}$, the actual rate constant value being dependent on pH and ionic strength [18]. During turnover, the reduction level of the CcOX redox sites, and particularly of the metals in the active site, depends on (i) the actual concentration of reduced cytochrome c and O_2 (weighted for their relative K_M values) at the redox competent sites and (ii) the internal electron transfer rate from the electron accepting pole (heme a-Cu_A), where cytochrome c reacts, to the active (heme a_3-Cu_B) site, where the O_2 reaction takes place. At saturating concentration of the physiological substrates, the rate limiting step in the CcOX catalytic cycle is the internal electron transfer [19–21]. Over and above the description of the reaction mechanisms, the aim of this work is to stress the idea that CcOX uses both O_2 and NO as physiological substrates [5, 14, 22, 23] and to review the experimental evidence pointing to a central role of the NO interplay with CcOX in cell bioenergetics.
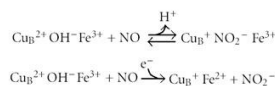
2. CcOX Binds Reversibly or Oxidizes NO to Nitrite at the Active Site Where O_2 Binds

In order to better understand the reciprocal interactions between CcOX and NO, it may help summarizing the intermediates populated by CcOX during turnover with physiological substrates. During the catalytic cycle the fully oxidized (**O**) heme a_3-Cu_B site accepts a first electron from Cu_A/heme a, leading to formation of a partially, single-electron, reduced (**E**) species; subsequently, a second electron is transferred to the active site, and the fully reduced (**R**) species is formed. Once in the **R** state, O_2 binds rapidly generating the short-lived (microseconds, at 20°C) compound **A**, in which O_2 is complexed to heme a_3^{2+} [24]. Electrons are rapidly delivered to bound O_2, and Compound **A** converts to a nominal peroxy (**P**) complex with both heme a_3 and Cu_B oxidized; actually, the experimental evidence suggests that the O–O (peroxy) bond in this **P** species is already cleaved off, showing heme a_3 in the ferryl ($Fe^{4+}=O$) form and a tyrosine residue in a radical state [25, 26]. By accepting a third electron, **P** decays quickly into a canonical ferryl (**F**) intermediate [27], that eventually converts back to the fully oxidized **O** state upon arrival of one last electron from Cu_A/heme a. The sequential steps and the intermediates populated during a single turnover are indicated, starting and ending with the fully oxidized **O** species:

$$\mathbf{O} \xrightarrow{e^-} \mathbf{E} \xrightarrow{e^-} \mathbf{R} \xrightarrow{O_2} \mathbf{A} \longrightarrow \mathbf{P} \xrightarrow{e^-} \mathbf{F} \xrightarrow{e^-} \mathbf{O}$$

Since first proposed as a unified picture based on experiments carried out using purified CcOX [28], the enzyme adducts formed upon reacting with NO have been spectroscopically identified as a nitrosyl-derivative (heme a_3^{2+}-NO) or as a nitrite-bound (heme a_3^{3+}-NO_2^-) derivative, or a mixture of these two species, depending on the steady-state fractional accumulation of all the intermediates [29]. It is worthy to notice that the Fe and Cu ions in the active site undergo redox changes only upon reacting in the oxidized state (i.e., Fe^{3+}, Fe^{4+}, Cu^{2+}) with NO. During the reaction NO is oxidized to NO_2^-, that is released in the medium; the whole event is identified as pathway 1 (PW1):

$$Cu_B^{2+} OH^- Fe^{3+} + NO \underset{H^+}{\rightleftharpoons} Cu_B^+ NO_2^- Fe^{3+}$$

$$Cu_B^{2+} OH^- Fe^{3+} + NO \xrightarrow{e^-} Cu_B^+ Fe^{2+} + NO_2^-$$

Otherwise, if the active site is partially or fully reduced, an affinity-driven NO binding to these metals takes place; the whole event is identified as pathway 2 (PW2) and occurs without further redox events:

$$Cu_B^+ Fe^{2+} + NO \rightleftharpoons Cu_B^+ Fe^{2+} NO$$
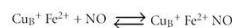
NO is very reactive towards the fully reduced **R** binuclear site. It binds to heme a_3^{2+} at a rate similar to that of O_2, that is, $k = 0.4 - 1 \times 10^8 \, M^{-1} \, s^{-1}$ [16, 17], yielding the high affinity Fe^{2+} nitrosyl adduct, whose accumulation is observable directly by spectroscopy or indirectly by NO amperometry [30, 31], when the fully reduced CcOX in detergent solution is mixed with NO. Interestingly, in the presence of NO, all circumstances favoring the electron donation to the catalytic site of CcOX or slowing down its oxidation by O_2 as during hypoxia (i.e., when the $[O_2] \leq K_{M,O_2}$ of CcOX) proved to favor CcOX nitrosylation [32]. Figure 1 shows schematically how accumulation of the turnover intermediates correlates with the build up of the nitrosylated ($Cu_B^+ Fe^{2+} NO$) or the nitrite-bound ($Cu_B^+ NO_2^- Fe^{3+}$) species.

It is worth mentioning that, contrary to a few bacterial oxidases [34–36], mitochondrial CcOX cannot reduce to N_2O the NO bound at reduced heme a_3 [30]. This implies that the functional recovery of the enzyme after NO binding necessarily lags behind the thermal dissociation of NO from the active site. The dissociation reaction is relatively slow ($k_{off} = 3.9 \times 10^{-3} \, s^{-1}$ at 20°C) and photosensitive [28]. Photosensitivity has been widely used by Sarti and coworkers to gain insight, through amperometric measurements, into the mechanism of CcOX inhibition by NO in mitochondria or whole cells [37], that is, under conditions unfavorable to spectroscopy. Since the fully reduced binuclear site reacts eagerly with both O_2 and NO, the inhibition of CcOX via
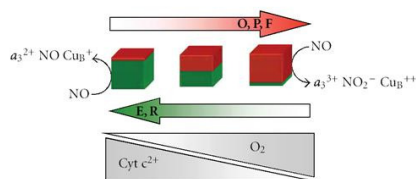
FIGURE 1: Dual-pathway model for the interaction of NO with mitochondrial cytochrome oxidase. The nature of the interaction between NO and CcOX depends on the catalytic intermediates targeted, and these are differently populated at different concentrations of O_2 and reduced cytochrome c. The oxidized intermediates **O**, **P**, **F** (see text) are overall more populated with increasing O_2 availability, and/or decreasing the concentration of reduced cytochrome c in the mitochondrion: these intermediates react with NO generating a nitrite-inhibited CcOX. The reduced species **E** and **R** (see text) buildup, instead, upon decreasing O_2 and/or increasing the concentration of reduced cytochrome c: upon reacting with NO, these intermediates generate a heme a_3^{2+}-NO complex, in competition with oxygen.

formation of a nitrosyl adduct is expected to occur in competition with O_2, that is, according to PW2. Consistently, the O_2 competition is more clearly observed when the concentration of the reducing substrates favors the reduction of the enzyme [29, 32]. In any case, the inhibition of the nitrosylated CcOX is reverted at the rate of the NO thermal dissociation from reduced heme a_3 [28]. It is worth noticing that, although the NO dissociation process is mechanistically independent of O_2 concentration, bulk O_2 shortens the duration of inhibition by oxidizing free NO in solution, thus hampering NO rebinding to CcOX.

3. The Fully- and Half-Reduced Binuclear Site

The ability of the single electron reduced **E** species to bind NO was investigated using the K354M mutant of the *Paracoccus denitrificans* CcOX [38]. In this mutant the internal electron transfer from the electron accepting pole to the active site is severely impaired, so that the full reduction of the active site and its reaction with O_2 is achieved very slowly, that is, within several minutes. Under these conditions the electron transferred intramolecularly from heme a/Cu_A resides on either heme a_3 or Cu_B, and the resulting **E** species can not react with O_2. Interestingly, however, **E** reacts promptly with NO generating the nitrosyl derivative. Thus, one can conclude that, unlike O_2, NO binds to the binuclear active site even before its complete reduction [12, 31]. Whether the reaction with **E** plays a role in the mechanism of CcOX inhibition by NO during turnover is still unclear, since it has been also suggested that at steady-state the reaction of NO with **E** is not required to account for fast inhibition [32, 39]. Regardless of whether the reaction of NO with either **E** or **R** is predominant, it seems feasible to conclude that all conditions leading to reduction of the binuclear site in the presence of NO favor nitrosylation of the enzyme.

4. The Role of Cu_B in the Reaction with NO

The reaction of NO with Cu_B in the fully oxidized CcOX to form nitrite was first reported by Brudvig and coworkers in the early 80s [40]. Later on this reaction was reinvestigated by Cooper et al. [41] and Giuffrè et al. [42], using a *pulsed* (*fast*) preparation of CcOX. The pulsing procedure that *in vitro* consists in preliminary reduction-reoxidation of CcOX [43], removes chloride from the oxidized active site of the enzyme thereby allowing fast reaction with NO [42]; indeed, CcOX is expectedly in the pulsed state *in vivo* where CcOX turnover takes place continuously. During the reaction with the oxidized Cu_B ($k = 2 \times 10^5$ M^{-1} s^{-1} at 20°C), NO is transiently oxidized to nitrosonium ion (NO^+), which is subsequently hydroxylated (or hydrated) to nitrite/nitrous acid.

Thus, after the reaction, the enzyme displays nitrite bound to ferric heme a_3 and is inhibited. The affinity of nitrite for the reduced heme a_3, however, is much lower than the affinity for the oxidized active site. The intramolecular electron transfer to heme a_3-Cu_B, therefore, causes the prompt dissociation of nitrite and the subsequent full restoration of activity [29, 44]. Relevant to possible pathophysiological effects of CcOX inhibition by NO, it is worthy to notice that the nitrite dissociation upon reduction of heme a_3 ($k\sim6 \times 10^{-2}$ s^{-1} at pH = 7.3, $T = 20°C$ [29]) is approximately one order of magnitude faster than the NO-dissociation from the nitrosylated site, accounting also for the observed production of nitrite by isolated mitochondria [45, 46].

It has been proposed that nitrite formation could follow an alternative route via reaction with O_2 of the NO bound to the fully reduced CcOX [46]. According to this proposal, a superoxide anion (O_2^-) forms by the reaction of O_2 with reduced Cu_B and reacts with NO bound to reduced heme a_3 to yield peroxynitrite; peroxynitrite is reduced in turn by the enzyme to nitrite, which is finally released in the bulk. The hypothesis, though feasible and intriguing, was not confirmed by independent experiments specifically designed to investigate the kinetics and the products of the reaction of fully reduced nitrosylated CcOX with O_2 [50]. Using myoglobin as an optical probe for free NO, the NO bound to reduced heme a_3 was shown to be displaced by excess O_2 at the low rate of thermal dissociation, to be eventually released in the bulk as such, and not as nitrite [50]. The NO dissociation from the heme iron takes minutes, also when assayed in mitochondria or intact cells, at 37°C and in the dark, that is, under conditions common *in vivo* in internal organs and tissues. The slow recovery of function of the nitrosylated CcOX is compatible with a more severe state of inhibition characteristic of PW2.

The role of Cu_B in the CcOX-mediated oxidation of NO to nitrite was also addressed in experiments carried out using the *E. coli* cytochrome *bd*. This oxidase lacks Cu_B and, consistently, reacts with NO much more slowly ($k = 1.5 \times 10^2$ M^{-1} s^{-1} at 20°C) than mitochondrial CcOX, without forming nitrite [51]. Interestingly, the NO dissociation from the Cu_B-lacking cytochrome *bd* oxidase (from *E. coli*) is much faster [52, 53], pointing to a specific property of heme *d* [54] and/or to a role of Cu_B also in the NO dissociation

TABLE 1: Cytochrome c oxidase versus NO—kinetic and thermodynamic parameters.

CcOX intermediate	CcOX adduct formed	K_I (nM)	k_{on} (M^{-1} s^{-1}) ($T = 20°C$)	k_{off} (s^{-1}) ($T = 20°C$)	O_2-competition
E, R	Nitrosylated CcOX-NO	0.2 [32]	0.4–1 $\times$ 10^8 [16, 17]	3.9 $\times$ 10^{-3} [28]	yes
O, P, F	Nitrite bound CcOX-NO$_2^-$	20 [32]	$\sim$1 $\times$ 10^5 (**O, P**) $\sim$1 $\times$ 10^4 (**F**) [29, 58]	6.0 $\times$ 10^{-2} [29]	no

from the active site. As a matter of fact, this peculiarity was suggested to confer to cytochrome *bd*-expressing bacteria a higher resistance to nitrosative stress [53, 55, 56], a hypothesis supported by *in vitro* studies on *E. coli* deletion mutants of each of the two alternative respiratory oxidases (cytochrome *bd* and cytochrome *bo₃*) [55].

5. Cells Respiring in the Presence of NO and Using Endogenous Substrates

The respiration of cells grown under *standard* conditions, that is, in the presence of (unlimited) O_2 and endogenous reducing substrates, is inhibited by NO but without detectable accumulation of nitrosylated CcOX [37, 57]. As a matter of fact, these standard culture conditions favor the overall accumulation of the CcOX intermediates **P**, **F** and **O** [29, 41, 42, 58]; these are the species responsible for the NO oxidation to nitrite. Consistently, upon rapid and efficient scavenging of bulk NO, respiration is promptly recovered. It is worthy to point out that nitrite, far from being a simple oxidation byproduct, represents a source of NO particularly important in view of the NO cell homeostasis [59–62]. When the oxygen tension decreases in tissues, not only respiration but also the production of NO by nitric oxide synthases (NOSs) is severely impaired, as the NOS uses O_2 as cosubstrate [63]. Anoxia, however, induces tissue acidification, which promotes the reduction of nitrite to NO, compensating for impairment of the NOS-dependent NO production [59, 60, 64]. Consistently, and apparently important for a cardiovascular response, low doses of nitrite ($\sim$50 nM) administered to ischemic, heart-arrested mice, early during resuscitation procedures, were shown to significantly improve survival of the treated animals compared to controls [61].

The CcOX NO-inhibition pathway prevailing in mitochondria under given metabolic conditions might be responsible for pathological responses of cells and tissues [57]. Compelling experimental evidence has been collected suggesting that the O_2-uncompetitive nitrite inhibition pathway (PW1) prevails under conditions of low electron flux through the respiratory chain and high O_2, whereas the O_2-competitive nitrosyl pathway (PW2) takes over as the electron flux increases and O_2 concentration decreases [32, 37].

The main features of the two pathways can be summarized as follows:

(i) both reactions lead to the rapid accumulation of a CcOX inhibited species, characterized by different stability, K_I, and O_2 competitiveness (Table 1);

(ii) one pathway prevails over the other one depending on the fractional accumulation of the NO-targeted CcOX turnover intermediates [28, 29], whose distribution depends in turn on the *in situ* availability of O_2 and reduced cytochrome c; the concentration of the latter ultimately depends on its absolute concentration and on the electron flow level trough the respiratory chain;

(iii) PW1 prevails under basal mitochondrial metabolic conditions;

(iv) PW2 prevails under conditions favoring the accumulation of **E** and **R**, that is, when the concentration of cytochrome c^{2+} at the CcOX site increases and/or the O_2 tension decreases;

(v) the accumulation of CcOX-NO or CcOX-NO$_2^-$ affects differently the mitochondrial bioavailability of NO: the nitrosyl-derivative releases NO in the medium as such, that is, still reactive, whereas the nitrite-derivative releases nitrite to be further oxidized to nitrate, eliminated or rereduced to NO.

The NO concentration level in the cell varies depending on the relative rate of its production, and degradation or scavenging. Unless exogenously supplemented to the cells (NO-donors), the enzymatic endogenous NO production is controlled via the activation/inhibition of the cell NO-synthases. Alternatively, as mentioned above, NO is generated by the protein-bound or free metal ions (Fe^{2+}, Cu^+) catalyzed reduction of NO$_2^-$, a reaction that commonly occurs in solution, at acidic pH [59, 60]. The NO bioavailability can be lowered, therefore, by specific cell-permeable NO-synthase inhibitors or by NO scavengers, such as heme-proteins or reduced glutathione [65].

As pointed out by Cooper and Giulivi [5], when the NOS activity is inhibited, one may expect the O_2 consumption by respiring mitochondria to increase. This event, however, has been often but not always observed [5], probably owing to the activation of alternative NO-releasing systems, such as nitrosoglutathione and S-nitrosated protein thiols, or the NO$_2^-$ reduction, all active regardless of the presence of NOS inhibitors.

6. Effectors and Pathophysiology

Over the years, the enzymatic NO release has been induced in cultured cells, tissues, and organs, either using effectors able to activate cell Ca^{2+} fluxes [66], thus stimulating the constitutive NOS, or by enhancing the expression of the inducible isoform of NOS (iNOS) [67]. Morphine is the prototype of a family of drugs used in analgesia and cancer pain treatment [68, 69]. Relevant to the NO chemistry,
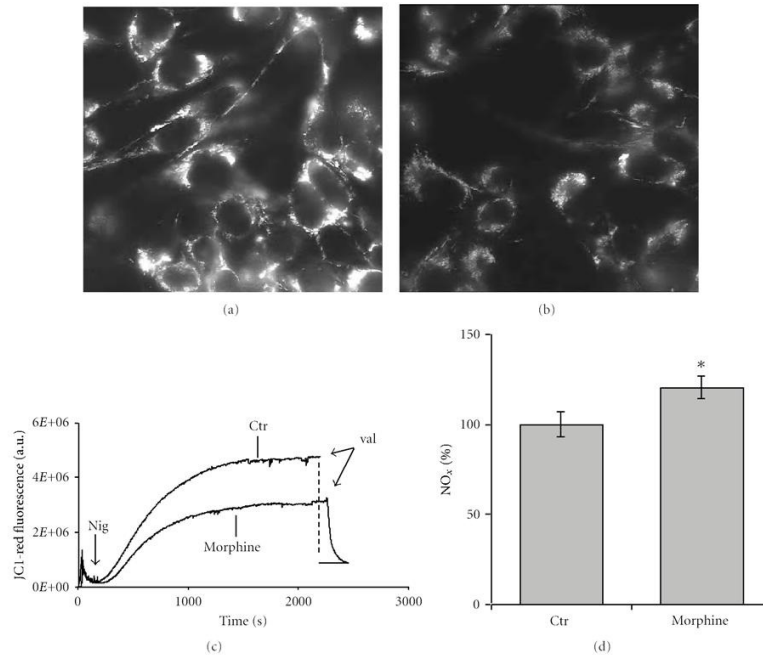
168

Attachments

FIGURE 2: Morphine-induced mitochondrial membrane potential and NO_x changes in Glioma cells. *Fluorescence microscopy*: control cells (a), 20 nM morphine incubated for 24 h (b). Mitochondrial membrane potential ($\Delta\Psi$) was probed using Rhodamine123; the dye is electrophoretically accumulated by the cell mitochondria. *Bulk fluorescence* (c). Control (ctr) versus morphine-treated (morphine) cells, assayed in air-equilibrated medium and in the presence of 2 μM ouabain and 0.4 μM JC-1; after signal stabilization, 0.6 μM nigericin is added and fluorescence changes followed over time. Addition of valinomycin abolishes the membrane potential. Excitation and emission wavelength, 575 nm and 590 nm, respectively. *Nitrite accumulation* (d). The release of NO_x (nitrite and nitrate) in the medium and during incubation with morphine was assessed spectrophotometrically by the Griess reaction; results expressed as percentage of control cells (ctr). *$P < 0,05$. Modified from [33].

morphine activates the opioid and the N-methyl-D-aspartate receptors of neuronal cells, triggering Ca^{2+} fluxes and NO release [70, 71]. In 2004, Mastronicola et al. [33] confirmed that the persistence of nanomolar morphine in the cell culture of glioma cells was able to induce the accumulation of nitrite/nitrate in the medium. Interestingly, the cell mitochondria displayed a membrane potential drop off, as probed by a significant decrease of the intramitochondrial JC-1 red-aggregates, whose accumulation requires high mitochondrial $\Delta\Psi$ values (Figure 2) [72]. Thus, over the same time scale of a cell Ca^{2+} transient (seconds to minutes) the NOS activation can affect the mitochondrial potential [33]. More recently, Arese et al. [48] have shown a transient inhibition of the mitochondrial respiratory chain in human adult low calcium temperature (HaCaT) cells, maintained in a standard culture medium, in the presence of nanomolar (or less) melatonin. After a few hours incubation compatible with a receptor-mediated process [73], and with a timecourse compatible with the circadian melatonin biorhythm, the basal mRNA expression level of the neuronal NOS (nNOS) in the cells was raised by a factor of ~4 (Figure 3(a)), returning, thereafter, to basal level [48]. As shown in the same figure, within the same time scale, the authors observed that: (i) the production of nitrite and nitrate (NO_x) was increased (Figure 3(b)) and (ii) the mitochondrial membrane potential was decreased (Figure 3(c)). Consistently, the ATP_{OXPHOS} production was also decreased and an increase of glycolytic ATP and lactate was detected [48]. Taken together, all these findings suggest

169

Attachments

that mediated by the melatonin receptors, NO is released and CcOX is reversibly inhibited, with significant bioenergetic consequences. Since cells are not likely facing conditions compatible with the accumulation of CcOX intermediates **E** or **R**, we can infer that inhibition has occurred via PW1. Interestingly, therefore, under physiological conditions, within the limits of a cell culture, a few hours exposure to hormonal-like concentrations of melatonin is able to exert some inhibition on mitochondrial OXPHOS and to raise the $\text{ATP}_{\text{glycolytic}}/\text{ATP}_{\text{OXPHOS}}$ ratio by a factor of ~ 2 (Figure 3(d)) as expected on the basis of a compensatory physiological Warburg effect [74]. All together these findings suggest that physiological concentrations of melatonin may play a mitochondrial role and interestingly in a circadian context. Indeed, the hypothesis that the melatonin-driven shift towards glycolysis might have a physiological role in the chemistry of the night rest, though attractive, is presently fully speculative, and remains to be investigated.

Based on the effects of melatonin and on the information collected about the NO inhibition of purified CcOX or mitochondria [75, 76], it is also tempting to speculate on how the mitochondrial state can affect the response to NO, particularly under conditions compatible with a limited, and transient raise of NO concentration. It is worthy to consider that isolated state 3 mitochondria proved to be inhibited by NO more effectively than state 4 mitochondria [75, 76]. This suggests that the sensitivity to NO inhibition increases with the electron flux level of the respiratory chain, and particularly with the turnover rate of CcOX; under these conditions the CcOX inhibition is oxygen competitive [32]. In state 3 mitochondria, therefore, and in the presence of suitable amounts of reduced cytochrome c, the fractional accumulation of the reduced (**E** and **R**) CcOX species is expected to increase; these species are promptly nitrosylated in the presence of NO. At low turnover rate, as in state 4, the oxidized catalytic intermediates (**O**, **P** and **F**) are expected to be more populated [29], and the NO inhibition predominantly occurs following PW1. Both in state 3 and state 4, if the NO concentration is low (e.g., subnanomolar), the fraction of CcOX inhibited is limited, and the depression of respiration is almost insignificant [77, 78], a finding consistent with an excess capacity of CcOX [79, 80]. When NO persists in the cell environment, as during a prolonged incubation with even low (nM) concentration of NO, and particularly if the turnover rate of CcOX is increased, a substantial inhibition of the respiratory chain is predictable and synthesis of $\text{ATP}_{\text{OXPHOS}}$ decreases [81]. Under these conditions, glycolysis likely takes place to compensate for ATP loss [82].

7. How Does the NO/CcOX Interplay Turn into Pathology

As just mentioned, the transient inhibition of mitochondrial OXPHOS may induce a physiological, compensatory activation of glycolysis [74]. This original observation by Warburg was recently reproposed by Almeida et al. [83], to rationalize the energetic changes of astrocytes and neurons
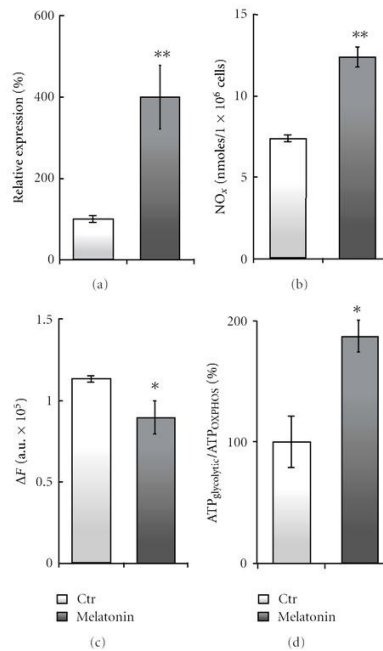
FIGURE 3: Melatonin-induced changes of the nNOS mRNA expression in HaCaT cells: effect on NO_x production and mitochondrial membrane potential. (a)—Real-time PCR quantification of nNOS mRNA (β-actin gene used for normalization). (b)—Fluorometric determination of the NO_x release in the cell culture medium. (c)—Mitochondrial membrane potential evaluated as the fluorescence difference, ΔF, from the maximal (*plateau*) to the minimal level reached after addition of valinomycin (see also Figure 2(c)). (d)—Contribution of oxidative phosphorylation and glycolysis to ATP production, directly evaluated according to [47]. The $\text{ATP}_{\text{glycolytic}}/\text{ATP}_{\text{OXPHOS}}$ ratio is indicative of the ability of a given cell line to compensate with glycolysis an OXPHOS impairment (so-called, Warburg effect) [48, 49]. The release of NO induced by melatonin almost doubles the glycolytic contribution to ATP synthesis in HaCaT cells. Cells were incubated with 1 nM melatonin for 6 h. (a), (b): $^{**}P < 0,01$ versus CTR; (c), (d): $^*P < 0,05$ versus CTR. Modified from [48].

inhibited by NO. In this respect, it is worth considering that neurons, astrocytes, lymphoid, keratinocytes cells, and in general different cell lines may possess a different glycolytic compensatory capacity of coping with OXPHOS NO-inhibition [48, 57, 83]. All the evidence so far collected shows that under standard cell culture conditions, a pulse of NO

leads to the accumulation of the CcOX-NO_2^- derivative [37], which is able to immediately and fully recover its function, provided that free NO is scavenged in the mitochondrial environment. On the contrary, when CcOX nitrosylation is induced by (artificially) rising the electron flux level at the CcOX site or by allowing the cells to respire towards hypoxia ($[O_2] \leq K_{M,O2}$), the respiratory chain remains inhibited for longer times at the CcOX site [28, 29, 32, 84]. It is worth recalling that indeed everything else being equal, the functional recovery of CcOX-NO is approximately 10–20 times slower than recovery of CcOX-NO_2^-. Thus, at least in a first approximation, it is feasible to propose that, compared to conditions promoting the formation of the CcOX-nitrite adduct, conditions favoring CcOX nitrosylation are expectedly more dangerous for cells, since causing a 10–20 times longer inhibition of the mitochondrial respiratory chain. One may indeed speculate that the compensatory glycolytic ATP synthesis might become insufficient, when CcOX is maintained nitrosylated for longer times.

In 2008 Masci et al. [57] characterized the mitochondria NO inhibition pattern of cells collected from patients affected by Ataxia Telangiectasia (AT). This is a multisystemic genetic human disorder characterized by a conjunctival telangiectasia and by a cerebellar degeneration leading to progressive ataxia [85, 86]. The disease is caused by mutations of the AT-mutated gene (ATM), coding for a nuclear 350 kDa protein that controls cell cycle and DNA damage repair [87–89]. AT patients are characterised by a genetic instability and vulnerability to radiation-induced oxidative stress [90–94]. Compared to control cells, AT cells display a defective reactive oxygen species (ROS) scavenging capacity [95, 96], with a decreased bioavailability of reduced glutathione [96].

Relevant to a possible pathological implication of the NO mitochondrial inhibition, AT patients show a bioenergetic deficiency [97]. The mitochondrial functional characterization, and the NO inhibition pattern of lymphoid cells collected from AT patients, proved to be significantly altered. Based on the rate of respiration recovery from inhibition, under otherwise identical conditions of substrates availability (O_2 and reductants), the CcOX in AT cells underwent nitrosylation to a substantially higher extent than in control cells [57]. As expected, based on the higher stability of the nitrosyl-adduct compared to the nitrite-adduct, after NO inhibition and subsequent removal of free NO, recovery of respiration of AT cells is slow, occurring at the rate of the NO displacement from the reduced CcOX active site, whereas control cells recover almost immediately (Figures 4(a) and 4(b)). As a matter of fact the inhibition of AT cells respiration was promptly removed upon shedding light on the cells (photosensitivity of the nitrosyl-adduct!). This peculiarity of AT cells has been correlated to their 1.7 fold higher concentration of mitochondrial cytochrome c compared to control cells (Figure 4(c)) [57]. The whole picture is consistent with the hypothesis that in AT cells, showing a lower ATP$_{glycolytic}$/ATP$_{OXPHOS}$ ratio compared to control cells (Figure 4(d)), the formation of **E** and **R** and thus CcOX nitrosylation is favored owing to the higher availability of reduced cytochrome c [29, 32].

8. The Dark Side of the Interplay between NO and CcOX

In conclusion, regardless of the pathway leading to inhibition of CcOX, in the presence of NO, mitochondrial OXPHOS is impaired to some extent. Impairment is due to the slow displacement of NO from the active site or to the involvement of the site in the NO oxidation to nitrite. The evidence so far collected suggests that, if NO remains available in the mitochondrial environment, the mitochondrial membrane potential decreases, and glycolysis begins to contribute significantly to ATP synthesis. Thus, it seems crucial that cells responding to NO pulses are endowed with an efficient glycolytic machinery able to compensate for the decreased aerobic ATP production [82, 83].

Finally, let us consider for the sake of the argument a chronic hypoxia induced by an impaired microcirculation, for instance in the brain. Under these conditions common to many age-related neurodegenerations, one might expect an increased NO release to enhance the blood flow in response to hypoxia. In this already pathological scenario, however, the blood flow and thus O_2 concentration may not increase significantly, owing to the vessel sclerosis; neurons could rather become hypoxic and in the presence of an increased NO concentration. These are the circumstances favouring PW2 (CcOX nitrosylation), even more so if the respiratory chain concentration of reducing substrates is still large enough. Under these conditions and in the absence of a suitable glycolytic compensation, the ATP levels could decrease dramatically, leading to cell death.

Abbreviations

|	
CcOX:	Cytochrome c oxidase
CcOX-NO:	Nitrosyl cytochrome c oxidase derivative
CcOX-NO_2^-:	Nitrite-bound cytochrome c oxidase
PW1:	NO reaction pathway leading to nitrite-bound CcOX
PW2:	NO reaction pathway leading to nitrosyl CcOX
OXPHOS:	Oxidative phosphorylation
$\Delta\Psi$:	Membrane electrical potential difference
O:	Fully oxidized CcOX
E:	CcOX with single-electron reduced heme a_3-Cu$_B$
R:	CcOX with fully reduced heme a_3-Cu$_B$
A:	CcOX with ferrous oxygenated heme a_3
P:	"Peroxy" CcOX intermediate
F:	"Ferryl" CcOX intermediate
NOS:	Nitric oxide synthase
nNOS:	Neuronal NOS
NO_x:	Nitrite-nitrate
AT:	Ataxia Telangiectasia
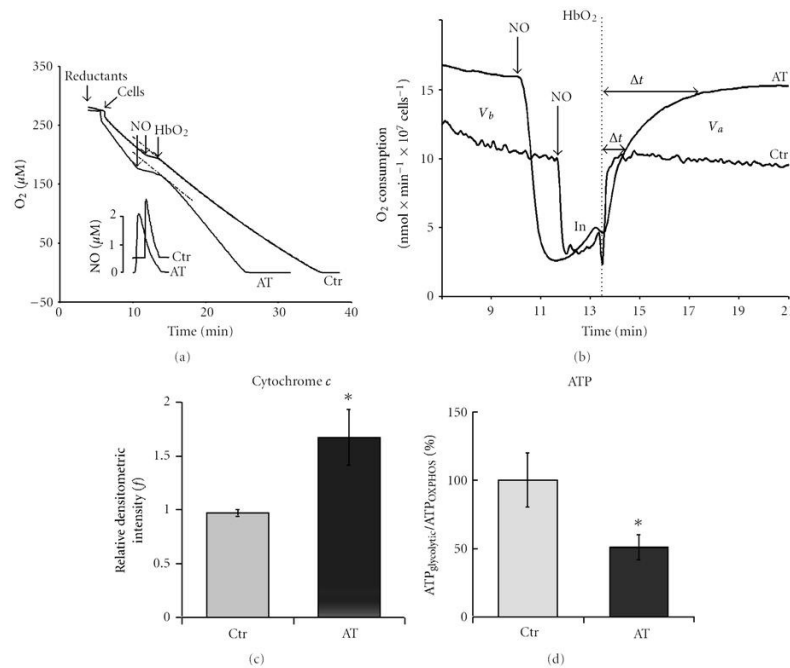
Figure 4: Oxygen consumption of Ataxia Telangiectasia (AT) cells: the inhibitory effect of NO. (a)—O_2consumption profiles of AT and control lymphoblastoid cells, recorded in the dark and in the presence of excess ascorbate and tetramethyl-p-phenylenediamine (TMPD). Inhibition of respiration was induced by adding a single bolus of pure NO gas solution (see lower NO profiles). In order to assess the fraction of residual inhibited CcOX-NO, the instantaneous rate was measured at 45 s after HbO_2 addition. (b)—First derivative plots (integration time $t = 2$ s). Rate of O_2 consumption before addition of NO (V_b), and after addition of oxygenated hemoglobin, HbO_2 (V_a), that is, in the absence of free NO. In: inhibited state (in the presence of free NO). The Δt value is the time necessary for complete recovery of activity after addition of HbO_2. $T = 25$ C. (c)—Cytochrome c immunoblot. Cell-lysate (30 μg/well) of AT patients and controls (ctr). (d)—Relative contribution of OXPHOS and glycolysis to ATP production in AT and control cells. Modified from [57].

HaCaT:	Human adult low calcium temperature, that is, keratinocytes cell line
HbO$_2$:	Oxygenated haemoglobin
State 3 respiration:	Induced by ADP, causing a burst of O$_2$ consumption and ATP synthesis and relaxing into the slower State 4 respiration after ADP consumption.

References

[1] J. J. Poderoso, M. C. Carreras, C. Lisdero, N. Riobó, F. Schöpfer, and A. Boveris, "Nitric oxide inhibits electron transfer and increases superoxide radical production in rat heart mitochondria and submitochondrial particles," *Archives of Biochemistry and Biophysics*, vol. 328, no. 1, pp. 85–92, 1996.

[2] S. Moncada and J. D. Erusalimsky, "Does nitric oxide modulate mitochondrial energy generation and apoptosis?" *Nature Reviews Molecular Cell Biology*, vol. 3, no. 3, pp. 214–220, 2002.

[3] F. Blandini, K. H. Braunewell, D. Manahan-Vaughan, F. Orzi, and P. Sarti, "Neurodegeneration and energy metabolism: from chemistry to clinics," *Cell Death and Differentiation*, vol. 11, no. 4, pp. 479–484, 2004.

[4] S. Shiva, J. Y. Oh, A. L. Landar et al., "Nitroxia: the pathological consequence of dysfunction in the nitric oxide-cytochrome c

oxidase signaling pathway," *Free Radical Biology and Medicine*, vol. 38, no. 3, pp. 297–306, 2005.

[5] C. E. Cooper and C. Giulivi, "Nitric oxide regulation of mitochondrial oxygen consumption II: molecular mechanism and tissue physiology," *American Journal of Physiology*, vol. 292, no. 6, pp. C1993–C2003, 2007.

[6] J. D. Erusalimsky and S. Moncada, "Nitric oxide and mitochondrial signaling: from physiology to pathophysiology," *Arteriosclerosis, Thrombosis, and Vascular Biology*, vol. 27, no. 12, pp. 2524–2531, 2007.

[7] P. Sarti, A. Giuffrè, M. C. Barone, E. Forte, D. Mastronicola, and M. Brunori, "Nitric oxide and cytochrome oxidase: reaction mechanisms from the enzyme to the cell," *Free Radical Biology and Medicine*, vol. 34, no. 5, pp. 509–520, 2003.

[8] C. E. Cooper and G. C. Brown, "The inhibition of mitochondrial cytochrome oxidase by the gases carbon monoxide, nitric oxide, hydrogen cyanide and hydrogen sulfide: chemical mechanism and physiological significance," *Journal of Bioenergetics and Biomembranes*, vol. 40, no. 5, pp. 533–539, 2008.

[9] A. Galkin and S. Moncada, "S-nitrosation of mitochondrial complex I depends on its structural conformation," *Journal of Biological Chemistry*, vol. 282, no. 52, pp. 37448–37453, 2007.

[10] E. Clementi, G. C. Brown, M. Feelisch, and S. Moncada, "Persistent inhibition of cell respiration by nitric oxide: crucial role of S-nitrosylation of mitochondrial complex I and protective action of glutathione," *Proceedings of the National Academy of Sciences of the United States of America*, vol. 95, no. 13, pp. 7631–7636, 1998.

[11] C. E. Cooper, N. A. Davies, M. Psychoulis et al., "Nitric oxide and peroxynitrite cause irreversible increases in the K_m for oxygen of mitochondrial cytochrome oxidase: in vitro and in vivo studies," *Biochimica et Biophysica Acta*, vol. 1607, no. 1, pp. 27–34, 2003.

[12] A. Giuffrè, P. Sarti, E. D'Itri, G. Buse, T. Soulimane, and M. Brunori, "On the mechanism of inhibition of cytochrome c oxidase by nitric oxide," *Journal of Biological Chemistry*, vol. 271, no. 52, pp. 33404–33408, 1996.

[13] C. E. Cooper, "Nitric oxide and cytochrome oxidase: substrate, inhibitor or effector?" *Trends in Biochemical Sciences*, vol. 27, no. 1, pp. 33–39, 2002.

[14] F. Antunes, A. Boveris, and E. Cadenas, "On the biologic role of the reaction of NO with oxidized cytochrome C oxidase," *Antioxidants and Redox Signaling*, vol. 9, no. 10, pp. 1569–1579, 2007.

[15] G. Benard, B. Faustin, E. Passerieux et al., "Physiological diversity of mitochondrial oxidative phosphorylation," *American Journal of Physiology*, vol. 291, no. 6, pp. C1172–C1182, 2006.

[16] Q. H. Gibson and C. Greenwood, "Reactions of cytochrome oxidase with oxygen and carbon monoxide," *The Biochemical Journal*, vol. 86, pp. 541–554, 1963.

[17] R. S. Blackmore, C. Greenwood, and Q. H. Gibson, "Studies of the primary oxygen intermediate in the reaction of fully reduced cytochrome oxidase," *Journal of Biological Chemistry*, vol. 266, no. 29, pp. 19245–19249, 1991.

[18] M. Brunori, S. R. Parr, C. Greenwood, and M. T. Wilson, "A temperature jump study of the reaction between azurin and cytochrome c oxidase from *Pseudomonas aeruginosa*," *Biochemical Journal*, vol. 151, no. 1, pp. 185–188, 1975.

[19] F. Malatesta, P. Sarti, G. Antonini, B. Vallone, and M. Brunori, "Electron transfer to the binuclear center in cytochrome oxidase: catalytic significance and evidence for an additional intermediate," *Proceedings of the National Academy of Sciences of the United States of America*, vol. 87, no. 19, pp. 7410–7413, 1990.

[20] M. I. Verkhovsky, J. E. Morgan, and M. Wikstrom, "Control of electron delivery to the oxygen reduction site of cytochrome c oxidase: a role for protons," *Biochemistry*, vol. 34, no. 22, pp. 7483–7491, 1995.

[21] M. Brunori, A. Giuffrè, E. D'Itri, and P. Sarti, "Internal electron transfer in Cu-heme oxidases: thermodynamic or kinetic control," *Journal of Biological Chemistry*, vol. 272, no. 32, pp. 19870–19874, 1997.

[22] P. Sarti, E. Forte, D. Mastronicola, A. Giuffrè, and M. Arese, "Cytochrome c oxidase and nitric oxide in action: molecular mechanisms and pathophysiological implications," *Biochimica et Biophysica Acta*, vol. 1817, no. 4, pp. 610–619, 2012.

[23] D. C. Unitt, V. S. Hollis, M. Palacios-Callender, N. Frakich, and S. Moncada, "Inactivation of nitric oxide by cytochrome c oxidase under steady-state oxygen conditions," *Biochimica et Biophysica Acta*, vol. 1797, no. 3, pp. 371–377, 2010.

[24] B. Chance, C. Saronio, and J. S. Leigh, "Functional intermediates in the reaction of membrane bound cytochrome oxidase with oxygen," *Journal of Biological Chemistry*, vol. 250, no. 24, pp. 9226–9237, 1975.

[25] L. Weng and G. M. Baker, "Reaction of hydrogen peroxide with the rapid form of resting cytochrome oxidase," *Biochemistry*, vol. 30, no. 23, pp. 5727–5733, 1991.

[26] M. Fabian, W. W. Wong, R. B. Gennis, and G. Palmer, "Mass spectrometric determination of dioxygen bond splitting in the "peroxy" intermediate of cytochrome c oxidase," *Proceedings of the National Academy of Sciences of the United States of America*, vol. 96, no. 23, pp. 13114–13117, 1999.

[27] S. Han, Y. C. Ching, and D. L. Rousseau, "Ferryl and hydroxy intermediates in the reaction of oxygen with reduced cytochrome c oxidase," *Nature*, vol. 348, no. 6296, pp. 89–90, 1990.

[28] P. Sarti, A. Giuffrè, E. Forte, D. Mastronicola, M. C. Barone, and M. Brunori, "Nitric oxide and cytochrome c oxidase: mechanisms of inhibition and NO degradation," *Biochemical and Biophysical Research Communications*, vol. 274, no. 1, pp. 183–187, 2000.

[29] A. Giuffrè, M. C. Barone, D. Mastronicola, E. D'Itri, P. Sarti, and M. Brunori, "Reaction of nitric oxide with the turnover intermediates of cytochrome c oxidase: reaction pathway and functional effects," *Biochemistry*, vol. 39, no. 50, pp. 15446–15453, 2000.

[30] G. Stubauer, A. Giuffrè, M. Brunori, and P. Sarti, "Cytochrome c oxidase does not catalyze the anaerobic reduction of NO," *Biochemical and Biophysical Research Communications*, vol. 245, no. 2, pp. 459–465, 1998.

[31] J. Torres, V. Darley-Usmar, and M. T. Wilson, "Inhibition of cytochrome c oxidase in turnover by nitric oxide: mechanism and implications for control of respiration," *Biochemical Journal*, vol. 312, no. 1, pp. 169–173, 1995.

[32] M. G. Mason, P. Nicholls, M. T. Wilson, and C. E. Cooper, "Nitric oxide inhibition of respiration involves both competitive (heme) and noncompetitive (copper) binding to cytochrome c oxidase," *Proceedings of the National Academy of Sciences of the United States of America*, vol. 103, no. 3, pp. 708–713, 2006.

[33] D. Mastronicola, E. Arcuri, M. Arese et al., "Morphine but not fentanyl and methadone affects mitochondrial membrane potential by inducing nitric oxide release in glioma cells," *Cellular and Molecular Life Sciences*, vol. 61, no. 23, pp. 2991–2997, 2004.

[34] A. Giuffrè, G. Stubauer, P. Sarti et al., "The heme-copper oxidases of *Thermus thermophilus* catalyze the reduction of

nitric oxide: evolutionary implications," *Proceedings of the National Academy of Sciences of the United States of America*, vol. 96, no. 26, pp. 14718–14723, 1999.

[35] E. Forte, A. Urbani, M. Saraste, P. Sarti, M. Brunori, and A. Giuffrè, "The cytochrome cbb₃ from *Pseudomonas stutzeri* displays nitric oxide reductase activity," *European Journal of Biochemistry*, vol. 268, no. 24, pp. 6486–6491, 2001.

[36] C. S. Butler, E. Forte, F. Maria Scandurra et al., "Cytochrome bo₃ from *Escherichia coli*: the binding and turnover of nitric oxide," *Biochemical and Biophysical Research Communications*, vol. 296, no. 5, pp. 1272–1278, 2002.

[37] D. Mastronicola, M. L. Genova, M. Arese et al., "Control of respiration by nitric oxide in Keilin-Hartree particles, mitochondria and SH-SY5Y neuroblastoma cells," *Cellular and Molecular Life Sciences*, vol. 60, no. 8, pp. 1752–1759, 2003.

[38] A. Giuffrè, M. C. Barone, M. Brunori et al., "Nitric oxide reacts with the single-electron reduced active site of cytochrome c oxidase," *Journal of Biological Chemistry*, vol. 277, no. 25, pp. 22402–22406, 2002.

[39] C. E. Cooper, M. G. Mason, and P. Nicholls, "A dynamic model of nitric oxide inhibition of mitochondrial cytochrome c oxidase," *Biochimica et Biophysica Acta*, vol. 1777, no. 7-8, pp. 867–876, 2008.

[40] G. W. Brudvig, T. H. Stevens, and S. I. Chan, "Reactions of nitric oxide with cytochrome c oxidase," *Biochemistry*, vol. 19, no. 23, pp. 5275–5285, 1980.

[41] C. E. Cooper, J. Torres, M. A. Sharpe, and M. T. Wilson, "Nitric oxide ejects electrons from the binuclear centre of cytochrome c oxidase by reacting with oxidised copper: a general mechanism for the interaction of copper proteins with nitric oxide?" *The FEBS Letters*, vol. 414, no. 2, pp. 281–284, 1997.

[42] A. Giuffrè, G. Stubauer, M. Brunori, P. Sarti, J. Torres, and M. T. Wilson, "Chloride bound to oxidized cytochrome c oxidase controls the reaction with nitric oxide," *Journal of Biological Chemistry*, vol. 273, no. 49, pp. 32475–32478, 1998.

[43] E. Antonini, M. Brunori, and A. Colosimo, "Oxygen 'pulsed' cytochrome c oxidase: functional properties and catalytic relevance," *Proceedings of the National Academy of Sciences of the United States of America*, vol. 74, no. 8, pp. 3128–3132, 1977.

[44] J. Torres, M. A. Sharpe, A. Rosquist, C. E. Cooper, and M. T. Wilson, "Cytochrome c oxidase rapidly metabolises nitric oxide to nitrite," *The FEBS Letters*, vol. 475, no. 3, pp. 263–266, 2000.

[45] C. Giulivi, "Characterization and function of mitochondrial nitric-oxide synthase," *Free Radical Biology and Medicine*, vol. 34, no. 4, pp. 397–408, 2003.

[46] L. L. Pearce, A. J. Kanai, L. A. Birder, B. R. Pitt, and J. Peterson, "The catabolic fate of nitric oxide. The nitric oxide oxidase and peroxynitrite reductase activities of cytochrome oxidase," *Journal of Biological Chemistry*, vol. 277, no. 16, pp. 13556–13562, 2002.

[47] G. Sgarbi, A. Baracca, G. Lenaz, L. M. Valentino, V. Carelli, and G. Solaini, "Inefficient coupling between proton transport and ATP synthesis may be the pathogenic mechanism for NARP and Leigh syndrome resulting from the T8993G mutation in mtDNA," *Biochemical Journal*, vol. 395, no. 3, pp. 493–500, 2006.

[48] M. Arese, M. C. Magnifico, D. Mastronicola et al., "Nanomolar melatonin enhances nNOS expression and controls HaCaT-cells bioenergetics," *IUBMB Life*, vol. 64, no. 3, pp. 251–258, 2012.

[49] M. Merlo-Pich, G. Deleonardi, A. Biondi, and G. Lenaz, "Methods to detect mitochondrial function," *Experimental Gerontology*, vol. 39, no. 3, pp. 277–281, 2004.

[50] A. Giuffrè, E. Forte, M. Brunori, and P. Sarti, "Nitric oxide, cytochrome c oxidase and myoglobin: competition and reaction pathways," *The FEBS Letters*, vol. 579, no. 11, pp. 2528–2532, 2005.

[51] V. B. Borisov, E. Forte, A. Giuffrè, A. Konstantinov, and P. Sarti, "Reaction of nitric oxide with the oxidized di-heme and heme-copper oxygen-reducing centers of terminal oxidases: different reaction pathways and end-products," *Journal of Inorganic Biochemistry*, vol. 103, no. 8, pp. 1185–1187, 2009.

[52] V. B. Borisov, E. Forte, A. A. Konstantinov, R. K. Poole, P. Sarti, and A. Giuffrè, "Interaction of the bacterial terminal oxidase cytochrome bd with nitric oxide," *The FEBS Letters*, vol. 576, no. 1-2, pp. 201–204, 2004.

[53] V. B. Borisov, E. Forte, P. Sarti, M. Brunori, A. A. Konstantinov, and A. Giuffrè, "Redox control of fast ligand dissociation from *Escherichia coli* cytochrome bd," *Biochemical and Biophysical Research Communications*, vol. 355, no. 1, pp. 97–102, 2007.

[54] S. Rinaldo, K. A. Sam, N. Castiglione et al., "Observation of fast release of NO from ferrous d1 haem allows formulation of a unified reaction mechanism for cytochrome cd1 nitrite reductases," *Biochemical Journal*, vol. 435, no. 1, pp. 217–225, 2011.

[55] M. G. Mason, P. Nicholls, and C. E. Cooper, "The steady-state mechanism of cytochrome c oxidase: redox interactions between metal centres," *Biochemical Journal*, vol. 422, no. 2, pp. 237–246, 2009.

[56] A. Giuffrè, V. B. Borisov, D. Mastronicola, P. Sarti, and E. Forte, "Cytochrome bd oxidase and nitric oxide: from reaction mechanisms to bacterial physiology," *The FEBS Letters*, vol. 586, no. 5, pp. 622–629, 2012.

[57] A. Masci, D. Mastronicola, M. Arese et al., "Control of cell respiration by nitric oxide in Ataxia Telangiectasia lymphoblastoid cells," *Biochimica et Biophysica Acta*, vol. 1777, no. 1, pp. 66–73, 2008.

[58] J. Torres, C. E. Cooper, and M. T. Wilson, "A common mechanism for the interaction of nitric oxide with the oxidized binuclear centre and oxygen intermediates of cytochrome c oxidase," *Journal of Biological Chemistry*, vol. 273, no. 15, pp. 8756–8766, 1998.

[59] J. O. Lundberg, E. Weitzberg, and M. T. Gladwin, "The nitrate-nitrite-nitric oxide pathway in physiology and therapeutics," *Nature Reviews Drug Discovery*, vol. 7, no. 2, pp. 156–167, 2008.

[60] S. Shiva and M. T. Gladwin, "Nitrite mediates cytoprotection after ischemia/reperfusion by modulating mitochondrial function," *Basic Research in Cardiology*, vol. 104, no. 2, pp. 113–119, 2009.

[61] A. Webb, R. Bond, P. McLean, R. Uppal, N. Benjamin, and A. Ahluwalia, "Reduction of nitrite to nitric oxide during ischemia protects against myocardial ischemia-reperfusion damage," *Proceedings of the National Academy of Sciences of the United States of America*, vol. 101, no. 37, pp. 13683–13688, 2004.

[62] J. L. Zweier, A. Samouilov, and P. Kuppusamy, "Non-enzymatic nitric oxide synthesis in biological systems," *Biochimica et Biophysica Acta*, vol. 1411, no. 2-3, pp. 250–262, 1999.

[63] A. R. Whorton, D. B. Simonds, and C. A. Piantadosi, "Regulation of nitric oxide synthesis by oxygen in vascular endothelial cells," *American Journal of Physiology*, vol. 272, no. 6, pp. L1161–L1166, 1997.

174

[64] R. O. Poyton, P. R. Castello, K. A. Ball, D. K. Woo, and N. Pan, "Mitochondria and hypoxic signaling: a new view," *Annals of the New York Academy of Sciences*, vol. 1177, pp. 48–56, 2009.

[65] G. Stubauer, A. Giuffrè, and P. Sarti, "Mechanism of S-nitrosothiol formation and degradation mediated by copper ions," *Journal of Biological Chemistry*, vol. 274, no. 40, pp. 28128–28133, 1999.

[66] E. N. Dedkova, X. Ji, S. L. Lipsius, and L. A. Blatter, "Mitochondrial calcium uptake stimulates nitric oxide production in mitochondria of bovine vascular endothelial cells," *American Journal of Physiology*, vol. 286, no. 2, pp. C406–C415, 2004.

[67] G. C. Brown, "Nitric oxide produced by activated astrocytes rapidly and reversibly inhibits cellular respiration," *Neuroscience Letters*, vol. 193, no. 3, pp. 201–204, 1995.

[68] S. Mercadante, "Managing breakthrough pain," *Current Pain and Headache Reports*, vol. 15, no. 4, pp. 244–249, 2011.

[69] G. E. Plante and T. B. Vanitallie, "Opioids for cancer pain: the challenge of optimizing treatment," *Metabolism*, vol. 59, supplement 1, pp. S47–S52, 2010.

[70] G. W. Pasternak, Y. A. Kolesnikov, and A. M. Babey, "Perspectives on the N-methyl-D-aspartate/nitric oxide cascade and opioid tolerance," *Neuropsychopharmacology*, vol. 13, no. 4, pp. 309–313, 1995.

[71] J. Mark Quillan, K. W. Carlson, C. Song, D. Wang, and W. Sadée, "Differential effects of μ-opioid receptor ligands on Ca^{2+} signaling," *Journal of Pharmacology and Experimental Therapeutics*, vol. 302, no. 3, pp. 1002–1012, 2002.

[72] M. Reers, T. W. Smith, and L. B. Chen, "J-aggregate formation of a carbocyanine as a quantitative fluorescent indicator of membrane potential," *Biochemistry*, vol. 30, no. 18, pp. 4480–4486, 1991.

[73] F. Luchetti, B. Canonico, M. Betti et al., "Melatonin signaling and cell protection function," *The FASEB Journal*, vol. 24, no. 10, pp. 3603–3624, 2010.

[74] O. Warburg, "On respiratory impairment in cancer cells," *Science*, vol. 124, no. 3215, pp. 269–270, 1956.

[75] P. S. Brookes, D. W. Kraus, S. Shiva et al., "Control of mitochondrial respiration by NO·, Effects of low oxygen and respiratory state," *Journal of Biological Chemistry*, vol. 278, no. 34, pp. 31603–31609, 2003.

[76] V. Borutaité and G. C. Brown, "Rapid reduction of nitric oxide by mitochondria, and reversible inhibition of mitochondrial respiration by nitric oxide," *Biochemical Journal*, vol. 315, no. 1, pp. 295–299, 1996.

[77] M. Palacios-Callender, V. Hollis, N. Frakich, J. Mateo, and S. Moncada, "Cytochrome c oxidase maintains mitochondrial respiration during partial inhibition by nitric oxide," *Journal of Cell Science*, vol. 120, no. 1, pp. 160–165, 2007.

[78] M. Palacios-Callender, V. Hollis, M. Mitchison, N. Frakich, D. Unitt, and S. Moncada, "Cytochrome c oxidase regulates endogenous nitric oxide availability in respiring cells: a possible explanation for hypoxic vasodilation," *Proceedings of the National Academy of Sciences of the United States of America*, vol. 104, no. 47, pp. 18508–18513, 2007.

[79] B. Chance, "Reaction of oxygen with the respiratory chain in cells and tissues," *Journal of General Physiology*, vol. 49, no. 1, pp. 163–195, 1965.

[80] J. P. Mazat, R. Rossignol, M. Malgat, C. Rocher, B. Faustin, and T. Letellier, "What do mitochondrial diseases teach us about normal mitochondrial functions... that we already knew: threshold expression of mitochondrial defects," *Biochimica et Biophysica Acta*, vol. 1504, no. 1, pp. 20–30, 2001.

[81] P. S. Brookes, J. P. Bolaños, and S. J. R. Heales, "The assumption that nitric oxide inhibits mitochondrial ATP synthesis is correct," *The FEBS Letters*, vol. 446, no. 2-3, pp. 261–263, 1999.

[82] J. P. Bolaños, A. Almeida, and S. Moncada, "Glycolysis: a bioenergetic or a survival pathway?" *Trends in Biochemical Sciences*, vol. 35, no. 3, pp. 145–149, 2010.

[83] A. Almeida, J. Almeida, J. P. Bolaños, and S. Moncada, "Different responses of astrocytes and neurons to nitric oxide: the role of glycolytically generated ATP in astrocyte protection," *Proceedings of the National Academy of Sciences of the United States of America*, vol. 98, no. 26, pp. 15294–15299, 2001.

[84] F. Antunes, A. Boveris, and E. Cadenas, "On the mechanism and biology of cytochrome oxidase inhibition by nitric oxide," *Proceedings of the National Academy of Sciences of the United States of America*, vol. 101, no. 48, pp. 16774–16779, 2004.

[85] M. S. Meyn, "Ataxia-telangiectasia, cancer and the pathobiology of the ATM gene," *Clinical Genetics*, vol. 55, no. 5, pp. 289–304, 1999.

[86] P. J. McKinnon, "ATM and ataxia telangiectasia," *EMBO Reports*, vol. 5, no. 8, pp. 772–776, 2004.

[87] K. Savitsky, S. Sfez, D. A. Tagle et al., "The complete sequence of the coding region of the ATM gene reveals similarity to cell cycle regulators in different species," *Human Molecular Genetics*, vol. 4, no. 11, pp. 2025–2032, 1995.

[88] G. Rotman and Y. Shiloh, "ATM: from gene to function," *Human Molecular Genetics*, vol. 7, no. 10, pp. 1555–1563, 1998.

[89] M. F. Lavin and Y. Shiloh, "The genetic defect in ataxia-telangiectasia," *Annual Review of Immunology*, vol. 15, pp. 177–202, 1997.

[90] A. Barzilai, G. Rotman, and Y. Shiloh, "ATM deficiency and oxidative stress: a new dimension of defective response to DNA damage," *DNA Repair*, vol. 1, no. 1, pp. 3–25, 2002.

[91] R. Reliene, E. Fischer, and R. H. Schiestl, "Effect of N-acetyl cysteine on oxidative DNA damage and the frequency of DNA deletions in Atm-deficient mice," *Cancer Research*, vol. 64, no. 15, pp. 5148–5153, 2004.

[92] C. Barlow, S. Hirotsune, R. Paylor et al., "Atm-deficient mice: a paradigm of ataxia telangiectasia," *Cell*, vol. 86, no. 1, pp. 159–171, 1996.

[93] Y. Xu, T. Ashley, E. E. Brainerd, R. T. Bronson, M. S. Meyn, and D. Baltimore, "Targeted disruption of ATM leads to growth retardation, chromosomal fragmentation during meiosis, immune defects, and thymic lymphoma," *Genes and Development*, vol. 10, no. 19, pp. 2411–2422, 1996.

[94] A. J. R. Bishop, C. Barlow, A. J. Wynshaw-Boris, and R. H. Schiestl, "Atm deficiency causes an increased frequency of intrachromosomal homologous recombination in mice," *Cancer Research*, vol. 60, no. 2, pp. 395–399, 2000.

[95] J. Reichenbach, R. Schubert, D. Schindler, K. Müller, H. Böhles, and S. Zielen, "Elevated oxidative stress in patients with Ataxia telangiectasia," *Antioxidants and Redox Signaling*, vol. 4, no. 3, pp. 465–469, 2002.

[96] Y. Aksoy, O. Sanal, A. Metin et al., "Antioxidant enzymes in red blood cells and lymphocytes of ataxia-telangiectasia patients," *Turkish Journal of Pediatrics*, vol. 46, no. 3, pp. 204–207, 2004.

[97] M. Ambrose, J. V. Goldstine, and R. A. Gatti, "Intrinsic mitochondrial dysfunction in ATM-deficient lymphoblastoid cells," *Human Molecular Genetics*, vol. 16, no. 18, pp. 2154–2164, 2007.

175

Attachments

Article

New Evidence for Cross Talk between Melatonin and Mitochondria Mediated by a Circadian-Compatible Interaction with Nitric Oxide

Paolo Sarti [1,2,*], Maria Chiara Magnifico [1], Fabio Altieri [1], Daniela Mastronicola [2] and Marzia Arese [1]

[1] Department of Biochemical Sciences, Sapienza University of Rome, Rome 00185, Italy;
    E-Mails: mariachiara.magnifico@uniroma1.it (M.C.M.); fabio.altieri@uniroma1.it (F.A.);
    marzia.arese@uniroma1.it (M.A.)
[2] CNR Institute of Molecular Biology and Pathology, Rome 00185, Italy;
    E-Mail: daniela.mastronicola@uniroma1.it

* Author to whom correspondence should be addressed; E-Mail: paolo.sarti@uniroma1.it;
    Tel.: +39-6-4450291 or +39-6-49910944; Fax: +39-6-4440062.

Abstract: Extending our previous observations, we have shown on HaCat cells that melatonin, at ~10^{-9} M concentration, transiently raises not only the expression of the neuronal nitric oxide synthase (nNOS) mRNA, but also the nNOS protein synthesis and the nitric oxide oxidation products, nitrite and nitrate. Interestingly, from the cell bioenergetic point of view, the activated NO-related chemistry induces a mild decrease of the oxidative phosphorylation (OXPHOS) efficiency, paralleled by a depression of the mitochondrial membrane potential. The OXPHOS depression is apparently balanced by glycolysis. The mitochondrial effects described have been detected only at nanomolar concentration of melatonin and within a time window of a few hours' incubation; both findings compatible with the melatonin circadian cycle.

Keywords: nitric oxide; cell bioenergetics; respiratory chain; circadian rhythm; cell culture; Warburg effect; reactive oxygen; nitrogen species

176

Attachments

1. Introduction

Melatonin, the *N*-acetyl-5-methoxytryptamine, is an amphiphilic molecule with remarkable antioxidant properties [1,2]. Originally recognized as the hormone of the pineal gland, melatonin is produced also by other extrapineal sites [3–8]. World-widely recommended as a pharmaceutical tool for elderly people with sleep disorders, melatonin is responsible for regulation of the sleep-wake cycle [9,10]. It is involved in a variety of physiological functions [11–13], including modulation of gene transcription [14], blockage of transcriptional factors [15] and control of mitochondrial activities [16]. The antioxidant properties of melatonin have been world-widely recognized, likely accounting for a number of protective effects exerted in different cellular compartments [17]. Melatonin is more effective than the majority of its naturally occurring molecular analogs [18,19], suggesting that the substituents of the central indole structure controls the reactivity of the adducts. Rate constants determined for the reaction of melatonin with hydroxyl radicals are very high, almost diffusion limited, approaching $k \approx 10^{10} \, \text{M}^{-1}\text{s}^{-1}$ [20,21]. Despite its common use, the molecular mechanism(s) underlying the functional effects of melatonin, particularly those related to cell bioenergetics, remain as yet only partly understood. The blood circulating melatonin concentration is genetically encoded [22] and varies within individuals [23–26], accounting for the existence of genetically encoded melatonin-dependent human syndromes [27].

As schematically represented in Figure 1, over and above the antioxidant redox function, melatonin exerts its hormonal effects via receptor-mediated signaling and activation of specific mRNAs [12]. At least dealing with mitochondria, both the hormonal and the antioxidant function coexist [2,16] and referenced therein [28]. The experimental evidence suggest that the mitochondrial antioxidant activity is more evident at the higher ($\geq \mu M$) concentrations of melatonin, while the hormonal-like function can be detected at the lower ($\leq nM$) concentrations.

Very recently, using HaCat cells in culture, we have shown that nM melatonin induces the increase of the mRNA expression of neuronal nitric oxide synthase (nNOS) [28]. The mRNA induction was proven to occur within a few hours of cells incubation with melatonin and followed a rise and fall kinetics. The overall process was suggested to be fully compatible with a circadian cycle, mediated by melatonin receptors and with a timing consistent with a nuclear DNA-activated process [28]. The upregulation by melatonin of the nNOS mRNA expression appeared specific, since the eNOS and the iNOS expression was insensitive to melatonin [28]. Interestingly, on a time scale compatible with the nNOS mRNA changes, the cells displayed a lowered ATP_{OXPHOS} production. This finding has been tentatively explained based on the reversible inhibition exerted by the NO on the respiratory chain Complex IV (cytochrome c oxidase, CcOX) [29,30], an event whose pathophysiological meaning is strengthened by the putative existence of a mitochondrial isoform of the nNOS.

In this paper, we report new evidence supporting a melatonin-induced synthesis of the nNOS enzyme occurring within a time scale compatible with the nNOS mRNA, and we show its effect on cell respiration. Over a circadian-compatible time window, we have evaluated the nNOS protein synthesis by HaCat cells incubated with physiological, nanomolar, melatonin. In agreement with previous results [28], we have evaluated those functional parameters, suitable to assess the cell bioenergetic state, correlating them in parallel with changes in composition of the cell culture medium, particularly focusing on the NO end products. The whole picture further suggests that NO chemistry

1 7 7

Attachments

plays a role in the mitochondrial circadian cycle [28,31]. The hypothesis is fully consistent with the finding that the production of nitrite and nitrate is also characterized by a circadian night peak [32] and that the nNOS activity is involved in sleep regulation [33,34].

Figure 1. Melatonin on the cell stage. Melatonin interacts with cells in a receptor-dependent or -independent manner. The receptors on the cell membrane, MT1 (*Mel 1a*) and MT2 (*Mel 1b*), consist of seven transmembrane helices, G protein-coupled. Activating G protein signaling, the receptors mediate a wide variety of effects; among others, inhibition of the adenylate cyclase (AC), with a consequent cyclic AMP (cAMP) decrease, regulation of gene transcription, activation of protein kinase C subtypes and changes of intracellular Ca^{++} levels. Independently of receptors, melatonin permeates cell membranes and, owing to its low redox potential, $E_o = -980$ mV [21], scavenges the ROS in the cell cytoplasm, mitochondria and nucleus. In the cytoplasm, melatonin maintains GSH homeostasis and interacts with proteins, such as calmodulin (CaCaM), calreticulin and the cytosolic quinone reductase 2 enzyme, (MT3). Melatonin is also a ligand for a nuclear retinoid related orphan nuclear hormone receptor (RZR/RORa) regulating the expression of anti-oxidant enzymes, such as glutathione peroxidase (GPx), glutathione reductase (GRd) and superoxide dismutase (SOD), and downregulating pro-oxidant enzymes, such as the NOSs, particularly the iNOS [35]. Melatonin is accumulated in mitochondria at high concentrations, where it scavenges ROS and RNS. Melatonin also protects cardiolipin from oxidation [36] and prevents respiratory chain complexes, as well as mtDNA from free radical attack, thus ultimately protecting the membrane permeability transition (mPT) pore, thus preventing cell apoptosis.
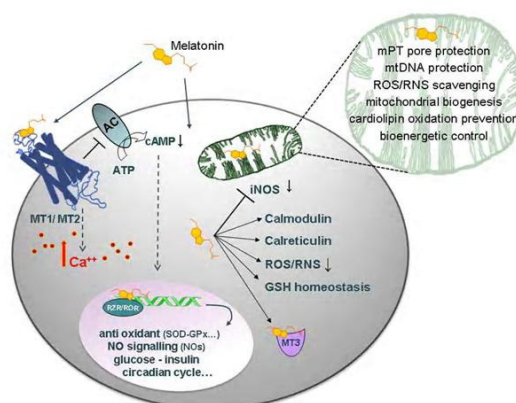
A bioenergetic involvement of melatonin is supported by the effects induced on the respiratory chain, though their interpretation is not always straightforward [16]. Difficulties in comparing data are partly linked to differences in the experimental set up. Experiments have been carried out, in fact, with fully integrated systems, such as animals or cells in culture, but also using isolated mitochondria. In the latter case, regardless of whether the organelles are functionally intact or not, the nuclear signaling-dependent reactions do not occur. In addition, it should be kept in mind that the intracellular

11262

concentration of melatonin putatively reached under the given conditions, unless directly measured, remains uncertain owing to the ability of different cell organelles, e.g., mitochondria [37], and compartments, e.g., nuclei [38], to accumulate melatonin to a different extent.

2. Results and Discussion

2.1. Experimental Results

The mitochondrial response to melatonin has been investigated using cultured HaCaT cells exposed to increasing amounts of melatonin, from 1 to 100 nM; the activation of nuclear-dependent reactions was also investigated by carrying the experiments within a time scale of hours.

Figure 2. Time-dependent effects of nM melatonin on nNOS expression and NOx production. HaCaT cells were incubated with 1 nM melatonin; at the times indicated, the nNOS mRNA (**a**), nNOS protein (**b**) and nitrite/nitrate (NOx) production (**c**) were assayed. (**a**) QRT-PCR analysis of mRNA expression was performed in the presence of specific primers for nNOS. The relative expression levels were calculated *vs.* untreated controls (ß-actin normalized). The maximal mRNA expression at 6 h (blue). Data +/− SEM, $n \geq 3$. ** $p \leq 0.01$ *vs.* control; * $p \leq 0.05$ *vs.* control; (**b**) Western blot analysis of nNOS protein. Data shown as fold increase *vs.* the nNOS protein expressed by control cells, as a function of incubation time. The maximal protein synthesis at 8 h (green). Data +/− SEM, $n \geq 3$. ** $p \leq 0.01$ *vs.* control; (**c**) NOx accumulation measured in the supernatant as a function of time. Data shown as fold increase *vs.* control (untreated). The maximal NOx production at 8 h (violet). Data +/− SEM, $n \geq 5$. ** $p \leq 0.01$ *vs.* control; (**d**) Time-dependent profile of the expression of the nNOS mRNA (blue) and nNOS protein (green); (**e**) Western Blot of cells incubated 8 h with 1 nM melatonin and controls (CTR); α-tubulin as reference.
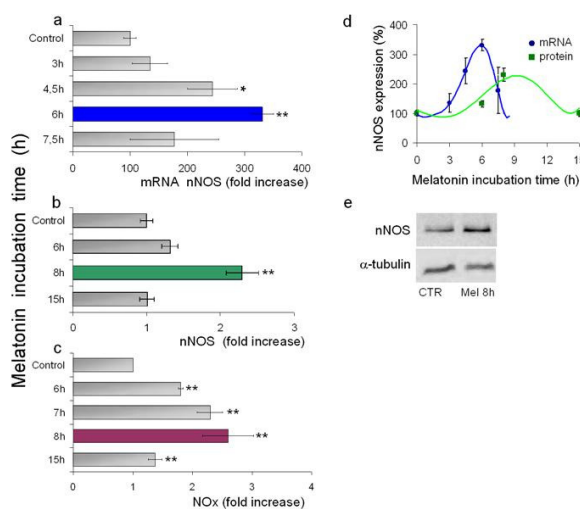
2.1.1. Neuronal NOS (nNOS) Expression and NOx Production

Cells were incubated with melatonin (1 nM) for up to ~15 h, and the bioavailability of nitric oxide has been evaluated indirectly by following changes of the cellular NOSs. As shown in Figure 2, the nNOS mRNA level and the nNOS protein expression changed as a function of time, together with the nitrites and nitrates (NOx) concentration, in the culture medium. The nNOS synthesis and the NOx production reach a maximum after ~8 h incubation, *i.e.*, ~2 h after cell rising of the nNOS mRNA; noticeably, timing of these processes is consistent with protein synthesis and maturation. The increase of the nNOS mRNA and of the protein concentration both occur in the presence of 1 nM melatonin, falling back to basal levels on a longer time scale, even increasing the concentration of melatonin by orders of magnitude (Figure 3). Interestingly, the maximal effect on the nNOS expression and the NOx accumulation is observed at ~1 nM melatonin, tending to the basal level, with increasing melatonin concentration by one or even two orders of magnitude.

**Figure 3.** Concentration dependence effect of melatonin (nanomolar) on nNOS expression and NOx production. HaCaT cells were treated with increasing melatonin concentrations (1, 10, 100 nM). (**a**) After 6 h of melatonin incubation, the RNA extracted (10 ng) was retro-transcribed and subjected to QRT-PCR in the presence of specific primers for nNOS. The relative expression levels were calculated *vs.* control after normalization for ß-actin. Data +/− SEM, $n = 3$. ** $p \leq 0.01$ *vs.* control; (**b**) NOx accumulation in the supernatant of HaCaT cells was quantified after 6 h (light bars) and 8 h (heavy bars) incubation with increasing melatonin concentrations. Data are expressed as means +/− SEM, $n \geq 5$. ** $p \leq 0.01$ *vs.* control.
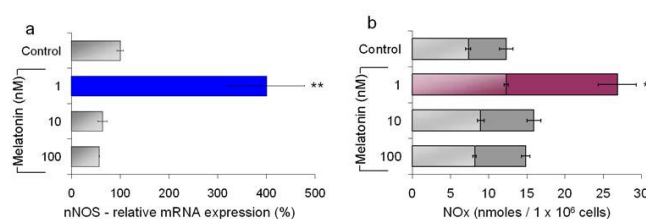
2.1.2. Mitochondrial Respiration and Membrane Potential

The spontaneous rate of oxygen consumption was measured amperometrically in intact HaCaT cells respiring on endogenous substrates and incubated 8 h with increasing amounts of melatonin. As shown in Figure 4a, when cells are treated with 1 nM melatonin, a ~10% loss of cell respiration is observed; the effect becomes insignificant at higher melatonin concentrations (up to two orders of magnitude), and it is also reverted by addition of the nNOS inhibitor 7-nitroindazole (7N), (Figure 4b). As shown in Figure 4c, following incubation with melatonin, the mitochondrial membrane potential ($\Delta\Psi$) is lowered, by approximately 20%, compared to control. Moreover, accumulation of the probe is maximal when arginine is removed from the cell culture medium, pointing to a correlation between the import of JC-1 and the availability of the NOS substrate.

Attachments

Figure 4. Effect of melatonin on respiration and mitochondrial membrane potential. (**a**) HaCaT cells were incubated 8 h with increasing concentrations of melatonin (1, 10, 100 nM). Respiration was measured and reported as percent of the O_2 consumption of control HaCaT cells. Cell density: 3.3×10^6 cells/mL; medium: Hank's containing 1 g/L glucose. Data are expressed as means +/− SEM, $n \geq 3$. ** $p \leq 0.01$ *vs.* control; (**b**) Typical O_2 consumption profiles of melatonin-treated HaCaT cells, in the presence (3, orange) and absence (2, green) of the nNOS inhibitor 7-nitroindazole (7-N); control untreated cells (1, blue). Inset: 1st derivative plot of the traces; (**c**) Mitochondrial membrane potential measured, following JC-1 accumulation, started by the addition to the cells of nigericin 0.6 μM (Nig). Valinomycin (Val) is added (at plateau) to collapse the membrane potential. Excitation wavelength = 490 nm, emission wavelength = 590 nm. Cells maintained in the absence of the NOS substrate arginine (red); control cells (blue). Cells after 8 h incubation with 1 nM melatonin (green).
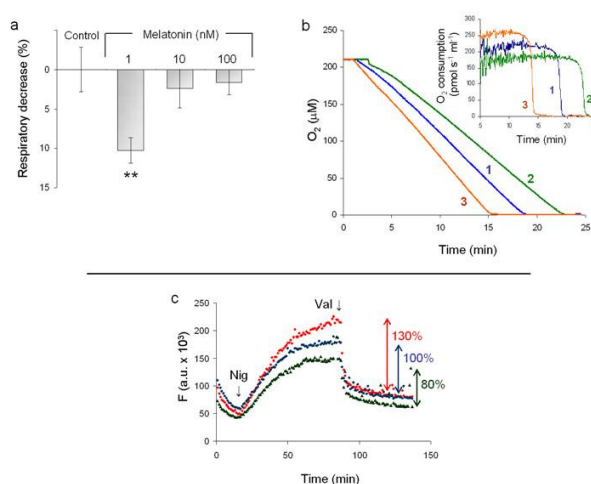
2.1.3. ATP and Lactate Production

Melatonin increases the nNOS synthesis; hence, the NO bioavailability of HaCaT cells as probed by the accumulation of the NOx. On the same time scale, the cell O_2 consumption is lowered, with predictable outcomes on the mitochondrial bioenergetics [39,40]. The cell oxidative phosphorylation and the glycolytic efficiency have been, therefore, evaluated, measuring the concentration of ATP and lactate. Compared to controls, the ATP_{OXPHOS} production by the cells incubated with 1 nM melatonin is ~25% lower (Figure 5a), while their glycolytic efficiency, monitored in parallel, is increased (Figure 5b). The lactate produced under basal conditions is indicative of the glycolytic contribution to ATP synthesis (gray bar in Figure 5b). In the presence of myxothiazol and antimycin inhibiting OXPHOS, some additional lactate is produced, due to glycolytic compensation of ATP loss (Warburg effect) (cyan bar in Figure 5b). This Warburg lactate is indicative of the OXPHOS contribution to ATP

1 8 1

synthesis. The basal lactate production of the melatonin treated cells is ~65% of the total lactate, to be compared to ~50% of the control cells, whereas the Warburg lactate production is ~48% in the melatonin treated cells and 35% in controls (Figure 5c). Overall, the data strengthen the hypothesis that several hours' incubation with 1 nM melatonin is able to induce a measurable depression of the OXPHOS function, compensated by glycolysis.

Figure 5. Effect of melatonin on the production of ATP$_{OXPHOS}$ and lactate. ATP and lactate were assayed in HaCaT cells incubated 6h with melatonin, 1 nM. (**a**) Rate of ATP synthesis: Complex II driven ATP synthesis was measured using cells permeabilized with 60 µg/mL digitonin in the presence of 20 mM succinate, 4 µM rotenone and 0.5 mM ADP. ATP measurements carried out according to the luciferin/luciferase assay [41]. Data +/− SEM, $n \geq 14$. ** $p \leq 0.01$ *vs.* control; (**b**) Lactate production by HaCaT cells incubated 3 h with glucose, 1 mM, and in the presence and absence of myxothiazol and antimycin A, 10 µM each. Basal lactate (gray bar) is produced by the cells in the absence of inhibitors and has been taken as ≈ ATP$_{glycolytic}$. The lactate produced in the presence of inhibitors has been taken as the maximal lactate (total, 100%). The difference between total and basal lactate is the Warburg lactate (cyan); Warburg lactate ≈ ATP$_{OXPHOS}$. Values are the means +/− SEM; $n = 4$. * $p \leq 0.05$ *vs.* control; (**c**) Synoptic table of the ATP and lactate amounts measured under the conditions described in (**a**) and (**b**).

Assay	Conditions		Control	Mel
ATP	+	digitonin/ADP/succinate/rotenone	0.69 nmol/min ± 0.03	0.51 nmol/min ± 0.04
	−	glucose		
Lactate basal	+	glucose	68.05 µg ± 5.3	80.02 µg ± 8.2
Lactate total	+	myxothiazol and antimycin A (Oxphos inhibitors)	132.0 µg ± 10.1	122.4 µg ± 11.9
	+	glucose		
Lactate Warburg	Lactate$_w$ = total − basal (oxphos compensatory)		64.0 µg	42.0 µg
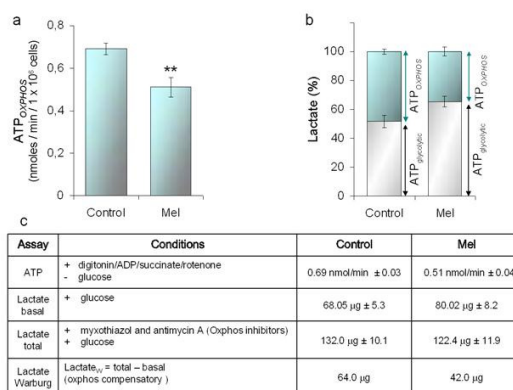
2.2. Discussion

2.2.1. Concentration of Melatonin and Protocol of Administration

Over the years, concentrations of melatonin from ~10^{-9} M up to ~10^{-4} M have been used to investigate the interactions between melatonin and mitochondria [16]. Measurements have been carried out in the presence of the melatonin cell receptors, as *in vivo* or *in vitro*, using cultured cells, but also in the absence of the receptors, when using intact mitochondria or sub-mitochondrial particles. To perform *in vivo* experiments, melatonin was injected intra-peritoneally (i.p.) or chronically

administered to the animals in drinking water, and their liver or brain mitochondria were isolated and assayed [42–44]. Protocols were compatible with a blood circulating drug concentration, variable [45–47], though somewhat higher, than the $\sim 10^{-9}$ M physiological one [48].

Alternatively, mitochondria were isolated first and then exposed to variable amounts of melatonin, down to $\sim 10^{-9}$ M concentrations [49]. In these experiments, a significant specific enhancement of the eT activity of Complex I and Complex IV, was observed and more patently at a concentration of melatonin $\geq 10^{-6}$ M. The authors proposed that the increase of activity was related to: (i) optimization of the mitochondrial membrane fluidity, due to melatonin prevention of membrane lipid peroxidation [50]; (ii) direct scavenging of the H_2O_2 [51,52]; and (iii) stabilization of mitochondrial GSH [53–55].

Somewhat in contrast, Lopez, A., *et al.* [37] have shown that melatonin added to mice liver mitochondria at concentrations from 1 nM to 1 mM is able to decrease respiration in a concentration-dependent manner, by inhibiting the ADP-dependent state 4 to state 3 transition. In the same line, Reyes-Toso [56] observed that melatonin added *in vitro* to mitochondria or chronically administered to the animals in the diet inhibits the substrate-induced (ADP) state 4 to state 3 transition, suggesting that this might protect mitochondria from oxidative damage. Our investigation on HaCaT keratinocytes allowed us to study the effect of nanomolar melatonin, without losing the contribution of the nuclear signaling. Interestingly, only under these conditions, it has been possible to observe the enhancement of the nNOS expression and the depression of mitochondrial activity (Figure 6).

Figure 6. Melatonin and the "keratinocyte hypothesis". At nanomolar and sub-nanomolar melatonin concentration, a melatonin-receptor-mediated transient nNOS overexpression is triggered. At this stage, calmodulin can predominantly interact with nNOS, leading to production of NO and modulation of mitochondrial function. Upon increasing the external concentration of melatonin (>1 nM) or its time of incubation, its intracellular concentration also rises: under these conditions, melatonin binds/inactivates calmodulin (CaCaM) leading to nNOS inhibition [57,58]. (**a**) Schematic drawing of melatonin traffic and signaling in a keratinocyte (HaCaT cells); (**b**) How the co-existing equilibrium of melatonin with calmodulin and NOS may affect NOS activity. Intracellular melatonin gradient (orange) and nNOS expression/activity (blue).
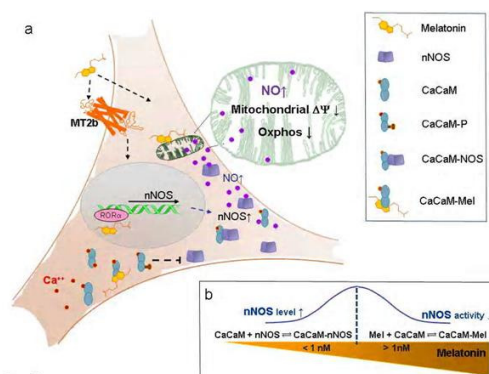
2.2.2. Nanomolar Melatonin, nNOS Synthesis and Involvement of Complex IV

Keratinocytes (HaCat cells), incubated for up to 15 h with nanomolar melatonin, after 6–8 h, display a transient rise of the nNOS and accumulate NOx (nitrite/nitrate) in the culture medium. The nNOS protein synthesis lags behind the rise of the corresponding nNOS mRNA: the protein increases transiently, and within hours, returns back to its basal level; the ~2 h shift between the protein and the mRNA synthesis is consistent with a nuclear DNA-dependent pathway. Following incubation with nanomolar melatonin and on a time scale similar to that of both the nNOS changes and the NOx accumulation, the mitochondrial respiration becomes slightly, but significantly, depressed (~10%). The mitochondrial membrane potential, instead, decreases to a larger extent, by ~20%, suggesting that under these conditions and at least in keratinocytes mitochondria, the mechanism(s) responsible for maintenance of $\Delta\Psi$ are more affected than respiration [59]. This observation is compatible with the hypothesis that, as a cell responds to melatonin, a small amount of free NO, nanomolar or less [60], is made available in the mitochondrial environment. NO, in fact, is able to rapidly and reversibly inhibit Complex IV in turnover with electrons and oxygen [61], a reaction whose occurrence has been demonstrated at all integration levels of the enzyme, from purified to fully integrated, in intact mitochondria and in cells [39,62,63]. Synchronously with the down regulation of the respiratory chain, we have also observed a decrease of the cell ability to synthesize ATP_{OXPHOS}, compensated by an increased production of glycolytic ATP, a behavior originally observed in astrocytes [64], the so-called Warburg effect [65].

Taken together, these findings suggest that nanomolar melatonin administered to intact HaCaT cells transiently activates the nNOS synthesis, with production of NO and reversible inhibition of Complex IV [61,62,66]. This leads, in turn, to a transient metabolic shift towards glycolysis [28]. It is worth recalling, in fact, that depending on the mechanism by which NO reacts with Complex IV, it is possible to detect either a physiological modulation of the electron transfer through the respiratory chain or a more persistent inhibition of mitochondrial respiration [63,67]. Relevant parameters controlling the reaction mechanism were shown to be the cell oxygenation state, the electron flux through the respiratory chain and, indeed, the NO concentration [63,68–70]. The fraction of mitochondria in state 3 and state 4 respiration is also important, as state 3 mitochondria are more prone to Complex IV nitrosylation (persistent inhibition) [71].

Based on independent measurements [68], under normal conditions of cell/tissues oxygenation and supply of mitochondrial reducing substrates, a pulse of NO, limited in extent and time, would lead to formation of a labile Complex IV-NO_2^- derivative. Interestingly, and relevant to the melatonin effects herein described, the activity of Complex IV is promptly recovered upon decreasing the NO bioavailability.

Melatonin, at pharmacological concentrations (10^{-6} M–10^{-3} M), either by signaling (Figure 1) or acting as a radical scavenger, optimizes the eT within the respiratory chain [16] and referenced therein cited, likely minimizing the effects of the NO inhibition of Complex IV. It is tempting to speculate that when the inhibition of Complex IV by NO prevails over the optimization of the electron transfer, then the radical scavenging capacity of melatonin might become insufficient to compensate for inhibition [63]. We suggest that this occurs at ~10^{-9} M melatonin in the extracellular environment, a concentration far too low to be effective in radical scavenging, but apparently ideal to activate the receptor-mediated

184

nNOS chemistry: the result is a transient release of NO with control of both the rate of respiration and the ATP$_{OXPHOS}$ synthesis. As expected, the Warburg effect is also clearly observed and, as a side effect, a higher fraction of O_2 becomes available for close by cells, the so called O_2-diversion [72]. Within the limits of a comparison between a cell culture system and an *in vivo* state, we suggest that the events involving 10^{-9} M melatonin and mitochondria are physiological and might occur in a circadian context.

Thus, under the conditions herein used to treat keratinocytes, 1 nM melatonin in the external medium depressed cell respiration and transiently increased the nNOS expression. Both effects were reverted upon increasing the concentration of melatonin or maintaining the cells in the presence of 1 nM melatonin for longer incubation times. The mechanism through which low melatonin concentrations in the extracellular medium might trigger the nNOS expression and, apparently, in a paradoxical biphasic mode, remains unclear. It is tempting to speculate that a time and concentration-dependent feed-back controls the effects of melatonin on the nNOS and that the basis of this control might involve the melatonin-calmodulin interaction and signaling [57].

In this frame, when the extracellular hormone concentration is low (nanomolar or less), the nuclear mediated nNOS activation occurs, also sustained by the cell availability of calmodulin (high affinity nNOS cofactor [73]). As the incubation time increases, the intracellular concentration of melatonin (and/or its metabolites) increases, too (Figure 6b). At this stage, due to the high affinity of melatonin for calmodulin [74] a competition between melatonin and nNOS for calmodulin occurs, inducing progressive nNOS inhibition [58] (Figure 6).

The existence of such equilibrium, if confirmed, would explain the biphasic behavior observed, also reconciling some discrepancies in the literature about the effects of melatonin, both on mitochondria and NOS.

3. Experimental Section

3.1. Chemicals

Dulbecco's modified Eagle's medium (DMEM) and fetal bovine serum (FBS) were from Invitrogen Life Technologies (GIBCO, Paisley, UK) and from PAA (Linz, Austria). Melatonin, JC-1 and all other reagents were from Sigma (St. Louis, MO, USA), unless otherwise specified. Real-time PCR reagents were from Stratagene (Santa Clara, CA, USA).

3.2. Cell Culture

HaCaT cells were grown in Dulbecco's modified Eagle's medium (DMEM), 10% fetal bovine serum (FBS), containing 4.5 g/L glucose, 0.05 mg/mL gentamycin and 2 mM L-glutamine, in 25 cm^2 flasks or multi-well plates. Cultures were maintained at 37 °C, under 5% CO_2 and 95% air. Before melatonin treatment, cells were grown for ~24 h in 1 g/L glucose DMEM, w/o FBS and phenol red. When required, cell lysis was carried out by TRIzol or CelLytic™ M Cell Lysis reagent in the presence of Protease Inhibitor Cocktail (1:100); protein content was determined by the Bradford reaction, and citrate synthase activity was assayed as representative of the mitochondrial mass.

3.3. nNOS mRNA Determination

The nNOS mRNA was determined according to the protocol detailed in [28]; briefly, HaCaT cells ($\sim 3 \times 10^6$ cells) were harvested and total RNA isolated; the reverse transcription was carried out using SideStep™ II QPCR cDNA Synthesis Kit (Agilent Technologies, Santa Clara, CA, USA). The QRT-PCR was performed using a Stratagene Mx3005p System (Agilent Technologies, Santa Clara, CA, USA). All reactions have been carried out in triplicate.

3.4. nNOS Detection by Western Blot

HaCaT cells were lysed with CelLytic™ M reagent (Sigma) in the presence of protease inhibitors (Sigma). The proteins were separated on 10% SDS-PAGE gels and transferred on nitrocellulose membranes (Whatman, GE Halthcare UK, Buckinghamshire, UK) 1 h at 100 mA. After 2 h blocking (PBS with 0.1% tween and 3% BSA), the membrane was incubated overnight at 4 °C with primary rabbit polyclonal anti-nNOS antibodies (from BD Transduction Laboratories, Buccinasco, MI, Italy); α tubulin was used as the reference. A secondary ECL TM anti-rabbit antibody HRP (Jackson, Baltimore, PA, USA) was thereafter incubated 1 h at 25 °C and chemiluminescence determined (Amersham, GE Halthcare UK, Buckinghamshire, UK). Densitometric analysis was carried out by the KODAK 1D Image Analysis Software (Eastman Kodak Company, Rochester, NY, USA).

3.5. Nitrite/Nitrate (NOx) Determination

Accumulation of the NOx in the culture medium of HaCaT cells ($\sim 2.5 \times 10^5$ cells/mL) was measured after 6 h and 8 h exposure to melatonin at the given concentrations or at different times of incubation with 1 nM melatonin (see text). The NOx content was determined fluorometrically (Fluorometric Assay Kit, Cayman Chemical Co., Ann Arbor, MI, USA).

3.6. Cell Respiration

HaCaT cells, grown overnight in an antibiotic/FBS-free DMEM medium, were incubated 8 h with increasing melatonin concentrations (1, 10, 100 nM); when required, the nNOS inhibitor, 7 N, was added (500 nM) 30 min before the measurement. For the assay, cells were resuspended in Hank's buffer containing 5.5 mM glucose at a final cell density, 3.3×10^6 cells/mL. Cell respiration was evaluated using high resolution respirometry (2k-Oxygraph OROBOROS Instruments, Innsbruck, Austria).

3.7. Mitochondrial Membrane Potential

The mitochondrial H^+ electrochemical potential gradient of intact cells ($\Delta\mu H^+$) was evaluated following the mitochondrial electrophoretic accumulation of JC-1 (Sigma) [75]. In the presence of the ionophore nigericin, converting ΔpH into $\Delta\Psi$ [76], the fluorescence reaches a maximum, whose level depends upon the membrane potential value. The fluorescence signal is rapidly dissipated by 0.2 μM valinomycin ($\Delta\Psi \approx 0$), thus allowing a ΔF to be evaluated (proportional to the membrane potential).

186

11270

3.8. ATP Measurements

The ATP concentration was quantified by chemiluminescence, as described in [28]. Briefly, cells were incubated with 1 nM melatonin for 6 h. The rate of ATP production was evaluated after cell membrane permeabilization with 60 μg/mL digitonin, 20 min at 25 °C; 20 mM succinate and 0.5 mM ADP were thereafter added, in the presence of 4 μM rotenone, to induce ATP synthesis. Measurements were performed using the ATPlite kit (Perkin Elmer, Waltham, MA, USA), on a VICTOR™ Multilabel Counter (Perkin Elmer, Waltham, MA, USA) equipped with 96-well (white) plates.

3.9. Lactate Measurements

Cells (~3 × 10⁶ cells), have been incubated 6 h with melatonin, 1 nM, and then, the lactate was measured. In order to energetically synchronize the cells, after the first 2 h, incubation cells were starved 1 h from glucose. Thereafter, glucose, 1 mM, was re-added to the cells for a further 3 h. Lactate determinations have been carried out in the absence of myxothiazol and antimycin A or in their presence (10 μM each) to fully inhibit OXPHOS. The lactate concentration was determined spectrophotometrically on the cell supernatant collected by centrifugation ($1000 \times g$, at 4 °C, 10 min).

3.10. Statistics

The number of independent measurements is indicated in the figure legend. Significance was determined using the Student *t*-test, run by Excel (Microsoft Windows platform). The error bars correspond to the standard error of the mean (SEM); all *p*-values correspond to two-sided sample *t*-test, assuming unequal variances. A *p*-value ≤ 0.05 was considered significant.

4. Conclusions

Based on our results, the physiological meaning of the effects induced by melatonin on the nNOS, and, thereby, on cell bioenergetics, is purely hypothetical, demanding further assessment and independent evaluation. All together, the experimental evidence points to two mechanistically-independent activities exerted by melatonin at the mitochondrial level. The first one is based on the antioxidant radical scavenging properties of melatonin: this is best observed at a high concentration of melatonin ($\geq 10^{-6}$ M); the second one is more consistent with a hormonal-like function and appears to be nuclear-dependent, possibly receptor-mediated, thus requiring a suitable time of cell incubation with nanomolar amounts of melatonin. Interestingly enough, these extracellular concentration values are compatible with those reached in our body during night peak, ~100–200 pg/mL [48,77], *i.e.*, ~1 nM melatonin. We believe that under these conditions, the intra-cellular concentration of melatonin increases gradually and allows its accumulation in the different cell compartments. In this respect, it is worth mentioning that the evaluation of the melatonin activity at the mitochondrial level can be particularly difficult *in vivo*, if we consider that: melatonin can be imported and accumulated in the mitochondrion [37], while metabolites of melatonin retain a substantial bioactivity [45]. Furthermore, calmodulin, in the cell, is in equilibrium with both melatonin and nNOS, indeed, among other targets: this peculiar state should be considered when addressing the melatonin effects on mitochondria. With these premises, the comparison between data obtained using different experimental approaches may

1 8 7

Attachments

not be straightforward. In conclusion, also based on the literature, our data suggest that melatonin controls mitochondrial efficiency at different levels, by: (i) favoring the eT through the respiratory chain, in a concentration-dependent manner and independently on nuclear-DNA-mediated reactions; while (ii) causing a mild transient inhibition of Complex IV, with a mitochondrial glycolytic shift, an effect mediated by nuclear signaling in a circadian compatible time-window.

Acknowledgements

Conflict of Interest

The authors declare no conflict of interest.

References

1. Maharaj, D.S.; Glass, B.D.; Daya, S. Melatonin: New places in therapy. *Biosci. Rep.* **2007**, *27*, 299–320.
2. Reiter, R.J.; Paredes, S.D.; Manchester, L.C.; Tan, D.X. Reducing oxidative/nitrosative stress: A newly-discovered genre for melatonin. *Crit. Rev. Biochem. Mol. Biol.* **2009**, *44*, 175–200.
3. Conti, A.; Conconi, S.; Hertens, E.; Skwarlo-Sonta, K.; Markowska, M.; Maestroni, J.M. Evidence for melatonin synthesis in mouse and human bone marrow cells. *J. Pineal Res.* **2000**, *28*, 193–202.
4. Slominski, A.; Tobin, D.J.; Zmijewski, M.A.; Wortsman, J.; Paus, R. Melatonin in the skin: Synthesis, metabolism and functions. *Trends Endocrinol. Metab.* **2008**, *19*, 17–24.
5. Champier, J.; Claustrat, B.; Besancon, R.; Eymin, C.; Killer, C.; Jouvet, A.; Chamba, G.; Fevre-Montange, M. Evidence for tryptophan hydroxylase and hydroxy-indol-*O*-methyl-transferase mRNAs in human blood platelets. *Life Sci.* **1997**, *60*, 2191–2197.
6. Carrillo-Vico, A.; Calvo, J.R.; Abreu, P.; Lardone, P.J.; Garcia-Maurino, S.; Reiter, R.J.; Guerrero, J.M. Evidence of melatonin synthesis by human lymphocytes and its physiological significance: Possible role as intracrine, autocrine, and/or paracrine substance. *FASEB J.* **2004**, *18*, 537–539.
7. Liu, C.; Fukuhara, C.; Wessel, J.H., 3rd; Iuvone, P.M.; Tosini, G. Localization of Aa-nat mRNA in the rat retina by fluorescence *in situ* hybridization and laser capture microdissection. *Cell Tissue Res.* **2004**, *315*, 197–201.
8. Reiter, R.J.; Tan, D.X. What constitutes a physiological concentration of melatonin? *J. Pineal Res.* **2003**, *34*, 79–80.
9. Escames, G.; Acuna-Castroviejo, D. Melatonin, synthetic analogs, and the sleep/wake rhythm. *Rev. Neurol.* **2009**, *48*, 245–254.

Attachments

10. Morris, C.J.; Aeschbach, D.; Scheer, F.A. Circadian system, sleep and endocrinology. *Mol. Cell. Endocrinol.* **2012**, *349*, 91–104.

11. Dollins, A.B.; Zhdanova, I.V.; Wurtman, R.J.; Lynch, H.J.; Deng, M.H. Effect of inducing nocturnal serum melatonin concentrations in daytime on sleep, mood, body temperature, and performance. *Proc. Natl. Acad. Sci. USA* **1994**, *91*, 1824–1828.

12. Luchetti, F.; Canonico, B.; Betti, M.; Arcangeletti, M.; Pilolli, F.; Piroddi, M.; Canesi, L.; Papa, S.; Galli, F. Melatonin signaling and cell protection function. *FASEB J.* **2010**, *24*, 3603–3624.

13. Ciftci, M.; Bilici, D.; Kufrevioglu, O.I. Effects of melatonin on enzyme activities of glucose-6-phosphate dehydrogenase from human erythrocytes *in vitro* and from rat erythrocytes *in vivo*. *Pharmacol. Res.* **2001**, *44*, 7–11.

14. Martin, V.; Herrera, F.; Carrera-Gonzalez, P.; Garcia-Santos, G.; Antolin, I.; Rodriguez-Blanco, J.; Rodriguez, C. Intracellular signaling pathways involved in the cell growth inhibition of glioma cells by melatonin. *Cancer Res.* **2006**, *66*, 1081–1088.

15. Korkmaz, A.; Ma, S.; Topal, T.; Rosales-Corral, S.; Tan, D.X.; Reiter, R.J. Glucose: A vital toxin and potential utility of melatonin in protecting against the diabetic state. *Mol. Cell. Endocrinol.* **2012**, *349*, 128–137.

16. Acuna-Castroviejo, D.; Escames, G.; Rodriguez, M.I.; Lopez, L.C. Melatonin role in the mitochondrial function. *Front. Biosci.* **2007**, *12*, 947–963.

17. Reiter, R.J.; Tan, D.X.; Rosales-Corral, S.; Manchester, L.C. The universal nature, unequal distribution and antioxidant functions of melatonin and its derivatives. *Mini Rev. Med. Chem.* **2013**, *13*, 373–384.

18. Poeggeler, B.; Reiter, R.J.; Tan, D.X.; Chen, L.D.; Manchester, L.C. Melatonin, hydroxyl radical-mediated oxidative damage, and aging: A hypothesis. *J. Pineal Res.* **1993**, *14*, 151–168.

19. Poeggeler, B.; Thuermann, S.; Dose, A.; Schoenke, M.; Burkhardt, S.; Hardeland, R. Melatonin's unique radical scavenging properties—Roles of its functional substituents as revealed by a comparison with its structural analogs. *J. Pineal Res.* **2002**, *33*, 20–30.

20. Poeggeler, B.; Saarela, S.; Reiter, R.J.; Tan, D.X.; Chen, L.D.; Manchester, L.C.; Barlow-Walden, L.R. Melatonin—A highly potent endogenous radical scavenger and electron donor: New aspects of the oxidation chemistry of this indole accessed in vitro. *Ann. N. Y. Acad. Sci.* **1994**, *738*, 419–420.

21. Mahal, H.S.; Sharma, H.S.; Mukherjee, T. Antioxidant properties of melatonin: A pulse radiolysis study. *Free Radic. Biol. Med.* **1999**, *26*, 557–565.

22. Srinivasan, V.; Spence, D.W.; Pandi-Perumal, S.R.; Brown, G.M.; Cardinali, D.P. Melatonin in mitochondrial dysfunction and related disorders. *Int. J. Alzheimers Dis.* **2011**, doi:10.4061/2011/326320.

23. Griefahn, B.; Brode, P.; Remer, T.; Blaszkewicz, M. Excretion of 6-hydroxymelatonin sulfate (6-OHMS) in siblings during childhood and adolescence. *Neuroendocrinology* **2003**, *78*, 241–243.

24. Bergiannaki, J.D.; Soldatos, C.R.; Paparrigopoulos, T.J.; Syrengelas, M.; Stefanis, C.N. Low and high melatonin excretors among healthy individuals. *J. Pineal Res.* **1995**, *18*, 159–164.

25. Grof, E.; Grof, P.; Brown, G.M.; Arato, M.; Lane, J. Investigations of melatonin secretion in man. *Prog. Neuropsychopharmacol. Biol. Psychiatry* **1985**, *9*, 609–612.

26. Wetterberg, L.; Iselius, L.; Lindsten, J. Genetic regulation of melatonin excretion in urine. A preliminary report. *Clin. Genet.* **1983**, *24*, 399–402.

11273

27. Galecki, P.; Szemraj, J.; Bartosz, G.; Bienkiewicz, M.; Galecka, E.; Florkowski, A.; Lewinski, A.; Karbownik-Lewinska, M. Single-nucleotide polymorphisms and mRNA expression for melatonin synthesis rate-limiting enzyme in recurrent depressive disorder. *J. Pineal Res.* **2010**, *48*, 311–317.

28. Arese, M.; Magnifico, M.C.; Mastronicola, D.; Altieri, F.; Grillo, C.; Blanck, T.J.; Sarti, P. Nanomolar melatonin enhances nNOS expression and controls HaCaT-cells bioenergetics. *IUBMB Life* **2012**, *64*, 251–258.

29. Cleeter, M.W.; Cooper, J.M.; Darley-Usmar, V.M.; Moncada, S.; Schapira, A.H. Reversible inhibition of cytochrome c oxidase, the terminal enzyme of the mitochondrial respiratory chain, by nitric oxide. Implications for neurodegenerative diseases. *FEBS Lett.* **1994**, *345*, 50–54.

30. Brown, G.C.; Bolanos, J.P.; Heales, S.J.; Clark, J.B. Nitric oxide produced by activated astrocytes rapidly and reversibly inhibits cellular respiration. *Neurosci. Lett.* **1995**, *193*, 201–204.

31. Kalinchuk, A.V.; Stenberg, D.; Rosenberg, P.A.; Porkka-Heiskanen, T. Inducible and neuronal nitric oxide synthases (NOS) have complementary roles in recovery sleep induction. *Eur. J. Neurosci.* **2006**, *24*, 1443–1456.

32. Tsikas, D.; Gutzki, F.M.; Stichtenoth, D.O. Circulating and excretory nitrite and nitrate as indicators of nitric oxide synthesis in humans: Methods of analysis. *Eur. J. Clin. Pharmacol.* **2006**, *62*, 51–59.

33. Chen, L.; Majde, J.A.; Krueger, J.M. Spontaneous sleep in mice with targeted disruptions of neuronal or inducible nitric oxide synthase genes. *Brain Res.* **2003**, *973*, 214–222.

34. Leonard, T.O.; Lydic, R. Pontine nitric oxide modulates acetylcholine release, rapid eye movement sleep generation, and respiratory rate. *J. Neurosci.* **1997**, *17*, 774–785.

35. Alonso, M.; Collado, P.S.; Gonzalez-Gallego, J. Melatonin inhibits the expression of the inducible isoform of nitric oxide synthase and nuclear factor kappa B activation in rat skeletal muscle. *J. Pineal Res.* **2006**, *41*, 8–14.

36. Petrosillo, G.; Moro, N.; Ruggiero, F.M.; Paradies, G. Melatonin inhibits cardiolipin peroxidation in mitochondria and prevents the mitochondrial permeability transition and cytochrome c release. *Free Radic. Biol. Med.* **2009**, *47*, 969–974.

37. Lopez, A.; Garcia, J.A.; Escames, G.; Venegas, C.; Ortiz, F.; Lopez, L.C.; Acuna-Castroviejo, D. Melatonin protects the mitochondria from oxidative damage reducing oxygen consumption, membrane potential, and superoxide anion production. *J. Pineal Res.* **2009**, *46*, 188–198.

38. Hevia, D.; Sainz, R.M.; Blanco, D.; Quiros, I.; Tan, D.X.; Rodriguez, C.; Mayo, J.C. Melatonin uptake in prostate cancer cells: Intracellular transport versus simple passive diffusion. *J. Pineal Res.* **2008**, *45*, 247–257.

39. Moncada, S.; Erusalimsky, J.D. Does nitric oxide modulate mitochondrial energy generation and apoptosis? *Nat. Rev. Mol. Cell Biol.* **2002**, *3*, 214–220.

40. Sarti, P.; Forte, E.; Giuffre, A.; Mastronicola, D.; Magnifico, M.C.; Arese, M. The chemical interplay between nitric oxide and mitochondrial cytochrome c oxidase: Reactions, effectors and pathophysiology. *Int. J. Cell Biol.* **2012**, doi:10.1155/2012/571067.

41. Sgarbi, G.; Baracca, A.; Lenaz, G.; Valentino, L.M.; Carelli, V.; Solaini, G. Inefficient coupling between proton transport and ATP synthesis may be the pathogenic mechanism for NARP and Leigh syndrome resulting from the T8993G mutation in mtDNA. *Biochem. J.* **2006**, *395*, 493–500.

190

42. Martin, M.; Macias, M.; Escames, G.; Reiter, R.J.; Agapito, M.T.; Ortiz, G.G.; Acuna-Castroviejo, D. Melatonin-induced increased activity of the respiratory chain complexes I and IV can prevent mitochondrial damage induced by ruthenium red *in vivo*. *J. Pineal Res.* **2000**, *28*, 242–248.

43. Okatani, Y.; Wakatsuki, A.; Reiter, R.J. Melatonin protects hepatic mitochondrial respiratory chain activity in senescence-accelerated mice. *J. Pineal Res.* **2002**, *32*, 143–148.

44. Jimenez-Ortega, V.; Cano, P.; Cardinali, D.P.; Esquifino, A.I. 24-Hour variation in gene expression of redox pathway enzymes in rat hypothalamus: Effect of melatonin treatment. *Redox Rep.* **2009**, *14*, 132–138.

45. Tan, D.X.; Manchester, L.C.; Terron, M.P.; Flores, L.J.; Reiter, R.J. One molecule, many derivatives: A never-ending interaction of melatonin with reactive oxygen and nitrogen species? *J. Pineal Res.* **2007**, *42*, 28–42.

46. Martin, M.; Macias, M.; Escames, G.; Leon, J.; Acuna-Castroviejo, D. Melatonin but not vitamins C and E maintains glutathione homeostasis in *t*-butyl hydroperoxide-induced mitochondrial oxidative stress. *FASEB J.* **2000**, *14*, 1677–1679.

47. Inarrea, P.; Casanova, A.; Alava, M.A.; Iturralde, M.; Cadenas, E. Melatonin and steroid hormones activate intermembrane Cu,Zn-superoxide dismutase by means of mitochondrial cytochrome P450. *Free Radic. Biol. Med.* **2011**, *50*, 1575–1581.

48. Zawilska, J.B.; Skene, D.J.; Arendt, J. Physiology and pharmacology of melatonin in relation to biological rhythms. *Pharmacol. Rep.* **2009**, *61*, 383–410.

49. Martin, M.; Macias, M.; Leon, J.; Escames, G.; Khaldy, H.; Acuna-Castroviejo, D. Melatonin increases the activity of the oxidative phosphorylation enzymes and the production of ATP in rat brain and liver mitochondria. *Int. J. Biochem. Cell Biol.* **2002**, *34*, 348–357.

50. Garcia, J.J.; Reiter, R.J.; Guerrero, J.M.; Escames, G.; Yu, B.P.; Oh, C.S.; Munoz-Hoyos, A. Melatonin prevents changes in microsomal membrane fluidity during induced lipid peroxidation. *FEBS Lett.* **1997**, *408*, 297–300.

51. Reiter, R.J.; Tan, D.X.; Manchester, L.C.; Qi, W. Biochemical reactivity of melatonin with reactive oxygen and nitrogen species: A review of the evidence. *Cell Biochem. Biophys.* **2001**, *34*, 237–256.

52. Tan, D.X.; Manchester, L.C.; Reiter, R.J.; Qi, W.B.; Karbownik, M.; Calvo, J.R. Significance of melatonin in antioxidative defense system: Reactions and products. *Biol. Signals Recept.* **2000**, *9*, 137–159.

53. Acuna-Castroviejo, D.; Martin, M.; Macias, M.; Escames, G.; Leon, J.; Khaldy, H.; Reiter, R.J. Melatonin, mitochondria, and cellular bioenergetics. *J. Pineal Res.* **2001**, *30*, 65–74.

54. Leon, J.; Acuna-Castroviejo, D.; Sainz, R.M.; Mayo, J.C.; Tan, D.X.; Reiter, R.J. Melatonin and mitochondrial function. *Life Sci.* **2004**, *75*, 765–790.

55. Leon, J.; Acuna-Castroviejo, D.; Escames, G.; Tan, D.X.; Reiter, R.J. Melatonin mitigates mitochondrial malfunction. *J. Pineal Res.* **2005**, *38*, 1–9.

56. Reyes-Toso, C.F.; Rebagliati, I.R.; Ricci, C.R.; Linares, L.M.; Albornoz, L.E.; Cardinali, D.P.; Zaninovich, A. Effect of melatonin treatment on oxygen consumption by rat liver mitochondria. *Amino Acids* **2006**, *31*, 299–302.

Attachments

57. Soto-Vega, E.; Meza, I.; Ramirez-Rodriguez, G.; Benitez-King, G. Melatonin stimulates calmodulin phosphorylation by protein kinase C. *J. Pineal Res.* **2004**, *37*, 98–106.

58. Leon, J.; Escames, G.; Rodriguez, M.I.; Lopez, L.C.; Tapias, V.; Entrena, A.; Camacho, E.; Carrion, M.D.; Gallo, M.A.; Espinosa, A.; *et al.* Inhibition of neuronal nitric oxide synthase activity by N^1-acetyl-5-methoxykynuramine, a brain metabolite of melatonin. *J. Neurochem.* **2006**, *98*, 2023–2033.

59. Palacios-Callender, M.; Quintero, M.; Hollis, V.S.; Springett, R.J.; Moncada, S. Endogenous NO regulates superoxide production at low oxygen concentrations by modifying the redox state of cytochrome c oxidase. *Proc. Natl. Acad. Sci. USA* **2004**, *101*, 7630–7635.

60. Mastronicola, D.; Genova, M.L.; Arese, M.; Barone, M.C.; Giuffre, A.; Bianchi, C.; Brunori, M.; Lenaz, G.; Sarti, P. Control of respiration by nitric oxide in Keilin-Hartree particles, mitochondria and SH-SY5Y neuroblastoma cells. *Cell. Mol. Life Sci.* **2003**, *60*, 1752–1759.

61. Sarti, P.; Giuffrè, A.; Barone, M.C.; Forte, E.; Mastronicola, D.; Brunori, M. Nitric oxide and cytochrome oxidase: Reaction mechanisms from the enzyme to the cell. *Free Radic. Biol. Med.* **2003**, *34*, 509–520.

62. Cooper, C.E.; Mason, M.G.; Nicholls, P. A dynamic model of nitric oxide inhibition of mitochondrial cytochrome c oxidase. *Biochim. Biophys. Acta* **2008**, *1777*, 867–876.

63. Sarti, P.; Forte, E.; Mastronicola, D.; Giuffre, A.; Arese, M. Cytochrome c oxidase and nitric oxide in action: Molecular mechanisms and pathophysiological implications. *Biochim. Biophys. Acta* **2012**, *1817*, 610–619.

64. Almeida, A.; Almeida, J.; Bolanos, J.P.; Moncada, S. Different responses of astrocytes and neurons to nitric oxide: The role of glycolytically generated ATP in astrocyte protection. *Proc. Natl. Acad. Sci. USA* **2001**, *98*, 15294–15299.

65. Warburg, O. On respiratory impairment in cancer cells. *Science* **1956**, *124*, 269–270.

66. Brown, G.C.; Cooper, C.E. Nanomolar concentrations of nitric oxide reversibly inhibit synaptosomal respiration by competing with oxygen at cytochrome oxidase. *FEBS Lett.* **1994**, *356*, 295–298.

67. Cooper, C.E.; Brown, G.C. The inhibition of mitochondrial cytochrome oxidase by the gases carbon monoxide, nitric oxide, hydrogen cyanide and hydrogen sulfide: Chemical mechanism and physiological significance. *J. Bioenerg. Biomembr.* **2008**, *40*, 533–539.

68. Sarti, P.; Giuffrè, A.; Forte, E.; Mastronicola, D.; Barone, M.C.; Brunori, M. Nitric oxide and cytochrome *c* oxidase: Mechanisms of inhibition and NO degradation. *Biochem. Biophys. Res. Commun.* **2000**, *274*, 183–187.

69. Brunori, M.; Forte, E.; Arese, M.; Mastronicola, D.; Giuffre, A.; Sarti, P. Nitric oxide and the respiratory enzyme. *Biochim. Biophys. Acta* **2006**, *1757*, 1144–1154.

70. Mason, M.G.; Nicholls, P.; Wilson, M.T.; Cooper, C.E. Nitric oxide inhibition of respiration involves both competitive (heme) and noncompetitive (copper) binding to cytochrome c oxidase. *Proc. Natl. Acad. Sci. USA* **2006**, *103*, 708–713.

71. Brookes, P.S.; Kraus, D.W.; Shiva, S.; Doeller, J.E.; Barone, M.C.; Patel, R.P.; Lancaster, J.R., Jr.; Darley-Usmar, V. Control of mitochondrial respiration by NO*, effects of low oxygen and respiratory state. *J. Biol. Chem.* **2003**, *278*, 31603–31609.

Attachments

72. Trimmer, B.A.; Aprille, J.R.; Dudzinski, D.M.; Lagace, C.J.; Lewis, S.M.; Michel, T.; Qazi, S.; Zayas, R.M. Nitric oxide and the control of firefly flashing. *Science* **2001**, *292*, 2486–2488.

73. Zoche, M.; Bienert, M.; Beyermann, M.; Koch, K.W. Distinct molecular recognition of calmodulin-binding sites in the neuronal and macrophage nitric oxide synthases: A surface plasmon resonance study. *Biochemistry* **1996**, *35*, 8742–8747.

74. Romero, M.P.; Garcia-Perganeda, A.; Guerrero, J.M.; Osuna, C. Membrane-bound calmodulin in Xenopus laevis oocytes as a novel binding site for melatonin. *FASEB J.* **1998**, *12*, 1401–1408.

75. Reers, M.; Smith, T.W.; Chen, L.B. J-aggregate formation of a carbocyanine as a quantitative fluorescent indicator of membrane potential. *Biochemistry* **1991**, *30*, 4480–4486.

76. Reed, P.W. Ionophores. *Methods Enzymol.* **1979**, *55*, 435–454.

77. Pandi-Perumal, S.R.; Srinivasan, V.; Maestroni, G.J.; Cardinali, D.P.; Poeggeler, B.; Hardeland, R. Melatonin: Nature's most versatile biological signal? *FEBS J.* **2006**, *273*, 2813–2838.

Attachments

Characterization of Mitochondrial Dysfunction in the 7PA2 Cell Model of Alzheimer's Disease

Nina Krako[a,c,1], Maria Chiara Magnifico[b,1], Marzia Arese[b], Giovanni Meli[c], Elena Forte[b],
Agnese Lecci[c], Annalisa Manca[c], Alessandro Giuffrè[d], Daniela Mastronicola[d],
Paolo Sarti[b,d] and Antonino Cattaneo[a,c,*]
[a] *Scuola Normale Superiore, Pisa, Italy*
[b] *Department of Biochemical Sciences and Istituto Pasteur – Fondazione Cenci Bolognetti,
Sapienza University of Rome, Italy*
[c] *European Brain Research Institute – "Rita Levi-Montalcini", Rome, Italy*
[d] *CNR Institute of Molecular Biology and Pathology, Rome, Italy*

Handling Associate Editor: ShiDu Yan

Abstract. The 7WD4 and 7PA2 cell lines, widely used as cellular models for Alzheimer's disease (AD), have been used to investigate the effects of amyloid-β protein precursor overexpression and amyloid-β (Aβ) oligomer accumulation on mitochondrial function. Under standard culture conditions, both cell lines, compared to Chinese hamster ovary (CHO) control cells, displayed an ∼5% decrease of O_2 respiration as sustained by endogenous substrates. Functional impairment of the respiratory chain was found distributed among the protein complexes, though more evident at the level of complex I and complex IV. Measurements of ATP showed that its synthesis by oxidative phosphorylation is decreased in 7WD4 and 7PA2 cells by ∼25%, this loss being partly compensated by glycolysis (Warburg effect). Compensation proved to be more efficient in 7WD4 than in 7PA2 cells, the latter cell line displaying the highest reactive oxygen species production. The strongest deficit was observed in mitochondrial membrane potential that is almost 40% and 60% lower in 7WD4 and 7PA2 cells, respectively, in comparison to CHO controls. All functional parameters point to a severe bioenergetic impairment of the AD cells, with the extent of mitochondrial dysfunction being correlated to the accumulation of Aβ peptides and oligomers.

Keywords: Alzheimer's disease, amyloid-β oligomers, bioenergetics, mitochondrial dysfunction

INTRODUCTION

The molecular mechanisms causing Alzheimer's disease (AD) are complex and still uncertain in their nature and progression. AD is characterized by a progressive increase of the amyloid-β peptide (Aβ), derived from abnormal processing of the amyloid-β protein precursor (AβPP), in brain regions serving memory and cognition, whose impairment is an invariant hallmark of the disease [1]. There is ample evidence coming, first of all, from genetic data that abnormal processing of the amyloid-β precursor protein (AβPP) leading to high Aβ peptide production, is sufficient to cause AD [2]. The Aβ peptides are produced proteolytically by β- and γ-secretase acting on AβPP, and are prone to aggregation in highly toxic oligomeric assemblies within the brain, inside and outside the

---

neuronal cells. There is considerable evidence implicating elevated oxidative stress, mitochondrial dysfunction, and energy metabolism deficiencies as early events in the pathogenesis of AD [3]. In this respect, little is known about whether and how Aβ production and oligomerization influence cellular bioenergetics and mitochondrial function. Both the AβPP and the Aβ peptides have been reported to actively interact with rat brain and muscle mitochondria, leading to a decrease of oxidative phosphorylation (OXPHOS) efficiency [4]. Aβ can be imported into mitochondria *via* the TOM import machinery, independently of the mitochondrial membrane potential, and can affect the functional mitochondrial state [5]. Heat shock protein 60 (HSP60), a membrane chaperone localized on mitochondria, has been reported to be involved in the translocation of AβPP to mitochondria [6], and its interaction with appoptosin, a novel pro-apoptotic protein involved in neuronal cell death, is gaining attention [7]. Relevant to Aβ production, an active γ-secretase complex has been found to be localized in mitochondria [8], linked to the mitochondrial associated membranes, at the contact sites between the endoplasmic reticulum (ER) and mitochondrial network [9]. Relevant to cell bioenergetics, using isolated mitochondria it has been reported that synthetic Aβ peptides inhibit *in vitro* cytochrome *c* oxidase activity and cellular respiration [10, 11], consistent with studies in neuroblastoma SHSY-5Y cells [12], or Tg2576 mice [13] both overexpressing AβPP.

Invariably, an increased generation of reactive oxygen species (ROS) has also been reported as an early event in AD patients [3]. In this regard, it is worth considering that mitochondria are the leading sites for ROS production, and that nitric oxide, as part of them, has been shown to play a major role in neurodegenerative diseases, AD included [14]. Therefore, mitochondria represent key pathophysiological targets for Aβ, particularly considering that the whole process of Aβ synthesis, oligomerization, and accumulation begins intracellularly [15].

The 7PA2 and 7WD4 cells are among the best characterized cellular models of Aβ toxicity and oligomerization. The 7PA2 cells are the most widely used source of naturally produced, biologically-relevant Aβ peptides and oligomers [16–19]. These are the Chinese hamster ovary cell lines (CHO): the 7WD4 cells stably express the wild type human AβPP isoform, 751 amino acids in length (wtAβPP$_{751}$), while the 7PA2 cells harbor the human Val717Phe (V717F) mutation of the wtAβPP$_{751}$ [20]. Both the 7WD4 and 7PA2 cells are sources of endogenously produced,

natural Aβ peptides. The AβPP V717F mutation [21, 22] is located 4-6 residues beyond the wtAβPP cleavage site where γ-secretase binds. The Aβ peptides produced proteolytically display changes in length and tertiary structures, and have been proposed to be responsible for the earlier clinical manifestations of dementia and death of patients that harbor the mutation [23]. Since these cells are the best cellular model to study Aβ processing and aggregation of natural oligomers and since the literature shows putative links between Aβ and oxidative stress, it is therefore of interest to investigate whether and how the intracellular production of Aβ peptides and oligomers, in this cellular model, influences mitochondrial functions and cell bioenergetics.

In this work, we have investigated the bioenergetic effects induced by endogenously produced Aβ peptides, in intact 7WD4 and 7PA2 AD cells.

MATERIALS AND METHODS

Cells lines

The 7WD4 and 7PA2 cell lines were kindly provided by Dr. Denis Selkoe, Harvard Medical School, Boston. These are CHO cell lines stably expressing human wtAβPP$_{751}$ (7WD4 cells) and AβPP$_{751}$ harboring mutation V717F (7PA2 cells) [20]. Controls are non-transfected CHO cells. Western blot analysis for the expression of AβPP is shown in Supplementary Figure 1 and anti-Aβ immunostaining is shown in Supplementary Figure 3. The cells were cultured in Ham's F12 media with L-glutamine, supplemented with 10% fetal bovine serum, penicillin/streptomycin and G418 for maintaining selection of hAβPP stable transfect (7WD4 and 7PA2). Before the experiments, cells were plated without G418 antibiotic in order to be in the same culture conditions as control CHO cells.

Mitochondrial membrane potential

The mitochondrial H$^+$ electrochemical potential gradient ($\Delta\mu$H$^+$) of intact cells was evaluated following the mitochondrial electrophoretic accumulation of the membrane permeable, fluorescent cationic probe JC-1 (Sigma Chemical Co.). Type and intensity of emission of this dye depends both on its concentration and on the light excitation wavelength. Upon exciting at 490 nm, JC-1 monomers display a fluorescence emission centered at 537 nm (green band). Beyond a critical concentration, better reached at high mitochondrial membrane potential values ($\Delta\Psi \geq 200$ mV), JC-1

195

aggregates are formed in the mitochondrion, characterized by an intense emission band centered at 590 nm (red band) [24]. Measurements were carried out in the presence of the ionophore nigericin, converting ΔpH into $\Delta\Psi$. Cells were pre-incubated in DMEM (without glucose) for 1 h at 37°C, 5% CO_2. For the experiment, cells were trypsinized, gently centrifuged at $1100\times g$ for 3 min at 25°C, and resuspended in DMEM (containing glucose, 1 g/L) without phenol red, to obtain a cell suspension of 3×10^6 cells/ml. The kinetics of JC-1 accumulation was followed in the presence of ouabain 2 μM, collapsing the cell membrane potential, thus avoiding an aspecific cytoplasmic accumulation of the fluorescent probe [24]. After addition of nigericin, the fluorescence level reached a maximum within approximately 60 min; thereafter, the fluorescence signal was rapidly dissipated by 0.2 μM valinomycin ($\Delta\Psi \cong$ 0). The kinetics of JC-1 accumulation was measured at 595 nm (VICTOR^{TM} Multilabel Counter, Perkin Elmer), under identical conditions for the three cell lines in 24-well black plates, 3×10^6 cells/ml.

Reactive oxygen species

Cell ROS generation was assessed using 2′,7′-dichlorodihydrofluorescein diacetate (DCFDA) from Molecular Probes (Eugene, OR). Before the experiment, cells were trypsinized, pelleted at $1100\times g$ for 3 min at 25°C, and resuspended in Hank's buffer, at the density 1×10^6 cells/ml. Cell suspensions, 1×10^6 cells/well, were plated in 24-well (black) plates, and the relative fluorescence emission after cell loading of DCFDA 100 μM, was followed after washing, at 520 nm (VICTOR^{TM} Multilabel Counter, Perkin Elmer).

Cell respiration

Cell respiration was evaluated using the High Resolution Respirometry (2k-Oxygraph, OROBOROS Instruments). Intact cells (3.3×10^6 cells/ml) were resuspended in DMEM, containing glucose 1 g/L. The respiratory control ratio was measured as the ratio between the rate of O_2 consumption, observed after the sequential addition of the ionophores 600 nM nigericin and 200 nM valinomycin, and the rate of respiration before their addition; these ionophores, when co-present in the assay medium, fully collapse mitochondrial $\Delta\mu H^+$ [25]. Respiration was evaluated under basal (not stimulated) metabolic conditions, thus limited by endogenous substrates availability and in cells permeabilized with digitonin, in the presence of excess substrates and ADP. The optimal digitonin concentration and the incubation time, determined according to [26], were $1.8 \mu g/ml \times 1 \times 10^6$ cells and 10 min, respectively. Putative membrane damage produced by digitonin was also evaluated, by independently assaying the onset of sensitivity of cell respiration to externally added cytochrome c^{2+} [27].

ATP measurements

The concentration of ATP was quantified by chemiluminescence under basal cell metabolic conditions, at equilibrium. The stationary ATP measurements were performed using cells suspended in phosphate-buffered-saline (PBS) containing L-glutamine (2 mM), in the presence of glucose, 2 g/L, or in its absence, for 3 h (starvation). When necessary, oligomycin (2.5 μg/ml) was added over the last 1.5 h incubation. ATP measurements were performed using the ATPlite kit (Perkin Elmer), on a VICTOR^{TM} Multilabel Counter (Perkin Elmer, Waltham, USA) equipped with 96-well (white) plates.

Lactate measurements

Cells were grown in 6-well plates to 80–90% confluence. Lactate production was evaluated according to [27] with minor modifications: before the experiment cells were pre-incubated for 1 h at 37°C, 5% CO_2 in 2 ml of DPBS containing Ca^{2+} 0.9 mM and Mg^{2+} 0.5 mM. Thereafter, cells were incubated in the same medium containing glucose (1 mM); when necessary myxothiazol and antimycin. A were added (5 μM each). Lactate was determined spectrophotometrically in the cell supernatant.

Citrate synthase

Cells (1×10^6) were lysed and centrifuged at $13,000\times g$ and supernatants assayed for citrate synthase [28] and for total protein content [29]. The CHO, 7WD4, and 7PA2 cells displayed very similar protein contents, about 0.22 mg/ml, and citrate synthase activity, about 0.27 units/ml with minor differences (within 2.5%) among cell lines.

Statistics

The number of independent measurements is indicated in the figure legends. Significance was determined using the Student *t*-test, run by Excel (Microsoft Windows platform). The error bars correspond to the

standard error of the mean (SEM); all p values correspond to two-sided sample t-test assuming unequal variances. A p value ≤ 0.05 was considered significant.

RESULTS

Cell respiration

Respiration of the three cell lines was evaluated oxygraphically using viable intact cells. Measurements were carried out under identical conditions either under basal metabolic conditions or in the presence of ionophores, nigericin and valinomycin, to abolish the control (inhibition) exerted on the respiratory chain by the H^+ electrochemical potential gradient. The basal, spontaneous, respiration rate of CHO, 7WD4, and 7PA2 cells corresponded to 85, 37, and 52 pmol O_2 s^{-1} mg^{-1} of proteins, respectively. In the presence of ionophores, cell respiration increased by a factor of $\sim$2.4 (CHO), 1.5 (7WD4), and 1.6 (7PA2), respectively, thus allowing the assignment of the respiratory control ratio to each cell line (see Fig. 1). Thus, respiration rate is reduced in 7WD4 and 7PA2 cells.

The functional state of the respiratory chain complexes was evaluated by a substrate/inhibitor titration approach, which allows the controlled addition of exogenous reducing substrates enabled by digitonin cell membrane permeabilization (modified from [27]). As shown in Fig. 2b, within 10 min incubation with digitonin, cell respiration slowly decreases to approximately 50% of the initial value, as expected due to partial membrane permeabilization and loss of reduc-

ing substrates and ADP. By the exogenous addition of excess ADP and substrates generating NADH (i.e., pyruvate and malate), cell respiration is restored to the initial values. Interestingly, the 7PA2 and 7WD4 oxygen consumption is about 40% lower than that of CHO control cells (Fig. 2c). At this stage, the addition of rotenone, by inhibiting Complex I, almost completely abolishes respiration, typically restored with succinate, the substrate that reacts directly with Complex II. As also shown in Fig. 2c, before inhibition by rotenone and after the addition of succinate, the differences of respiration rate between AD and control cells are maintained, although attenuated, as if the impairment of Complex I was higher than that of Complex II. Similarly to rotenone, antimycin A stops respiration by inhibiting Complex III. In this case, respiration is restored by donating electrons directly to cytochrome c and cytochrome c oxidase, i.e., using the reductants ascorbate and TMPD. These conditions ensure the highest electron transfer efficiency at the complex IV site, so that the O_2 consumption rate increases in all cell lines, though to a different extent, reaching 230 pmol O_2 s^{-1} mg^{-1} of proteins for CHO, and 170 pmol O_2 s^{-1} mg^{-1} of proteins for both 7WD4 and 7PA2 cells; the addition of exogenous cytochrome c^{2+} to the respiring cells did not affect respiration, proving the integrity of the mitochondrial outer membrane, and suggesting that, as performed, the mild digitonin treatment causes small ions and molecules permeabilization, but not loss of cytochrome c, at least on the time window explored (Fig. 2c). In conclusion, both the 7WD4 and 7PA2 cells show an electron transfer
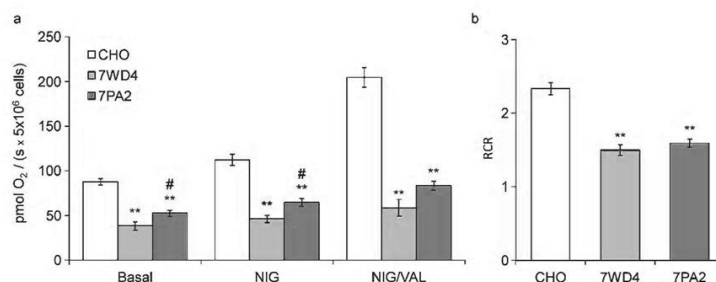

Fig. 1. Cell respiration and respiratory control ratio of CHO, 7WD4, and 7PA2 cells. a) Oxygen consumption of intact cells (5×10^6 cells/chamber) resuspended in DMEM containing 1 g/L glucose. Basal: endogenous respiration rate; NIG: respiration rate after addition of nigericin (600 nM) to cells undergoing basal respiration; NIG/VAL: respiration rate measured after addition of valinomycin (200 nM) to cells respiring in the presence of nigericin. b) Respiratory control ratio (RCR) obtained as the ratio between the rate observed in the presence of both nigericin and valinomycin (NIG/VAL) and in their absence (basal respiration). Data values are the means $\pm$ SEM; $n \geq 5$. **$p \leq 0.001$ versus Control (CHO); #$p \leq 0.05$ versus 7WD4.
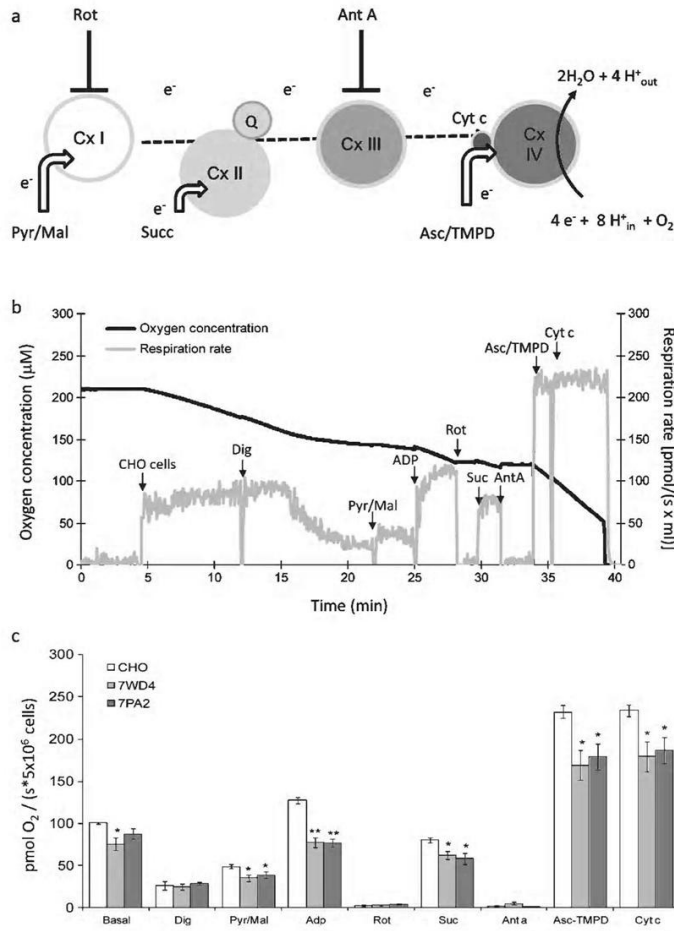
Attachments

Fig. 2. Respiratory complexes activity in digitonin-permeabilized CHO, 7WD4, and 7PA2 cells. a) Sequential representation of the mitochondrial respiratory chain. Experimental design of oxygraphic titration, using specific substrate and inhibitors. Cx I-IV: mitochondrial complex I-IV. Rot: rotenone (0.5 μM, inhibitor of Cx I), Ant A: antimycin A (5 μM, inhibitor of Cx III). Pyr/Mal: Pyruvate+Malate (8.8 mM and 4.4 mM respectively); Succ: succinate (10 mM); Asc/TMPD: ascorbate+TMPD (2 mM and 0.5 mM respectively, reductants of CxIV); Q: ubiquinol, Cyt c: cytochrome c. b) Typical oxygraphic trace of 5×10^6 CHO cells. Black line: oxygen concentration trace, gray line: O_2 flux, i.e., oxygen consumption rate. Dig: digitonine (6 μg/ml), ADP: adenosine diphosphate (4 mM); cytochrome c (10 mM). c) Respiration rate values in CHO, 7WD4, and 7PA2 cells recorded after each addition step (of substrate/inhibitor) during the trace. Data values are the means ± SEM; $n \geq 5$. $*p \leq 0.05$ versus Control (CHO); $**p \leq 0.001$ versus Control (CHO).

198

deficit, which is particularly evident for the activity of complex I and complex IV.

ATP and lactate

The ATP concentration was determined in cells preliminarily starved from glucose for 3 h. Starvation from glucose of cultured cells, that commonly rely on glycolysis, has been necessary to stimulate OXPHOS [30]. As shown in Fig. 3a, in the absence of glucose sustaining glycolysis, the ATP concentration level in 7WD4 and 7PA2 cells is $\sim$20% lower than in CHO. As also shown in the figure, the addition of oligomycin to the cells induces a dramatic decrease of ATP due to OXPHOS inhibition. Under these conditions, the difference between the ATP measured in the absence and presence of oligomycin is, within the error, indicative of the level of ATP produced by oxidative phospho-

rylation (ATP$_{OXPHOS}$) present in each cell line. In the presence of glucose, glycolysis can take place and compensate for loss of ATP$_{OXPHOS}$ (Warburg effect). Under these conditions, the dramatic ATP drop induced by oligomycin is no longer evident (Fig. 3b). Interestingly, the 7PA2 cells display an $\sim$20% decrease of the total ATP concentration even if able to sustain a glycolytic response, as proved by the lactate measurements (see below). The 7WD4 cells, on the contrary, display the same ATP content of CHO cells.

The relative contribution of OXPHOS and glycolysis to the overall ATP production in the three cell lines was independently evaluated by comparing the concentration of lactate produced by the cells preincubated for 2.5 h with glucose. Determination of lactate production was carried out in the absence and presence of antimycin A and myxothiazol (complex III
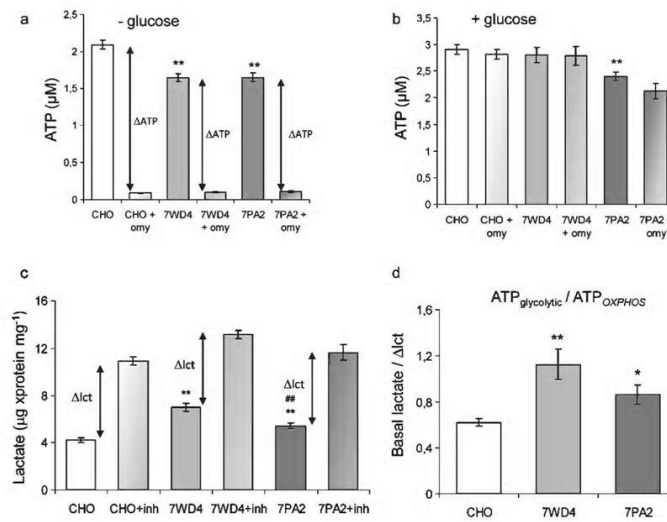

Fig. 3. ATP concentration in CHO, 7WD4, and 7PA2 cells and lactate accumulation in the cell medium. a, b) ATP measurements carried out by the luciferin/luciferase assay under stationary conditions in intact cells (5×10^5/ml). Relative contribution of OXPHOS and glycolysis to the ATP production was evaluated in the presence and absence of oligomycin 2.5 µg/ml and glucose 1 mM. a) Measurement of ATP in the absence of glucose (to avoid glycolysis) after 3 h cell starvation in the presence of PBS containing L-glutamine. Omy: oligomycin; ΔATP: difference of ATP measured in the absence and in the presence of oligomycin (corresponding to ATP$_{OXPHOS}$). b) Measurements of ATP in the presence of glucose to allow glycolysis. Data $\pm$ SEM collected using 3 cell preparations; $n \geq 6$. **$p \leq 0.001$ versus CHO cells. c) Basal lactate $\approx$ ATP$_{glycolytic}$; Δlct $\approx$ ATP$_{OXPHOS}$. Cells were incubated 2.5 h in the presence of glucose 1 mM and in the presence and absence of myxothiazol and antimycin A (inh), 5 µM each. d) Ratio between basal lactate and Δlct, as indicative of the ATP$_{glycolytic}$/ATP$_{OXPHOS}$ ratio. Values are the means $\pm$ SEM; $n \geq 5$. *$p \leq 0.05$ versus CHO; **$p \leq 0.001$ versus CHO; ##$p \leq 0.001$ versus 7WD4.

199

Attachments

and OXPHOS inhibitors, respectively) (Fig. 3c). The glycolytic ATP synthesized under basal metabolic conditions is proportional to the lactate produced in the absence of inhibitors: the basal lactate concentration in CHO cells is $4.2\,\mu g \times mg^{-1}$ of protein, to be compared, respectively, with the 5.4 and $7.0\,\mu g \times mg^{-1}$ of protein of 7PA2 and 7WD4 cells. In the presence of antimycin A and myxothiazol the lactate production increases proportionally in CHO as in 7WD4 and 7PA2 cells (Fig. 3c). The difference between the lactate detected in the presence and absence of inhibitors, Δlct in Fig. 3c, since it has been induced by the OXPHOS inhibition, is proportional to ATP_{OXPHOS}. Therefore, the basal lactate concentration value divided by Δlct was taken as indicative of the $ATP_{glycolytic}/ATP_{OXPHOS}$ ratio [30]. As shown in Fig. 3d, this ratio is 0.62 in CHO cells, 1.12 in 7WD4, and 0.86 in 7PA2 cells. We conclude therefore that 7WD4 and 7PA2 cells exhibit a greater glycolytic efficiency, compensating for the OXPHOS deficit observed above.

Mitochondrial $\Delta\mu H^+$

The 7WD4 and 7PA2 cells as well as the CHO cells, grown under standard culture conditions, can generate and maintain a mitochondrial proton electrochemical potential gradient. The amplitude of the mitochondrial membrane potential built up by the three cell lines was evaluated following the mitochondrial accumulation of the JC-1 (red) aggregates. Upon addition of nigericin, the JC-1 red fluorescence reaches a maximum in about 60 minutes. The subsequent addition of valinomycin suddenly dissipates the membrane potential leading to a fast bleaching of the fluorescence signal; this allows the evaluation of a ΔF proportional to the mitochondrial membrane potential built up by any cell line. Typical kinetics of JC-1 import into 7WD4, 7PA2, and CHO cells are shown in Fig. 4a: under identical conditions, the 7WD4 and the 7PA2 cells express a mitochondrial ΔF whose value corresponds to 66% and 43% of the CHO control cells value (Fig. 4b).
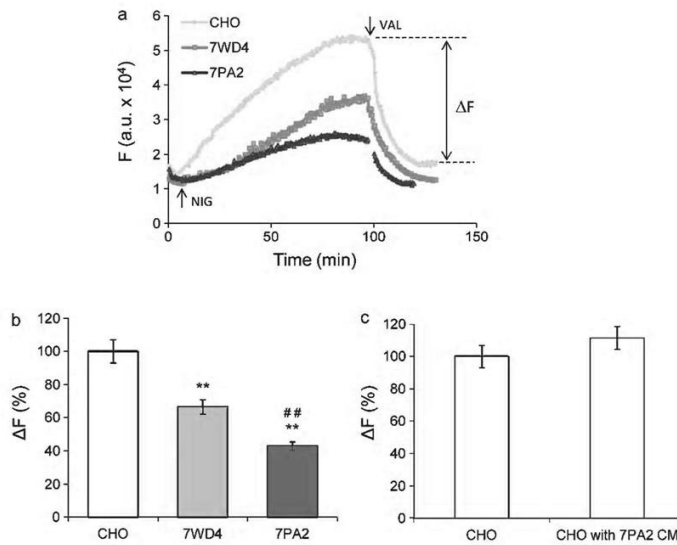

Fig. 4. Mitochondrial membrane potential in CHO, 7WD4, and 7PA2 cells. a) Time-dependent JC-1 accumulation in cell mitochondria following addition of nigericin $0.6\,\mu M$ (NIG). Valinomycin $0.2\,\mu M$ (VAL) is added at plateau to dissipate the $\Delta\Psi$. ΔF values were calculated as the difference between the maximal fluorescence and the final level reached after valinomycin addition. b) ΔF values (% of Control cells). Data $\pm$ SEM, $n \geq 13$. **$p \leq 0.001$ versus Control (CHO); ##$p \leq 0.001$ versus 7WD4. c) ΔF values of CHO control cells and CHO cells incubated overnight with 7PA2 conditioned medium. Data values are the means $\pm$ SEM; $n = 3$.

200

Attachments

In conclusion, both 7WD4 and 7PA2 cells have decreased mitochondrial membrane potential with respect to CHO control cells. This is more evident in 7PA2 than in 7WD4, thus could be associated to the $A\beta PP_{V717F}$ mutation (7PA2), causing a higher $A\beta$ oligomer production, inducing stronger effect on mitochondrial membrane potential.

The 7PA2 cells are the best characterized model of naturally occurring $A\beta$ peptides and oligomers. In this line, we asked whether the conditioned medium of 7PA2 cells would affect the mitochondrial membrane potential in CHO cells, similarly to the effect of endogenously produced $A\beta$ in 7PA2 cells. Thus, we incubated the CHO cells overnight with the 7PA2 conditioned medium, which is enriched with naturally occurring $A\beta$ oligomers, and observed no differences in mitochondrial membrane potential (Fig. 4c). We conclude that, under these conditions, extracellular $A\beta$ peptides and oligomers from 7PA2 cells do not influence mitochondrial membrane potential of CHO cells when delivered extracellularly. Data support that the intracellular balance of $A\beta$ in 7PA2 cells is the main cause of the observed mitochondrial potential deficit.

Reactive oxygen species

The evaluation of ROS production, carried out using cells pre-loaded with the DCFDA fluorescent probe, showed that the ROS accumulation is higher in 7PA2 and 7WD4 than in CHO cells, by ∼20% (Fig. 5b). As expected, both 7WD4 and 7PA2 cells have higher ROS production with respect to CHO basal ROS level. The ROS production is higher in 7PA2 than in 7WD4 cells correlating with depolarization of their mitochondrial membrane potential shown above.

DISCUSSION

Over the last decade, the hypothesis that mitochondrial dysfunction contributes significantly to pathogenesis and evolution of AD has gained attention. The experiments, carried out *in vitro* [11], in cell cultures [12], or *in vivo* [3, 31, 32], all seem to suggest that the mitochondrial dysfunction is related to interactions between mitochondria and $A\beta$ as a proteolytic product of $A\beta PP$ [33]. The molecular mechanisms underlying the mitochondrial impairment in AD are still uncertain. That is in part due to the difficulty of studying mechanisms in complex or ill-defined systems, such as the AD brain. In order to undertake and investigate the mechanisms of mitochondrial dysfunction in AD, we exploit the simple and well-defined AD-related model system of 7PA2 and 7WD4 cells. In this work we have therefore readdressed this issue by investigating the bioenergetic behavior of 7WD4 and 7PA2 cells. These cells naturally produce $A\beta$ oligomers [15, 17, 34], although the 7PA2 cells are able to accumulate them to a higher concentration [16, 20, 35].

The step by step titration approach applied to 7WD4 and 7PA2 cells shows a fairly uniform gradual depression of the functional activity of the respiratory chain, though more evident at the level of complex I and complex IV. Our finding in cells with intact mitochondria adds significant evidence to the recent study that demonstrates an impairment of complex I and complex IV activity by synthetic $A\beta$ added *in vitro* [36]. We show that a less efficient electron flux within the respiratory chain, compatible with a lower mitochondrial trans-membrane electrochemical potential gradient ($\Delta\mu H^+$), and thus a lower respiratory control ratio, are the features of the AD cells, particularly of 7PA2 cells. According to our results, respiration of the 7WD4 and 7PA2 cells, as well as their ability to build up and maintain a mitochondrial trans-membrane electrochemical potential gradient ($\Delta\mu H^+$), are impaired. The mitochondrial membrane potential of the 7WD4 and 7PA2 cells, measured by following the electrophoretic import of JC-1, is about half of that built up by control cells, and respiration is also depressed in 7WD4 and 7PA2 cells. Interestingly, the respiratory chain deficiency appears more evident in the 7PA2 than in the 7WD4 cell line. This finding is consistent with the observation that the concentration of $A\beta$ peptides, responsible for the mitochondrial toxicity, is higher in 7PA2 cells, whose culture condition medium proved to inhibit, *in vivo,* the hippocampus long-term potentiation [17], more efficiently than the conditioned medium of the 7WD4 cells [34].

Both the 7WD4 and 7PA2 cells display a lower (∼20%) stationary production of OXPHOS-ATP. In addition, the 7PA2 cells proved to be less efficient than CHO control and 7WD4 cells in compensating with glycolysis the olygomicin-induced OXPHOS impairment, as if the bioenergetic machinery of 7PA2 cells was less properly organized in both the oxidative and glycolytic metabolic compartments. Overall, the functional data herein presented suggest that the 7PA2 cells are bioenergetically less active than controls, and more severely damaged than 7WD4 cells, probably due to the their higher expression of toxic $A\beta$ oligomers. The 7PA2 and the 7WD4 cells proved to compensate to some extent their bioenergetic impairment, by glycolysis, though compensation was less efficient in 7PA2 cells than in 7WD4 cells. It is worth to keep in mind
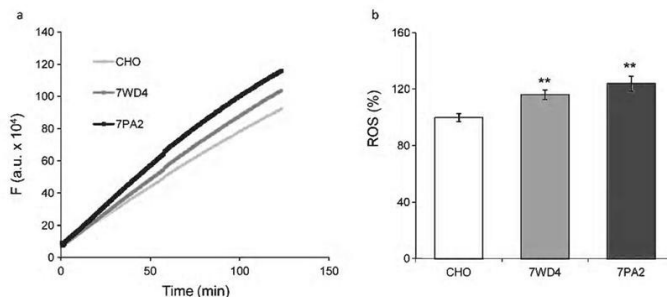
Attachments

Fig. 5. Reactive oxygen species (ROS) production in CHO, 7WD4, and 7PA2 cells. ROS production was measured in cell suspension in Hank's buffer containing DCFDA 0.1 mM. a) The kinetics of DCFDA fluorescence followed for 120 min. b) The percentage of ROS production is taken at 60 min. Data values are the means ± SEM; $n = 8$. $**p \leq 0.001$ versus Control (CHO).

that CHO and CHO-derived cells are ovary cell lines, not neurons. Here we show that these ovary cells, commonly used as a cellular model system for AD-related mechanism, display a Warburg effect. Neurons, however, do not perform glycolysis, so that a more severe bioenergetic impairment is expected in neuronal cells of AD patients, due to an intrinsically reduced ability to compensate with glycolysis [37].

Changes in mitochondrial physiology have as consequence alterations in mitochondrial morphology, shape, dynamics, and mitophagy, all processes involved in neurodegenerative diseases, including AD [38]. It has been reported that Aβ causes structural changes of mitochondria, decreases their trafficking, and alters mitochondrial fission/fussion dynamics [39–42]. These studies have been done in neurons since these kinds of mitochondrial changes are very relevant for neuronal survival. Our preliminary observations indicate altered mitochondrial morphology in 7WD4 and 7PA2 cells with respect to CHO controls (Supplementary Figure 2). More detailed studies regarding structural mitochondrial characteristics in these cell models are in progress.

It is well established that Aβ impairs mitochondrial redox activity and increases the generation of ROS [36, 43–46]. Interestingly, cell toxicity of Aβ peptides may also rely on their ability to bind Cu^{2+} ions and to catalyze bio-oxidations [47, 48]. These literature data are fully consistent with the higher ROS production herein detected particularly in the 7PA2 cells, but also in the 7WD4 cells. In both cases, the Aβ peptide produces its detrimental effect, particularly when interacting with the inner mitochondrial membrane complexes, that

was recently shown to occur for subunit I of respiratory complex IV[49] and subunit 3 of respiratory complex I *in vitro* [50].

It has been shown that AβPP possesses mitochondrial targeting signals and can localize to mitochondria in a membrane arrested form, with inside orientated N-terminus [51]. More recently it has been shown that structural features within the nascent chain of AβPP can regulate its alternative targeting to mitochondria [52]. Even if γ-secretase components have been found to localize to mitochondria [8], still the generally accepted idea is that Aβ is imported in mitochondria via TOM import machinery [5] from other intracellular compartments such as ER and endosomes that seems to be primary sites of Aβ production.

The interaction between the Aβ peptides and membrane bilayers has been previously demonstrated [53]. The Aβ peptides are able to deeply penetrate and perturb membrane structure, altering its viscosity and permeability properties, also contributing to formation of membrane channels in artificial membranes [53]. Recently, the hypothesis of Aβ oligomer pore formation has been sustained [54–56]. If the formation of membrane pores by Aβ oligomers [53] also occurs in mitochondria of 7WD4 and 7PA2 cells, this could possibly contribute to explanations of malfunctioning proteo-membrane complexes and observed lower respiratory capacity in these cells.

Observed mitochondrial deficits are not necessarily and exclusively due to a direct interaction of Aβ within mitochondria, but could reflect an indirect interaction probably mediated by events occurring in the ER and/or at the ER-mitochondria interface. Indeed,

202

Attachments

similar mitochondrial deficits observed in HEK293, COS-7 cells, and a mouse model overexpressing AβPP with Osaka mutation, were associated with ER-stress, ER associated degradation, and endosomal/lysosomal leakage [57, 58]. Recent findings implicate the role of mitochondrial associated membrane subcellular compartment (mitochondria-associated ER membrane) in AD pathogenesis [9, 59]. These studies demonstrate an increased significance of the ER-mitochondria crosstalk, with roles in lipid metabolism, Ca^{2+} signaling and other processes, which as a consequence, could influence mitochondrial functions, resulting in the mitochondrial deficits observed in AD. The observed co-immunostaining for Aβ and Tom20 mitochondrial marker in 7PA2 cells demonstrate that while the bulk intracellular localization of Aβ is generally extramitochondrial, a partial mitochondrial colocalization can be found (Supplementary Figure 3).

Our results demonstrate the effects of intracellular and endogenously generated Aβ peptides and oligomers on mitochondrial physiology in 7WD4 and 7PA2 cells. It remains to be ascertained whether Aβ peptides and/or oligomers exert their effects on mitochondrial functions by a direct or indirect mechanism. A new way to investigate how and where the Aβ oligomers induce mitochondrial changes would be a conformational-selective interference by the intracellular antibodies (intrabodies) approach [60]. Indeed, the use of conformational specific anti-Aβ oligomers recombinant antibody fragments [61] intrinsically suited for intracellular expression and targeting in different subcellular compartments [60, 62, 63] would allow clarifying the roles of subcellular Aβ processing and oligomerization on mitochondrial physiology, providing an answer to a well-established but still obscure role of mitochondrial deficit in AD pathology.

Authors' disclosures available online (http://www.j-alz.com/disclosures/view.php?id=1820) .

SUPPLEMENTARY MATERIAL

Supplementary methods and figures are available in the electronic version of this article: http://dx.doi.org/10.3233/JAD-130728.

REFERENCES

[1] Masters CL, Selkoe DJ (2012) Biochemistry of amyloid beta-protein and amyloid deposits in Alzheimer disease. *Cold Spring Harb Perspect Med* **2**, a006262.

[2] Schellenberg GD, Montine TJ (2012) The genetics and neuropathology of Alzheimer's disease. *Acta Neuropathol* **124**, 305-323.

[3] Nunomura A, Perry G, Aliev G, Hirai K, Takeda A, Balraj EK, Jones PK, Ghanbari H, Wataya T, Shimohama S, Chiba S, Atwood CS, Petersen RB, Smith MA (2001) Oxidative damage is the earliest event in Alzheimer disease. *J Neuropathol Exp Neurol* **60**, 759-767.

[4] Aleardi AM, Benard G, Augereau O, Malgat M, Talbot JC, Mazat JP, Letellier T, Dachary-Prigent J, Solaini GC, Rossignol R (2005) Gradual alteration of mitochondrial structure and function by beta-amyloids: Importance of membrane viscosity changes, energy deprivation, reactive oxygen species production, and cytochrome c release. *J Bioenerg Biomembr* **37**, 207-225.

[5] Hansson Petersen CA, Alikhani N, Behbahani H, Wiehager B, Pavlov PF, Alafuzoff I, Leinonen V, Ito A, Winblad B, Glaser E, Ankarcrona M (2008) The amyloid beta-peptide is imported into mitochondria via the TOM import machinery and localized to mitochondrial cristae. *Proc Natl Acad Sci U S A* **105**, 13145-13150.

[6] Walls KC, Coskun P, Gallegos-Perez JL, Zadourian N, Freude K, Rasool S, Blurton-Jones M, Green KN, LaFerla FM (2012) Swedish Alzheimer mutation induces mitochondrial dysfunction mediated by HSP60 mislocalization of amyloid precursor protein (APP) and beta-amyloid. *J Biol Chem* **287**, 30317-30327.

[7] Zhang H, Zhang YW, Chen Y, Huang X, Zhou F, Wang W, Xian B, Zhang X, Masliah E, Chen Q, Han JD, Bu G, Reed JC, Liao FF, Chen YG, Xu H (2012) Appoptosin is a novel pro-apoptotic protein and mediates cell death in neurodegeneration. *J Neurosci* **32**, 15565-15576.

[8] Hansson CA, Frykman S, Farmery MR, Tjernberg LO, Nilsberth C, Pursglove SE, Ito A, Winblad B, Cowburn RF, Thyberg J, Ankarcrona M (2004) Nicastrin, presenilin, APH-1, and PEN-2 form active gamma-secretase complexes in mitochondria. *J Biol Chem* **279**, 51654-51660.

[9] Area-Gomez E, Del Carmen Lara Castillo M, Tambini MD, Guardia-Laguarta C, de Groof AJ, Madra M, Ikenouchi J, Umeda M, Bird TD, Sturley SL, Schon EA (2012) Upregulated function of mitochondria-associated ER membranes in Alzheimer disease. *EMBO J* **31**, 4106-4123.

[10] Crouch PJ, Blake R, Duce JA, Ciccotosto GD, Li QX, Barnham KJ, Curtain CC, Cherny RA, Cappai R, Dyrks T, Masters CL, Trounce IA (2005) Copper-dependent inhibition of human cytochrome c oxidase by a dimeric conformer of amyloid-beta1-42. *J Neurosci* **25**, 672-679.

203

[11] Casley CS, Canevari L, Land JM, Clark JB, Sharpe MA (2002) Beta-amyloid inhibits integrated mitochondrial respiration and key enzyme activities. *J Neurochem* **80**, 91-100.

[12] Rhein V, Baysang G, Rao S, Meier F, Bonert A, Muller-Spahn F, Eckert A (2009) Amyloid-beta leads to impaired cellular respiration, energy production and mitochondrial electron chain complex activities in human neuroblastoma cells. *Cell Mol Neurobiol* **29**, 1063-1071.

[13] Manczak M, Anekonda TS, Henson E, Park BS, Quinn J, Reddy PH (2006) Mitochondria are a direct site of A beta accumulation in Alzheimer's disease neurons: Implications for free radical generation and oxidative damage in disease progression. *Hum Mol Genet* **15**, 1437-1449.

[14] Sarti P (2013) Nitric oxide: Role in human disease. *eLS*, doi: 10.1002/9780470015902.a0003390.pub2.

[15] Walsh DM, Tseng BP, Rydel RE, Podlisny MB, Selkoe DJ (2000) The oligomerization of amyloid beta-protein begins intracellularly in cells derived from human brain. *Biochemistry* **39**, 10831-10839.

[16] Portelius E, Olsson M, Brinkmalm G, Ruetschi U, Mattsson N, Andreasson U, Gobom J, Brinkmalm A, Holtta M, Blennow K, Zetterberg H (2012) Mass spectrometric characterization of amyloid-beta species in the 7PA2 cell model of Alzheimer's disease. *J Alzheimers Dis* **33**, 85-93.

[17] Walsh DM, Klyubin I, Fadeeva JV, Cullen WK, Anwyl R, Wolfe MS, Rowan MJ, Selkoe DJ (2002) Naturally secreted oligomers of amyloid beta protein potently inhibit hippocampal long-term potentiation *in vivo. Nature* **416**, 535-539.

[18] O'Hare E, Scopes DI, Kim EM, Palmer P, Jones M, Whyment AD, Spanswick D, Amijee H, Nerou E, McMahon B, Treherne JM, Jeggo R (2013) Orally bioavailable small molecule drug protects memory in Alzheimer's disease models. *Neurobiol Aging* **34**, 1116-1125.

[19] Li S, Jin M, Zhang D, Yang T, Koeglsperger T, Fu H, Selkoe DJ (2013) Environmental novelty activates beta2-adrenergic signaling to prevent the impairment of hippocampal LTP by Abeta oligomers. *Neuron* **77**, 929-941.

[20] Podlisny MB, Ostaszewski BL, Squazzo SL, Koo EH, Rydell RE, Teplow DB, Selkoe DJ (1995) Aggregation of secreted amyloid beta-protein into sodium dodecyl sulfate-stable oligomers in cell culture. *J Biol Chem* **270**, 9564-9570.

[21] Murrell J, Farlow M, Ghetti B, Benson MD (1991) A mutation in the amyloid precursor protein associated with hereditary Alzheimer's disease. *Science* **254**, 97-99.

[22] Chartier-Harlin MC, Crawford F, Houlden H, Warren A, Hughes D, Fidani L, Goate A, Rossor M, Roques P, Hardy J et al. (1991) Early-onset Alzheimer's disease caused by mutations at codon 717 of the beta-amyloid precursor protein gene. *Nature* **353**, 844-846.

[23] Roher AE, Kokjohn TA, Esh C, Weiss N, Childress J, Kalback W, Luehrs DC, Lopez J, Brune D, Kuo YM, Farlow M, Murrell J, Vidal R, Ghetti B (2004) The human amyloid-beta precursor protein770 mutation V717F generates peptides longer than amyloid-beta-(40-42) and flocculent amyloid aggregates. *J Biol Chem* **279**, 5829-5836.

[24] Reers M, Smiley ST, Mottola-Hartshorn C, Chen A, Lin M, Chen LB (1995) Mitochondrial membrane potential monitored by JC-1 dye. *Methods Enzymol* **260**, 406-417.

[25] Brunori M, Sarti P, Colosimo A, Antonini G, Malatesta F, Jones MG, Wilson MT (1985) Mechanism of control of cytochrome oxidase activity by the electrochemical-potential gradient. *EMBO J* **4**, 2365-2368.

[26] Gnaiger E, Kuznetsov A, Lassnig B, Fuchs A, Reck M, Renner K, Stadlmann S, Rieger G, Margreiter R (1998) High-resolution respirometry - optimum permeabilization of the cell membane by digitonin. *BioThermoKinetics in the Post Genomic Era* 89-95.

[27] Kuznetsov AV, Veksler V, Gellerich FN, Saks V, Margreiter R, Kunz WS (2008) Analysis of mitochondrial function in situ in permeabilized muscle fibers, tissues and cells. *Nat Protoc* **3**, 965-976.

[28] Srere PA, Brooks GC (1969) The circular dichroism of glucagon solutions. *Arch Biochem Biophys* **129**, 708-710.

[29] Bradford MM (1976) A rapid and sensitive method for the quantitation of microgram quantities of protein utilizing the principle of protein-dye binding. *Anal Biochem* **72**, 248-254.

[30] Merlo-Pich M, Deleonardi G, Biondi A, Lenaz G (2004) Methods to detect mitochondrial function. *Exp Gerontol* **39**, 277-281.

[31] Du H, Guo L, Fang F, Chen D, Sosunov AA, McKhann GM, Yan Y, Wang C, Zhang H, Molkentin JD, Gunn-Moore FJ, Vonsattel JP, Arancio O, Chen JX, Yan SD (2008) Cyclophilin D deficiency attenuates mitochondrial and neuronal perturbation and ameliorates learning and memory in Alzheimer's disease. *Nat Med* **14**, 1097-1105.

[32] Lustbader JW, Cirilli M, Lin C, Xu HW, Takuma K, Wang N, Caspersen C, Chen X, Pollak S, Chaney M, Trinchese F, Liu S, Gunn-Moore F, Lue LF, Walker DG, Kuppusamy P, Zewier ZL, Arancio O, Stern D, Yan SS, Wu H (2004) ABAD directly links Abeta to mitochondrial toxicity in Alzheimer's disease. *Science* **304**, 448-452.

[33] Lin MT, Beal MF (2006) Mitochondrial dysfunction and oxidative stress in neurodegenerative diseases. *Nature* **443**, 787-795.

[34] Townsend M, Shankar GM, Mehta T, Walsh DM, Selkoe DJ (2006) Effects of secreted oligomers of amyloid beta-protein on hippocampal synaptic plasticity: A potent role for trimers. *J Physiol* **572**, 477-492.

[35] Podlisny MB, Walsh DM, Amarante P, Ostaszewski BL, Stimson ER, Maggio JE, Teplow DB, Selkoe DJ (1998) Oligomerization of endogenous and synthetic amyloid beta-protein at nanomolar levels in cell culture and stabilization of monomer by Congo red. *Biochemistry* **37**, 3602-3611.

[36] Bobba A, Amadoro G, Valenti D, Corsetti V, Lassandro R, Atlante A (2013) Mitochondrial respiratory chain complexes I and IV are impaired by beta-amyloid via direct interaction and through Complex I-dependent ROS production, respectively. *Mitochondrion* **13**, 298-311.

[37] Moncada S, Bolanos JP (2006) Nitric oxide, cell bioenergetics and neurodegeneration. *J Neurochem* **97**, 1676-1689.

[38] Chen H, Chan DC (2009) Mitochondrial dynamics–fusion, fission, movement, and mitophagy–in neurodegenerative diseases. *Hum Mol Genet* **18**, R169-R176.

[39] Manczak M, Calkins MJ, Reddy PH (2011) Impaired mitochondrial dynamics and abnormal interaction of amyloid beta with mitochondrial protein Drp1 in neurons from patients with Alzheimer's disease: Implications for neuronal damage. *Hum Mol Genet* **20**, 2495-2509.

[40] Manczak M, Reddy PH (2012) Abnormal interaction between the mitochondrial fission protein Drp1 and hyperphosphorylated tau in Alzheimer's disease neurons: Implications for mitochondrial dysfunction and neuronal damage. *Hum Mol Genet* **21**, 2538-2547.

[41] Reddy PH (2009) Amyloid beta, mitochondrial structural and functional dynamics in Alzheimer's disease. *Exp Neurol* **218**, 286-292.

[42] Wang X, Su B, Lee HG, Li X, Perry G, Smith MA, Zhu X (2009) Impaired balance of mitochondrial fission and fusion in Alzheimer's disease. *J Neurosci* **29**, 9090-9103.

204

Attachments

[43] Behl C, Davis JB, Lesley R, Schubert D (1994) Hydrogen peroxide mediates amyloid beta protein toxicity. *Cell* **77**, 817-827.

[44] Kadowaki H, Nishitoh H, Urano F, Sadamitsu C, Matsuzawa A, Takeda K, Masutani H, Yodoi J, Urano Y, Nagano T, Ichijo H (2005) Amyloid beta induces neuronal cell death through ROS-mediated ASK1 activation. *Cell Death Differ* **12**, 19-24.

[45] Hensley K, Carney JM, Mattson MP, Aksenova M, Harris M, Wu JF, Floyd RA, Butterfield DA (1994) A model for beta-amyloid aggregation and neurotoxicity based on free radical generation by the peptide: Relevance to Alzheimer disease. *Proc Natl Acad Sci U S A* **91**, 3270-3274.

[46] Shearman MS, Ragan CI, Iversen LL (1994) Inhibition of PC12 cell redox activity is a specific, early indicator of the mechanism of beta-amyloid-mediated cell death. *Proc Natl Acad Sci U S A* **91**, 1470-1474.

[47] Kontush A (2001) Amyloid-beta: An antioxidant that becomes a pro-oxidant and critically contributes to Alzheimer's disease. *Free Radic Biol Med* **31**, 1120-1131.

[48] Roberts BR, Ryan TM, Bush AI, Masters CL, Duce JA (2012) The role of metallobiology and amyloid-beta peptides in Alzheimer's disease. *J Neurochem* **120**(Suppl 1), 149-166.

[49] Hernandez-Zimbron LF, Luna-Munoz J, Mena R, Vazquez-Ramirez R, Kubli-Garfias C, Cribbs DH, Manoutcharian K, Gevorkian G (2012) Amyloid-beta peptide binds to cytochrome C oxidase subunit 1. *PLoS One* **7**, e42344-.

[50] Munguia ME, Govezensky T, Martinez R, Manoutcharian K, Gevorkian G (2006) Identification of amyloid-beta 1-42 binding protein fragments by screening of a human brain cDNA library. *Neurosci Lett* **397**, 79-82.

[51] Anandatheerthavarada HK, Biswas G, Robin MA, Avadhani NG (2003) Mitochondrial targeting and a novel transmembrane arrest of Alzheimer's amyloid precursor protein impairs mitochondrial function in neuronal cells. *J Cell Biol* **161**, 41-54.

[52] Pfeiffer NV, Dirndorfer D, Lang S, Resenberger UK, Restelli LM, Hemion C, Miesbauer M, Frank S, Neutzner A, Zimmermann R, Winklhofer KF, Tatzelt J (2013) Structural features within the nascent chain regulate alternative targeting of secretory proteins to mitochondria. *EMBO J* **32**, 1036-1051.

[53] Seelert H, Dani DN, Dante S, Hauss T, Krause F, Schafer E, Frenzel M, Poetsch A, Rexroth S, Schwassmann HJ, Suhai T, Vonck J, Dencher NA (2009) From protons to OXPHOS supercomplexes and Alzheimer's disease: Structure-dynamics-function relationships of energy-transducing membranes. *Biochim Biophys Acta* **1787**, 657-671.

[54] Sciacca MF, Kotler SA, Brender JR, Chen J, Lee DK, Ramamoorthy A (2012) Two-step mechanism of membrane disruption by Abeta through membrane fragmentation and pore formation. *Biophys J* **103**, 702-710.

[55] Prangkio P, Yusko EC, Sept D, Yang J, Mayer M (2012) Multivariate analyses of amyloid-beta oligomer populations indicate a connection between pore formation and cytotoxicity. *PLoS One* **7**, e47261.

[56] Connelly L, Jang H, Arce FT, Capone R, Kotler SA, Ramachandran S, Kagan BL, Nussinov R, Lal R (2012) Atomic force microscopy and MD simulations reveal pore-like structures of all-D-enantiomer of Alzheimer's beta-amyloid peptide: Relevance to the ion channel mechanism of AD pathology. *J Phys Chem B* **116**, 1728-1735.

[57] Nishitsuji K, Tomiyama T, Ishibashi K, Ito K, Teraoka R, Lambert MP, Klein WL, Mori H (2009) The E693Delta mutation in amyloid precursor protein increases intracellular accumulation of amyloid beta oligomers and causes endoplasmic reticulum stress-induced apoptosis in cultured cells. *Am J Pathol* **174**, 957-969.

[58] Umeda T, Tomiyama T, Sakama N, Tanaka S, Lambert MP, Klein WL, Mori H (2011) Intraneuronal amyloid beta oligomers cause cell death via endoplasmic reticulum stress, endosomal/lysosomal leakage, and mitochondrial dysfunction *in vivo*. *J Neurosci Res* **89**, 1031-1042.

[59] Hedskog L, Pinho CM, Filadi R, Ronnback A, Hertwig L, Wiehager B, Larssen P, Gellhaar S, Sandebring A, Westerlund M, Graff C, Winblad B, Galter D, Behbahani H, Pizzo P, Glaser E, Ankarcrona M (2013) Modulation of the endoplasmic reticulum-mitochondria interface in Alzheimer's disease and related models. *Proc Natl Acad Sci U S A* **110**, 7916-7921.

[60] Cattaneo A, Meli G (2012) Protein silencing with intracellular antibodies: Targeting Alzheimer's disease. *Eur J Neurodegener Dis* **1**, 147-163.

[61] Meli G, Visintin M, Cannistraci I, Cattaneo A (2009) Direct *in vivo* intracellular selection of conformation-sensitive antibody domains targeting Alzheimer's amyloid-beta oligomers. *J Mol Biol* **387**, 584-606.

[62] Biocca S, Cattaneo A (1995) Intracellular immunization: Antibody targeting to subcellular compartments. *Trends Cell Biol* **5**, 248-252.

[63] Biocca S, Neuberger MS, Cattaneo A (1990) Expression and targeting of intracellular antibodies in mammalian cells. *EMBO J* **9**, 101-108.

205